Charles University in Prague
Faculty of Science
Department of Physical and Macromolecular Chemistry

Institute of Macromolecular Chemistry
Academy of Sciences of the Czech Republic

Nanostructures produced by conducting polymer, polyaniline

Doctoral Thesis

Elena Konyushenko

Supervisor: Jaroslav Stejskal, PhD.

Prague 2008

Univerzita Karlova v Praze
Přírodovědecká fakulta
Katedra fyzikální a makromolekulární chemie

Ústav makromolekulární chemie
Akademie věd České republiky, v.v.i.

Nanostruktury vytvářené vodivým polymerem, polyanilinem

Doktorská disertační práce

Ing. Elena Konyushenko

Školitel: RNDr. Jaroslav Stejskal, CSc.

Praha 2008

This Dissertation describes my original work except where acknowledgement is made in the text. It is not substantially the same as any work that has been or is being submitted to any other University for any degree, diploma or any other qualification.

Elena Konyushenko

Acknowledgment

While working for my PhD Thesis, I have learnt how difficult is to do any research and that the results obtained are a result of many people's hard work. In consequence, I would like to start my Thesis by expressing my gratitude to all those people who have helped me and inspired me during my work.

Firstly, I would like to thank my supervisor Dr. Jaroslav Stejskal, whom I am deeply indebted for his patient guidance and motivation. His enthusiasm for research was my permanent inspiration and his immense knowledge of macromolecular chemistry and chemistry of conducting materials have made my study much easier. This Thesis would not be completed without his encouragement and support.

My consultant, Prof. Dr. Miroslava Trchová, has been invaluable as well. The discussions with her were the source of many ideas and impulses which advanced my work. I would like to thank her especially for her patience in elucidating to me, time after time, the knowledge about FTIR and Raman spectroscopies. The research summarized in this Thesis would not be possible without the spectra of the samples from her Laboratory. Many of the samples were kindly prepared by the Laboratory technician, M. Brunclíková, and her PhD student Mgr. Ivana Šeděnková.

I would like to thank Dr. Irina Sapurina, who has been helping with understanding of fundamentals of macromolecular chemistry and love for polyaniline. Thanks are also due to all co-workers and friends who were helping and supporting me during my PhD studies.

Contents

1. Introduction: Polyaniline

Polyaniline (PANI) is one of the most interesting conducting polymers. Polyaniline has a high level of electrical conductivity, good redox and ion-exchange properties, excellent environmental stability, and easy way of preparation from common chemicals (Gospodinova *et al.* 1998, Kang *et el.* 1998, Stejskal *et al.* 2002a). That is why PANI has a good application potential and has been studied for more than last three decades.

The preparation of PANI is a simple chemical process from the technical point of view. In fact, the aniline oxidation is represented by an intricate interplay of consecutive reactions, which are still far from being completely understood. The synthesis of PANI depends on the reaction conditions. There are many parameters that are regarded to be important in the control the properties and PANI morphology (Focke *et al.* 1987, Wei *et al.* 1987). These include especially the chemical nature of the oxidants, the acid protonating aniline and reaction intermediates during the oxidation, concentration of reactants (especially that of aniline and oxidant) and their molar proportions, temperature, solvent components, the presence of additives (*e.g.*, colloidal stabilizers and surfactants), templates added to reaction mixture, *etc.* It is not completely obvious to the experimentalists, which of these parameters can aim the synthesis in the direction of the desired products. The organized supramolecular structures of PANI, like nanotubes and nanowires, have been discovered during the search for the optimum reaction conditions and so far there are no unambiguous concepts of their genesis. Despite the considerable effort exploited in this direction, the complete and generally accepted reaction scheme of aniline oxidation under the various reaction conditions has not been produced. Even less is known of the reaction between the molecular and supramolecular structures. The simple concepts are needed, which would explains the generation of all types of supramolecular structures and, at the same time, relate them to the molecular structure produced in the individual phases of aniline oxidation.

1.1. Preparation of polyaniline

The understanding of the molecular mechanism of aniline oxidation sets the basis of the successful control of the PANI synthesis. Namely, the molecular processes, determining the molecular structure of the oxidation products, predetermine the physical and chemical properties of products and their supramolecular structure. The present

knowledge about aniline oxidative polymerization can briefly be summarized as follows.

Aniline can be oxidized by the two main methods, chemically or electrochemically. In this work the chemical method for the polymerization has been used. The oxidation typically takes place in various aqueous media and variety of oxidants can be used for this purpose (Figure 1). The synthesis may yield a product having different properties and various supramolecular morphologies. Depending on the preparation conditions, they can be soluble in various organic solvent or insoluble in any solvent.

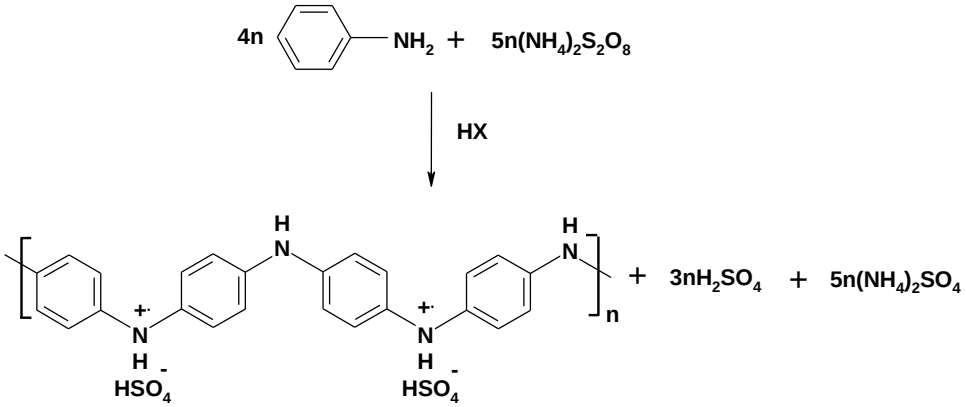

Figure 1. The scheme of the aniline polymerization.

Komentář [E1]:

The oxidative polymerization of aniline at pH<2 belongs to the class of chain reactions (Stejskal *et al.* 1996, Wei *et al.* 2001). The growth of chains proceeds by the addition of monomer aniline molecules to the active chain end. Emeraldine form of PANI is formed during the standard polymerization of aniline and the sulfuric acid is a by-product.

The conducting PANI macromolecules have a regular structure. More than 95 % of constitutional units are linked in head-to-tail *para* positions. The fraction of molecules linked in other way is small (Bacon *et al.* 1968, Hagiwara *et al.* 1987). It is quite surprising that such a regular structure is produced at relatively high temperature and during a fast reaction. As a rule, the chains of ordinary polymers produced under such conditions are composed of units having various microstructure. The regular

chains are produced only with specific catalysts, such as of Ziegler-Natta type, during the slow polymerizations at low-temperature (Ledwith *et al.* 1974).

1.2. Properties of polyaniline

The oxidative polymerization of aniline gives rise to PANI which exists in a variety of forms, differing in the degree of oxidation or extent of protonation, or both (Stejskal *et al.* 1995b). For the discussion of PANI forms and their interconversions, the following scheme of PANI forms was proposed (Figure 2).

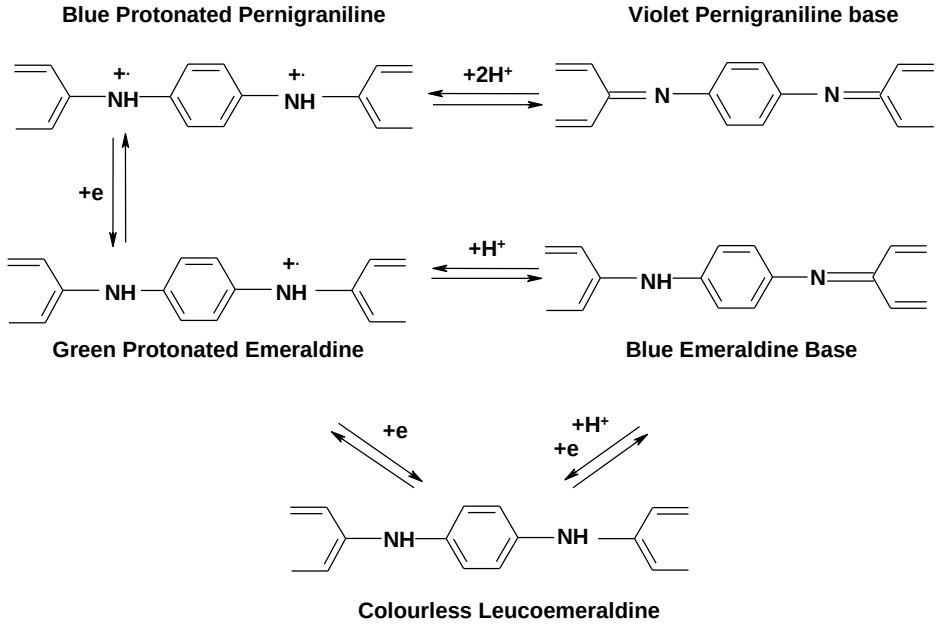

Figure 2. Forms of polyaniline (Stejskal *et al.* 1996).

The most important form of PANI, protonated emeraldine, is produced by the oxidative polymerization of aniline in aqueous acids, it is green and conducting. The positive charge on aniline units is balanced by negatively-charged counter ions of organic or inorganic nature. This form of PANI is stable. Protonated emeraldine converts to the blue emeraldine base in alkaline medium. This transition proceeds already at pH 6–7. The emeraldine base has the same number of non-protonated imine and amine groups (Epstein *et al.* 1987); it is non-conducting and it has blue colour.

If stronger oxidizing conditions are applied, PANI is converted to protonated pernigraniline (MacDiarmid *et al.* 1985, Stejskal *et al.* 1993), which is blue and may be expected to be conducting, a subsequent treatment with an alkali results in the pernigraniline base, which is violet and non-conducting. The acid–base transition occurs at pH 0-1. The two blue forms, protonated pernigraniline and emeraldine base, are of different colour shades.

Polyaniline can be reduced to colourless, non-conducting, leucoemeraldine. The scheme shows a set of interrelated structures which require only the exchange of protons or electrons or both to undergo interconversion. Such a scheme is compatible with all the known facts.

1.3. Morphology of polyaniline

Polyaniline is a unique conducting polymer. It exists in variety of protonated and oxidation forms and it also has different supramolecular morphologies. Polyaniline nanogranules can be prepared when aniline is polymerized in the strongly acidic aqueous media and is currently used for the synthesis of a conducting PANI (Stejskal *et al.* 1993, Gospodinova *et al.* 1993).

A lot of work has been done on the preparation of the PANI nanotubes and nanowires. The pioneering papers have been published by Wan group (Huang *et al.* 1999, Qiu *et al.* 2001a, Qiu *et al.* 2001b). It has been proposed that the presence of organic acids produce the soft template by the reaction with aniline. Such salts have been assumed to organize into micelles. Later, however, the nanotubes have been synthesized in the presence of inorganic acids or without any acids, just in water (Konyushenko *et al.* 2006a). It should be mentioned that when polymerization proceeds just in water, PANI nanosheets can also be formed in addition to nanotubes. Another type of morphology is represented by microspheres (Venancio *et al.* 2006, Stejskal *et al.* 2008). When aniline has been oxidized in the presence of ammonium peroxide, in alkaline media when pH>7. Under those conditions oligo-aniline microspheres are formed.

1.4. Composite materials

One of the most interesting and novel materials are the carbon nanotubes (CNT). Carbon nanotubes have a high degree of constitutional organization. They exist as two fundamental forms, single-wall and multi-wall carbon nanotubes (MWCNT). Since the

discovery of CNT, attention has been given to its surface modification in order to get separated and uniformly dispersed CNT and thus to produce useful composite materials. MWCNT have been coated by a conducting polymer PANI, as the method to modify the surface of CNT. In such composite materials, PANI acts as an adhesive of the individual CNT. Polyaniline coating converts the original hydrophobic surface of CNT to hydrophilic one and provides a good compatibility with other hydrophilic compounds. PANI is a mixed proton and electron conductor. This is important in processes than involve the simultaneous transport of protons and electrons, *e.g.* in hydrogen evolution reaction (Damian *et al.* 2006) or in fuel-cell electrodes (Deng *et al.* 2005). Conducting polymers exhibits redox properties; in the combination with CNT they have also been used as electrodes in the supercapacitors (Frackowiak *et al.* 2006, Gupta *et al*. 2006).

CNT prepared by chemical-vapour deposition method often include metal nanoparticels, which serve as catalytic centers for the nanotubular growth during CNT preparation. The ferromagnetic materials (Fe, Co and Ni) and their alloys are used as catalysts and their nanoparticels are incorporated into CNT. Iron-filled aligned multi-wall CNT shows significant uniaxial magnetic anisotropy related to the cylindrical shape of the aligned iron particles. Such materials may find application in future magnetic storage devices (Mehl *et al*. 2003). Other examples of such materials are CNT or PANI nanotubes filled with nickel, which have the coercivity an order of magnitude higher than that of bulk nickel (Bao *et al*. 2002, Cao *et al*. 2001).

1.5. Applications

The great variety of properties are displayed by the organic conducting polymers have led to a large array of applications that are at various stages of development. These include electromagnetic shielding for computers and other electronic apparatuses, conducting coatings for loudspeaker membrane, gas sensors (‘electronic noses’) to identify the presence of small quantities of different gases, battery electrodes, membranes to separate unwanted ions from solutions, corrosion-resistant coatings to prevent rusting, and cheap disposable electronic chips for automatic pricing of supermarket goods, and many others (Kaiser *et al.* 2001).

2. The aim of the Thesis

It has been shown that PANI exists in variety of forms, differing in degree of oxidation or extent of protonation, or both. Recently, few mechanisms of aniline polymerization have been proposed in the literature, but so far the complete and generally accepted reaction scheme of aniline oxidation under the various reaction conditions has not been produced. That is why this work is concentrated on the formation of different structures of PANI under various reaction conditions and on the explanation of processes occurring during the polymerization. Also, it has been studied how the polymerization conditions influence the supramolecular morphology of PANI. The second part of the Thesis is concentrated on the preparation of the composite materials of PANI and multi-wall carbon nanotubes.

In this work, the course of aniline polymerization in various acidic media has been investigated by following the dependences of temperature and pH on time. Aniline was oxidized under different conditions: the temperature has been changed from – 25 ^{o}C to + 25 ^{o}C; the polymerization has started in different acidic solutions (pH was changed from 10 to 2.5); the various doping acids have been used – organic or inorganic; the ratio of monomer to oxidant has been changed, *etc*. Polyaniline prepared under these conditions have been studied by different methods. FTIR and Raman spectra were used to analyze the molecular structure; scanning and transmission electron microscopies were employed to see the supramolecular structures; gel permeation chromatography was used to determine the molecular weight, and the conductivity was measured.

The mechanism of the aniline oxidation was proposed and related to the formation of supramolecular structures of PANI under different reaction conditions. The special attention has been paid to PANI nanotubes.

The composites PANI/CNT have been prepared at various conditions like, the concentration of CNT was changed from 0 to 80 wt%, and the doping level of conducting polymer films was also varied. There two kinds of CNT have been coated: pure CNT and CNT with incorporated nickel nanoparticles. All composite materials have been studied by different methods and possible application has been proposed.

The Thesis consists of five papers published in international journals, one accepted for the publication, and one submitted manuscript after a minor revision (Appendices A–E). They can be divided into two groups: (1) the synthesis of various morphologies of PANI and (2) the preparation of composite materials, CNT/PANI. Another three papers have not been included in the present Thesis.

3. Polyaniline nanostructures

3.1. The mechanism of aniline oxidation

Aniline is oxidized *in-situ* by ammonium peroxydisulfate in aqueous media to PANI. Aniline, a primary amine with moderate basicity, has $pK_a = 4.6$ (CRC 1995). The most of aniline molecules become protonated already at pH<4 (Figure 3) (Stejskal *et al.* 2008). Oligomers and polymer chains have terminal primary amine groups with the pK_a value close to that of aniline. There are many 'internal' secondary amine units in the chains that are much weaker base and become protonated only at pH<2 and lower (Perrin *et al.* 1972, Barton *et al.* 1979). The phenazine units are protonated still at lower pH<1 (Wu *et al.* 1997, Komura *et al.* 2000).

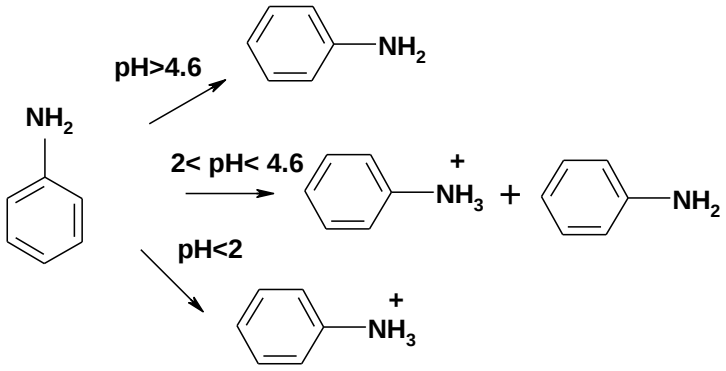

Figure 3. The protonation of neutral aniline molecules depends on pH.

It is very important to realize that the protonated and non-protonated amino groups have different reactivity. The oxidation potential of protonated amines is considerably higher due to the reduced electron density of the molecule, in the connection with the localization of a positive charge on this molecule (Ćirić-Marjanović *et al.* 2006). The oxidation of both the protonated aniline and the terminal primary amino groups in oligomers is much more difficult compared with the non-protonated analogues.

The oxidation of aniline to the chain structures always involves abstraction of hydrogen atoms as new covalent bonds are produced between the aniline molecules. One monomer addition needs the elimination of two protons (Figure 1). That is why the acidity of the reaction mixture always increases during the oxidation. The originally predominant deprotonated molecules thus gradually convert to protonated forms and the mechanism of the oxidation changes as the oxidation proceeds (Stejskal *et al.* 2008). In

this way, the oxidation of aniline is a complex albeit well-defined dynamic process. We can say that the reaction pathway of aniline oxidation changes during the transition from the non-protonated to protonated amines. The oxidation process itself can be analyzed by following time dependences of acidity that increases in the course of reaction because sulfuric acid is a by-product, and/or temperature, the oxidation is exothermic (Konyushenko *et al.* 2006a).

3.1.1. Oxidation in the solutions of strong acids

The oxidation of aniline in the solutions of strong acids; like sulfuric or hydrochloric acids, starts at pH 2.4 and decreases during the reaction up to 1 (Figure 4). The pH decreases from the very beginning of the reaction, indicating that some process took place during the induction period, which precedes the exothermic polymerization.

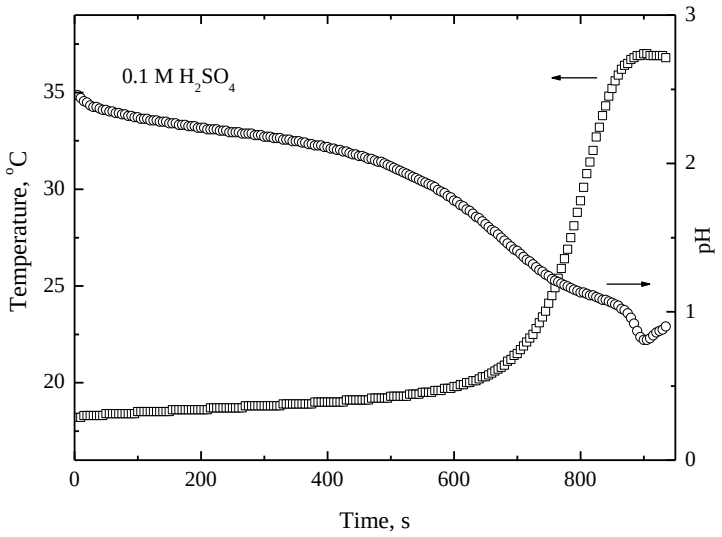

Figure 4. The changes in temperature (squares) and acidity (circles) during the oxidation of 0.2 M aniline with 0.25 M ammonium peroxydisulfate in 0.1 M sulfuric acid (Konyushenko *et al.* 2006a).

Aniline molecules are present dominantly in the form of anilinium cations in the solutions of strong acids; the concentration of neutral aniline molecules is very low. That is why the process of oxidation is slow (we can observed the induction period Figure 4). During the induction period, there is virtually no heat evolved during this stage, and also the changes in pH are hardly spotted. Under such conditions, anilinium

cations are formed as oligomers, dimers and trimers. The blue colour at the beginning of the induction period corresponds to the oxidized forms of semidines, amino-diphenylamines (Figure 5) (Ćirić-Marjanović *et al.* 2006).

The induction period is followed by the fast exothermic process associated with the growth of the polymer chains. The reaction mixture becomes heterogeneous because the reaction intermediates and products are not soluble in the medium. The blue colour of the reaction mixture deepens (the absorption maximum is located at 690 nm (Stejskal *et al.* 1995a), the thin polymer film is produced at the air/solution interface having a violet metallic tint.

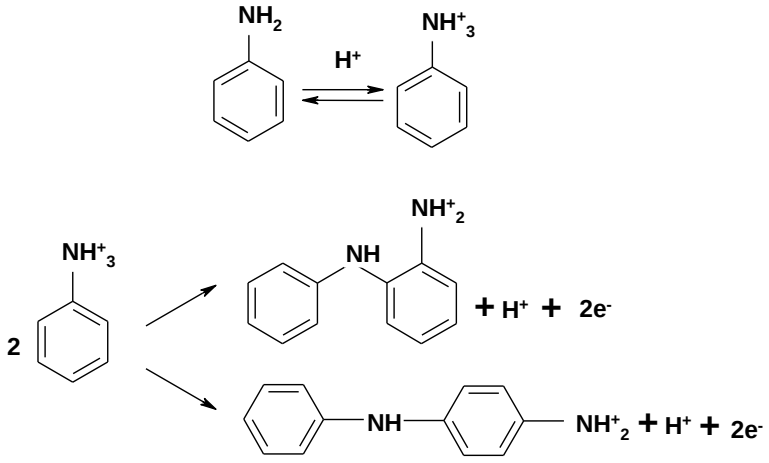

Figure 5. Formation of aniline dimers.

We assume that the subsequent oxidative reaction of aniline dimer, *o*-semidine with aniline or intramolecular cyclization of trimers yields the stable structures of phenazine types: phenazine and *N*-phenylenphenazine (Figure 6).

The formation of a phenazine heterocycle is promoted by the acidic medium. They play the role of nucleates and initiation centres in the further propagation of polymer chains (Stejskal *et al.* 2006). The formation of the phenazine structures is confirmed by different methods, such as UV–visible spectra (Stejskal *et al.* 1993) and FTIR and Raman spectroscopies (Šeděnková *et al.* 2007, Trchová *et al.* 2006). FTIR spectra of the early oxidation product are presented on the Figure 7.

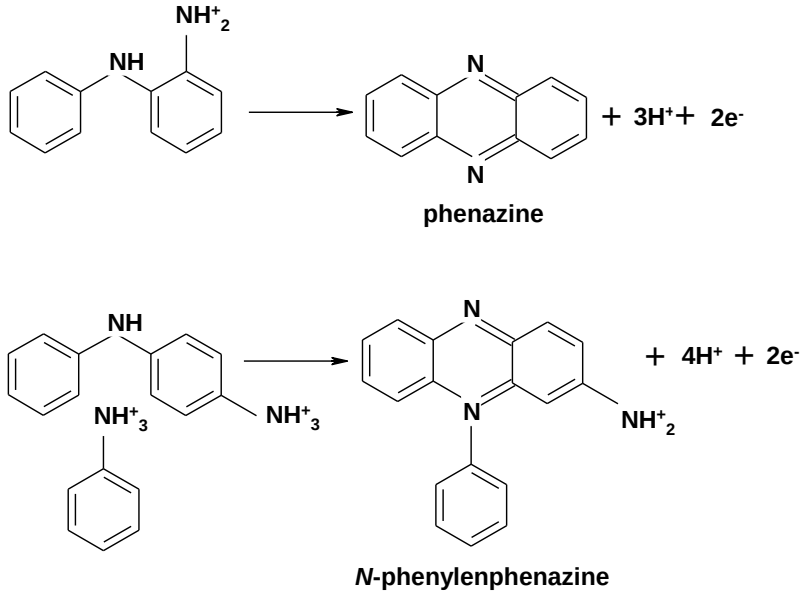

Figure 6. Formation of aniline trimers.

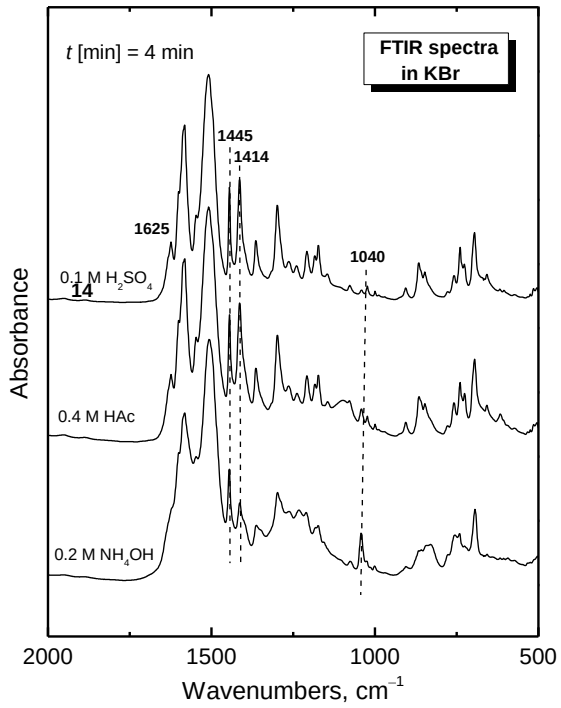

Figure 7. FTIR spectra of products isolated in the early stages of aniline oxidation (after 4 min) in 0.1 M sulfuric acid, 0.4 M acetic acid, or 0.2 M ammonium hydroxide (Stejskal *et al.* 2008).

FTIR spectra of oxidation products collected in the early stages of oxidation in the solutions of a strong and weak acid are virtually identical. This is one of the most important observations of this study (Stejskal *et al.* 2008). The presence of the peaks at 1625, 1445, and 1414 cm^{-1} is a common feature of all the early oxidation product. The last peak may be assigned to a totally symmetric stretching of the phenazine ring (Viva *et al.* 1999, Dines *et al.* 2001). Phenazine-like units can also be detected by the bands at 1208 and 1136 cm^{-1} and their contribution to the band at 1145 cm^{-1} is possible. The bands observed at 1445 and 1414 cm^{-1} in the spectrum of *o*-semidine (2-aminodiphenylamine), where they are much stronger than in the spectrum of *p*-semidine (4-aminodiphenylamine), support the presence of *ortho*-linked aniline constitutional units in the oligomers. The band at 1625 cm^{-1}, with a shoulder at ~ 1630 cm^{-1}, corresponds to the C=C stretching vibration in a phenazine-like segment (Li *et al.* 2005), including a contribution from C=N stretching vibrations (Malinauskas *et al.* 1998).

Further oligomer growth is suppressed due to its high oxidation potential and the low concentration of available neutral aniline. When pH becomes sufficiently low, the chain propagation starts from the initiation centers: phenazines and *N*-phenylphenazines (Figure 8). The concrete chemical structure of such a centre is still open to discussion and the formula shown in Figure 8 is only one of possible structures.

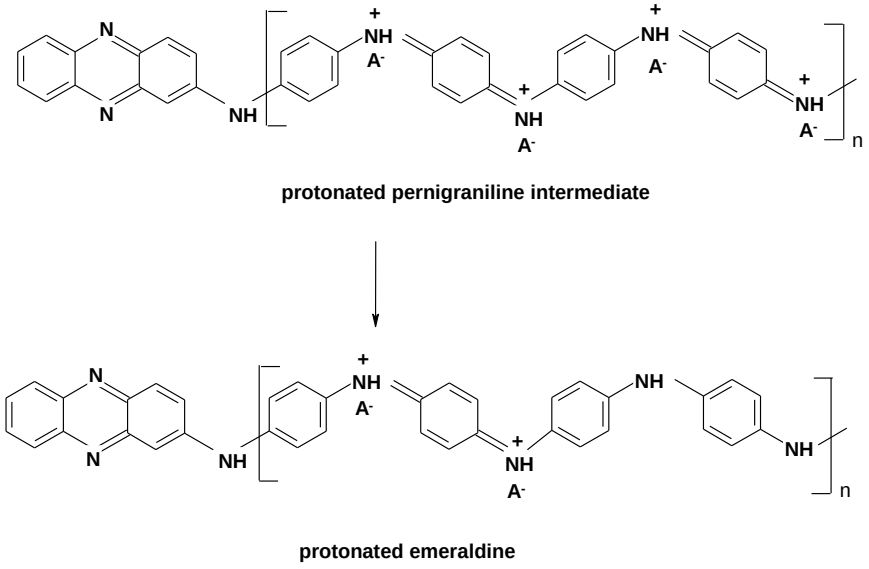

Figure 8. Propagation: The formation of the polyaniline chain.

The first attachment of aniline monomer to a phenazine nucleate takes place at the high oxidation potential, 1.5 V. If it takes place, the formation of future initiation centers of the chain growth proceeds. The propagation produces the conjugated system over which the electrons can be delocalized. At the propagation stage, the oxidation potential of the products decreases and the chain growth takes place (Zhang *et al.* 2006a, Genies *et al.* 1990, Bejan *et al.* 1998). The regular polymer-chain structure is formed due to the many times repeated reactions of *para*-substitutions. The oxidation degree of the growing chains is between emeraldine and pernigraniline forms (Madathil *et al.* 2004). It is confirmed by the optical spectra, a broad absorption band of pernigraniline at 690 nm is observed (Stejskal *et al.* 1995a). The protonated pernigraniline oxidation state implies the large fraction of imine groups in polymer chain carries a positive charge. The polymer chain has the possibility to reduce its energy, to delocalize the charge along the conjugated system. This can be achieved when the polymer chain has a flat configuration with alternating benzenoid rings and amino groups. Such structure is found with the polymer chains constituted by *para*-linked aniline units connected in head-to-tail type. The benzene rings lay in a plane in a zig-zag configuration (Pouget *et al.* 1991). In this configuration, the macromolecules have a maximum conjugation and charge delocalization.

The oxidation of aniline proceeds until one of the reactants or both become depleted. After the depletion of one of the reactants or both, the polymerization stops. The structure of PANI depends on the reactant, which was present in excess. If there was an excess of oxidant, the resulting polymer remains in the pernigraniline form (Manohar *et al.* 1991). This applies especially at the molar ratio [peroxydisulfate]/[aniline]>1.5. If the reaction has been carried out at stoichiometric conditions, the molar ratio [peroxydisulfate]/[aniline]=1.25 (Stejskal *et al.* 2002b), or at aniline excess, pernigraniline is reduced in the end of the reaction to emeraldine and aniline oxidized at the same time to emeraldine (Stejskal *et al.* 1996, Kolla *et al.* 2005).

Some authors have proposed that the hydrolysis of reactive centers takes place during the oligomerization as well as in the polymerization and can be regarded as a termination step (Gospodinova *et al.* 1994). The hydrolyzed terminal amino group effectively blocks any further growth reactions. It is well known that the molecular weight of PANI can be increased by the reduction of polymerization temperature (Zengin *et al.* 2007, Mattoso *et al.* 1994, Stejskal *et al.* 1998, Stejskal *et al.* 2004). This

experimental facts well correspond to the concept of hydrolytic termination, when the rate of the hydrolysis is reduced at lower temperature.

3.1.2. Oxidation in the solution of weak acids

When the polymerization is conducted in the solutions of weak acids, the aniline and primary amino groups in oligomers become protonated but the intrinsic secondary amino groups are not. The temperature and acidity profiles during the oxidation of aniline with ammonium peroxydisulfate are shown in Figure 9.

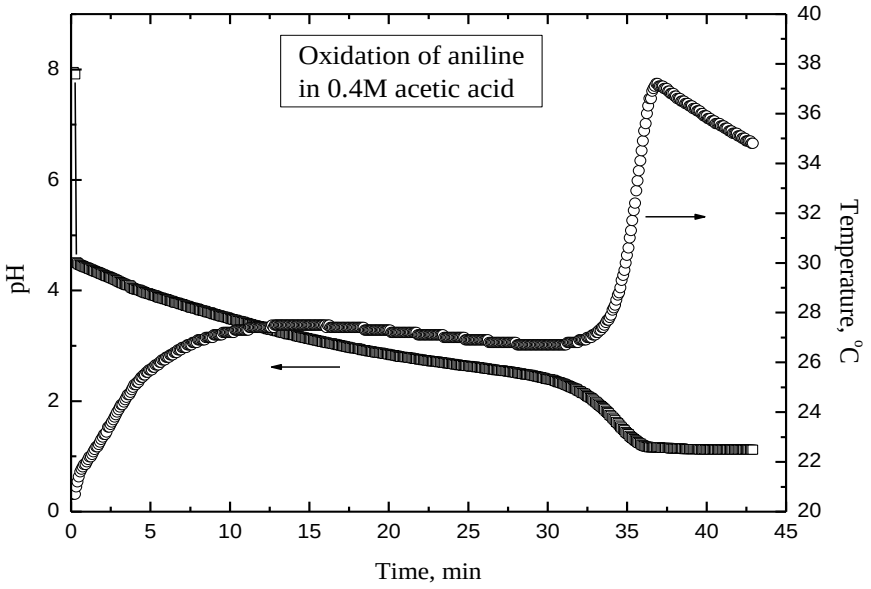

Figure 9. Time dependence of pH and temperature during the polymerization of aniline in 0.4 M acetic acid.

The polymerization in the aqueous solutions of weak acids (acetic, succinic, phosphoric acids and *etc.*) starts at pH~4.5 and drops, as sulfuric acid has been produced by the decomposition of peroxydisulfate, and hydrogens are removed from aniline as protons. When the oxidation of aniline starts at mildly acidic conditions, at pH 4.5 in the weak organic or inorganic acids; the reaction mixture is rich of both neutral aniline molecules and anilinium cations. Neutral aniline molecules are easily oxidized to oligomers (Figure 10), and the released protons reduce the pH (Figure 9). The equilibrium between the aniline molecules and anilinium cations shifts in favour of

latter species. Anilinium cations are much more difficult to be directly oxidized, because the electron pair on nitrogen, which is delocalized in neutral aniline molecules, becomes localized in anilinium cations (Cram *et al.* 1964). That is why the reaction virtually stops (Fu *et al.* 1994, Stejskal *et al.* 2006), and the temperature starts to decrease (Figure 9). Yet, there is always equilibrium between the protonated and neutral species, both species always coexist, and the oxidation of neutral aniline molecules still proceeds with preference even if their content is very low (Stejskal *et al.* 2008). This is manifested by a continuing decreasing pH under such conditions (Figure 9). The situation corresponds to the induction period observed in the classical polymerization of aniline in the acidic media. The situation changes when pH<2 (Figure 9). Such conditions correspond to those of oxidation in the solutions of strong acids, and indeed sulfuric acid is produced in the course of oxidation (Figure 1). The exothermic polymerization then follows (Figure 9).

During the induction period, the highly deficient neutral aniline is still the only species which is oxidized; the predominating anilinium cations are not prone to direct oxidation. The *ortho*- and *para*-linked aniline units produced (Figure 10).

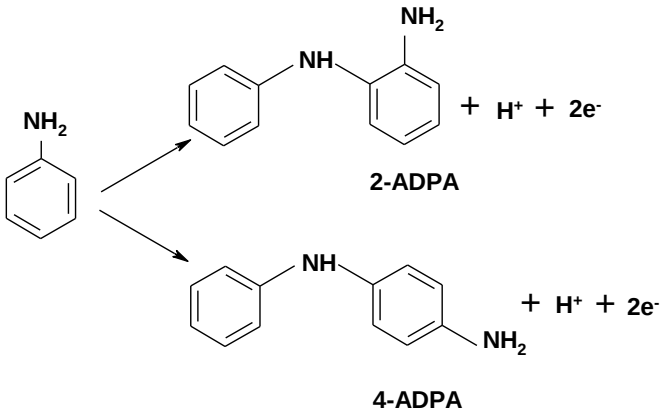

Figure 10. The formation of aniline dimers.

The aniline dimers, 4-aminodiphenylamine (4-ADPA) and 2-aminodiphenylamine (2-ADPA), show complex redox and acid–base behavior (Ćirić-Marjanović *et al.* 2006). The 4-aminodiphenylamine has a considerably lower electrochemical potential compared with aniline (Gospodinova *et al.* 1993). This is the reason for the instantaneous oxidation of 4-aminodiphenylamine. The 2-aminodiphenylamine base form is slightly more oxidizable than aniline, but less oxidizable than

4-aminodiphenylamine (Figure 11).

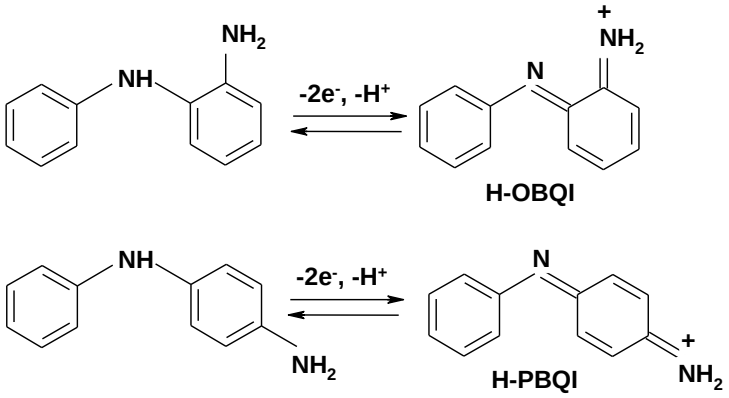

Figure 11. The formation of oxidized forms of 4-ADPA and 2-ADPA (Ćirić-Marjanović *et al.* 2006).

The oxidized form of 4-aminodiphenylamine, *N*-phenyl-*p*-benzoquinonediimine (PBQI), has been identified at the initial stage of the aniline oxidative polymerization by using UV–visible absorption spectroscopy (Gospodinova *et al.* 1993). The reaction take places when pH<4, so the further step is the conversion of dimers to trimers (Figure 12).

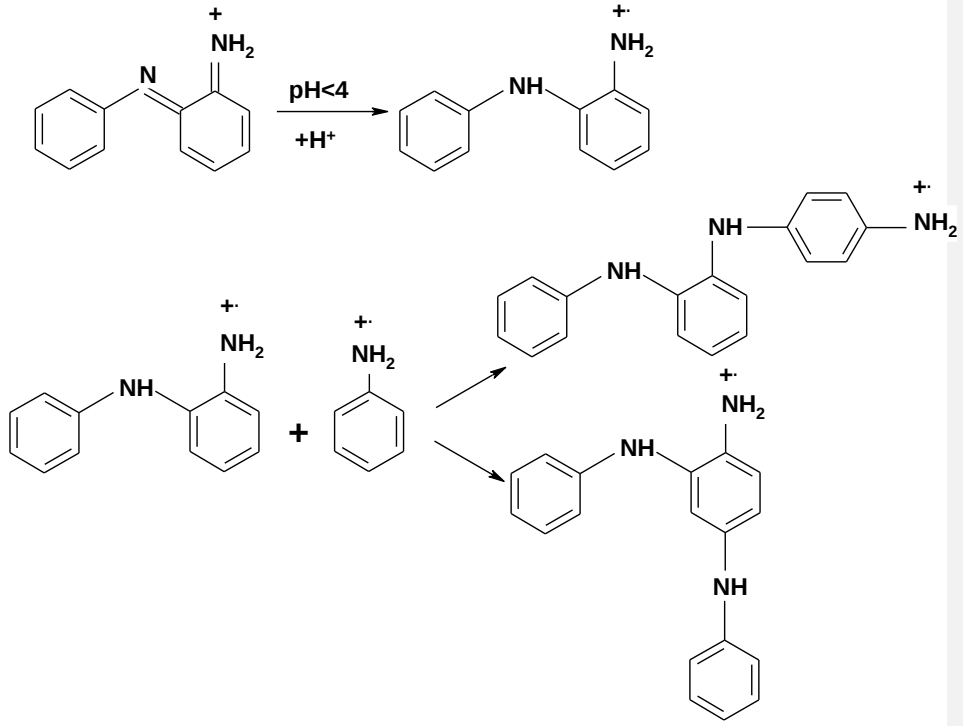

Figure 12. The formation of trimers (Ćirić-Marjanović *et al.* 2006).

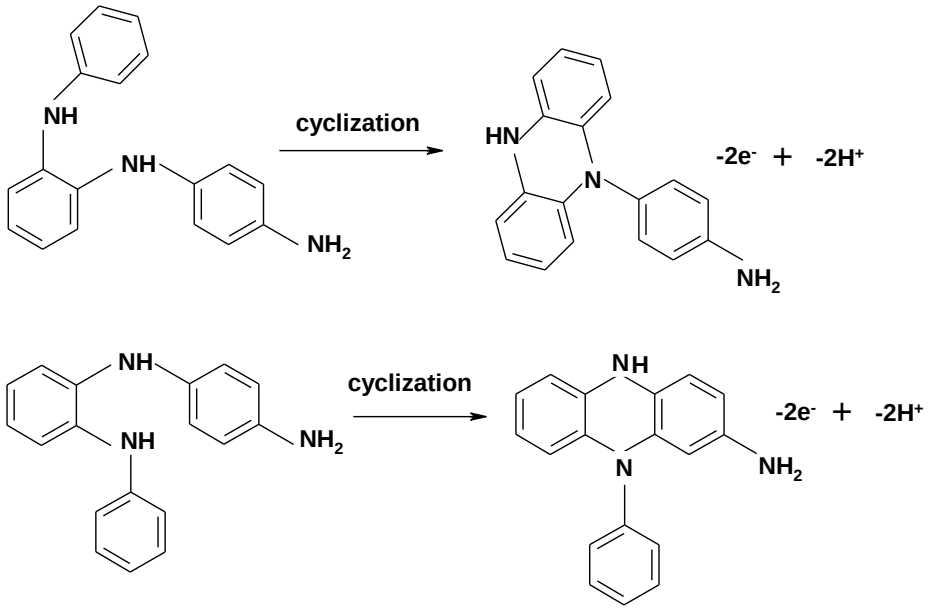

Figure 13. Formation of phenazine-like cycles (Ćirić-Marjanović *et al.* 2006).

The trimers can have different structures. Some of them during further oxidation can form the phenazine cycles (Figure 13). The produced phenazine units, or their segments, may act as initiation centers for the growth of conventional PANI, subject to the condition that pH<2 and the intermediate pernigraniline unites become protonated. Once growth starts, the aniline constitutional units are linked in the *para*-position, due to the formation of the conducting conjugating system represented by protonated pernigraniline (Figure 8). The propagation proceeds with the preference over initiation of PANI chains. The resulting chains are thus having a phenazine head segment and a tail of *para*-linked aniline constitutional units (Figure 8).

3.1.3. Oxidation in the alkaline media

The oxidation of aniline in alkaline media proceeds when pH>7. Under such acidity conditions all kinds of amino groups (the aniline monomer, the terminal amino groups in oligomers and the secondary amino groups) are not protonated. The pH and temperature dependences are shown in (Figure 14).

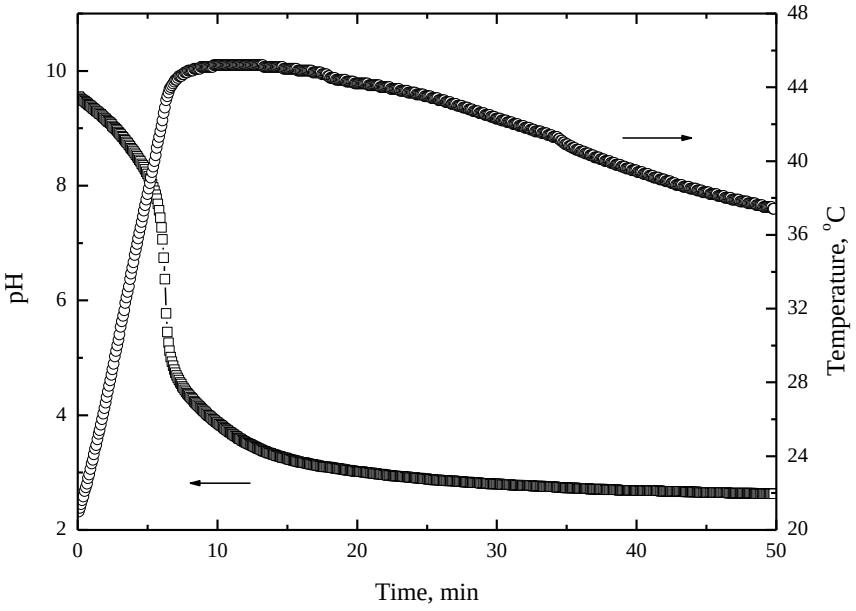

Figure 14. The pH and temperature dependences of the aniline oxidation.

The oxidation starts at pH 10 and pH decreases due to the generation of protons. The exothermic oxidation starts immediately after mixing of reactants, without any induction period and proceeds with a high rate. Temperature monotonously increases during the whole oxidation process and cools only after one of the reactant or both become depleted.

The slow-down of the reaction is observed at later stages (Liu *et al.* 2006). The protons produced in the oxidation reduce pH to 4. The reaction terminates by the depletion of neutral aniline molecules that have reacted or became converted to anilinium cations. The pH does not reach the acidity needed for the protonation of imine groups in pernigraniline, *i.e.* for the polymer growth (Stejskal *et al.* 2008).

The molecular mechanism of oxidation at pH>4 can be proposed as follows. Under the conditions when all kinds of amino groups are not protonated, the monomer and terminal primary amino groups of oligomers have a low ionization potential and are easily oxidized (Gospodinova *et al.* 1998, Ćirić-Marjanović *et al.* 2006). The attack is oriented to *ortho*- and *para*-positions of benzenoid ring, which is given by the electron-withdrawing effect of its substituent, amino group (Zimmermann *et al.* 1998). The

ability of an aniline dimer and oligomers to be oxidized is higher compared with the aniline monomer alone due to the better delocalization of the positive charge of the reaction centre on longer molecules (Gospodinova *et al.* 1993). That is why the oxidant oxidizes oligomers with a higher probability than monomer (Ćirić-Marjanović *et al.* 2008a).

The intramolecular cyclization of *ortho*-coupled units and intermolecular cyclization involving *para*-linked units and aniline monomer are the parallel reactions. Phenazine cycles are produced in the oligomers. The reaction of aniline addition, *i.e.* the oligomer growth, proceeds, too. There is no marked difference in the energy of the subsequent addition and cyclization; that is why the average degree of oligomerization is 20–30 constitutional units (Trchová *et al.* 2006).

The oligomers are non-conducting, having mixed *ortho*- and *para*-coupled units. Due to the irregular molecular structure of oligomer chains, there is no conjugated system produced that would results in the charge delocalization and consequent conductivity. The material is brown, absorbing the light in the range below 600 nm. The absorption bands typical of phenazine structures are present in the FTIR and Raman spectra (Trchová *et al.* 2006, Ćirić-Marjanović *et al.* 2008b).

3.2. The formation of nanotubes

The oxidation of aniline in acidic aqueous media yields conducting polymers in various forms, such as insoluble precipitates, nanofilms deposited on template surfaces, or as colloidal dispersions in aqueous or organic media. At the same time, PANI particles exist in a variety of forms: nanogranules (MacDiarmid *et al.* 2001, Stejskal *et al.* 2002a), nanowires (Zhang *et al.* 2004, Li *et al.* 2006, Zhang *et al.* 2006b), nanotubes (Zhang *et al.* 2005, Stejskal *et al.* 2006, Zhang *et al.* 2007), nanorods (Zhang *et al.* 2003), nanosheets and microspheres (Wang *et al.* 2005, Venancio *et al.*2006). The mechanism of the formation is somewhat different for each structure. It has been proposed that the acidity of the reaction medium is the key factor controlling the oxidation of aniline (Venancio *et al.* 2006, Konyushenko *et al.* 2006a, Stejskal *et al.* 2006) and the water-born oligomers self-assemble into the supramolecular structures that serve as a template for the nanotubular growth of polymer (Trchová *et al.* 2006).

Polyaniline nanotubes represent probably the most interesting PANI structure. To understand the mechanism of their formation, we have investigated the genesis of such nanotubular structures (Stejskal *et al.* 2006, Trchová *et al.* 2006). During the

oxidation of aniline beginning in neutral media, we have observed the evolution of the water-insoluble products of the reaction. The silicon windows were placed into the reaction mixture and removed at various stages of aniline oxidation (Figure 15).

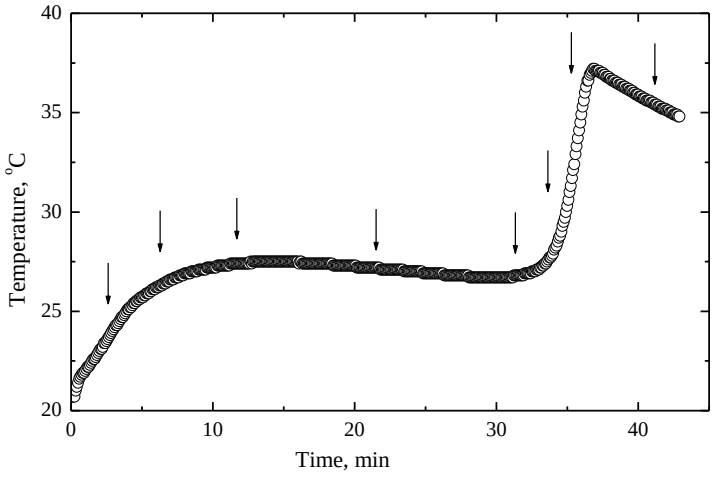

Figure 15. Change in temperature during the oxidation of aniline by ammonium peroxydisulfate. The times of samples collection are marked by arrows.

The aniline oligomers produced in the early stages of the oxidation are insoluble in the reaction medium; the solubility of aniline dimers, semidines, is low. The oxidation products, deposited on the windows, have been studied by optical microscopy (Figure 16). There is a link between the course of the polymerization and the supramolecular morphology produced at various times. The product obtained in the first stage of aniline oxidation, after 2–8 min, are composed mostly of crystals, which are obviously insoluble in water, having the size of several micrometers (Figure 16A). The crystals grow to trees (dendrimers) with branches of tens of micrometers in length. On the window removed at 21 min (Figure 16B), we observed, in addition to the granular precipitate, the first nanotubes. After 31 min (Figure 16C), nanotubes are well visible.

The nanotubes extend often to a few micrometers, their external diameter being ca. 200 nm and internal diameter of the cavity ca. 20–40 nm. The granular PANI precipitate is produced close to the end of polymerization (Figure 16D). As it sediments, it covers the nanotubular structure deposited on the silicon windows. This precipitate virtually always accompanies the nanotubes (Figure 17).

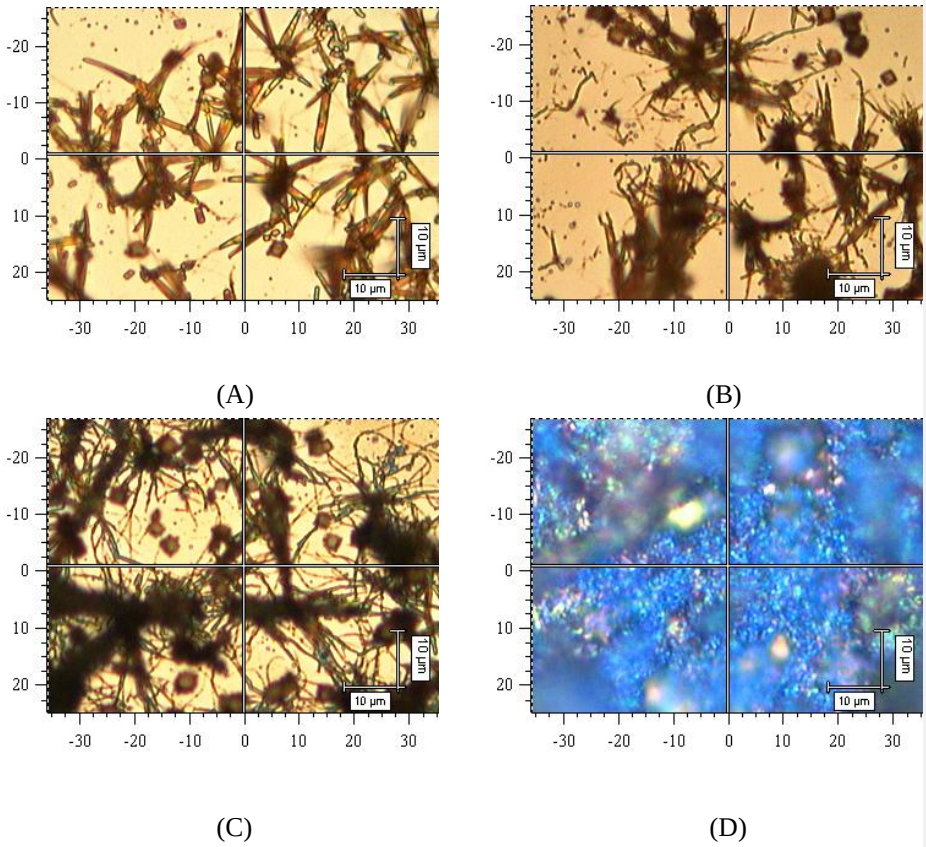

Figure 16. Optical microscopy of the oxidation products deposited on silicon windows after reaction times t = (A) 5, (B) 21, (C) 31, and (D) 38 min (Stejskal *et al.* 2006).

The presence of nanotubes is confirmed by transmission electron microscopy (Figure 17), which shows the internal cavity of the nanotubes in the final precipitated product of polymerization. Nanorods of the similar morphology, but without a cavity, have also been detected in the samples (Figure 17).

The scanning electron microscopy images (Figure 18) show the complex structure of nanotubes. The internal cavity in broken nanotube is easily visible (Figure 18B). The typical outer diameter of nanotubes is 100–200 nm, the inner diameter is 0–100 nm.

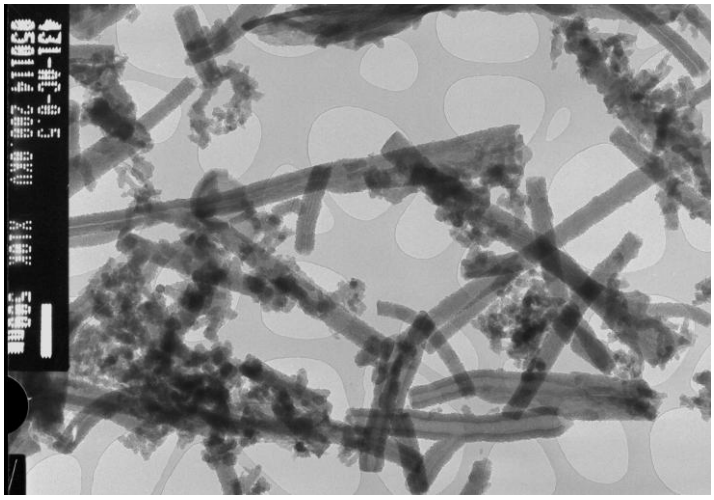

Figure 17**.** TEM micrograph of PANI nanotubes and related structures (Stejskal *et al.* 2006).

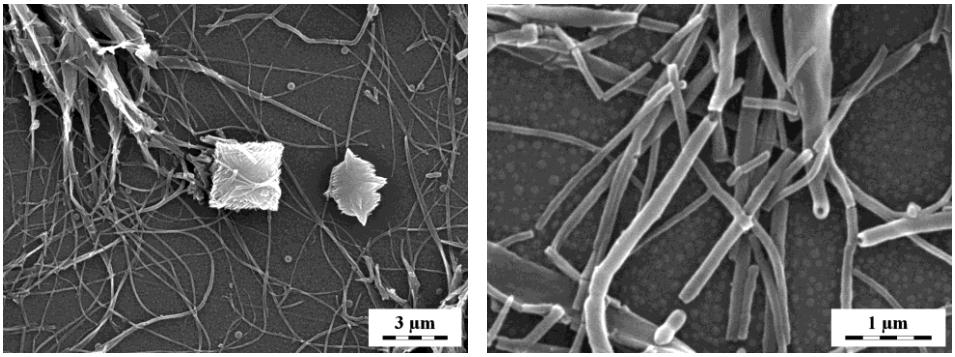

A B

Figure 18. Polyaniline nanotubes produced on silicon windows after the reaction time t = 31 min. Two magnifications (A, B) (Stejskal *et al.* 2006).

3.2.1. The nucleation of nanotubes

The aniline oligomers produced in the early stages of the oxidation are insoluble in the reaction medium. Oligomers precipitate, often with frequent needle-like crystallite off-springs (Figure 16A). These crystallites serve as the templates for the future nucleation of PANI nanotubes.

When the acidity of the reaction mixture becomes sufficiently high, the phenazine units may initiate the propagation of polymer chains. Due to their flat structure, shuch hydrophobic units absorb on the available surfaces (Stejskal *et al.*

2005). The absorption of phenazine units at the surface of needle-like oligomer off-springs is selective, due to the obvious anisotropy of the crystallites. We assume that the phenazine units are absorbed on the walls of the oligomer crystallites, leaving the front surfaces uncoated. In this way, the nucleus of the nanotubes is produced as a sleeve on an oligomer needle (Stejskal *et al.* 2006, Trchová *et al.* 2006). The size of the crystallites determines the inner diameter of the future nanotube. The thickness of the nanotube wall corresponds to the thickness of the deposited PANI film and is proportional to the molecular weight of the PANI chains. The front surface of this nanotubular nucleus has exposed phenazine units adjacent to the crystallite front.

3.2.2. The growth of the nanotube

The process of the formation of supramolecular structure reflects the simultaneously proceeding chemical reactions. Similarly like in the molecular reactions, there are two subsequent stages in morphology development: the nucleation period and the growth of polymer structure.

The phenazine structures have a flat molecular structure. They have tendency to self-assembling to regular one-dimensional columns, stacks (Figure 19) and the associates based on the π–π interactions (Sun *et al.* 2005, Kokunov *et al.* 2004, Crispin *et al.* 2004).

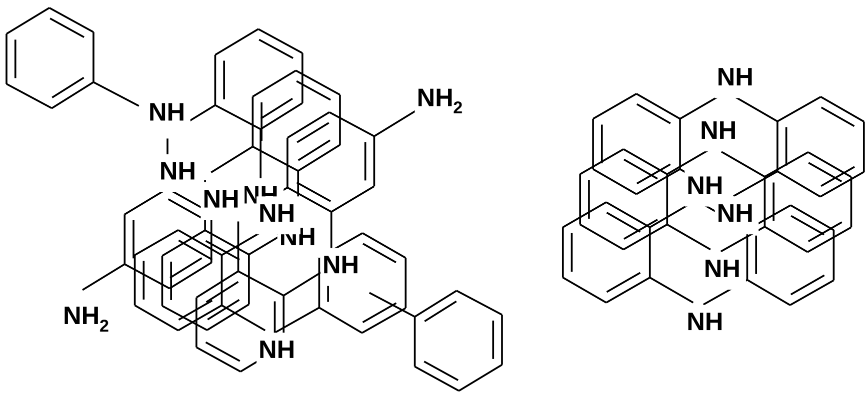

Figure 19. The phenazines and *N*-phenylphenazines can form stacks of oligomers.

The random agglomeration of phenazine units in the solutions leads to the formation of precipitate. On the other hand, the sorption of oligomers on the surface immersed in the reaction mixture give rise to thin films during the subsequent polymerization. The type of organization of phenazine cycles on the template surface or

in the volume of the reaction mixture predetermines the future morphology of the supramolecular polymer growth. Depending on the reaction conditions and nature of the template, the sorption or agglomeration of phenazines may be random or organized. The PANI chains are growing from them in the preferred direction given by molecular geometry. The assembly of the terminal phenazine units thus binds the PANI chain-starts together. The self-ordering produced is further stabilized during the chain growth of PANI counterparts by hydrogen bonding and ionic interactions (Figure 20). That is why the nanotube continues to grow without any guide and with an internal cavity determined by nucleus size. This concept can be supported by the observation of nanotubular growth in polycarbonate membranes, which continue to grow beyond the membrane limits, still preserving the nanotubular morphology (Tagowska *et al.* 2004).

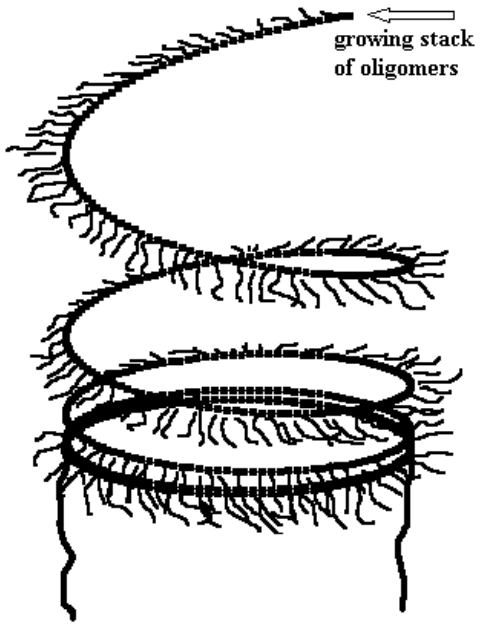

Figure 20. The phenazine units at the start of PANI chains stack on each other, and PANI chains extend from them as they grow during the polymerization. The individual spiral threads are shown as being separated just for the clarity of illustration; we believe, however, that each thread closely copies the previous one and there is no separation between them (Stejskal *et al.* 2006).

The growth of one-dimensional structures can also be initiated without any template. In this case, we assume that phenazine terminal units associate with each other more loosely. Stacks of one-dimensional fibrils of phenosafranines (including

phenazine structures) of 1 nm diameter, which corresponds approximately to the size of a phenazine heterocycle (Saez *et al.* 1993), have been reported in the literature (Komura *et al.* 2000). Polyaniline chains extending from them produce a brush. A nanorod without an internal cavity results instead of a nanotube. Such nanorods are observed to accompany the nanotubes (Figure 17), and their mutual proportions are likely to be the pH-dependent.

The pH of the reaction plays the crucial role in the formation of nanotubes. We have found that the nature of the acids controls not only the acidity of the reaction but also the surface morphology of the nanotubes (Figure 21).

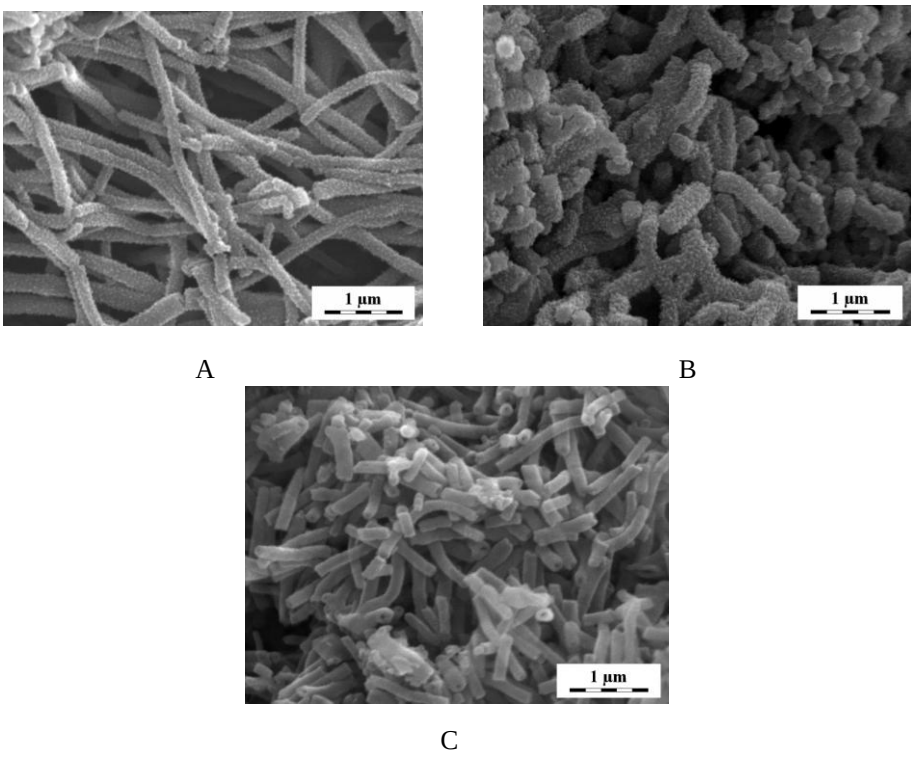

Figure 21. The polyaniline nanotubes prepared in 0.4 M succinic acid (A), 0.1 M picric acid (B), and 0.4 M acetic acid (C).

3.3. The formation of nanogranules

Granular morphology is the most typical for PANI prepared in a classical way in the acidic aqueous media (Stejskal *et al.* 2002a, Konyushenko *et al.* 2006a) (Figure 22). Polyaniline nanogranules have a size of tens to a few hundreds of nm. The mechanism of their formation has not been analyzed in the literature. We assume that the globules

are produced as a result of random association of phenazine nucleates. Such association takes place when the concentration of nucleates is high, the solubility of nucleates is reduced and the polymer chain starts to grow before the phenazine structures are organized.

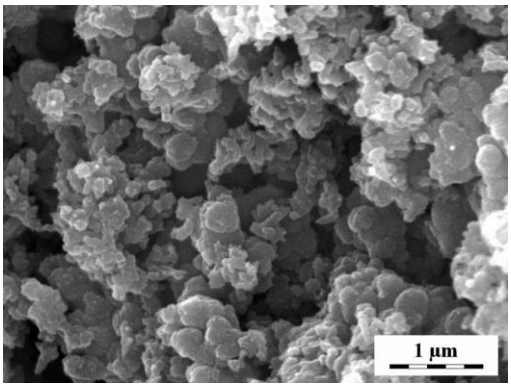

Figure 22. The granular morphology of polyaniline prepared in the presence of 0.1 M sulfuric acid (Konyushenko *et al.* 2006a).

3.4. The formation of microspheres

The formation of microspheres, which is observed in the oxidation of aniline (Wang *et al.* 2005, Venancio *et al.* 2006, Stejskal *et al.* 2008) or aniline derivatives (Han *et al.* 2006) at low acidity and at alkaline conditions, has another background. The neutral aniline is not always completely miscible with aqueous medium and constitutes a separate phase. The oxidation then proceeds at the interface between aniline droplets and liquid phase containing the oxidant. The non-conducting aniline oligomers form microspheres having a diameter of a few micrometres (Figure 23).

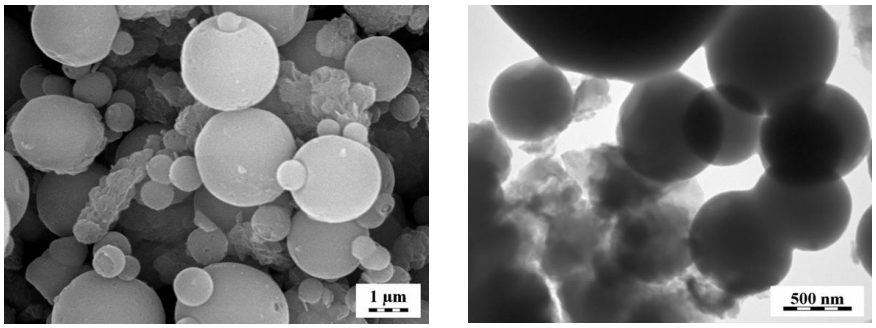

Figure 23. SEM (left) and TEM (right) images of microspheres which are formed during the oxidation of aniline in 0.2 M ammonium hydroxide.

The oxidation of aniline by the oligomerization mechanism takes place at the droplet interface. The droplet surface becomes coated with a non-conducting oligomer. Aniline diffuses through the interface and the thickness of the oligomer layer increases. The synthesis on the surface of the droplets is similar to the oxidation at the interface water-organic liquid, where aniline itself takes a role of an inorganic liquid.

Polyaniline microspheres may be hollow or compact (Hang *et al.* 2007, Stejskal *et al.* 2008, Venancio *et al.* 2006). In the latter case, the interior of this sphere is filled with aniline or with aniline oligomers or with both. The hollow sheres have an opening as a rule (Venancio *et al.* 2006, Zhang *et al.* 2003). The hole in the microsphere surface is caused the liquid aniline, which is expelled from the interior of the sphere. This takes place during the synthesis, *e.g.* during the thermal expansion in the strongly exothermic oxidation, or during the processing of product, *e.g.*by drying at elevated temperature vacuum. The eruption of aniline during the exothermic polymerization is demonstrated by the formation of a tail of subsequently produced oligomers (Figure 23 left). Similar morphologies have also been reported in the literature (Venancio *et al.* 2006).

3.5. The polymerization in ice and the formation of nanowires

It was observed that the oxidative polymerization of aniline proceeded well not only in the liquid mixture (20 ^{o}C or –5 ^{o}C) but also at sub-zero temperatures, when the reaction mixture becomes frozen. The polymerization carried out at reduced temperature yielded PANI with a higher molecular weight (Adams *et al.* 1996) and degree of crystallinity, although the improvement of conductivity was marginal (Stejskal *et al.* 1998). The higher molecular weight is a benefit when the mechanical properties of PANI are important, *e.g.*, when the solutions of PANI base in *N*-methylpyrrolidone are used to cast PANI membranes (Kocherginsky *et al.* 2005) or spun to produce PANI fibres (Pomfret *et al.* 2000) or nanofibres (Kameoka *et al.* 2003).

At –24 ^{o}C, in ice, the process takes place in the solid state; the reaction is slower, yet still feasible. The originally white ice becomes gradually dark green. The morphology of PANI is different from the polymerizations made in the liquid media. Polyaniline is constituted by particles of submicrometre size, mutually connected by nanofibres of *ca* 20 nm thickness (Figure 24).

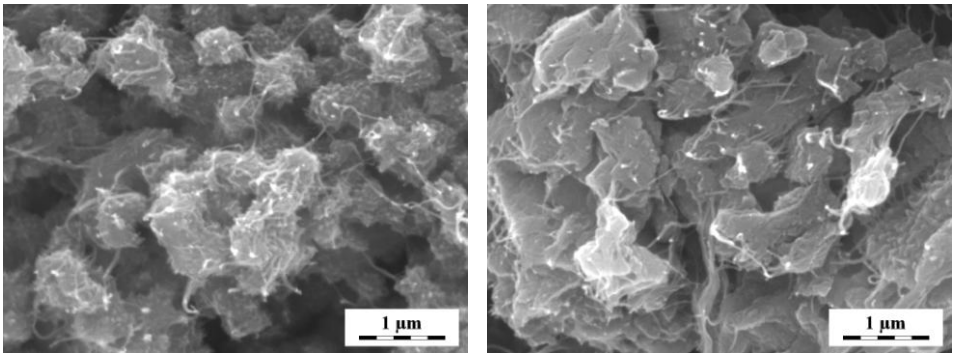

Figure 24. Polyaniline prepared in frozen mixture of 0.1 M H_2SO_4 (left) and 0.4 M acetic acid (right).

Kocherginsky *et al.* (Kocherginsky *et al.* 2005, Kocherginsky *et al.* 2006) have investigated redox processes occuring at PANI membranes. They have shown that the molecule the reductant and the oxidant can react and exchange electrons without being in a direct contact, when separated by a conducting PANI membrane. This concept was extended to the polymerization of aniline (Blinova *et al.* 2007). Solutions of aniline hydrochloride and ammonium peroxydisulfate, separated by a PANI membrane, react to yield PANI by exchanging the electrons through the conducting polymer. Polyaniline was produced entirely on aniline side of the membrane.

The concept outlined above explains why the polymerization also takes place in a frozen aqueous media, in ice. Once the first traces of PANI have been formed, the molecules of aniline and peroxydisulfate produce further PANI by transferring the electrons through the mass of existing PANI (Figure 25).

The abstraction of two electrons is needed for the formation of a chemical bond between the aniline and growing PANI chain. These are accepted by the oxidant molecule, peroxydisulfate, which is reduced to sulfate. The electrons travel through the conducting PANI phase from the locus of polymerization to the oxidant. Consequently, neither the aniline monomer nor the oxidant molecules need to diffuse to meet each other in order to react. As PANI grows by this mechanism, it gradually expands and penetrates the whole volume of the solidified reaction mixture. The resulting PANI structure thus has a connective character, and electrical contact between its parts is maintained.

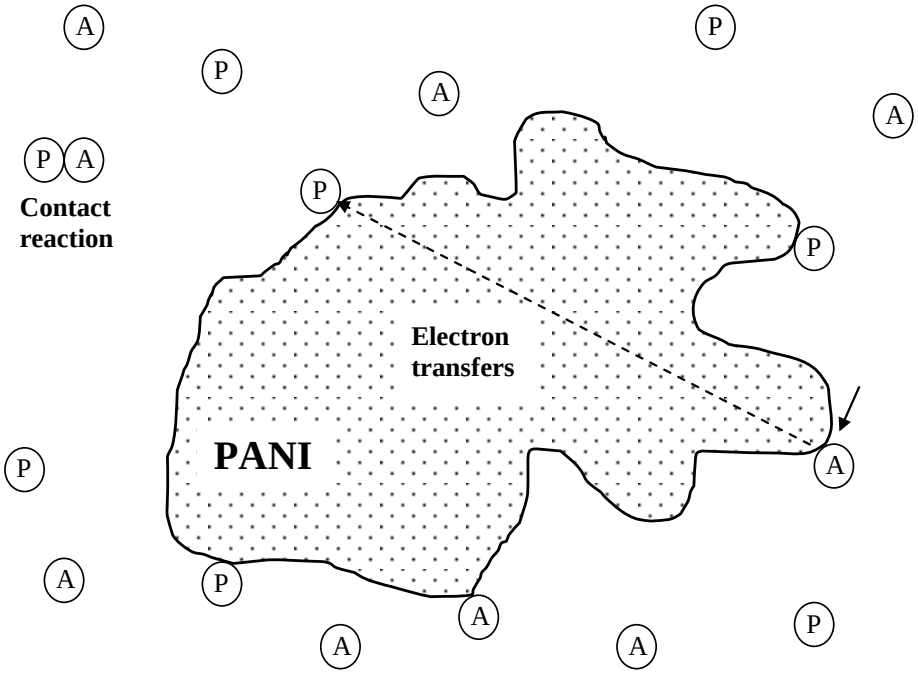

Figure 25. The mechanism of the aniline polymerization in the solid state (Konyushenko *et al.* 2008b).

4. Multi-wall carbon nanotubes coated by polyaniline

Carbon in various forms is an inert material in many aggressive media, it has good thermal stability, and good electrical conductivity. Carbon is a material of a choice as a catalyst support or as electrodes in batteries, supercapacitors, and fuel cells. Multi-wall carbon nanotubes (CNT) are one of the most studies allotropic forms of carbon. The high degree of organization and high aspect ratio are responsible for their unique electric, magnetic, and mechanical properties.

Carbon nanotubes prepared by the chemical-vapour deposition method often include metal nanoparticles, which serve as catalytic centers for the nanotubular growth during CNT preparation. The ferromagnetic metals (Fe, Co and Ni) and their alloys are used as catalysts and their nanoparticles are incorporated into CNT. The residual catalyst is removed as a rule, by dissolution in strong acids, leaving pure CNT. On the other hand, if left in CNT, the presence of ferromagnetic metals results in magnetically functionalized CNT.

4.1. The coating of carbon nanotubes

Multi-wall carbon nanotubes (CNT) have been coated with a conducting polymer, PANI, directly during the oxidation of aniline in ethanol (50 vol%)–water mixture. The content of CNTs in the samples was 0–80 wt%. The monomer and then the oxidant solutions were added to various portions of CNT to start the polymerization of aniline. Composites containing more than 80 wt% CNT could not be prepared in this way because the volume of the reaction mixture was too low to accommodate all the CNT.

The oxidation of aniline is an exothermic reaction and its course is easily monitored by recording the reaction temperature (Figure 26) (Stejskal *et al.* 2002). A solution of aniline hydrochloride in ethanol containing CNT has been mixed with an aqueous solution of the oxidant. After an induction period, the increase in the temperature is associated with the exothermic polymerization of aniline.

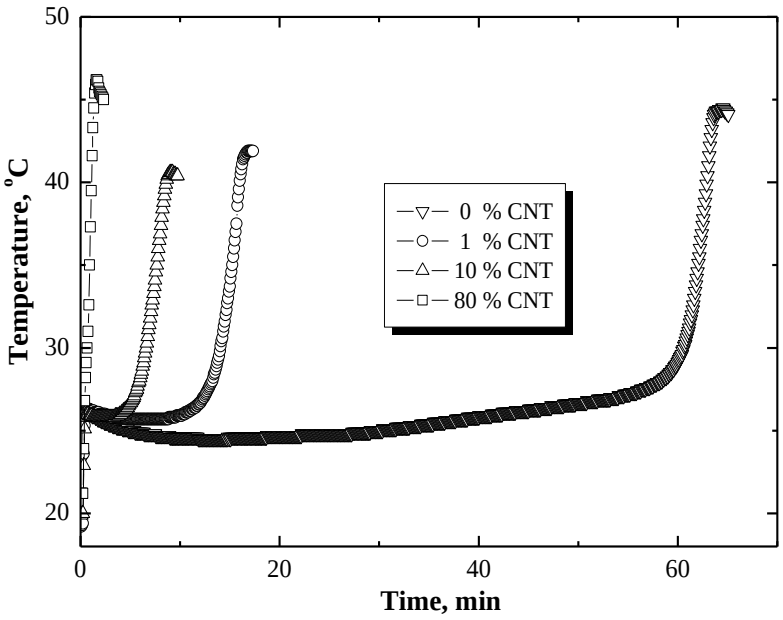

Figure 26. The course of aniline polymerization in the presence of CNT. The compositions are given in wt.% of CNT in the composite (Konyushenko *et al.* 2006b).

The presence of CNT in the reaction mixture significantly accelerates the rate of aniline oxidation. Even 1 wt% of CNT (relative to aniline) reduces the reaction time from 64 min to 17 min by shortening the induction period. There are two possible explanations for the observed acceleration of oxidation. The first is based on the assumption of heterogeneous catalysis. The oligomeric aniline intermediates adsorbed at the substrate, having a large surface area, like silica gel, start the growth of PANI chains more readily than those in the liquid phase (Stejskal *et al.* 2003). The CNT have also a high surface area and that is why they could act in a similar manner. Philip *et al.* (Philip *et al.* 2005) proposed the principle of heterogeneous catalysis to be operative in the case of CNT; the oxidation of aniline gets faster at the surface of CNT, resulting in the core–shell morphology of the products, it can be see on the SEM and TEM micrographs (Figure 27).

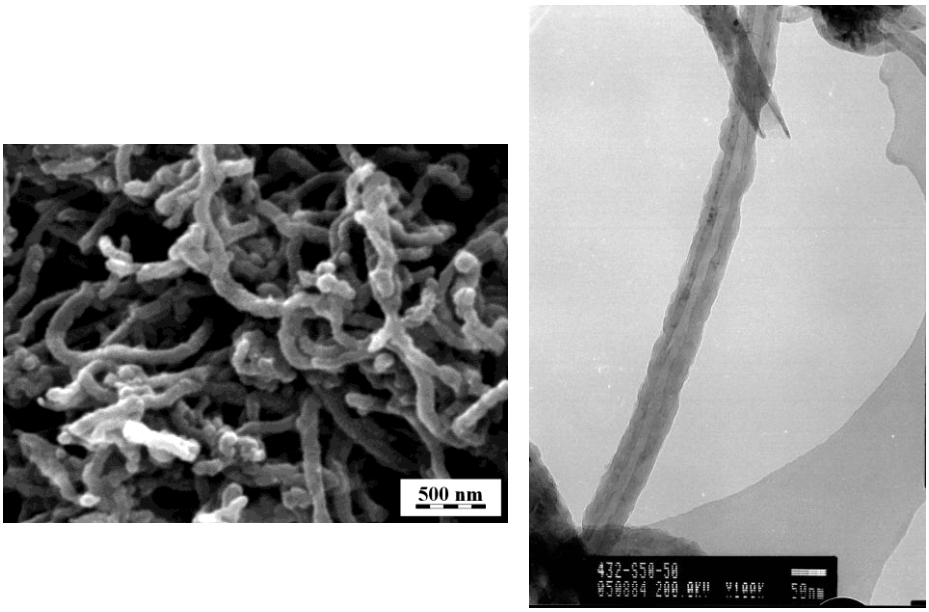

Figure 27. SEM (left) and TEM (right) images of CNT coated by PANI (Konyushenko *et al.* 2006b).

The second explanation is based on the fact that CNTs are conducting, *i.e.* they are able to transfer electrons. The oxidation of aniline is a typical redox reaction, in which the electrons are abstracted from aniline molecules and accepted by an oxidant, peroxydisulfate, which converts to sulfate (Figure 1). In a classical reaction concept, the molecules of aniline and oxidant are expected to meet, and consequently to react. It has recently been proposed that conducting materials can mediate the transfer of electrons (Kocherginsky *et al.* 2006); CNTs can obviously undertake such a role and transfer the electrons between the reductant and oxidant. This means, that the aniline molecule at the surface of CNT can exchange electrons, and thus convert to PANI, with any oxidant molecule that is also in contact with CNT, and not only with the oxidant in the close vicinity of the aniline molecule involved. This fact dramatically increases the probability for an aniline molecule to be oxidized to a PANI constitutional unit. The PANI chain growing at the CNTs surface is also conducting and thus participates in the electron transfer from the aniline unit that is being added to the PANI chain-end and CNTs.

Scanning electron microscopy (SEM) illustrates a uniform coating of CNTs with PANI (Figure 27). The coated CNTs become thicker as the amount of deposited PANI increases. The uniform deposition of PANI on the CNTs is similarly demonstrated by transmission electron microscopy (TEM), which shows the bilayered structure of coated CNTs (Figure 27). As the internal cavity is well discernible, we conclude that the coating with PANI takes place only at the outer surface of the CNTs (Konyushenko *et al.* 2006b). The conducting polymer is not covalently bonded to the carbon nanotubes. The aniline oligomers are absorbed (Stejskal *et al.* 2005) at the surface of CNT and starts the growth of PANI coating there.

4.2. Properties of the composite CNT/PANI

The conductivity of the composites is a characteristic of prime interest. It was measured by a four-point van der Pauw method on pellets compressed at 700 MPa. For non-conducting PANI bases, a two-point method was used. Before such measurements, circular gold electrodes were deposited on the both sides of the pellets. The dependence of conductivity on CNT content for CNT coated by PANI film is shown on the Figure 28. At low fractions of CNT, the conductivity is determined by the PANI as the main component (Figure 28).

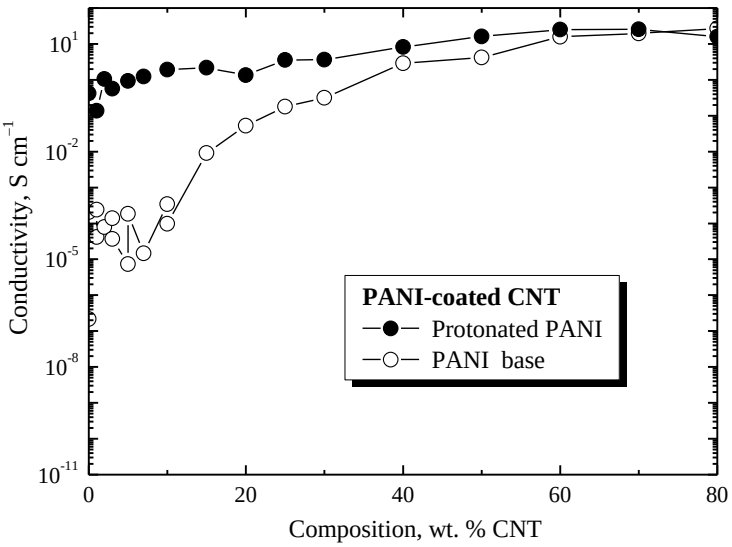

Figure 28. The conductivity of carbon nanotubes coated with protonated PANI (full circles) and PANI base (open circles) (Konyushenko *et al.* 2006b).

The increase in the conductivity of CNT coated with non-conducting PANI base with increasing content of CNT is slow, compared with the CNT coated by protonated conducting PANI. At low concentrations of CNT, the direct electrical contact between CNT is prevented by the surface coating with a non-conducting PANI base and the percolation threshold is practically not distinguishable. Yet, the coating with PANI base seems to reduce the contact resistance between CNT. The resulting conductivity of CNT coated with PANI base thus reaches 19.6 S cm^{-1} at 70 wt% CNT. The conductivity is thus comparable with that of the CNT coated with protonated PANI. We are obvious dealing with interfacial phenomena between the CNT separated with a thin coating of PANI. A non-conducting PANI base is not a true insulator, and it can probably mediate the charge-carrier transfer over short distances between the neighboring CNT, similarly to the protonated conducting form (Konyushenko *et al.* 2006b).

The contact angle of water on 'standard' PANI hydrochloride is 49 ° (Shishkanova *et al.* 2005). When PANI has been prepared in ethanol (50 vol %)–water mixtures, the contact angle was 43 °. The enhanced wettability is possibly due to the sulfonation of aromatic rings under these reaction conditions. The contact angles of CNTs coated with protonated PANI are about ~40° up to 60 wt% CNTs in the composite. The composite is thus hydrophilic and behaves as a neat PANI. This is not surprising considering the core–shell morphology of the composite (Figure 27). At higher contents of CNT, the contact angles could not be measured. The water droplet penetrated into the composite, possibly as a result of higher porosity. This means that the contact angle of neat CNTs could not be determined but we expect that, by analogy with graphite, they are more hydrophobic; the contact angle of water on graphite is 79 ° (Konyushenko *et al.* 2006b).

4.3. Coating carbon nanotubes containing the residual nickel catalyst nanoparticles

One type of the multi-wall carbon nanotubes was prepared by the decomposition of methane on nickel catalyst (Tomishko *et al.* 1999). Such CNT contain nickel particles; the metal particles having the size of tens of nanometers are well visible in transmition electron microscopy micrographs (Figure 29). Some of them are located outside the CNT, a part of them is integrated into CNT.

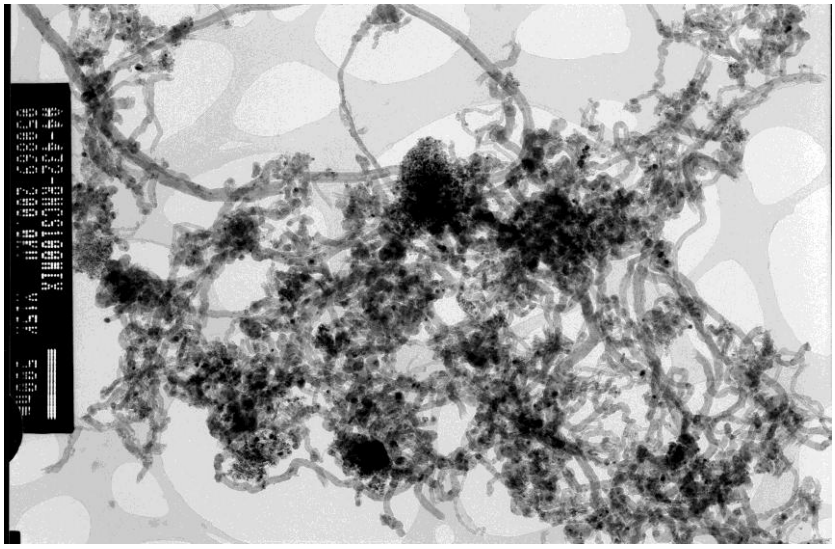

Figure 29. TEM micrograph of CNT containing nickel nanoparticels (Konyushenko *et al.* 2008a).

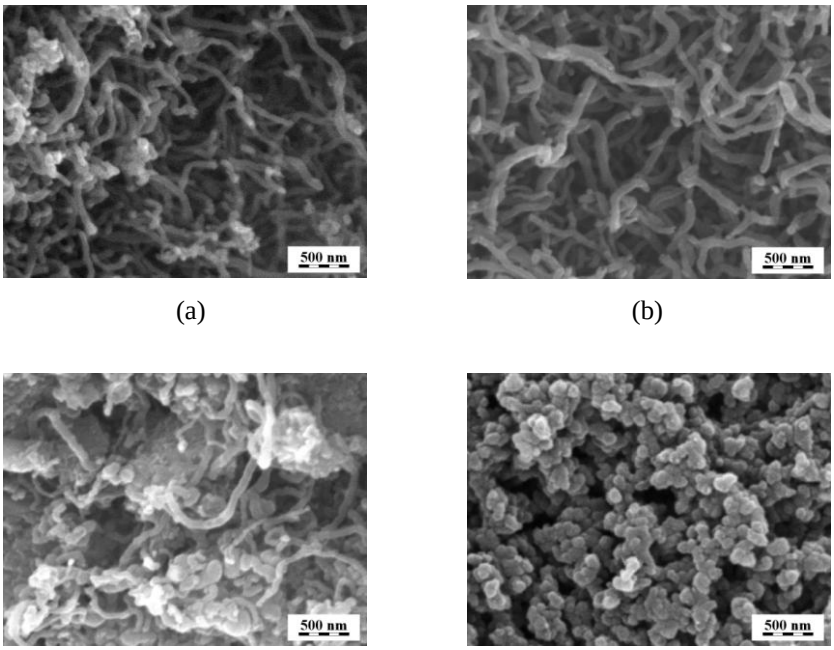

(a) (b)

(c) (d)

Figure 30. SEM micrographs of (a) original CNT, (b) those coated with 20 wt.% PANI and (c) 50 wt. % PANI, and (d) neat PANI (Konyushenko *et al.* 2008a).

Polyaniline coating was produced again by the oxidation of aniline hydrochloride dissolved in ethanol with an aqueous solution of ammonium peroxydisulfate. Polyaniline film grows on the surface of CNT producing a core-shell morphology for the samples containing majority of CNT (Figure 30).

The large diameter of the PANI-coated CNT compared with neat CNT is well visible. The thickness of the coating estimated by TEM was 20-30 nm. In the composite having comparable amount of components, 50 wt% PANI, the conducting polymer constitutes separate regions (Figure 30 c). The addition of ethanol to reaction mixture has been reported to change the common granular morphology of PANI to fibrillar (Kan *et al.* 2006). In the present study, however, the morphology of PANI prepared in ethanol (50 vol%)–water was strictly granular (Figure 30 d). The thermogravimetric analysis (TGA) demonstrates the presence of nickel as a residue, that the composites of PANI and CNT have been prepared (Figure 31).

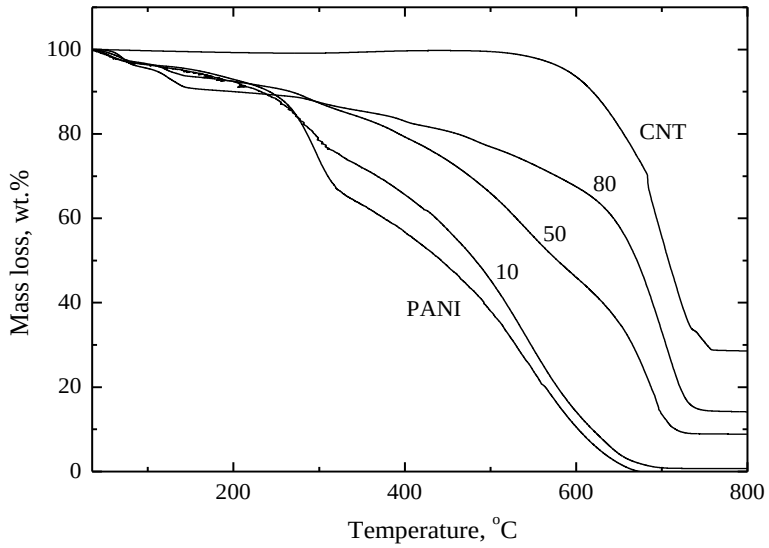

Figure 31. Thermogravimetric analysis of PANI-coated CNT. The content of CNT (wt.%) is given at the individual curves (Konyushenko *et al.* 2008a).

The typical features of PANI degradation are observed (Konyushenko *et al.* 2006b). The mass loss in temperature range below 200 °C reflects the deprotonation of PANI, the loss of its acid, and humidity. The decomposition of PANI starts above 300 °C. We can see an improvement of PANI stability with increasing content of CNT in the composite. CNT destruction begins above 550 °C. CNT with a removed catalyst

leave after exposure to 800 ^{o}C a residue less than 1 wt% (Konyushenko *et al.* 2006b). In the present case, the residue is 28.5 wt% and can be attributed to the nickel catalyst and/or its oxidation products.

The conductivity of PANI-coated CNT practically does not depend on the content of CNT in the composite (Figure 32). The conductivity of PANI, 1.0 S cm^{-1}, is lower that in the case of 'standard' PANI (Stejskal *et al.* 2002b), 4.4 S cm^{-1}, because the preparation took place in ethanol-water mixture instead of water. An unpronounced increase in the conductivity to 1–2 S cm^{-1} is marginal and suggests that the CNT are slightly more conducting than PANI. The PANI glues and decreases the contact resistance between individual CNT (Cochet M 2001). A possible small decrease in conductivity at high CNT contents may be interpreted as being caused by the increasing contact resistance, due to the insufficient availability of PANI in the interstitial space (Konyushenko *et al.* 2008a).

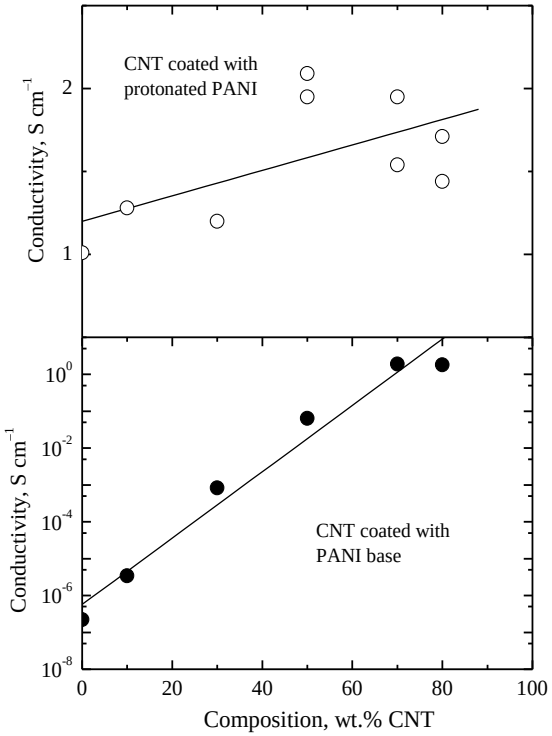

Figure 32. The dependence of conductivity of CNT coated with protonated PANI (top) and with PANI base (bottom) for composites having various CNT content (Konyushenko *et al.* 2008a).

The conversion of protonated PANI coating to a non-conducting PANI base reduces the conductivity down to 10^{-7} S cm^{-1} at low CNT contents (Figure 32). The conductivity increases with increasing CNT content, without any percolation transition.

The mechanical integrity of compressed samples was poor, considerably lower compared with analogous CNT that have not contained the residual catalyst (Konyushenko *et al.* 2006b). The attempts to test the thermal stability of composites (Prokeš *et al.* 2004) at 175 ^{o}C have failed because the electrical contact with the samples has been lost even before reaching the working temperature.

4.3.1. Density and wettability

The specific mass of neat CNT is 0.5 g cm^{-3}, the density determined by helium pycnomentr was 2.36 g cm^{-3} (Tomishko *et al.* 1999). The densities of PANI-coated CNT have been measured by the Archimedes method on compressed pellets and they have an apparent character reflecting their porosity. The density of composites increases with increasing content of CNT (Figure 33), and its value extrapolated for neat CNT is 1.72 g cm^{-3}.

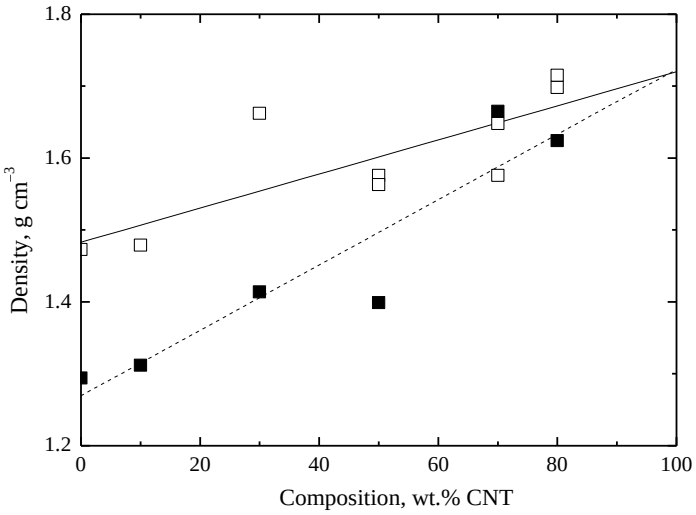

Figure 33. Density of CNT coated with protonated PANI (open squares) or with PANI base (full squares) (Konyushenko *et al.* 2008a).

The composites thus contain voids and are likely to have a good permeability for vapours and gases. This is important for the applications in the fuel-cell electrodes and sensors.

Water contact angle could be measured only at 0–30 wt% CNT in the samples and was 42 °, close to the value of 49 ° reported for bulk PANI hydrochloride (Shishkanova *et al.* 2005). At higher content of CNT, water droplet placed on the pellet penetrated the sample, and contact angle could not be determined. This implies that PANI-coated CNT are hydrophilic (Konyushenko *et al.* 2006b) and, similarly like density results, suggest the porous structure of the composites.

4.3.2. Complex permeability and magnetic hysteresis

Magnetic spectra frequency of complex permeability, $\mu^*(f)$, of PANI–CNT composites with different ratio of PANI and CNT are presented in Figure 34.

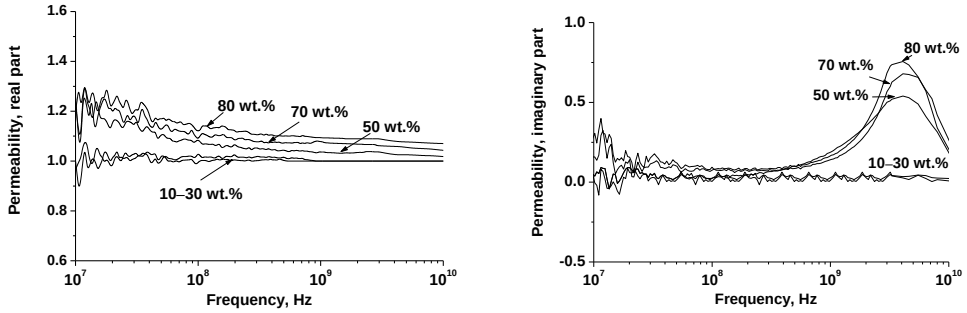

Figure 34. The frequency dependence of real (left) and imaginary (right) parts of complex permeability of CNT coated with protonated conducting PANI. The content of CNT is given at the individual curves (Konyushenko *et al.* 2008a).

The composites with 10–40 wt% CNT do not exhibit any ferromagnetic properties; the real part of permeability, μ′, is around the unity and the magnetic losses, μ'', are close to zero in the frequency range from 1 MHz to the 10 GHz. The ferromagnetic behaviour of composites appears when the CNT content increases to 50 wt%, which approximately corresponds to 10 wt% of nickel. The character of $\mu^*(f)$ indicates that single-domain nickel nanoparticles (single-domain-size criterion for

nickel particles is 6–7 nm) in CNT are exchange-coupled (Vonsovskii *et al.* 1998, Bukhaev *et al.* 1998). This is revealed by magnetic dispersion and two resonance peaks on the $\mu''(f)$, the first located in low-frequency range, 1–10 MHz, and the second in high-frequency range, 1–3 GHz. By increasing CNT up to 80 wt% nickel content increases, and thus enhances both permeability components in specified frequency regions.

The dynamic magnetic behaviour of PANI-CNT composites is in a good agreement with magnetostatic measurements of nickel-incorporating CNT powders. It is a ferromagnetic material with saturation magnetization M_s=0.5 emu g^{-1} (Figure 35) and low remanent magnetization M_r=0.035 emu g^{-1}.

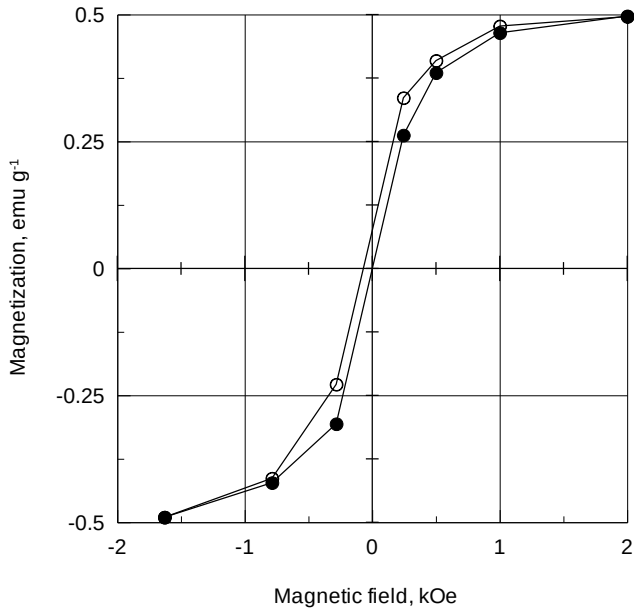

Figure 35. Magnetic hysteresis loop of neat CNT containing nickel nanoparticles (full circles – forward trace, open circles – reverse trace) (Konyushenko *et al.* 2008a).

By comparison with few tens oersted coercivities of bulk nickel, the coercivity H_c=35 Oe was observed in CNT (Figure 35). Such high coercivity of nickel-incorporating CNT can be explained by the high value of the effective anisotropy in one-dimensional exchange-coupled system formed by nickel nanoparticles encapsulated in thin carbon shells (Figure 29) (Iskhakov *et al.* 2003, Komagortsev *et al.* 2005).

Consequently, the ferromagnetism of CNT containing nickel nanoparticles has two reasons: (1) the carbon shell protects nickel from oxidation, and (2) the large shape anisotropies and inner diameter of CNT give rise to single-domain one-dimensional system. Two types of particle interactions, *viz.* magnetic–dipole and exchange interactions, are operative (Iskhakov *et al.* 2003). The cooperative effects lead to the increase in the internal magnetic field that acts on each particle. Taking into account a few works that provide evidence that in some carbon structure, *e.g.* fullerene encapsulated nickel nanoparticels (Lee *et al.* 2002) or CNT produced by arc-discharge method (Kotosonov *et al.* 2002), and under special treatment of graphitic structure (Esquinazi *et al.* 2003), the unusual magnetic properties of CNT maybe due to the enhanced interaction between ferromagnetic nanoparticles under the influence of electronic structure of graphene layers.

5. Conclusions

We have synthesized different morphologies of PANI under various conditions. Polyaniline nanotubes have been prepared in the solutions of weak organic acids. The nature of the acid has an influence on the surface morphology of the nanotubes. For example, when aniline is oxidized in the presence of acetic acid, the nanotubes have smooth surface, in the solutions of picric acid, the surface is rough. On the other hand, regardless of any acid, at the end of the polymerization PANI is protonated by the sulfuric acid, which is produced a by product. The nanotubes are produced even in the absence of any acid. This means that any kind of acids and their salts with aniline are not needed as templates for the polymerization of aniline. In our opinion, the self-assembly of aniline oligomers, rather than that of aniline monomers, predetermines the supramolecular structure of the final products. Polyaniline nanogranules are prepared when the aniline is oxidized in the solutions of strong acids and aniline microspheres can be formed when aniline is oxidized in the alkaline solutions. The decreasing of the polymerization temperature leads to the formation of nanowires.

We have demonstrated the course of aniline oxidation as reflected by the dependences of pH and temperature on time. The dependences are different for the oxidation at various acidities. It has been found that the aniline oxidation proceeds in two steps in the solutions of strong acids. The short induction period is observed at the beginning of the polymerization. During this period the phenazine structures are

formed. They act as nucleates for the further growing of the polymer chains. The second period is a very fast exothermic process, which corresponds to the formation of the PANI chains. When the oxidation starts in mild acidic conditions, in the solutions of weak organic acids, the pH and temperature dependences have three steps. The first step corresponds to the formation of phenazine structures. The pH is around 3. The second period is very slow. The pH decreases due to the formation of the sulfuric acid and the release of the protons from aniline molecules. When pH is less then 2, the third period is started. This is the fast formation of polymer chains, the process is exothermic. Another pH and temperature dependences have been observed when aniline is oligomerized in the alkaline media. The reaction starts with a fast increase of temperature and by decreasing pH. The phenazine structures are formed. The reactions stops at pH approximately 5; the acidity of the reaction mixture is not enough for the formation of polymer chains. That is why during the oxidation of aniline started in alkaline media only oligomers are obtained.

It is proposed that needle-like oligomer crystallites serve as template sites for the growth of nanotubes after they become coated with PANI. Nanotubular growth proceeds beyond the template nucleus, without any external guide. The terminal phenazine units self-assemble and guide the growth of PANI chains, thus producing a nanotube wall. Once the tubular growth has started, each thread of the produced spiral copies the previous one. Hydrogen bonding and ionic interactions between the neighbouring PANI chains stabilize the supramolecular nanotubular structure. The theoretical expectations were confirmed by FTIR spectra, optical microscopy, and gel permission chromatography.

We have synthesized composite materials of multi-wall carbon nanotubes with PANI under different reaction conditions. It has been chosen two types of carbon nanotubes: 1) pure carbon nanotube and carbon nanotubes containing nickel nanoparticles. The presence of CNT in the reaction mixture used for the oxidation of aniline dramatically increases the rate of PANI formation. Electron microscopy shows that CNT become coated with PANI during *in situ* polymerization of aniline. The coating is uniform and its thickness increases with increasing content of PANI in the composite.

It was shown that the thermal stability of PANI in the composites with CNT is better than the stability of neat PANI. The coating of CNT with protonated PANI

changes the originally hydrophobic surface to hydrophilic, the water contact angle for protonated PANI coating being 42 ^{o}.

We have observed that the conductivity of protonated CNT/PANI composites was 1–2 S cm^{-1}, regardless of the composition, 0–80 wt% CNT. Protonated PANI coating is converted to a non-conducting one by immersion in ammonium hydroxide solution and conductivity of composites can be reduced down to 10^{-7} S cm^{-1} at low CNT contents. The compositional dependence of conductivity does not exhibit the percolation behaviour.

It was found that the ferromagnetism of neat CNT and CNT-rich composites is due to the presence of incorporated nickel-catalyst nanoparticles inside the holes and defects of nanotubes. In spite of the fact that nickel nanoparticles are single-domain particles, they display cooperative magnetic properties, due to the formation of one-dimensional nanosystem, which manifest itself in the presence of frequency dispersion of complex permeability in broad frequency range.

References

(Adams *et al.* 1996) Adams P N, Laughlin P J, Monkman A P, *Synth Met* **76**:157 (1996).

(Bacon *et al.* 1968) Bacon J, Adams RN, *J Am Chem Soc* **90**:6596 (1968).

(Bao *et al.* 2002) Bao JC, Zhou QF, Hong JM, Xu Z, *Appl Phys Lett* **81**:4592 (2002).

(Barton *et al.* 1979) Barton D , Ollis BD, *Comprehensive Organic Chemistry*, I.O. Suntherland, Ed. **2**:151 (1979).

(Bejan *et al.* 1998) Bejan D, Duca A, *Croatica Chim Acta*, **71**:745 (1998).

(Blinova *et al.* 2007) Blinova NV, Stejskal J, Trchová M, Ćirić-Marjanović G, Sapurina I, *J Phys Chem B* **111**:2240 (2007).

(Bukhaev *et al.* 1998) Bukhaev AA, Ovchinnikov DV, Nurgazizov NI, Kukovitskii EF, Klaiber M, Weisendanger R, *J Phys Solid State* **40**:1163 (1998).

(Cao *et al.* 2001) Cao H, Tie C, Xu Z, Hong J, Sang H, *Appl Phys Lett* **78**:1592 (2001).

(Ćirić-Marjanović *et al.* 2006) Ćirić-Marjanović G, Trchová M, Stejskal J, *Collect Czech Chem Commun* **71**:1407 (2006).

(Ćirić-Marjanović *et al.* 2008a) Ćirić-Marjanović G, Trchová M, Stejskal J, *Int J Quantum Chem* **108**:318 (2008).

(Ćirić-Marjanović *et al.* 2008b) Ćirić-Marjanović G, Konyushenko EN, Trchová M, Stejskal J, *Synth Met* **158**:200 (2008).

(Cochet *et al.* 2001) Cochet M, Maser WK, Benito AM, Callejas MA, Martínez MT, Benoit J-M, Schreiber J, Chauvet O, *Chem Commun* 1450 (2001).

(CRC 1995) *CRC Handbook of Chemistry and Physics*, Lide DR, Frederikse HPR, Eds., 76th Ed., CRC Press, New York 1995; p. 8-49.

(Cram *et al.* 1964) Cram DJ, Hammond GS, *Organic Chemistry*, McGraw Hill, New York 1964, pp 210–211.

(Crispin *et al.* 2004) Crispin X, Cornil J, Friedlein R, Okudaira KK, Lemaur V, Grispin A, Kestemont G, Lehman M, Fahlman M, Lazzaroni R, Geerts Y, Wendin G, Ueno N, Bredas J-L , Salaneck WR, *J Am Chem Soc* **126**:11889 (2004).

(Damian *et al.* 2006) Damian A, Omanovic S, *J Power Sources* **158**:464 (2005).

(Deng *et al.* 2005) Deng MG, Yang BC, Hu YD, *J Mater Sci* **40**:5021 (2005).

(Dines *et al.* 2001) Dines TJ, MacGregor LD, Rochester CH, *Phys Chem Chem Phys* **13**:2676 (2001).

(Epstein *et al.* 1987) Epstein AJ, Ginder JM, Zuo F, *Synth Met* **18**:303 (1987).

(Esquinazi *et al.* 2003) Esquinazi P, Spemann D, Hohne R, Setzer A, Han K-H, Butz T, *Phys Rev Lett* **91**:227201 (2003).

(Focke *et al.* 1987) Focke WW, Wnek GE, Wei Y, *J Phys Chem* **91**:5813 (1987).

(Frackowiak *et al.* 2006) Frackowiak E, Khomenko V, Jurewicz K, Lota K, Beguin F, *J Power Sources* **153**:413 (2006).

(Fu *et al.* 1994) Fu Y, Elsenbaumer RL, *Chem Mater* **6**:671 (1994).

(Genies *et al.* 1990) Genies EM, Boyle A, Lapkowski M , Tsintavis C, *Synth Met* **36**:139 (1990).

(Gospodinova *et al.* 1993) Gospodinova N, Mokreva P, Terlemezyan L, *Polymer* **34**:2438 (1993).

(Gospodinova *et al.* 1994) Gospodinova N, Mokreva P, Terlemezyan L, *Polymer* **35**:3102 (1994).

(Gospodinova *et al.* 1998) Gospodinova N, Termlemezyan L, *Prog Polym Sci* **23**: 1443 (1998).

(Gupta *et al.* 2006) Gupta V, Miura N, *Electrochim Acta* **52**:1721 (2006).

(Hagiwara *et al.* 1987) Hagiwara T, Akiyama K, *Bunseki Kagaku* **36**:73 (1987).

(Han *et al.* 2006) Han J, Song G, Guo R, *Adv Mater* **18**:3140 (2006).

(Han *et al.* 2007) Han J, Song G, Guo R, *Eur Polym J* **43**:4229 (2007).

(Huang *et al.* 1999) Huang J, Wan M, *J Appl Polym Sci* **37**:1277 (1999).

(Iskhakov *et al.* 2003) Iskhakov RS, Komagortsev SV, Balaev AD, Okotrub AV, Kudashov AG, Kuznetsov VL, Butenko YuV, *JETP Lett* **78**:236 (2003).

(Kameoka *et al.* 2003) Kameoka J, Orth R, Yang YN, Czaplewski D, Mathers R, Coates GW, Craighead HG, *Nanotechnology* **14**:1124 (2003).

(Kan *et al.* 2006) Kan J, Zhang S, Jing G, *J Appl Polym Sci* **99**:1848 (2006).

(Kang *et al.* 1998) Kang ET, Neoh KG , Tan KL, *Prog Polym Sci* **23**:277 (1998).

(Kocherginsky *et al.* 2005) Kocherginsky NM, Lei W, Wang Z, *J Phys Chem A* **109**:4010 (2005).

(Kocherginsky *et al.* 2006) Kocherginsky NM, Wang Z, *Synth Met* **156**:558 (2006).

(Kokunov *et al.* 2004) Kokunov YV, Gorbunova YE, Khmelevskaya LV, *Russ J Inorg Chem* **49**:1498 (2004).

(Kolla *et al.* 2005) Kolla HS, Surwade SP, Zhang X, MacDiarmid AG, Manohar SK, *J Am Chem Soc* **127**:16770 (2005).

(Komagortsev *et al.* 2005) Komagortsev SV, Iskhakov RS, Denisova EA, Balaev AD, Myagkov VG, Bulina NV, Kudashov AG, Okotrub AV, *Tech Phys Lett* **31**:454 (2005).

(Komura *et al.* 2000) Komura T, Ishihara M, Yamaguchi T , Takachashi K, *J Electroanal Chem* **493**:84 (2000).

(Konyushenko *et al.* 2006a) Konyushenko EN, Stejskal J, Šeděnková I, Trchová M, Sapurina I, Cieslar M , Prokeš J, *Polym Int* **55**:31 (2006).

(Konyushenko *et al.*2006b) Konyushenko EN, Stejskal J, Trchová M, Hradil J, Kovářová J, Prokeš J, Cieslar M, Hwang J-Y, Chen K-H, Sapurina I, *Polymer* **47**:5715 (2006).

(Konyushenko *et al*, 2008a) Konyushenko EN, Kazantseva NE, Stejskal J, Trchová M, Kovářová J, Sapurina I, Tomishko MM, Demicheva OV, Prokeš J, *J Magn Magn Mater* **320**:231 (2008).

(Konyushenko *et al.* 2008b) Konyushenko EN, Stejskal J, Trchová M, Blinova NV, Holler P, *Synth Met*, submitted.

(Kotosonov *et al.* 2002) Kotosonov AS, Shilo DV, Moravsky AP, *Phys Solid State* **44**:666 (2002).

(Ledwith *et al.* 1974) Ledwith A , Sherrington DC, in *Reactivity, Mechanism and Structure in Polymer Chemistry*, Jenkins AD, Ledwith A, Eds., Chap. 12, pp 384–430, Wiley, London 1974.

(Lee *et al.* 2002) Lee GH, Hun SH, Jeong JW, Ri H-C, *J Magn Magn Mater* **246**:404 (2002).

(Li *et al.* 2005) Li XG, Duan W, Huang M-R, Rodriguez LNJ, *React Funct Polym* **62**:261 (2005).

(Li *et al.* 2006) Li D, Kaner RB, *J Am Chem Soc* **128**:968 (2006).

(Liu *et al.* 2006) Liu XX, Zhang L, Li Y-B, Bian L-J, Huo YQ, Su Z, *Polym Bull* **57**:825 (2006).

(MacDiarmid *et al.* 1985) MacDiarmid AG, Chiang JC, Halpern M, *Mol Cryst Liq Cryst* **121**:173 (1985).

(MacDiarmid *et al.* 2001) MacDiarmid AG, Jones EW Jr, Norris ID, Gao J, Johnson AT Jr, Pinto NJ, Hone J, Han B, KO F, Okuzaki H, Llangune M, *Synth Met* **119**:27 (2001).

(Madathil *et al.* 2004) Madathil R, Ponrathnam S, Byrne HJ, *Polymer* **45**:546 (2004).

(Malinauskas *et al.* 1998) Malinauskas A, Bron M, Holze R, *Synth Met* **92**: 127 (1998).

(Manohar *et al.* 1991) Manohar SK, MacDiarmid AG, Epstein AJ, *Synth Met* **41**:711 (1991).

(Mattoso *et al.* 1994) Mattoso LHC, MacDiarmid AG, Epstein AJ, *Synth Met* **68:**1 (1994).

(Mehl *et al.* 2003) Mehl T, Elefant D, Graff A, Kozhuharova R, Leonhardt A, Monch I, Ritshel M, Simon P, Graudeva-Zotova S, Schneider CM, *J Appl Phys* **93**:7894 (2003).

(Perrin *et al.* 1972) Perrin DD, *Dissociation Constants of Organic Bases in Aqueous Solution*, IUPAC Chem Data Ser: Suppl 1972. Butterworths, London 1972

(Philip *et al.* 2005) Philip B, Xie J, Abraham JK, Varadan VK, *Polym Bull* **53**:127 (2005).

(Pomfret *et al.* 2000) Pomfret SJ, Adams PN, Comfort NP, Monkman AP, *Polymer* **41**:2265 (2000).

(Pouget *et al.* 1991) Pouget JP, Jozefowicz ME, Epstein AJ, Tang X, MacDiarmid AG, *Macromolecules* **24**:779 (1991).

(Qiu *et al.* 2001a) Qiu H, Wan M, Matthews B, Dai L, *Macromolecules* **34**:675 (2001).

(Qiu *et al.* 2001b) Qiu H, Wan M, *J Polym Sci, Part A: Polym Chem* **39**:3485 (2001).

(Saez *et al.* 1993) Saez EI , Corn RM, *Electrochim Acta* **38**:1619 (1993).

(Šeděnková *et al.* 2007) Šeděnková I, Trchová M, Stejskal J, Bok J, *App Spectrosc* **61**:1153 (2007).

(Shishkanova *et al.* 2005) Shishkanova TV, Sapurina I, Stejskal J, Král V, Volf R, *Anal Chim Acta* **553**:160 (2005).

(Stejskal *et al.* 1993) Stejskal J, Kratochvil P, Radhakrishnan N, *Synth Met* **61**:225 (1993).

(Stejskal *et al.* 1995a) Stejskal J, Kratochvíl P, Špírková M, *Polymer* **36**:4135 (1995).

(Stejskal *et al.* 1995b) Stejskal J, Kratochvil P, Jenkins AD, *Collect Czech Chem Commun* **60**:1747 (1995).

(Stejskal *et al.* 1996) Stejskal J, Kratochvil P,, Jenkins AD, *Polymer* **37**: 367 (1996)

(Stejskal *et al.* 1998) Stejskal J, Riede A, Hlavatá D, Prokeš J, Helmstedt M, Holler P, *Synth **Met*** **96**:55 (1998).

(Stejskal *et al.*2002a) Stejskal J in *Dendrimers, Assemblies, Nanocomposites*, The MML Ser. Vol. 5, Arshady R , Guyot A, Ads, Chap. 6 and 7, pp. 195– 281, Citus Books, London 2002.

(Stejskal *et al.* 2002b) Stejskal J, Gilbert RG, *Pure Appl Chem* **74**:857 (2002).

(Stejskal *et al.* 2003) Stejskal J, Trchová M, Fedorova S, Sapurina I, *Langmuir* **19**:3018 (2003).

(Stejskal *et al.* 2004) Stejskal J , Sapurina I, *J Colloid Interface Sci* **274**:489 (2004).

(Stejskal *et al.* 2005) Stejskal J , Sapurina I, *Pure App Chem* **77**:815 (2005).

(Stejskal *et al.* 2006) Stejskal J, Sapurina I, Trchová M, Konyushenko EN, Holler P, *Polymer* **47**:8253 (2006).

(Stejskal *et al.* 2008) Stejskal J, Sapurina I, Trchová M, Konyushenko EN, *Macromolecules*, in press.

(Sun *et al.* 2005) Sun X, Dong S , Wang E, *Macromol Rapid Commun* **26**:1504 (2005).

(Tagowska *et al.* 2004) Tagowska M, Palys B, Jackowska K, *Synth Met* **142**:223 (2004).

(Tomishko *et al.* 1999) Tomishko M.M, Permyakov GN, Zezin MYu, Beskov VS, Mikhailova AV, Alekseev AM, Putilov AV, *Theor Found Chem Eng* **33**:370 (1999).

(Trchová *et al.* 2005) Trchová M, Šeděnková I, Stejskal J, *Synth Met* **154**:1 (2005).

(Trchová *et al.* 2006) Trchová M, Konyushenko EN, Stejskal J, Šeděnková I, Holler P , Ćirić-Marjanović G., *J Phys Chem B* **110**:9461 (2006).

(Venancio *et al.* 2006) Venancio EC, Wang P-C, MacDiarmid AG, *Synth Met* **156**:357 (2006).

(Viva *et al.*1999) Viva FA, Andrade EM, Molina FM, Florit MI, *J Electroanal Chem* **471**:180 (1999).

(Vonsovskii *et al.* 1998) Vonsovskii SV, *Magnetism*, Nauka, Moscow, 1971. Chapter 23, pp. 800–805.

(Wang *et al.* 2005) Wang X, Liu N, Yan X, Zhang W, Wei Y, *Chem Lett* **34**:42 (2005).

(Wei *et al.* 1987) Wei Y, Tang X, Sun Y, Focke WW, *J Polym Sci, Part A: Polym Chem* **27**:2385 (1989).

(Wei *et al.* 2001) Wei Y, *J Chem Educ* **78**:551(2001).

(Wu *et al.* 1997) Wu L-L, Luo J, Lin Z-H, *J Electroanal Chem* **417**:53 (1996).

(Zengin *et al.* 2007) Zengin H, Spencer HG, Zengin G, Gregory RV, *Synth Met* **157**:147 (2007).

(Zhang *et al.* 2003) Zhang Z, Wan M, *Synth Met* **132**:205 (2003).

(Zhang *et al.* 2004) Zhang X, Goux WJ, Manohar SK, *J Am Chem Soc* **126**:4502 (2004).

(Zhang *et al.* 2003) Zhang L , Wan M, *Adv Funct Mater* **13**:815 (2003).

(Zhang *et al.* 2005) Zhang Z, Wei Y, Zhang L, Wan M, *Acta Mater* **53**:1373 (2005).

(Zhang *et al.* 2006a) Zhang X, Kolla HS, Wang X, Raja K , Manohar SK, *Adv Funct Mater* **16**:1145 (2006).

(Zhang *et al.* 2006b) Zhang L, Wan M , Wei Y, *Macromol Rapid Commun* **27**:888 (2006).

(Zhang *et al.* 2007) Zhang LJ, Peng H, Hsu CF, Kilmartin PA, Travas-Sejdic J, *Nanotechnology* **18** :115607 (2007).

(Zimmermann *et al.* 1998) Zimmermann A, Kunzelmann U , Dunsch L, *Synth Met* **93**:17 (1998).

List of papers included in the Thesis:

1. **Konyushenko EN**, Stejskal J, Šeděnková I, Trchová M, Sapurina I, Cieslar M, Prokeš J,
Polyaniline nanotubes: conditions of formation,
POLYMER INTERNATIONAL 55: 31–39 (2006).
Times cited : 33 (21) IF: 1.475

2. Trchová M, Šeděnková I, **Konyushenko EN**, Stejskal J, Holler P, Ćirić-Marjanović G,
Evolution of polyaniline nanotubes: The oxidation of aniline in water,
JOURNAL OF PHYSICAL CHEMISTRY B 110: 9461–9468 (2006)
Times cited : 27 (17) IF: 4.115

3. **Konyushenko EN**, Stejskal J, Trchová M, Hradil J, Kovářová J, Prokeš J, Cieslar M, Hwang J-Y, Chen K-H, Sapurina I,
Multi-wall carbon nanotubes coated with polyaniline ,
POLYMER 47: 5715–5723 (2006).
Times cited : 9 (7) IF: 2.773

4. Stejskal J, Sapurina I, Trchová M, **Konyushenko E**, Holler P,
The genesis of polyaniline nanotubes,
POLYMER 47: 8253–8262 (2006).
Times cited : 12 (8) IF: 2.773

5. **Konyushenko EN**, Kazantseva NE, Stejskal J, Trchová M, Kovářová J, Sapurina I, Tomishko MM, Demicheva OV, Prokeš J,
Ferromagnetic behaviour of polyaniline-coated multi-wall carbon nanotubes containing nickel nanoparticles,
JOURNAL OF MAGNETISM AND MAGNETIC MATERIALS 320: 231–240 (2008).
Times cited :0 IF: 1.212

6. Stejskal J, Sapurina I, Trchová M, **Konyushenko EN**,
Oxidation of aniline: Polyaniline granules, nanotubes, and oligoaniline microspheres,
MACROMOLECULES, proofs.
IF: 4.277

7. **Konyushenko EN**, Stejskal J, Trchová M, Blinova NV, Holler P,
Polymerization of aniline in ice,
SYNTHETIC METALS, after revision.
IF: 1.685

The citations as in 19 May 2008 according to SCOPUS database. The number after subtraction of autocitations is given in parentheses. The impact factors (IF) = 2007.

SCOPUS H-factor (Konyushenko EN): 4 (May 2008)

Other papers not included in the Thesis:

1. Stejskal J, Trchová M, Blinova NV, **Konyushenko EN**, Reynaud S, Prokeš J, *The reaction of polyaniline with iodine,* POLYMER 49: 180–185 (2008).
   Times cited :0 IF: 2.773

2. Ćirić-Marjanović G, **Konyushenko EN**, Trchová M, Stejskal J, *Chemical oxidative polymerization of anilinium sulfate versus aniline: Theory and experiment,* SYNTHETIC METALS 158:200–211 (2008).
   Times cited :0 IF: 1.685

3. **Konyushenko EN**, Trchová M, Stejskal J, Sapurina I, *The acidity control in the nanotubular growth of polyaniline*, POLYMER, after revision.
   IF: 2.773

Appendix A

Elena N. Konyushenko, Jaroslav Stejskal, Ivana Šeděnková. Miroslava Trchová, Irina Sapurina, Miroslav Cieslar and Jan Prokeš,

Polyaniline nanotubes: conditions of formation,

Polym Int **55:** 31–39 (2006).

Polymer International

Polym Int 55:31–39 (2006)
DOI: 10.1002/pi.1899

Polyaniline nanotubes: conditions of formation

Elena N Konyushenko,[1] Jaroslav Stejskal,[1]* Ivana Šeděnková,[1] Miroslava Trchová,[1] Irina Sapurina,[2] Miroslav Cieslar[3] and Jan Prokeš[3]

[1]*Institute of Macromolecular Chemistry, Academy of Sciences of the Czech Republic, Heyrovsky Sq. 2, 162 06 Prague 6, Czech Republic*
[2]*Institute of Macromolecular Compounds, Russian Academy of Sciences, St Petersburg 199004, Russia*
[3]*Charles University Prague, Faculty of Mathematics and Physics, 121 16 Prague 2, Czech Republic*

Abstract: The courses of aniline oxidation with ammonium peroxydisulfate in aqueous solutions of strong (sulfuric) and in weak (acetic) acids, followed by temperature and acidity changes, are different. In solutions of sulfuric acid, granular polyaniline (PANI) was produced; in solutions of acetic acid, PANI nanotubes were obtained. The external diameter of the nanotubes was 100–300 nm, the internal cavity 20–100 nm, and the length extended to several micrometres. The morphology of PANI, granular or tubular, depends on the acidity conditions during the reaction rather than on the chemical nature of the acid. PANI nanotubes were also produced when aniline was oxidized in the absence of any acid. The bulk conductivity of PANI prepared in solutions of acetic acid was 0.08–0.27 S cm^{-1}, depending on the acid concentration. Protonated PANI prepared in sulfuric and acetic acids were deprotonated with ammonium hydroxide to obtain PANI bases and the ammonium salt of the protonating acid. FTIR spectroscopy showed the differences in the molecular structure of the PANI bases. Irrespective of whether the polymerization was performed in solutions of sulfuric or acetic acid, PANI had hydrogen sulfate counter-ions only. The PANI morphology is thus not controlled by the nature of counter-ions. The acidity of the reaction medium determines the protonation of monomer, oligomer and polymer species. The chemistry of aniline oxidation is likely to be affected especially by the protonation of an intermediate in the pernigraniline form. It is proposed that, in the course of aniline oxidation, pH-dependent self-assembly of aniline oligomers predetermines the final PANI morphology.

Keywords: conducting polymer; conductivity; morphology; nanotube; nanorod; polyaniline; polyaniline base; protonation

INTRODUCTION

Conducting-polymer nanotubes have recently become the object of numerous investigations because of the potentially interesting electrical properties conferred to polymer morphology produced at the nano-scale level. The understanding of the principles of nanotube formation and knowledge of the factors that control the nanotubular morphology constitute a challenge.

There are three approaches to the preparation of conducting polymer nanotubes. The first, pioneered by Martin *et al.*,[1,2] uses a membrane with holes produced by, for example, heavy-ion bombardment as a template for the polymerization. Polyaniline (PANI) or polypyrrole is then grown *in situ* on the surface of the pores (Fig. 1(a)).[3–7] After mechanical abrasion of membrane surfaces, followed by dissolution of the membrane body, conducting polymer nanotubes are obtained.

The reverse method uses suitable rod-like objects as templates for the polymerization and growth of polymer films (Fig. 1(b)), followed by template dissolution. It is helpful if the template is negatively charged[8] to attract positively charged aniline or pyrrole monomers. This technique has been illustrated by the polymerization of pyrrole on rods produced by pyrrole and β-naphthalenesulfonic acid complex.[9] The coating of sulfonated carbon nanotubes[10] and of polymer nanofibres[11,12] with PANI serves as additional examples.

The last approach is based on the polymerization of aniline in the absence of templates of fixed morphology. Aniline is oxidized in acidic aqueous medium as a rule. It has been proposed that acids present in the reaction mixture or, more precisely, micelles or assemblies produced by their salts with aniline act as 'soft' templates.[13–18] The polymerization at template interfaces would give rise to PANI nanotubes, perhaps in a similar manner as polymerization at macroscopic liquid–liquid interfaces produces PANI nanowires.[19,20] Wan *et al.*[17] observed the formation of PANI nanotubes when aniline was oxidized in solutions of hydroxycarboxylic acids. The authors

* Correspondence to: Jaroslav Stejskal, Institute of Macromolecular Chemistry, Academy of Sciences of the Czech Republic, Heyrovsky Sq. 2, 162 06 Prague 6, Czech Republic
E-mail: stejskal@imc.cas.cz
Contract/grant sponsor: Grant Agency of the Academy of Sciences of the Czech Republic; contract/grant number: A4050313
(*Received 24 March 2005; revised version received 25 April 2005; accepted 15 July 2005*)
Published online 3 November 2005

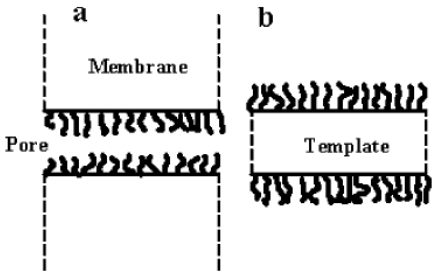

Figure 1. Nanotubes are produced by the growth of polymer chains (a) inside membrane pores or (b) on the surface of solid template structures.

stressed the role of hydroxy groups in stabilizing the nanotubular structure by hydrogen bonding. The polymerizations of aniline in the presence of naphthalenesulfonic acids,[15,21,22] camphorsulfonic acid,[16] 2-acrylamido-2-methyl-1-propanesulfonic acid[23] or sulfoxy-terminated dendrons[24] have all led to PANI nanotubes. Nanotubes were obtained even in the presence of inorganic acids.[14] It thus seems that nanotubes can be prepared in a solution of virtually *any* acid.

Although the concept of micellar templates is attractive to explain the formation of nanotubes, it can easily be criticized. The existence of cylindrical template micelles has been assumed but their presence has never been proved. The observed inner diameter of the nanotubes raises some questions, too. It is found to be typically in the range 10–120 nm.[16,17,22] This is a much larger value than the diameter of the potential micelles produced by aniline salts, unless they were considerably swollen with aniline base. Some authors therefore talk about polymerization without any shape-guiding template[25] or templateless polymerization[13,26] without specifying the tubular growth mechanism.

In the present study, we have selected aqueous solutions of acetic acid to be a medium for the polymerization of aniline. We demonstrate that PANI nanotubes are produced under conditions where potential template micelles can hardly be present.

EXPERIMENTAL

Preparation of PANI

0.2 mol L^{-1} aniline was oxidized with 0.25 mol L^{-1} ammonium peroxydisulfate[27] in an aqueous medium of 0–0.8 mol L^{-1} acetic acid and in 0.1 mol L^{-1} sulfuric acid at room temperature. On the following day the precipitated PANI was collected on a filter, rinsed with a corresponding solution of acid, and dried over silica gel.

Part of the protonated PANI was deprotonated with excess 1 mol L^{-1} ammonium hydroxide, and the resulting PANI base was again dried. The supernatant solutions of ammonium hydroxide containing the ammonium salt of the original protonating acid were separated and evaporated, and the ammonium salts were collected and dried.

Characterization

Infrared spectra in the range 400–4000 cm^{-1} were recorded at 64 scans per spectrum at 2 cm^{-1} resolution using a fully computerized Thermo Nicolet NEXUS 870 FTIR spectrometer with a DTGS TEC detector. Measurements of the powdered samples were performed *ex situ* in the transmission mode in KBr pellets. Spectra of the corresponding liquid acetic acid were measured by an attenuated total reflectance (ATR) technique on a ZnSe crystal. All spectra were corrected for the presence of moisture and carbon dioxide in the optical path.

Conductivity was determined by a four-point van der Pauw method on PANI powders which had been compressed into pellets 13 mm in diameter and ~1 mm thick using a Keithley 237 high-voltage source measurement unit and a Keithley 2010 multimeter equipped with a 2000-SCAN 10 channel scanner card.

RESULTS AND DISCUSSION

In order to prepare PANI as a material having a good level of electrical conductivity, sufficient acidity of the reaction medium is essential. In most experiments, the molar ratio of acid to aniline has been at least equal to unity and an excess of acid has often been used.[28–30] A granular morphology of PANI has invariably been observed under such conditions.[26,30,31]

Low concentrations of acids have usually been avoided because the conductivity of PANI becomes reduced[29] from 10^0 to 10^{-2} S cm^{-1}. On the other hand, studies reporting the formation of PANI nanotubes have used an acid-to-aniline molar ratio lower than unity.[14,16,20,22,24] Wang *et al.*[32] added sodium hydroxide to the reaction mixture to reduce the acidity, and nanotubes were also produced in that case. We thus decided to investigate the polymerization of aniline under both strongly and mildly acidic conditions, in solutions of strong and weak acids, especially with respect to the course of polymerization and the produced morphology. The results are compared with the polymerization of aniline in the absence of any added acid.

The course of polymerization

The oxidation of aniline with ammonium peroxydisulfate (Fig. 2) is exothermic and its course is easily followed by monitoring the reaction temperature.[27,33] As the aniline molecules are chained into PANI, the hydrogens from the amino group of aniline and from the *para* positions of benzene rings are released as protons, as sulfuric acid. Consequently, the acidity of the reaction mixture also increases during polymerization[34] and can be recorded to assess the progress of reaction.

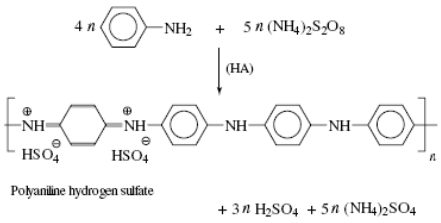

Figure 2. Oxidation of aniline with ammonium peroxydisulfate in aqueous acidic medium yields PANI hydrogen sulfate. Sulfuric acid and ammonium sulfate are by-products.

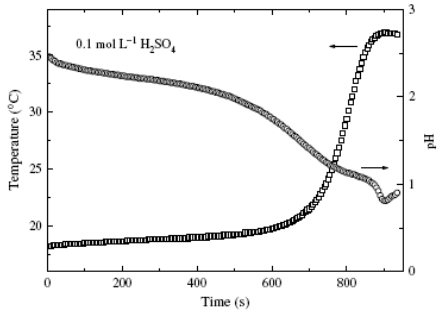

Figure 3. Changes in temperature (squares) and acidity (circles) during oxidation of 0.2 mol L^{-1} aniline with 0.25 mol L^{-1} ammonium peroxydisulfate in 0.1 mol L^{-1} sulfuric acid.

Polymerization in a strong acid

When 0.2 mol L^{-1} aniline was oxidized with ammonium peroxydisulfate at an equimolar concentration of sulfuric acid, we observed a so-called induction period, where the temperature of the reaction mixture stayed almost constant or increased only slightly (Fig. 3). This phase was followed by the exothermic process, attributed to aniline polymerization, which was manifested by the increase in temperature. The pH decreased from the very beginning of the reaction, indicating that some chemical processes took place during the induction period. The exothermic polymerization was linked to a drop in pH, as expected. The last drop in pH, observed after the temperature had reached its maximum, could be connected with the conversion of the pernigraniline to the emeraldine form of PANI. It should be stressed that all reaction processes took place at pH < 2.5, and they were completed in 14 min.

Polymerization in a weak acid

When polymerization was conducted with an equivalent concentration of acetic acid, the polymerization pattern was different. The temperature started to increase from the very beginning of the reaction, but then the temperature increase slowed down and then

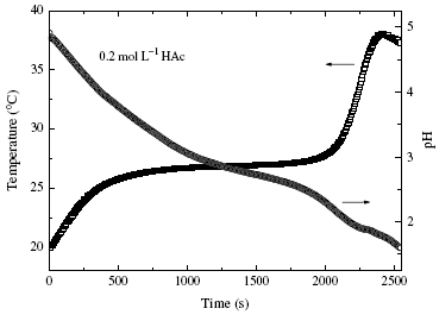

Figure 4. Changes in temperature (squares) and acidity (circles) during oxidation of 0.2 mol L^{-1} aniline with 0.25 mol L^{-1} ammonium peroxydisulfate in 0.2 mol L^{-1} acetic acid.

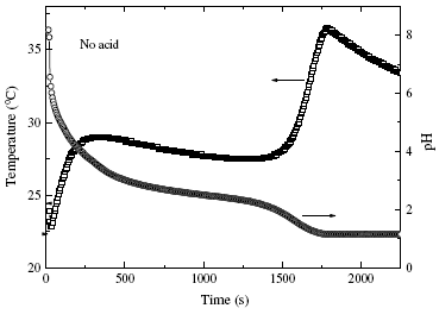

Figure 5. Changes in temperature (squares) and acidity (circles) during the oxidation of 0.2 mol L^{-1} aniline with 0.25 mol L^{-1} ammonium peroxydisulfate in water.

increased again in the next stage (Fig. 4). Two exothermic processes obviously followed in succession. The reaction started at pH 5, acetic acid being much weaker than sulfuric acid. As the oxidation proceeded, the pH fell below 2, as sulfuric acid had been produced by the decomposition of peroxydisulfate, and hydrogens were removed as protons from aniline. On the acidity curve we can also distinguish two subsequent phases. During the first one, the acidity reduction tended to level off, and then during the second exothermic oxidation process it dropped again. The reaction was over in 38 min.

Polymerization with no acid

The oxidative polymerization of aniline in the absence of any acid is the most interesting case. The two exothermic oxidation phases were well separated (Fig. 5). It seems that, in the first step, the aniline became exhausted by the formation of oligomers (Fig. 6). The reaction stopped for the following reason: with the exception of the terminal amine group, the intermediate pernigraniline structure[28,35] was not protonated at pH 3–4 in the reaction medium (Fig. 5),

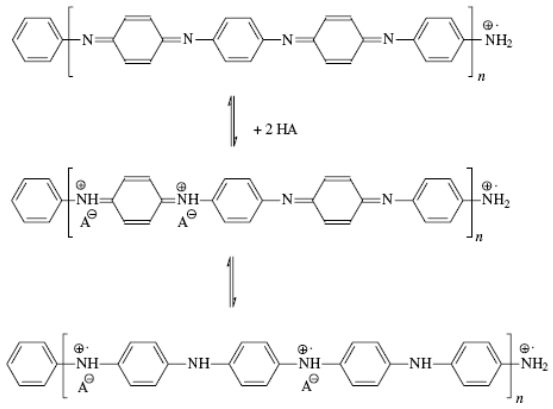

Figure 6. Growth of PANI chains in the pernigraniline form. At moderate acidity (pH > 3) the pernigraniline is not protonated (with the possible exception of the terminal amine group). The protonation takes place at pH < 2 and produces cation-radicals along the chain.

because the protonation of pernigraniline only takes place in more acidic media,[36] i.e. pH < 2. There is only a single unpaired electron at the growing end of the PANI chain (Fig. 6). The pernigraniline chain contains a system of conjugated double bonds. The unpaired electron at the end of the molecule becomes more and more delocalized along the chain as the degree of polymerization increases. That is why it soon loses its reactivity, and the polymerization stops at the oligomer stage. This is a general feature of all conjugated polymers and that is why most of them have a low molecular weight.

When the pH of the reaction mixture gradually reached a value where pernigraniline started to be protonated, the concentration of electrons with unpaired spins on pernigraniline chains dramatically increased (Fig. 6). The unpaired electrons at the end of oligomer molecules became re-localized and, because of that, were re-activated so that they could again participate in polymerization reactions. As there seemed to be no aniline monomer available any more, the existing aniline oligomers were likely to be coupled into longer polymer chains. This mechanism may account for the often-observed bimodal distribution of molecular weights in PANI. In contrast, in a solution of sulfuric acid, once the pernigraniline had been produced, it was directly protonated because the pH was sufficiently low.

The polymerization in the absence of acid took 29 min (Fig. 5), i.e. it was considerably faster than in solutions of acetic acid, which took 38 min. We observed generally that the addition of strong acid to water accelerated the oxidation reaction but the presence of a weak acid made the oxidation process slower. The initial pH of aniline solution in the absence of acid was 8 (pH 5 in 0.2 mol L^{-1} acetic acid) and the terminal value was close to 1 (pH 2 in 0.2 mol L^{-1} acetic acid). This means that acetic acid acted as a sort of not very efficient buffer, and narrowed the pH range in which the oxidation takes place.

The course of aniline oxidation is different in solutions of strong and weak acids. We propose that the kinetics of polymerization is controlled by the acidity level and its changes during the polymerization, rather than by the chemical nature of the acid. The pH level is likely to control (a) the protonation of aniline to an anilinium cation, (b) the protonation of the terminal amine group in the aniline oligomer and (c) the pernigraniline structures produced during polymerization (Fig. 6). It is obvious that the reactivity of the protonated and non-protonated forms will be different, and their oxidation may lead to different products at various reaction rates.

Morphology

Polymerization in sulfuric acid led to the granular morphology (Fig. 7) that has often been reported in the literature.[30,31] The presence of PANI nanotubes was observed in all the products prepared in solutions of acetic acid (Fig. 8). A granular PANI precipitate, i.e. a non-tubular morphology, was also present in the samples to some extent. Nanotubes of 100–300 nm diameter were produced, regardless of the acetic acid concentration (0–0.8 mol L^{-1}). The diameter within a single nanotube was relatively uniform but various nanotubes had different thicknesses. Some of the nanotubes were several micrometres long; others were shorter than 0.5 μm. It should be mentioned that the nanotubular morphology was preserved after deprotonation of PANI to the corresponding base, i.e. it was not dependent on the presence of an acid protonating PANI. A similar observation has also been reported for PANI nanowires.[37]

The rich variety of PANI structures prepared in 0.5 mol L^{-1} acetic acid is better visualised on TEM micrographs (Fig. 9) and may be the result

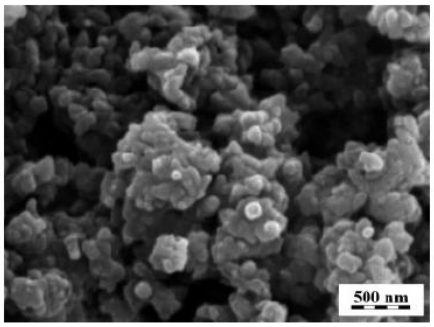

Figure 7. SEM micrograph of PANI prepared in 0.1 mol L^{-1} sulfuric acid.

of the acidity conditions that change in the course of aniline oxidation. Two-thirds of the sample was constituted by nanotubes, the rest by a granular precipitate. The cavities in the nanotubes were easily visible (Figs 9 and 10). The inner diameter differed substantially among the individual nanotubes, in the range 20–100 nm, but it was relatively constant within individual nanotubes. Some nanotubes had no discernible cavity (Figs 9(d) and 11) and could rather be regarded as nanorods. Such nanostructures have also been reported in the radiolytic synthesis of PANI to accompany PANI nanowires.[26] As a matter of interest, some objects resembling hollow spheres were also observed in the present samples (Fig. 9(e)), as well as in the literature.[15,26] Polymerization on the surface of aniline droplets has been offered as an explanation.[15] Alternatively, such objects could be the result of an interfacial polymerization of aniline on oxygen microbubbles[38] produced as by-products in the decomposition reactions of peroxydisulfate.

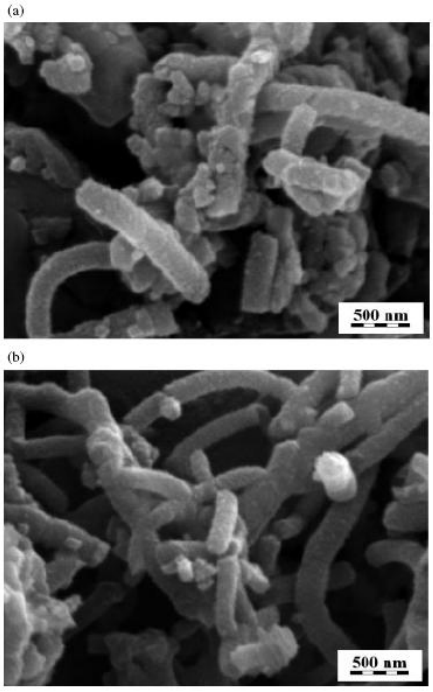

Figure 8. SEM micrographs of PANI prepared in (a) 0.2 mol L^{-1} and (b) 0.5 mol L^{-1} acetic acid.

The most important observation is that nanotubes were generated even in the absence of any added acid (Fig. 12). The quality of the nanotubes was inferior

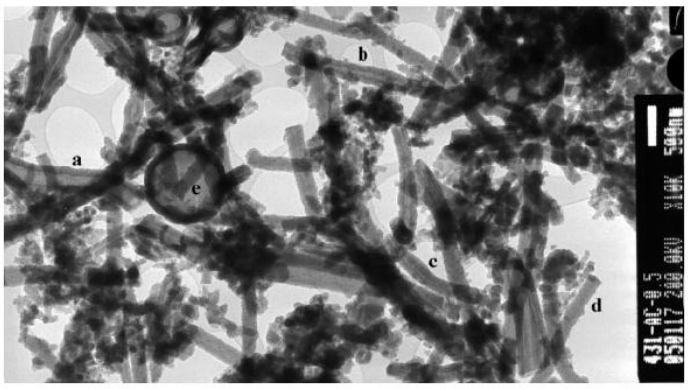

Figure 9. TEM micrograph of PANI structures prepared after 0.2 mol L^{-1} aniline was oxidized with 0.25 mol L^{-1} ammonium peroxydisulfate in 0.5 mol L^{-1} acetic acid at 20 °C. The products contained PANI nanotubes with external diameter *ca* 100–300 nm. The internal diameter varied from (a) 100 nm to (b) 40 nm and (c) 20 nm. There were also nanorods without any cavity (d). Some spherical objects were also present (e).

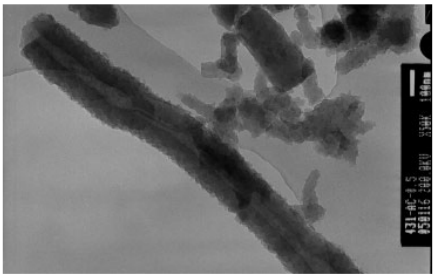

Figure 10. A PANI nanotube.

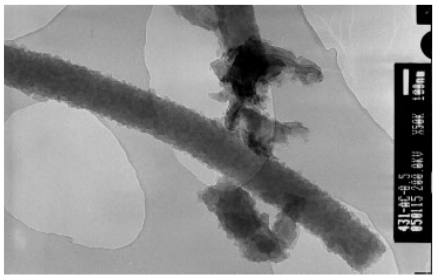

Figure 11. A PANI nanorod.

compared with those prepared in acetic acid solutions. On closer inspection, the SEM micrographs suggest the presence of PANI sheets (Fig. 12), of thickness 150–200 nm. Similar sheets or flakes were observed by Cheng *et al*.[24] when the polymerization of aniline was carried out at low content of organic acid.

There seems to be a link between the course of polymerization and the supramolecular PANI morphology that is produced. It is difficult to imagine any monomer micelles that would produce a template for the polymerization of aniline in solutions of acetic acid. On the other hand, aniline *oligomers* produced in the early stages of the polymerization are hydrophobic. They may aggregate to constitute a template-like structure that further predetermines the directional growth of PANI. Again, once they become protonated at low pH, their hydrophobicity is reduced and they become soluble in the reaction medium. This may result in a lower extent and altered procedure for oligomer aggregation and, consequently, in the change in the produced morphology. This concept may explain why organized nanotubular structures are obtained at lower acidity, and disordered granular ones at high acidity of the reaction medium.

Protonation of PANI

Other important questions are whether acetic acid constitutes a part of the PANI nanotubes and whether it may affect the produced morphology. During oxidation of aniline with ammonium peroxydisulfate,

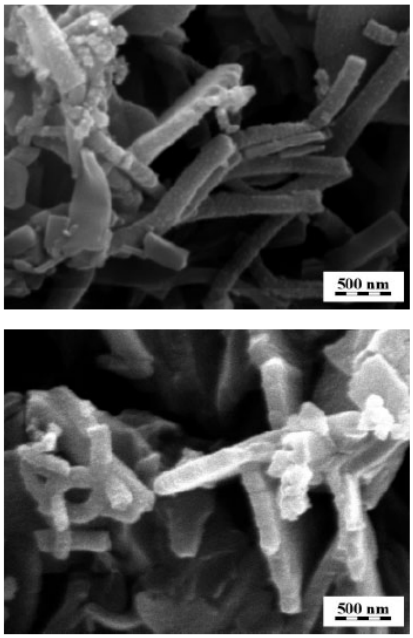

Figure 12. SEM micrographs of PANI prepared in the absence of any added acid.

sulfuric acid is produced as a by-product (Fig. 2). Its concentration is not negligible: from 0.25 mol L^{-1} concentration of an oxidant, 0.25 mol L^{-1} sulfuric acid is produced at 100 % conversion of aniline into PANI, which is practically achieved in the experiment.[27] Such an amount of strong acid is able to protonate PANI fully,[29,39] as 0.1 mol L^{-1} sulfuric acid is sufficient to provide all hydrogen sulfate counter-ions The FTIR spectra of all protonated PANI are similar (Fig. 13), which suggests that all samples of PANI are protonated in approximately the same way.

More detailed information is obtained after deprotonation of PANI with ammonium hydroxide (Fig. 14). In the present case, the ammonium salts obtained by evaporation of ammonium hydroxide extracts could be either ammonium sulfate or ammonium acetate. FTIR spectra (Fig. 15) show that the salts were ammonium sulfate, regardless of the acetic acid concentration used in the synthesis. There was not even a trace of acetate counter-ions detected in PANI.

The fact that hydrogen sulfate counter-ions were present in PANI is in accordance with information given in the literature. Wang *et al*.[32] observed that the ammonia solution used for the deprotonation of PANI gave a white precipitate with barium chloride. This proved the presence of sulfate ions in PANI. When polymerization of aniline was performed in solutions of citric acid, the citric counter-ions were not detected in

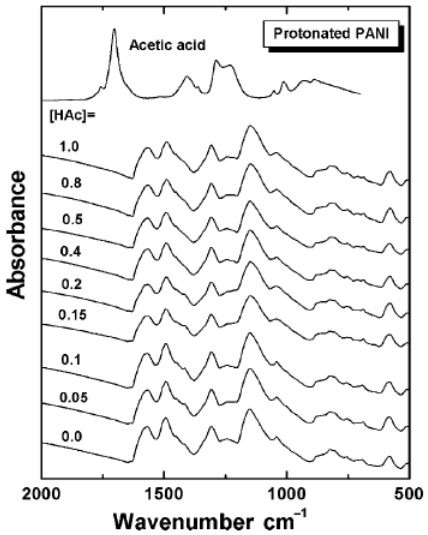

Figure 13. FTIR spectra of PANI prepared in solutions of acetic acid of various concentrations. The spectrum of acetic acid is shown at the top for the comparison.

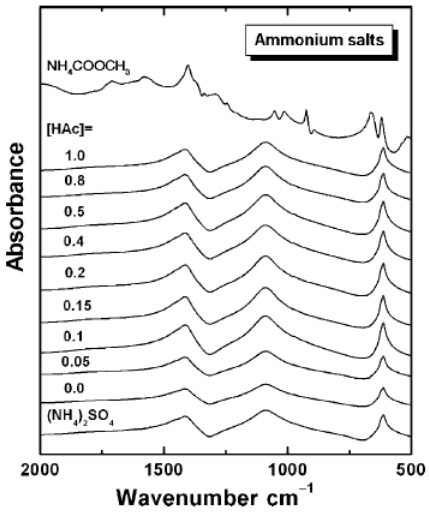

Figure 15. FTIR spectra of ammonium salts obtained after deprotonation of PANI samples prepared in solutions of acetic acid. The spectra of ammonium acetate (top) and ammonium sulfate (bottom) are shown for comparison.

PANI.[29] Other carboxylic acids, however, constituted a part of protonated PANI.[17] Whether, and to what extent, the sulfuric acid produced in the reaction could compete with other acids for the protonation of PANI would depend on the individual strength and structure of the acids.

PANI structure and properties

PANI bases obtained after deprotonation of samples prepared in solutions of acetic acid and in water have similar FTIR spectra (Fig. 16). It has to be stressed that the spectrum of the PANI base corresponding to the PANI prepared in a strong acid, 0.1 mol L^{-1} sulfuric acid, is different (Fig. 17). This means that the molecular structure of PANI prepared under mildly acidic conditions was different from that of samples prepared in solutions of strong acids. The spectrum of the PANI base prepared in the presence of sulfuric acid is similar to that reported in the literature.[40–43] Characteristic bands in the spectra of PANI prepared in acetic acid, observed in addition to the typical bands of PANI base, are at 1446, 1412, 1040, 756 and 695 cm^{-1} (Fig. 17). The bands at 1446 and 1412 cm^{-1} are related to mixed C–C stretching, and C–H and C–N bending vibrations observed in the spectra of the aromatic oligomers.[30,41] The peak at 1040 cm^{-1} is possibly due to the S=O stretching vibration and suggests the presence of sulfonic groups on the aromatic rings.[44] These groups could result from peroxydisulfate radical attack of the benzene rings. The bands at 754 and 695 cm^{-1} are characteristic of mono-substituted aromatic rings which are located

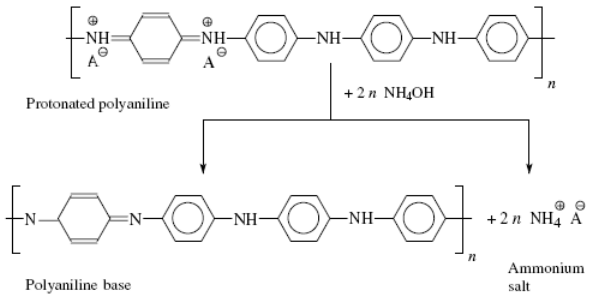

Figure 14. The protonated PANI was deprotonated with ammonium hydroxide to PANI base. The ammonium salt was produced from the acid which had protonated PANI.

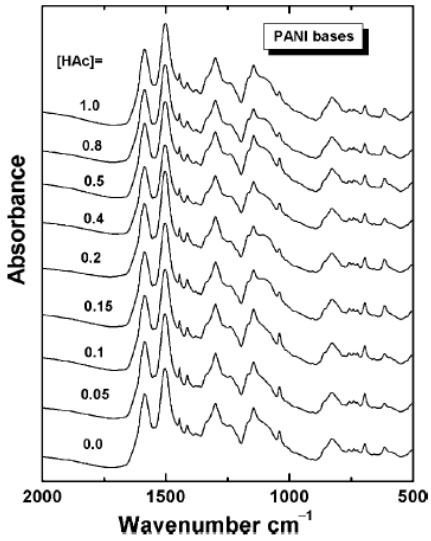

Figure 16. FTIR spectra of PANI bases obtained after deprotonation of samples prepared in solutions of acetic acid.

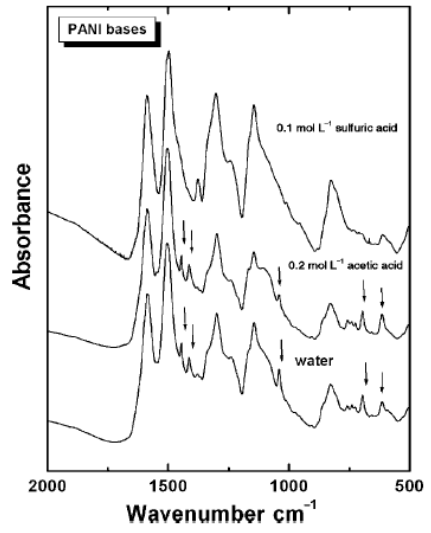

Figure 17. FTIR spectra of PANI bases corresponding to PANI prepared in 0.1 mol L^{-1} sulfuric acid, in 0.2 mol L^{-1} acetic acid, and in water without any added acid. The bands typical of the products prepared in weak acids and in water are marked by arrows.

at chain ends. Their observation thus indicates the presence of short-chain oligomers.[30]

The variations in molecular structure are reflected in the conductivity. PANI prepared in the absence of added acid had a conductivity of 0.083 S cm^{-1}. As the concentration of acetic acid in the mixture increased from 0.05 mol L^{-1} to 0.8 mol L^{-1}, the conductivity of PANI increased from 0.12 to 0.27 S cm^{-1}. These data are comparable with the results reported for PANI nanotubes prepared in solutions of camphorsulfonic acid.[16] Their conductivity in a compressed pellet was 0.03 S cm^{-1} but the conductivity of a single nanotube was three orders of magnitude higher. The conductivity of PANI prepared in sulfuric acid was 1.6 S cm^{-1}. Since, as we have learned, all samples are protonated with hydrogen sulfate counter-ions, the structure of PANI chains has to be structurally different as suggested by FTIR spectra.

Some indication of the ring sulfonation also comes from the results of elemental analysis. The theoretical composition of PANI base (Fig. 14) is 79.5 % C, 5.0 % H and 15.5 % N.[27] While the PANI base prepared in 0.8 mol L^{-1} acetic acid had 64.4 % C, 5.0 % H, 13.7 % N and 3.1 % S, the synthesis in 0.8 mol L^{-1} sulfuric acid yielded a base with a composition 67.0 % C, 4.8 % H, 12.5 % N and 1.9 % S. The most obvious difference is in the sulfur content, i.e. in the content of sulfo groups on the PANI chain. The interaction between the sulfo and imine groups in the individual chains may affect the supramolecular morphology. Also, the presence of oxygen suggested by elemental analysis may be important and its role has practically never been discussed in the literature.

Concluding remarks

Thin PANI films grow at virtually any surface in contact with the reaction mixture.[28,45] It is assumed that aniline oligomers are adsorbed at the interface, their reactivity being increased as a result of altered electron-density distribution caused by adsorption.[46,47] The polymer chains growing from these oligomers produce a film with a brush-like chain-ordering morphology.[47] It has recently been proposed that the formation of colloidal particles by conducting polymers may have the same origin,[48,49] an adsorption of aniline oligomers on the steric stabilizer present in the reaction mixture. This concept can be extended to the polymerization at liquid–liquid interface that produces nanofibres; it was suggested that the formation of nanofibres is not determined by the interface but more likely by the nature of the oxidative polymerization of aniline.[50] Indeed, the growth of nanowires from a liquid–liquid interface resembles the growth of the film at the solid–liquid interface. The formation of nanotubes is likely to be governed by similar principles, based on the adsorption of oligomers at available interfaces. In the case of nanotubes, such interfaces could be provided by oligomer aggregates produced in the early stages of aniline oxidation. A simple model thus has to be sought that could account for the formation of thin films, colloidal particles, nanowires, nanofibres, nanorods, nanotubes, and related morphologies produced by conducting polymers.

CONCLUSIONS

(1) The course of aniline polymerization in solutions of strong and weak acids is different. In strong acid, an athermal induction period is followed by exothermic polymerization. In weak acid, or in the absence of any acid, two exothermic processes follow in succession.

(2) PANI prepared in the presence of acetic acid is produced mainly as nanotubes. These are accompanied by a globular precipitate. The external diameter of the nanotubes is 100–300 nm, and the length reaches up to a few micrometres. The internal diameter substantially differs between nanotubes, in the range 20–100 nm, but within a single nanotube it is relatively constant. In some cases, nanorods, without an internal cavity, are produced.

(3) The nanotubes are produced even in the absence of any acid. This means that organic acids and their salts with aniline are not needed as templates for the polymerization of aniline. In our opinion, the self-assembly of aniline oligomers, rather than that of aniline monomers, predetermines the supramolecular structure of the final products.

(4) A mildly acidic medium is favourable for the production of nanotubes at the cost of reduced conductivity in the bulk, 10^{-1} S cm^{-1}. In strongly acidic conditions, e.g. in solutions of sulfuric acid, a product with better conductivity, 10^{0} S cm^{-1}, but of a granular morphology, is produced.

(5) There are differences between the molecular structures of PANI prepared in strong and weak acids, as is reflected by the FTIR spectra of the corresponding PANI bases. The ring sulfonation and the formation of oligomer species in solutions of acetic acid may be responsible for this fact.

(6) When aniline is oxidized in the presence of acetic acid, the resulting PANI is protonated only by sulfuric acid produced by the decomposition of an oxidant, ammonium peroxydisulfate. Acetate counter-ions have not been detected in PANI.

ACKNOWLEDGEMENTS

The authors thank the Grant Agency of the Academy of Sciences of the Czech Republic (A4050313) for financial support. Special thanks are due to Ms J Hromádková from the Institute of Macromolecular Chemistry, Prague, for scanning electron microscopy.

REFERENCES

1 Cai Z and Martin CR, *J Am Chem Soc* **111**:4138 (1989).
2 Martin CR, in *Handbook of Conducting Polymers*, ed. by Skotheim TA, Elsenbaumer RL and Reynolds JR. Marcel Dekker, New York, pp. 409–421 (1998).
3 Ermolaev SV, Jitariouk N and La Moël A, *Nuclear Instr Meth Phys Res B* **185**:184 (2001).
4 Mazur M, Tagowska M, Palys B and Jackowska K, *Electrochem Commun* 5:403 (2003).
5 Xiong S, Wang Q and Xia H, *Synth Met* **146**:37 (2004).
6 Tagowska M, Pałys B and Jackowska K, *Synth Met* **142**:223 (2004).
7 Dauginet L and Demoustier-Champagne S, *Polymer* **46**:1575 (2005).
8 Shinkai S, Takeuchi M and Bae AH, *Supramol Chem* **17**:181 (2005).
9 Diez I, Tauer K and Schulz B, *Colloid Polym Sci* **283**:125 (2004).
10 Wei Z, Wan M, Lin T and Dai L, *Adv Mater* **15**:136 (2003).
11 Dong H, Nyame V, MacDiarmid AG and Jones WE Jr, *J Polym Sci, Part B: Polym Phys* **42**:3934 (2004).
12 Dong H, Prasad S, Nayme V and Jones WE Jr, *Chem Mater* **16**:371 (2004).
13 Qiu H, Wan M, Matthews B and Dai L, *Macromolecules* **34**:675 (2001).
14 Zhang Z, Wei Z and Wan M, *Macromolecules* **35**:5937 (2002).
15 Wei Z and Wan M, *Adv Mater* **14**:1314 (2002).
16 Long Y, Zhang L, Ma Y, Chen Z, Wang N, Zhang Z and Wan M, *Macromol Rapid Commun* **24**:938 (2003).
17 Zhang L, Long Y, Chen Z and Wan M, *Adv Funct Mater* **14**:693 (2004).
18 Xia H, Chan HSO, Xiao C and Cheng D, *Nanotechnology* **15**:1807 (2004).
19 Huang J and Kaner RB, *J Am Chem Soc* **126**:851 (2004).
20 Zhang X, King RCY, Jose A and Manohar SK, *Synth Met* **145**:23 (2004).
21 Wei Z, Zhang Z and Wan M, *Langmuir* **18**:917 (2002).
22 Zhang Z, Wei Z, Zhang L and Wan M, *Acta Mater* **53**:1373 (2005).
23 Pinto NJ, Carrión OL, Ayala AM and Ortiz-Marciales M, *Synth Met* **148**:271 (2005).
24 Cheng C, Jiang J, Tang R and Xi F, *Synth Met* **145**:61 (2004).
25 Yan H, Inokuchi M, Kinoshita M and Toshima N, *Synth Met* **148**:93 (2005).
26 Pillalamarri SK, Blum FD, Tokuhiro AT, Story JG and Bertino MF, *Chem Mater* **17**:227 (2005).
27 Stejskal J and Gilbert RG, *Pure Appl Chem* 74:857 (2002).
28 MacDiarmid AG and Epstein AJ, *Faraday Discuss Chem Soc* **88**:317 (1989).
29 Stejskal J, Hlavatá D, Holler P, Trchová M, Prokeš J and Sapurina I, *Polym Int* 53:294 (2004).
30 Laska J and Widlarz J, *Polymer* **46**:1485 (2005).
31 Stejskal J, Riede A, Hlavatá D, Prokeš J, Helmstedt M and Holler P, *Synth Met* **96**:55 (1998).
32 Wang X, Liu N, Yan X, Zhang W and Wei Y, *Chem Lett* **34**:42 (2005).
33 Fu Y and Elsenbaumer RL, *Chem Mater* 6:671 (1994).
34 Gospodinova N, Mokreva P and Terlemezyan L, *Polymer* **34**:2438 (1993).
35 Stejskal J, Kratochvíl P and Jenkins AD, *Polymer* **37**:367 (1996).
36 Stejskal J, Kratochvíl P and Jenkins AD, *Collect Czech Chem Commun* **60**:1747 (1995).
37 Sarno DM, Manohar SK and MacDiarmid AG, *Synth Met* **148**:237 (2005).
38 Chowdhuri D, Paul A and Chattopadhyay A, *J Phys Chem B* **106**:4343 (2002).
39 Palaniappan S, *Eur Polym J* **37**:975 (2002).
40 Quillard S, Louarn G, Lefrant S and MacDiarmid AG, *Phys Rev* **50**:12 496 (1994).
41 Boyer MI, Quillard S, Rebourt E, Louarn G, Buisson JP, Monkman A and Lefrant S, *J Phys Chem B* **102**:7382 (1998).
42 Trchová M, Stejskal J and Prokeš J, *Synth Met* **101**:840 (1999).
43 Trchová M, Matějka P, Brodinová J, Kalendová A, Prokeš J and Stejskal J, *Polym Degrad Stab* (in press).
44 Silverstein RM, Bassler GC and Morrill TC, *Spectrometric Identification of Organic Compounds*, 5th edn. J Wiley, New York (1991).
45 Stejskal J, Sapurina I, Prokeš J and Zemek J, *Synth Met* **105**:195 (1999).
46 Fedorova S and Stejskal J, *Langmuir* **18**:5630 (2002).
47 Sapurina I, Osadchev AY, Volchek BZ, Trchová M, Riede A and Stejskal J, *Synth Met* **129**:29 (2002).
48 Stejskal J and Sapurina I, *J Colloid Interface Sci* **274**:489 (2004).
49 Stejskal J and Sapurina I, *Pure Appl Chem* 77:743 (2005).
50 Huang J and Kaner RB, *Angew Chem Int Ed* **43**:5817 (2004).

Appendix B

Miroslava Trchová, Ivana Šeděnková, Elena N Konyushenko, Jaroslav Stejskal, Petr Holler, and Gordana Ćirić-Marjanović,

Evolution of Polyaniline Nanotubes: The oxidation of Aniline in Water,

J. Phys. Chem. B **110:** 9461–9468 (2006).

Evolution of Polyaniline Nanotubes: The Oxidation of Aniline in Water

Miroslava Trchová,*,† Ivana Šeděnková,† Elena N. Konyushenko,† Jaroslav Stejskal,† Petr Holler,† and Gordana Ćirić-Marjanović‡

Institute of Macromolecular Chemistry, Academy of Sciences of the Czech Republic, 162 06 Prague 6, Czech Republic, and Faculty of Physical Chemistry, University of Belgrade, Studentski Trg 12-16, 11001 Belgrade, Serbia and Montenegro

Received: December 27, 2005; In Final Form: March 8, 2006

The course of aniline oxidation with ammonium peroxydisulfate in aqueous solutions has been investigated. The reaction was terminated at various times and the intermediates collected. Besides the precipitates, the films deposited in situ on silicon windows have also been studied. The kinetic course of polymerization is controlled by the acidity level, which changes during the polymerization from pH 8 to a final value close to pH 1. It has two distinct exothermic phases. Gel-permeation chromatography indicates that aniline oligomers are produced at first at high pH, while polyaniline follows after the pH becomes sufficiently low. The growth of polyaniline nanotubes was observed by optical microscopy and confirmed by electron microscopy. The molecular structure of the reaction intermediates was studied in detail by FTIR spectroscopy. Oxidation products are markedly sulfonated, and they contain phenazine units. Aniline oligomers are more soluble in chloroform than the polymer fraction, which contains nanotubes.

Introduction

Polyaniline (PANI) is one of the most investigated conducting polymers. It is prepared easily by the oxidation of aniline in aqueous medium (Figure 1). The reaction itself seems to be simple, yet it represents interplay of complex multilevel processes. Various supramolecular structures of the final product are obtained, depending on the conditions of the reaction, but the mechanism of their formation has not yet been elucidated. When aniline is oxidized in an acidic aqueous medium with ammonium peroxydisulfate, a PANI precipitate is produced.[1,2] The blue pernigraniline form present during the polymerization converts to a green protonated emeraldine at the end of the polymerization.[3−5] The reaction is exothermic and yields, in addition to PANI, sulfuric acid as a byproduct. The progress of polymerization thus can be followed in situ by recording either the temperature[6−8] or the pH.[9,10] Open-circuit potential measurements[5,11,12] and UV−visible spectroscopy[13,14] may be examples of other methods used for the same purpose. The progress of the chemical polymerization of aniline has newly been monitored in situ by ATR FTIR spectroscopy.[15]

Another group of techniques suitable to reflect the course of polymerization is based on the isolation of the reaction intermediates and their ex situ characterization. The oxidative polymerization of aniline with peroxydisulfate in dilute solutions of perchloric or hydrochloric acid of various concentrations was studied by Neoh et al.[16] The products thus obtained at various reaction times during the course of polymerization have been characterized by FTIR and X-ray photoelectron spectroscopies. The growth of PANI films on glass has been investigated by using UV−visible spectroscopy.[17] Studies of the development of morphology, however, are still missing.

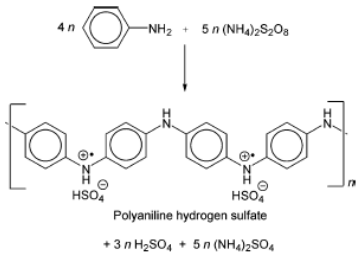

Figure 1. Oxidation of aniline with ammonium peroxydisulfate in water yields PANI hydrogen sulfate. *Para* addition of constitutional units is shown, but the *ortho* addition can also be important. Sulfuric acid and ammonium sulfate are byproducts.

It has been reported recently that the courses of aniline oxidation with ammonium peroxydisulfate in aqueous solutions of strong (sulfuric) or weak (acetic) acids, followed by temperature and pH changes, are substantially different.[10] In solutions of sulfuric acid, granular PANI was produced; in solutions of acetic acid, PANI nanotubes were obtained. The morphology of PANI, granular or tubular, depends on the acidity conditions during the reaction rather than on the chemical structure of the acid.[10] The understanding of the principles of nanotube formation and knowledge of the factors that control the nanotubular morphology constitute a challenge.

It has been demonstrated by Gospodinova et al.[9] that the polymerization of aniline also proceeds well in water, without any added acid, when ammonium peroxydisulfate was used as an oxidant. Such a system is the simplest from the chemical point of view because it includes just two reactants and no other component, and is thus well suited for fundamental studies of aniline oxidation. The sulfuric acid produced by the decomposition of peroxydisulfate (Figure 1) gradually provides the

* To whom correspondence should be addressed. Phone: +420-296-809-381. Fax: +420-296-809-410. E-mail: trchova@imc.cas.cz.
† Academy of Sciences of the Czech Republic.
‡ University of Belgrade.

10.1021/jp057528g CCC: $33.50
Published on Web 04/21/2006

necessary acidity, and the final PANI is protonated with this acid.[18,19] Although the conductivity of PANI thus prepared is rather low,[20] ~10^{-2} S cm^{-1}, the observed nanotubular morphology of the products[10] makes such a system of substantial interest.

In the present paper, we analyze the course of aniline oxidation with ammonium peroxydisulfate in aqueous solutions in the absence of any added acid, as it is observed by temperature and pH measurement. The oxidation reaction was terminated at various stages, and the molecular structure and morphology of the reaction intermediates have been assessed. Both PANI films deposited on silicon windows and the accompanying PANI precipitates have been collected and characterized. The *molecular* structure of the products of aniline polymerization was studied by FTIR spectroscopy. The *macromolecular* parameters, like molecular weights and their distributions, were checked by gel-permeation chromatography. Finally, the evolution of *supramolecular* structure, that is, of the PANI nanotubes formed during aniline oxidation, has been followed by optical microscopy and confirmed by electron microscopy.

Experimental Section

Sample Preparation. Aniline (0.2 M) was oxidized with ammonium peroxydisulfate (0.25 M) in water. Solutions of monomer and oxidant dissolved in water were mixed at room temperature to start the oxidation. The reaction mixture was quickly poured over silicon windows, that are used in FTIR spectroscopy (26 mm in diameter), placed in Petri dishes. The windows were slightly lifted on a support so that the reaction mixture had access to both the top and bottom sides. After a specified time, selected on the basis of the preliminary determination of the course of polymerization, the silicon windows were removed from the mixture. The oxidation reaction was stopped by rinsing the PANI films deposited on the windows with water, which removed both aniline and oxidant. The films were dried in air. After FTIR spectroscopic characterization, the windows were immersed in 1 M ammonium hydroxide to convert protonated intermediate forms to the corresponding bases, and FTIR spectra were again recorded.

The residual reaction mixture left after the removal of silicon windows was poured at the same time into excess of 1 M ammonium hydroxide to stop the polymerization. The precipitate was quickly collected on a filter, thus separated from the residual monomer and oxidant, and also dried in air. Selected samples have been suspended in chloroform for 24 h and the soluble and insoluble fractions have been separated.

FTIR Spectroscopy. Infrared spectra in the range of 400−4000 cm^{-1} were recorded at 64 scans per spectrum at 2 cm^{-1} resolution using a fully computerized Thermo Nicolet NEXUS 870 FTIR Spectrometer with a DTGS TEC detector. The spectra of thin films deposited on silicon substrates were measured in the transmission mode. An absorption subtraction technique was applied to remove the spectral features of the silicon. FTIR spectra of powders were recorded ex situ in the transmission mode, after dispersion of the samples in potassium bromide pellets. The spectra were corrected for the presence of carbon dioxide and water vapor in the optical path.

Microscopy. A research-grade Leica DM LM Microscope equipped with a 50× Olympus objective lenses has been used for optical microscopy. Scanning electron micrographs have been taken with a JEOL 6400 microscope, transmission microscopy with a JEOL JEM 2000 FX.

Gel-Permeation Chromatography (GPC). Molecular weights were assessed by a GPC/SEC using a 8 × 600 mm PLMixedB column (Polymer Laboratories, U.K.) operating with *N*-methylpyrrolidone and calibrated with polystyrene standards with spectrophotometric detection at the wavelength of 650 nm. The samples were dissolved in *N*-methylpyrrolidone containing 0.025 g cm^{-3} triethanolamine for deprotonation of PANI, and 0.005 g cm^{-3} lithium bromide to prevent aggregation.

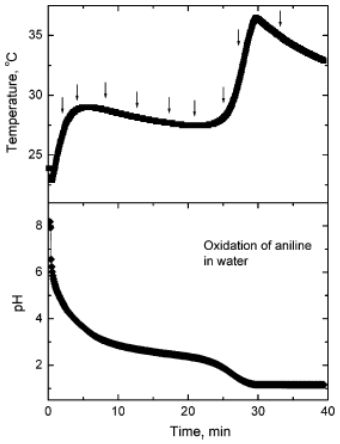

Figure 2. Changes in temperature (top, squares) and acidity (bottom, diamonds) during the oxidation of 0.2 M aniline with 0.25 M ammonium peroxydisulfate in water. There are two reaction phases: the first starts after mixing the reactants at time $t = 0$, the second after $t = 17-21$ min. The times of sample collections are marked by arrows.

Results

Course of Polymerization. The oxidation of aniline with ammonium peroxydisulfate is exothermic and its course is followed easily by monitoring the reaction temperature.[2,6] As aniline molecules are chained to produce PANI, the hydrogen atoms from the amino groups and from the benzene rings of the aniline are released in the form of protons, as sulfuric acid (Figure 1). Consequently, the pH of the reaction mixture decreases during the polymerization and can be recorded to assess the progress of reaction.[9]

The oxidative polymerization of aniline in the absence of any acid has been studied recently.[10] Unlike the oxidation in acid media, where an athermal induction period is followed by exothermic polymerization, two exothermic oxidation phases are well separated in water (Figure 2). The acidity of the medium, and the consequent protonation of the monomer and reaction intermediates, seem to be responsible for the existence of two reaction steps. In the beginning of the reaction, at pH > 4, aniline exists as a neutral molecule and is easily attacked by an oxidant. This is manifested by the fast increase in the temperature (Figure 2). At pH < 4, aniline is protonated to anilinium cation and the reaction mechanism changes. The oxidation then proceeds as in strong acids; an induction period is observed, followed by the exothermic polymerization of aniline.

Morphology. The polymerization of aniline in solutions of sulfuric acid has invariably lead to the granular morphology that has often been reported in the literature.[21] Polyaniline prepared in the presence of acetic acid has been produced mainly as nanotubes[10] accompanied by a globular precipitate; the

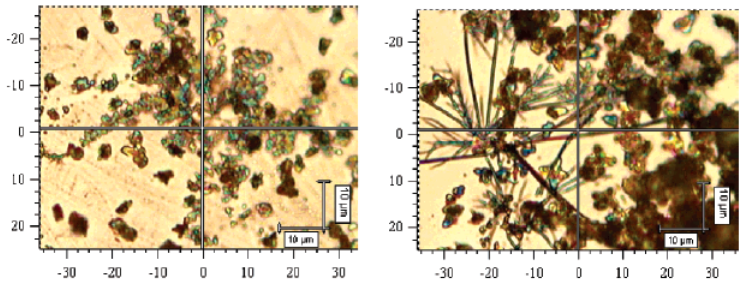

Figure 3. Morphology of the oligomeric products obtained after 8 min (left) and 13 min (right) of reaction time.

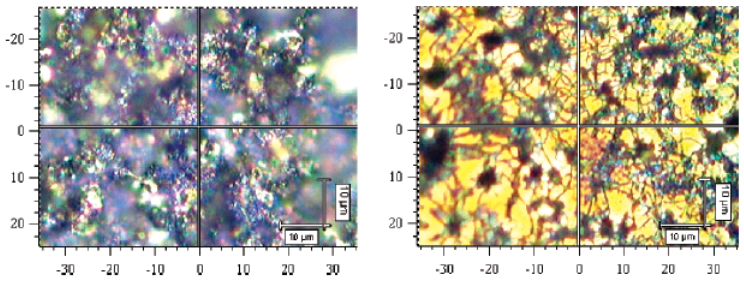

Figure 4. Top (left) and bottom side (right) of the silicon window observed after the 29 min polymerization time. Note the PANI nanotubes at the right micrograph.

nanotubes were produced, even in the absence of any acid. Here, we have investigated the genesis of such nanotubular structures.

During the oxidation of aniline beginning in neutral media, we have observed the evolution of the water-insoluble products of the reaction. The silicon windows were placed into the reaction mixture and removed at various stages of aniline oxidation. The oxidation products, deposited on the windows, have been studied by optical microscopy (Figures 3 and 4). There is a link between the course of polymerization and the supramolecular morphology produced at various times. The products obtained in the first stages of aniline oxidation, after 2−8 min, are composed mostly of crystals, which are obviously insoluble in water, having the size of several micrometers (Figure 3, left). They grow to trees (dendrimers) with branches of tens of micrometers in length, after the reaction time of 13 min (Figure 3, right). Brown granular objects several micrometers in size are also present. On the window removed at $t = 17$ min, we observed, in addition to the granular precipitate, the first nanotubes growing on the top side of the window. Later, at $t = 29$ min, only the unresolved structure is found on the top side of the windows, as a result of precipitate sedimentation (Figure 4, left). On the bottom side of silicon windows, we have observed the formation of nanotubes (Figure 4, right). Their occurrence increased at longer times of reaction.

The presence of nanotubes is confirmed by transmission electron microscopy (Figure 5), which shows the internal cavity of the nanotubes in the final precipitated product of polymerization ($t = 33$ min). The nanotubes extend often to a few micrometers, their external diameter being ca. 200 nm and internal diameter of the cavity ca. 20 nm. Nanorods of similar morphology, but without a cavity, have also been detected in the samples, and occasionally a nanosphere was spotted in the micrographs. Some nanosheets seem to be accompanying nanotubes (Figures 5 and 6) and, of course, a PANI precipitate of undefined morphology is also found in the final product.

Molecular Weights. GPC reveals that the reaction intermediates can be divided into two distinct groups. All of the samples separated before $t < 17$ min, that is, produced by the oxidation of neutral aniline, have a molecular-weight distribution similar to that shown for $t = 2$ min (Figure 7a). This corresponds to oligomers having the weight-average molecular weight $M_w = 5000-6000$ (Table 1). All of the products obtained at longer times, when the oxidation of anilinium cations has taken place, have bimodal distributions resembling that shown in Figure 7a for the reaction time $t = 33$ min. This is reflected in a high polydispersity index, M_w/M_n (Table). This means that oligomers are produced at the first stage of reaction, and polymers in the second. The average molecular weight of the polymer part could be estimated as $M_w = 40\,000-70\,000$. We conclude that, at higher pH (lower acidity, Figure 2, bottom), oligomeric products are obtained. Only at lower pH < 2 (at high acidity) are polymeric products produced in addition to the oligomers originated earlier.

We have also determined the distributions of the molecular weights of the chloroform-soluble and chloroform-insoluble fractions of the final product (Figure 7b). The soluble portion contains mainly oligomers. The fraction insoluble in chloroform has a polymeric character, but it also contains an oligomeric part, which is either entrapped in the polymer or due to the crystallization became insoluble. This again leads us to conclude that the oligomers are produced at the beginning of oxidation and the polymers in its advanced stage.

Sulfonation of Polyaniline. There is practically no difference in the elemental compositions of the intermediates. There is, however, a notable amount of sulfur, 5−6 wt %, present in the samples (Table). The observed content of sulfur corresponds

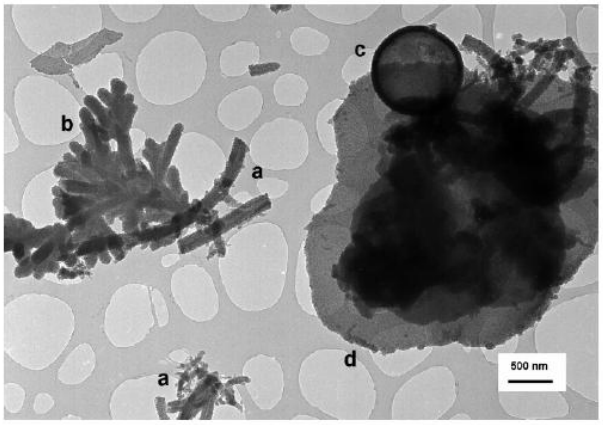

Figure 5. Nanotubes (a) are present along with nanorods (b), nanospheres (c), nanosheets (d), and objects of unresolved morphology in the final product of polymerization (t = 33 min).

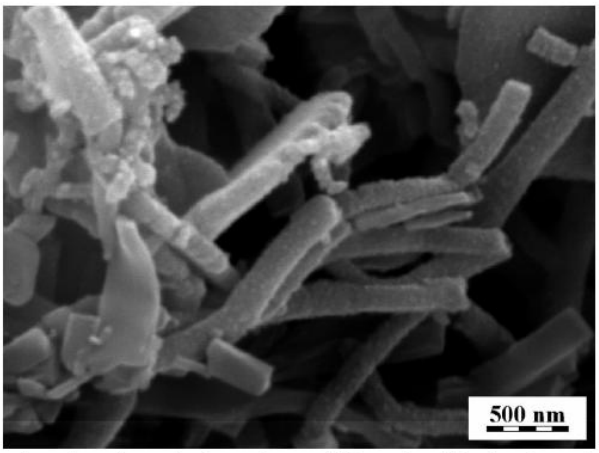

Figure 6. Polyaniline nanotubes as observed by scanning electron microscopy.[10] The nanosheets, 2D analogy of nanorods, accompany the nanotubes in the final product of polymerization (t = 33 min).

to approximately one sulfonate group per five nitrogens, that is, five aniline constitutional units. Such a degree of sulfonation should have a marked effect on the properties of the PANI, and could account for the reduced conductivity of such PANI in the protonated state.[22] The sulfonation is typical of oxidation products prepared in the presence of weak acids or in the absence of any acid.[10] It has to be stressed that the samples are PANI bases, and the sulfur cannot come from the hydrogen sulfate counterions (Figure 1) associated with imine nitrogens, and it has to be mainly in covalently bound sulfonate groups. When the polymerization has been carried out in solutions of strong acids, the PANI bases contained only 0.3 wt % of sulfur.[2]

The sulfonation of benzene rings is therefore offered as a plausible explanation for the presence of sulfur in PANI. Because the sulfur content in the intermediates obtained at the different reaction times is approximately constant (Table), it seems that the aniline monomer and low-molecular-weight oligomers, rather then the completed polymer, become sulfonated by interaction with ammonium peroxydisulfate or its derived radicals. The proposed aniline sulfonation would lead to a mixture of aniline with sulfanilic (4-anilinesulfonic acid) and orthanilic acid (2-anilinesulfonic acid). Therefore, the following process can be assumed to be a copolymerization of aniline with such sulfonic acids.[23] However, competitive sulfonation of low-molecular-weight oligomers cannot be ruled out. For example, in the case of aniline dimer, 4-aminodiphenylamine, its 1,4-diamino-substituted benzene ring is more reactive toward electrophilic aromatic substitution reaction, a sulfonation, than the mono-amino-substituted benzene ring. It can reasonably be expected that sulfonation of aniline trimers, tetramers, and so forth, leads mainly to products with the sulfonated aniline-oligomer head (a benzene ring with primary

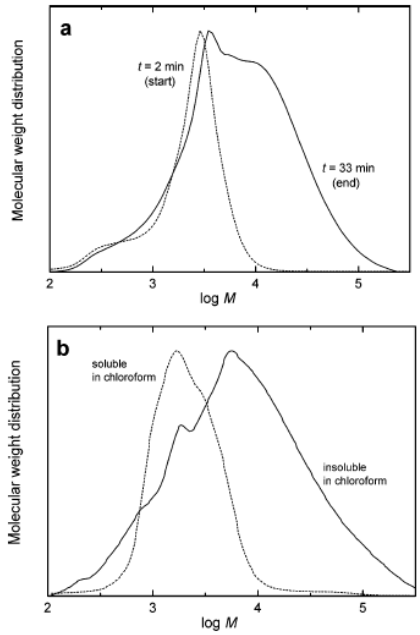

Figure 7. Weight distributions of molecular weights as obtained by GPC for the sample produced (a) at the start (dotted line) and at the end (full line) of aniline polymerization in water and (b) the chloroform-soluble and chloroform-insoluble fraction of the final product. The functions are normalized to a peak value.

TABLE 1: Elemental Composition of Reaction Intermediates Isolated in Their Base Form after Time t and Their Weight-Average Molecular Weight, M_w, and Polydispersity, Weight-to-Number Average Molecular Weight Ratio M_w/M_n, Obtained by GPC

t, min	%C	%H	%N	%S	$10^{-3} M_w$	M_w/M_n
2	58.0	5.4	15.0	6.1	6.2	3.1
4	59.3	5.5	14.7	5.5	5.2	3.3
8	63.0	5.9	14.3	4.9	6.0	3.6
13	59.5	5.3	14.5	5.6	5.4	4.0
17	58.5	5.2	14.4	6.3	14.1	5.3
21	57.8	5.1	13.8	6.0	41.8	14.1
25	56.4	5.1	13.4	5.1	38.1	11.3
27	55.6	5.1	13.4	6.0	56.5	15.9
29	54.5	5.0	13.7	6.3	87.2	15.8
33	57.9	5.1	13.5	6.3	64.8	13.1

amino group). Such aniline-sulfonated oligomers can also be copolymerized with aniline and other aniline oligomers in the reaction mixture.

FTIR Spectra. The molecular structure of the products arising during oxidation of aniline in water was studied by the FTIR spectroscopy. We have analyzed first the as-prepared samples deposited on silicon windows at various times after the beginning of the reaction (Figure 8). The spectra can be divided into two groups. The intensity of the absorption is very small for the samples obtained in the first stage of aniline oxidation (t < 17 min) (Figure 2) and later it increased dramatically as the thickness of the films grew. The shape of

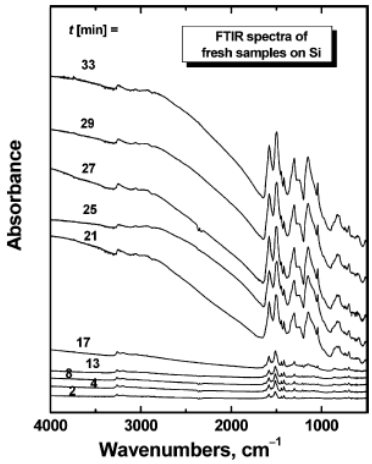

Figure 8. FTIR spectra of the reaction intermediates of the oxidation of aniline in water deposited on silicon windows separated after time t from the beginning of the reaction. The spectra are vertically shifted for separation in Figures 8−10.

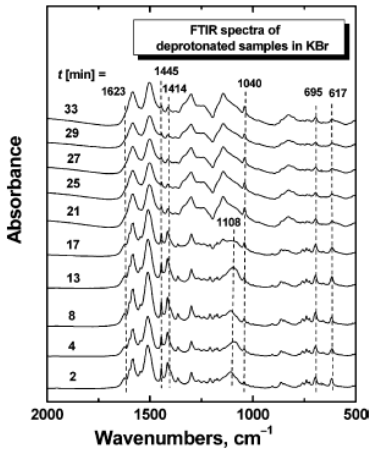

Figure 9. FTIR spectra of the precipitated reaction intermediates collected after time t.

the spectra changed, too. The products obtained in the second stage of the reaction show high absorption in the region above 2000 cm^{-1}.

We have also analyzed the spectra of the samples deposited on silicon windows after immersion in 1 M ammonium hydroxide, that is the deprotonated forms, and the spectra of corresponding powders obtained as precipitates. The spectra of samples deposited on silicon windows are very similar to the spectra of the corresponding powders; therefore, only the latter spectra are discussed (Figure 9). They can also be divided into two groups with an intermediate spectrum recorded for the sample isolated at t = 17 min. In the early stages of the reaction (t < 17 min), they are more similar to those of aniline oligomers.

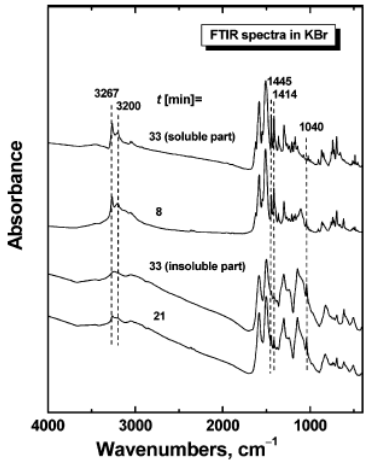

Figure 10. FTIR spectra of fractions soluble and insoluble in chloroform after extraction of intermediate collected at $t = 33$ min and comparison with the typical spectra of the first and second group of products (oligomers and polymers) collected after $t = 8$ and 21 min.

For longer times, the spectra resemble those of standard PANI[22] with some additional peaks marked by dashed lines in Figure 9.

The FTIR spectra of chloroform-soluble and chloroform-insoluble fractions of precipitated reaction intermediates collected at $t = 33$ min were compared with the typical spectra of the first and second group of products (Figure 10). One can see that the spectrum of the soluble fraction is very close to that of the aniline oligomer intermediate obtained at short reaction time, $t = 8$ min, while the spectrum of the insoluble fraction is similar to that of the final product of the polymerization reaction. Additional peaks are still present in the spectra of the insoluble part but they have a lower intensity. This observation will be discussed later.

Discussion Based on FTIR Spectroscopy

Spectroscopic Evidence of Sulfonation. The sulfonate SO_3^- groups attached to the aromatic rings have been identified by the absorption peaks at 1040, 695, and 617 cm^{-1} in all of the spectra[24] (Figure 9). These bands correspond, consecutively, to the S=O, S−O, and S−C stretching vibration modes. The presence of these bands in the spectra of alkali-treated samples confirms that sulfo-groups are covalently bound to the reaction intermediates during reaction. The aniline molecule and low-molecular-weight aniline oligomers, available in sufficient amount in the reaction mixture in the early stage of polymerization (at pH 4−8, Figure 2), are much more suitable for electrophilic attack than the anilinium cation and protonated aniline oligomers, and can thus be sulfonated. Additionally, the sulfonate group is likely to force the chain out of planarity,[25] inducing changes in the product conformation and in this way to reduce conjugation in the PANI chain. The conductivity of sulfonated PANI is indeed at least 2 orders of magnitude lower compared with common PANI.[2] We suppose that a broad band at 1144 cm^{-1} may be due to the asymmetric stretching vibration of the sulfonate group, and the band at 1108 cm^{-1} is attributed to the sulfate-ion stretching vibration.[26]

In the FTIR spectra of all the products obtained at short reaction times, one can observe two relatively strong bands with maxima at 3267 and 3200 cm^{-1} (only the spectrum of the sample obtained after 8 min is shown in Figure 10). They are less pronounced in the spectra of samples collected at longer times, $t > 17$ min (only the spectrum of the final product is shown in Figure 10). They could be assigned to terminal primary amine groups, but, considering the GPC data (Table), they are not likely to be present to a discernible extent. These bands have often been assigned to different types of intra- and intermolecular hydrogen-bonded N−H stretching vibrations of secondary amines, N−H···N. We also assume the presence of intramolecular hydrogen bonding in N−H···O, where the oxygen belongs to the sulfonate group.[27−31] The broad peak at 3182 cm^{-1} has also been reported to reflect the presence of an intermolecular hydrogen bonding to imine groups.[32] The bands due to secondary amine stretching at 3460 cm^{-1} and imine stretching[26,30,33] at 3370 cm^{-1} are very broad, and weaker than bands appearing at ~3267 and 3200 cm^{-1}.

Internal Protonation. The sulfonation of PANI units[25,34] may lead to internal, intramolecular or intermolecular, interaction between sulfonate groups and neighboring imine sites in PANI chains.[23] It is obvious that interactions of this type might help to stabilize supramolecular structures produced by PANI. As we expect to analyze the spectra of products converted to the base form, there are indeed indications for reluctance of the polymer toward deprotonation. The feature of internal protonation of the products isolated at longer times of polymerization, $t > 17$ min, is well manifested by the shape of the spectra above 2000 cm^{-1} (Figure 10).

All of the spectra contain the band at 1547 cm^{-1} of medium intensity, which is not expected to appear in the spectrum of undoped PANI (Figure 9). Cases et al.[35] assigned the band at 1547 cm^{-1} to semi-quinonoid rings, and Boyer et al.[36] reported the band at 1558 cm^{-1} for the emeraldine salt, with the proposed assignment of C=C stretching and C−H deformation vibrations in a semi-quinone structure. A strong and broad band observed at 1144 cm^{-1} is reported to be a band of a conducting PANI, associated with a high degree of electron delocalization in protonated PANI,[16,37−39] and it is also interpreted as a B−NH−B or Q=NH^+−B stretching mode[37] (B denotes a benzene ring, Q is a quinonoid ring in PANI chain, cf. Figure 1).

Phenazine-like Units. In the spectra of the present samples we have observed a set of bands corresponding to phenazine-like units (Figure 11). The presence of phenazinium structures in the structure of aniline oxidation products is not surprising. The phenazine rings are produced in chains containing both the *ortho* and *para*-linked aniline constitutional units. These are likely to be produced especially at low acidity of the reaction medium[40] at pH 4−8. They can constitute either branching sites (Figure 11a) or end-groups (Figure 11b). The band at 1623 cm^{-1}, with the shoulder at ~1630 cm^{-1}, is observed clearly in the spectra of the products obtained for $t < 21$ min, and for longer times they become overlapped with the band at 1582 cm^{-1}. We suppose that these modes correspond to C=C stretching vibration in a phenazine-like segment,[41] including a contribution from C=N stretching vibrations.[26,42] The spectrum of phenazine itself shows the band at 1627 cm^{-1}. The band at ~1600 cm^{-1} is well observed only in the spectra of products isolated at $t < 17$ min. This absorption, corresponding to a C−C benzene ring-stretching vibration, is situated very close to the positions 1597 and 1602 cm^{-1} found for aniline dimers, *p*-semidine (4-aminodiphenylamine), and *o*-semidine (2-aminodiphenylamine), respectively.

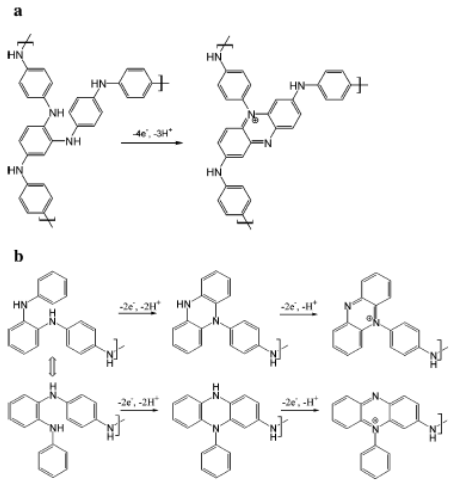

Figure 11. Phenazine-like unit can be formed: (a) at the branching site after oxidation of 1,2,4-trisubstituted ring structure; (b) at the beginning of the chain after oxidation of 1,2-disubstituted ring structure.

The band at ~1414 cm^{-1}, which is present in all the spectra, but is more intense in samples collected at t < 21 min, is a strong indication of the formation of phenazine-like segments (Figure 9). In the polymeric part produced at pH < 4, their presence becomes significantly reduced. This band is not observed in the spectra of standard PANI bases,[36,37] but heterocycles containing several nitrogen atoms are active in this wavenumber region. The band at ~1410 cm^{-1} has been observed in the spectra of pyrazine, phenazine, and polymers containing phenazine units, and it is assigned to a totally symmetric stretching of the phenazine ring.[43,44] Phenazine-like units can be also recognized through the bands at 1208 and 1136 cm^{-1} and its contribution to the bands at 1144 and 1108 cm^{-1} is possible (in the phenazine spectrum, the bands at 1210, 1136, 1147, and 1109 cm^{-1} are present). Their presence may thus be expected, and is indeed observed (Figures 8 and 9), especially in oligomeric products.

Evolution of FTIR Spectra. The strong band at 1582 cm^{-1}, observed at t < 21 min in the spectra of deprotonated samples (Figure 9), becomes even stronger and shifted to 1585 cm^{-1} after this reaction time. This band corresponds to C═C stretching in newly formed quinonoid rings, (the N═Q═N stretching mode).[35,37,45] The massive band at ~1510 cm^{-1} (with a shoulder at ~1496 cm^{-1}) appears in all of the spectra for the reactions times up to 21 min, and a strong band at ~1502 cm^{-1} is observed for longer times. This absorption is characteristic of benzenoid ring-stretching in the N−B−N mode.[37,45] The intensity ratio of the bands due to aromatic C═C stretching vibrations at 1445 and 1414 cm^{-1} (the last one corresponding to phenazine-like segments) is changed at 21 min.

The bands corresponding to C−N stretching vibrations are observed at 1364 cm^{-1} (for all polymerization times), 1378 cm^{-1} (arising at t = 21 min), and 1300 cm^{-1} (present in all the spectra, strengthened (and with a shoulder at 1336 cm^{-1}) for t > 17 min). Kang et al.[37] attributed the 1380 cm^{-1} band in the PANI spectrum to C−N stretching in QB_tQ unit (B_t denotes a trans-benzenoid unit), and the 1315 cm^{-1} band to C−N stretching in QB_cQ, QBB, and BBQ units (B_c denotes a *cis*-benzenoid unit). A band at ~1240 cm^{-1} due to C−N stretching in BBB units is noted in emeraldine-base spectra,[36,37] while we observed two bands at 1240 and 1266 cm^{-1} for all polymerization times. The band at 1266 cm^{-1} is possibly due to C−N vibrations in tertiary arylamine, in phenazine-like units.[27,28]

In the region 900−650 cm^{-1} many bands are observed, attributed to aromatic C−H out-of-plane deformation vibrations γ(C−H), while the spectrum of standard PANI usually has only one band typical of a para-disubstituted benzene ring.[46,47] Besides the presence of 1,4-disubstituted rings as prevalent for all polymerization times, indicating linear elements of chain, FTIR spectroscopy revealed the presence of a significant number of 1,2,4-trisubstituted rings, indicative of branched and/or substituted phenazine-like elements (Figure 11). The band at 827 cm^{-1} corresponding to 1,4-disubstituted rings[16,26,27,46,48] is drastically strengthened at 21 min, becoming the dominant band in this region. The 1,2,4-substitution pattern is revealed by the bands at 864 and 857 cm^{-1} (2 H) before and after t = 17 min, respectively, at 906 cm^{-1} (1 H) during all times,[26] and by the band at 880 cm^{-1} (1 H),[26,33] which appears after t = 17 min. The band at 880 cm^{-1} may be correlated with detected changes in the morphology of the polymeric products in this period. The band at 848 cm^{-1}, well resolved only at t < 21 min, can be due to 1,4- and/or 1,2,4-substituted rings. The mono and 1,2-disubstituted rings correspond to the bands[26] at 726 and 740 cm^{-1}. The bands at 906, 880 (1 isolated H), and 864 (857) cm^{-1} (2H) are attributable to γ(C−H) vibrations of substituted phenazines, too.[26] The 974 cm^{-1} band, strengthened at t > 17 min, corresponds to C−H in-plane deformation vibration of the quinonoid form of a 1,2,4-trisubstituted ring.[29,33]

FTIR spectra of the intermediates corresponding to longer times (t > 17 min) may be assigned to the spectra of standard PANI base[22] with some features of the spectra of samples obtained for t < 17 min (Figure 10). As has been shown, the samples are only partly soluble in chloroform. The insoluble polymer fraction is composed of nanotubes and granular precipitate. We suppose that both parts of this fraction are sulfonated and that the additional peaks, which are also present in the spectra of the insoluble part, belong to the observed nanotubes. The nanotubes also contain phenazine units.

Concluding Remark on Nanotube Formation. It has been proposed[10] that the aniline oligomers produced in the early stages of the polymerization at low acidity of the medium are insoluble in water, and that they aggregate to constitute a template-like structure, which further predetermines the directional growth of PANI, that is, the production of nanotubes. The present study provides additional insight into such a concept. The PANI nanotubes are produced within an intermediate acidity interval; at lower acidity, the products are oligomers, and at higher acidity, PANI has the granular morphology.

The occurrence of nanotubes is clearly associated with the presence of oligomer crystal-like structures that act as templates where the nanotubes growth starts. The presence of phenazine-like units in PANI (Figure 11) is also invariably connected with the existence of nanotubes. We propose that phenazinium units act as discotics that guide the stacking of oligomers as they are produced during the oxidation of aniline, providing the necessary organization and order that predetermine the growth of nanotubes. The sulfonation of PANI, occurring at the same time, may help to stabilize the produced structures by internal protonation, that is, by ionic bonding between sulfonate groups and protonated imine sites in neighboring polymer chains.

Although such a model is speculative, it stimulates the further experiment work in this direction.

Conclusions

The oxidation of aniline in water, that is, in the absence of any added acid, has two distinct exothermic phases. The acidity also increased in two steps from pH 8 at the beginning of the reaction to pH ≈ 1 at its end, the sulfuric acid being a byproduct. The evolution of PANI nanotubes during this process has been observed. Aniline oligomers are produced in the first part of the reaction, a polymer (PANI) in the subsequent regime. The development of oligomer crystals, and later of PANI nanotubes growing from them, has been observed by optical microscopy in PANI films deposited in situ during the polymerization on silicon windows. Precipitated oligomers thus act as a sort of a template, with nanotubes growing from them as branches. The presence of nanotubes of ca. 200 nm external diameter has been confirmed by scanning electron microscopy. The transmission electron microscopy revealed that, besides the nanotubes with an internal cavity, PANI nanorods, nanobubbles, and possibly nanosheets are found in the samples. The final oxidation products are composed of oligomers produced at short reaction times (soluble in chloroform); the polymer component is produced later and contains PANI nanotubes and precipitate (both insoluble in chloroform).

The molecular structure after deprotonation to bases is similar for both oligomers and polymers. Oligomers are not protonated during the reaction while the polymers generated later are. In contrast to the common PANI prepared in acid media, a notable content of sulfur in the samples has been found by elemental analysis. This has been attributed to the sulfonation of benzenoid rings in PANI and confirmed by identifying sulfonate vibrations in the FTIR spectra. Aniline monomers may become sulfonated in the course of the oxidation reaction and they are only later incorporated into the growing chains. The formation of phenazine units in PANI has also been proved with FTIR spectra. Such units are absent in the spectra of standard PANI. It is speculated that phenazine-like units promote the ordering of oligomers by a stacking mechanism, as with discotics. Such structures then provide a template from which PANI nanotubes emerge. The internal protonation, leading to ionic interaction between sulfonate groups and protonated imine sites of PANI chain, helps to stabilize the produced structure.

Acknowledgment. We thank the Grant Agency of the Academy of Sciences of the Czech Republic (A4050313 and A400500504) and the Ministry of Science and Environmental Protection of the Republic of Serbia (Contract no. 142047) for financial support. Thanks are also due to M. Cieslar from the Charles University in Prague for transmission electron micrograph.

References and Notes

(1) MacDiarmid, A. G.; Epstein, A. J. *Faraday Discuss. Chem. Soc.* **1989**, *88*, 317.
(2) Stejskal, J.; Gilbert, R. G. *Pure Appl. Chem.* **2002**, *74*, 857.
(3) Stejskal, J.; Kratochvíl, P.; Jenkins, A. D. *Polymer* **1996**, *37*, 367.
(4) Geng, Y.; Li, J.; Sun, Z.; Jing, X.; Wang, F. *Synth. Met.* **1998**, *96*, 1.
(5) Job, A. E.; Herrmann, P. S. P., Jr.; Vaz, D. O.; Mattoso, L. H. C. *J. Appl. Polym. Sci.* **2001**, *79*, 1220.
(6) Fu, Y.; Elsenbaumer, R. L. *Chem. Mater.* **1994**, *6*, 671.
(7) Beadle, P. M.; Nicolau, Y. F.; Banka, E.; Rannou, P.; Djurado, D. *Synth. Met.* **1998**, *95*, 25.
(8) Sulimenko, T.; Stejskal, J.; Prokeš, J. *Colloid Interface Sci.* **2001**, *236*, 328.
(9) Gospodinova, N.; Mokreva, P.; Terlemezyan, L. *Polymer* **1993**, *34*, 2438.
(10) Konyushenko, E. N.; Stejskal, J.; Šeděnková, I.; Trchová, M.; Sapurina, I.; Cieslar, M.; Prokeš, J. *Polym. Int.* **2006**, *55*, 31.
(11) Ponzio, E. A.; Echevarria, R.; Morales, G. M.; Barbero, C. *Polym. Int.* **2001**, *50*, 1180.
(12) Kolla, H. S.; Surwade, S. P.; Zhang, X.; MacDiarmid, A. G.; Manohar, S. K. *J. Am. Chem. Soc.* **2005**, *127*, 16770.
(13) Stejskal, J.; P. Kratochvíl, P.; Radhakrishnan, N. *Synth. Met.* **1993**, *61*, 225.
(14) Chakraborthy, M.; Mukherjee, D. C.; Mandal, B. M. *Langmuir* **2000**, *16*, 2482.
(15) Trchová, M.; Šeděnková, I.; Stejskal, J. *Synth. Met.* **2005**, *154*, 1.
(16) Neoh, K. G.; Kang, E. T.; Tan, K. T. *Polymer* **1993**, *34*, 3921.
(17) Sapurina, I.; Riede, A.; Stejskal, J. *Synth. Met.* **2001**, *123*, 503.
(18) Palaniappan, S. *Eur. Polym. J.* **2002**, *37*, 975.
(19) Stejskal, J.; Sapurina, I.; Trchová, M.; Prokeš, J. *Chem. Mater.* **2002**, *14*, 3602.
(20) Stejskal, J.; Hlavatá, D.; Holler, P.; Trchová, M.; Prokeš, J.; Sapurina, I. *Polym. Int.* **2004**, *53*, 294.
(21) Stejskal, J.; Sapurina, I. *Pure Appl. Chem.* **2005**, *77*, 815.
(22) Trchová, M.; Šeděnková, I.; Tobolková E.; Stejskal, J. *Polym. Degrad. Stab.* **2004**, *86*, 179.
(23) Yang, C.-H.; Chih, Y.-K.; Cheng, H.-E.; Chen, C.-H. *Polymer* **2005**, *46*, 10688.
(24) Şahin, Y.; Pekmez, K.; Yildiz, A. *Synth. Met.* **2002**, *131*, 7.
(25) Şahin, Y.; Pekmez, K.; Yildiz, A. *Synth. Met.* **2002**, *129*, 107.
(26) Socrates, G. *Infrared and Raman Characteristic Group Frequencies*; Wiley: New York, 2001; pp 78−167.
(27) Vien, D. L.; Colthup, N. B.; Fateley, W. G.; Grasselli, J. G. *The Handbook of Infrared and Raman Characteristic Frequencies of Organic Molecules*; Academic Press: New York, 1991.
(28) Kieffel, Y.; Travers, J. P.; Ermolieff, A.; Rouchon, D. *J. Appl. Polym. Sci.* **2002**, *86*, 395.
(29) Lin, X.; Zhang, H. *Electrochim. Acta* **1996**, *41*, 2019.
(30) Coates, J. In *Encyclopedia of Analytical Chemistry, Interpretation of Infrared Spectra, a Practical Approach*; Meyers, R. A., Ed.; Wiley: Chichester, 2000; pp 10815−10837.
(31) Sapurina, I.; Osadchev, A. Yu.; Volchek, B. Z.; Trchová, M.; Riede, A.; Stejskal, J. *Synth. Met.* **2002**, *129*, 29.
(32) Harada, I.; Furukawa, Y.; Ueda, F. *Synth. Met.* **1989**, *29*, E303.
(33) Bellamy, L. J. *The Infrared Spectra of Complex Molecules*; Richard Clay and Co.: Bungay, Suffolk, 1962; pp 65−84, 249−261.
(34) Wu, Q.; Qi, Z.; Wang, F. *Synth. Met.* **1999**, *105*, 191.
(35) Cases, F.; Huerta, F.; Lapuente, R.; Quijada, C.; Morallón, E.; Vázquez, J. L. *J. Electroanal. Chem.* **2002**, *529*, 59.
(36) Boyer, M. I.; Quillard, S.; Rebourt, E.; Louarn, G.; Buisson, J. P.; Monkman, A.; Lefrant, S. *J. Phys. Chem. B* **1998**, *102*, 7382.
(37) Kang, K. G.; Neoh, K. L.; Tan, T. C. *Prog. Polym. Sci.* **1998**, *23*, 277.
(38) Neoh, K. G.; Pun, M. Y.; Kang, E. T.; Tan, K. L. *Synth. Met.* **1995**, *73*, 209.
(39) Lee, J. Y.; Cui, C. Q.; Su, X. H.; Zhou, M. S. *J. Electroanal. Chem.* **1993**, *360*, 177.
(40) Ćirić-Marjanović, G.; Trchová, M.; Stejskal, J. *Collect. Czech. Chem. Commun.*, submitted for publication.
(41) Li, X.-G.; Duan, W.; Huang, M.-R.; Yang, Y.-L. *J. Polym. Sci. Part A: Polym. Chem.* **2001**, *39*, 3989.
(42) Malinauskas, A.; Bron, M.; Holze, R. *Synth. Met.* **1998**, *92*, 127.
(43) Viva, F. A.; Andrade, E. M.; Molina, F. M.; Florit, M. I. *J. Electroanal. Chem.* **1999**, *471*, 180.
(44) Dines, T. J.; MacGregor, L. D.; Rochester, C. H. *Phys. Chem. Chem. Phys.* **2001**, *13*, 2676.
(45) Kulszewicz-Bajer, I.; Różalska, I.; Kurylek, M. *New J. Chem.* **2004**, *28*, 669.
(46) Geniès, E. M.; Penneau, J. F.; Lapkowski, M.; Boyle, A. *J. Electroanal. Chem.* **1989**, *269*, 63.
(47) Thiemann, C.; Brett, C. M. A. *Synth. Met.* **2002**, *125*, 445.
(48) Zhang, L.; Long, Y.; Chen, Z.; Wan, M. *Adv. Funct. Mater.* **2004**, *14*, 693.

Appendix C

Jaroslav Stejskal, Irina Sapurina, Miroslava Trchová, Elena N. Konyushenko, and Petr Holler,

The genesis of polyaniline nanotubes,

Polymer **47:** 8253–8262 (2006).

Available online at www.sciencedirect.com
ScienceDirect
Polymer 47 (2006) 8253–8262
polymer
www.elsevier.com/locate/polymer

The genesis of polyaniline nanotubes

Jaroslav Stejskal [a,*], Irina Sapurina [b], Miroslava Trchová [a], Elena N. Konyushenko [a], Petr Holler [a]

[a] *Institute of Macromolecular Chemistry, Academy of Sciences of the Czech Republic, Heyrovsky Sq. 2, 162 06 Prague 6, Czech Republic*
[b] *Institute of Macromolecular Compounds, Russian Academy of Sciences, St. Petersburg 199004, Russia*

Received 26 June 2006; received in revised form 26 September 2006; accepted 1 October 2006
Available online 27 October 2006

Abstract

Aniline has been oxidized with ammonium peroxydisulfate in 0.4 M acetic acid. Protons are produced in the course of oxidation and the pH decreases as the reaction proceeds. The oxidation had two subsequent phases: (1) the oxidation of the neutral aniline molecules and the initially produced low-molecular weight aniline oligomers at low acidity, followed by (2) the oxidation of the anilinium cation after the acidity became higher. The two phases of oxidation gave different products, aniline oligomers with mixed *ortho*- and *para*-coupling of aniline molecules, and polyaniline nanotubes, respectively.

The aniline oligomers are produced at first at low acidity, pH > 4, some of them as rod-like crystals. The molecular weight of the oligomers has been assessed by gel-permeation chromatography to be of several thousands. The 2–3 wt.% content of sulfur in deprotonated samples suggests that the oxidation products are partly sulfonated. The oxidation of *ortho*-coupled anilines combined with intramolecular cyclization produces phenazine units or their blocks, as indicated by FTIR spectra. A high-molecular weight polyaniline is produced at pH < 2. The protonation of the intermediate pernigraniline form of polyaniline is a prerequisite for the polymerization.

The nano-sized oligomer crystallites serve as starting templates for the nucleation of PANI nanotubes. Further growth of nanotubes proceeds by the self-organization of the phenazine units or their blocks located at the ends of the PANI chains. Polyaniline nanotubes have a typical outer diameter of 100–200 nm, with a wall thickness of 50–100 nm, an inner diameter of 0–100 nm, and a length extending to several micrometres.

Keywords: Conducting polymer; Conductivity; Polyaniline nanotubes

1. Introduction

The importance of the conducting polymers, like polyaniline (PANI) and polypyrrole, has been recognized for many years [1–3]. The observation that these polymers can produce "one-dimensional" morphologies, like nanotubes [4–8], nanowires [9–16] or non-spherical colloidal nanoparticles [17–22], made them the exciting object of many investigations. The polymerization of aniline on "soft" templates, micellar structures involving aniline or aniline salts, has been offered as an explanation for the nanotube formation [6,11,12,16]. The oxidation of pyrrole on "hard" templates, afforded by inorganic nanofibers [8] or crystals of pyrrole salts [21,22], has also been reported. Low concentrations of acids with respect to aniline [11,23] and the use of organic acids [5,24] have usually been needed to obtain PANI nanotubes. Under these conditions, the oxidation of aniline starts at relatively low acidity of the medium. In a previous communication [7], we have proposed that the morphology development is controlled by the acidity of the reaction mixture and the consequent protonation of aniline, the reaction intermediates, and PANI. The *process* by which PANI nanotubes are generated has not been discussed so far. In this study, we report the individual phases of aniline oxidation, demonstrate the growth of nanotubes, and propose a model for nanotube formation.

* Corresponding author. Tel.: +42 0296809351; fax: +42 0296809410.
E-mail address: stejskal@imc.cas.cz (J. Stejskal).

0032-3861/$ - see front matter © 2006 Elsevier Ltd. All rights reserved.
doi:10.1016/j.polymer.2006.10.007

2. Experimental

2.1. Oxidation of aniline

Aniline (0.2 M) was oxidized with ammonium peroxydisulfate (APS, 0.25 M) in 0.4 M acetic acid (Fig. 1). Solutions of aniline monomer and oxidant were mixed at room temperature to start the oxidation. The reaction mixture was quickly poured over silicon windows, used in FTIR spectroscopy (26 mm in diameter), and placed in separate Petri dishes. The windows were slightly raised on a support so that the reaction mixture had access to both the top and bottom sides. After specified times, based on the preliminary determination of the course of polymerization, the silicon windows were removed from the mixture. The oxidation reaction was stopped by rinsing the oxidation products deposited on the windows with water, which removed aniline and oxidant, followed by drying in air.

The residual reaction mixture left after the removal of the silicon window was poured immediately into an excess of 1 M ammonium hydroxide to stop the polymerization. The precipitate was quickly collected on a filter, thus separated from the residual monomer and oxidant, and dried in air.

2.2. Microscopy

The research-grade optical Leica DM LM Microscope, equipped with 50× Olympus objective lenses, a scanning electron microscope (SEM) JEOL 6400 and a transmission electron microscope (TEM) JEOL JEM 2000 FX have been used to characterize the morphology of the samples.

2.3. Gel-permeation chromatography

Molecular weights were assessed with a GPC/SEC apparatus using a 8 × 600 mm PLMixedB column (Polymer Laboratories, UK) operating with *N*-methylpyrrolidone and calibrated with polystyrene standards with spectrophotometric detection at the wavelength of 650 nm. The samples were dissolved in *N*-methylpyrrolidone containing 0.025 g cm^{-3} triethanolamine for deprotonation of samples, and 0.005 g cm^{-3} lithium bromide to prevent aggregation.

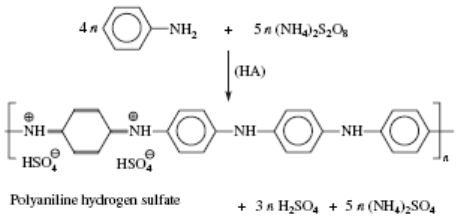

Fig. 1. The oxidation of aniline with ammonium peroxydisulfate in water yields PANI hydrogen sulfate. The *para* addition of constitutional units is shown but *ortho* addition can also be important. Sulfuric acid and ammonium sulfate or ammonium hydrogen sulfate are the by-products.

2.4. FTIR spectroscopy

Infrared spectra in the range of 400–4000 cm^{-1} were recorded at 64 scans per spectrum at 2 cm^{-1} resolution using a fully computerized Thermo Nicolet NEXUS 870 FTIR Spectrometer with a DTGS TEC detector. The spectra of the thin films deposited *in situ* on a silicon substrate were measured in the transmission mode. An absorption-subtraction technique was applied to remove the spectral features of the silicon wafers. FTIR spectra of powders were measured in the transmission mode after dispersion of the samples in potassium bromide pellets. The spectra were corrected for the presence of carbon dioxide and humidity in the optical path.

3. Results

We have recently reported [7] that the morphology of PANI, obtained after the oxidation of aniline under various acidity conditions, varies: in solutions of strong (sulfuric) acid, a common granular PANI was produced, while in solutions of weak (acetic) acid, PANI nanotubes were obtained. The internal cavity of the PANI nanotubes is easily visible in TEM micrographs (Fig. 2). Nanorods without a bore accompany

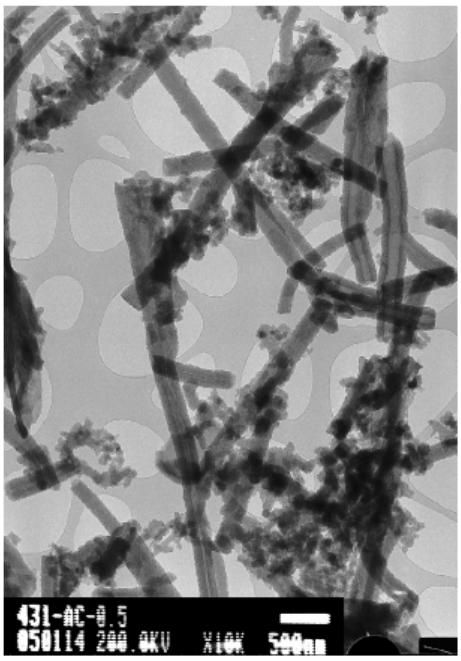

Fig. 2. TEM micrographs of PANI nanotubes and related structures.

the nanotubes. In the present paper, we concentrate on the process of nanotube formation.

3.1. The course of aniline oxidation

The oxidation of aniline is an exothermic process, and its course is easily followed by recording the reaction temperature [25,26] (Fig. 3A). The oxidation of aniline in water or in mildly acidic solution proceeds in two consecutive phases [7,25,27]. This is illustrated in the present study on the oxidation of aniline in 0.4 M acetic acid (Fig. 3A).

The oxidation of aniline starts [28] at pH 4.5 (Fig. 3B). The pK_a of aniline [25,29] is 4.6. Under such conditions, aniline exists as an approximately equimolar mixture of neutral molecules, which are easily oxidized, and anilinium cations, which are oxidized much more slowly [28]. The temperature of the reaction mixture increases as the oxidation proceeds. At the same time, the pH decreases [25,27,30], because hydrogen atoms, abstracted during the oxidation from amino groups and benzene rings, are released as protons, *i.e.*, as sulfuric acid [31–33] (Fig. 1) or hydrogen sulfate salt [25]. The pH value at the end of polymerization is 1.2.

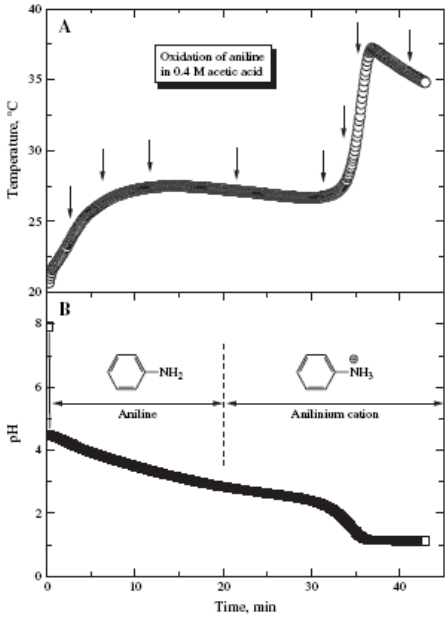

Fig. 3. (A) Temperature and (B) acidity changes during the oxidation of 0.2 M aniline with 0.25 M ammonium peroxydisulfate in 0.4 M acetic acid, started at ~22 °C. The times of sample collection are marked with arrows. The border between the predominance of neutral aniline molecules and anilinium cations is only approximate.

As the pH becomes lower than 4 (Fig. 3B), aniline molecules become protonated and convert to anilinium cations [28]. That is why the mechanism of the oxidation changes and the oxidation proceeds as in solutions of strong acids. In strongly acidic media, an athermal induction period is followed by the exothermic polymerization [25,31]. Thus, after 14 min of reaction, an induction period intervenes, which extends to 32 min (Fig. 3A).

The induction period extends this far, as the pH drops below 2, when the oxidized oligomeric intermediate, pernigraniline, becomes protonated [25,34]. The protonation of the pernigraniline form of PANI, manifested by the typical blue colour of the reaction mixture, is a prerequisite for the formation of conducting PANI of high molecular weight. We can thus conclude that the mechanism of aniline oxidation depends on whether the aniline molecules and the reaction intermediates based on aniline are protonated or not.

3.2. Evolution of nanotubes

The preparation of PANI nanotubes has been well documented [3,5,7,23]; studies related to the *process* of their formation, however, are scarce [35]. The oxidation of aniline in 0.4 M acetic acid yields products, which are insoluble in the aqueous medium. After the beginning of oxidation, they precipitate from the reaction medium as semi-crystalline oligomers, rod-like objects, which have the dimensions of several micrometres. They are easily visible by optical microscopy (Fig. 4A), and the SEM reveals details of their complex structure (Fig. 5). Only in the advanced stage of aniline oxidation, $t > 21$ min, we can observe nanotubes growing from them (Fig. 4B,C). The fact that they are nanotubes is demonstrated, in addition to TEM images (Fig. 2), also by SEM images (Fig. 6) – the internal cavity in broken nanotubes is easily visible (Fig. 6B). The typical outer diameter of nanotubes is 100–200 nm, the inner diameter is 0–100 nm.

Optical microscopy illustrates the fact that the nanotubes grow from macroscopic templates just as tree branches stem from trunks (Fig. 4B,C). There are no loose nanotubes, and the PANI structure has a connective character. This reflects the basic principle of PANI formation: chain growth beyond the dimer stage occurs in the solid-state structure that has already been produced, not in solution [36]. The granular PANI precipitate is produced close to the end of polymerization (Fig. 4D). As it sediments, it covers the nanotubular structure deposited on the silicon windows. This precipitate virtually always accompanies the nanotubes (Fig. 2).

In addition to nanotubes, other objects are also present. Nanospheres of *ca* 50 nm diameter are observed by SEM (Figs. 5A,6A). In fact, nanospheres could be in the same relation to the nanotubes, as fullerene and single-wall nanotubes are related in the realm of carbon chemistry. They are hardly discernible by optical microscopy (Fig. 4B). Our previous study [7] as well as other papers [23,37] has also shown nanospheres in TEM micrographs. Hollow PANI nanospheres were also produced when aniline was polymerized in the presence of triblock copolymers [38]. The role of the acidity of the

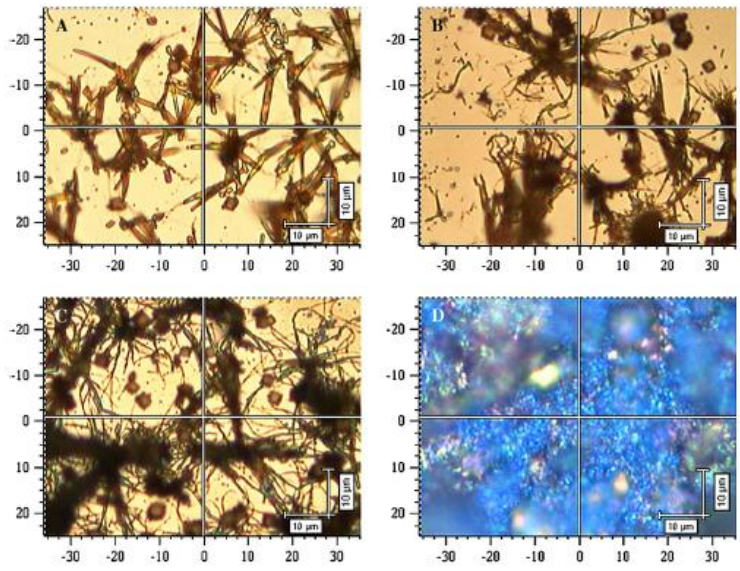

Fig. 4. Optical microscopy of the oxidation products deposited on silicon windows after reaction times t = (A) 5, (B) 21, (C) 31, and (D) 38 min.

reaction mixture in the formation of hollow PANI microspheres has also recently been reported [33].

3.3. The characterization of reaction intermediates by GPC

Samples of reaction intermediates have been collected in the course of oxidation at the times t marked by arrows in Fig. 3. The oxidation products produced at the beginning of reaction are the oligomers having a molecular weight of the order of thousands (Fig. 7). Their molecular weight does not change as the oxidation proceeds. Only after the reaction time $t = 35$ min, polymers are produced in the second oxidation step. This is illustrated by the shoulder of the molecular weight distribution extending into the region of high molecular weights (Fig. 7). Oligomer products are still present in samples collected in the end of oxidation. This indicates that oligomers have not been converted to polymers but only accompany them.

3.4. Separation by solubility in chloroform

The product collected in the early stages of aniline oxidation, $t = 3$ min, is only partly soluble in chloroform (24.8 wt.%). When the chloroform solution was evaporated on a silicon support, the square cross-like and branched crystals have been observed. This means that similar objects of 2–3 μm^2 size, observed in Figs. 4B,5A,6A, are composed of oligomers and not by polymers.

The final oxidation products typically contain both oligomeric and polymeric components (Fig. 7). We have attempted to separate them by extraction of the oligomeric fraction with chloroform. GPC in *N*-methylpyrrolidone proves that the fraction of the oxidation product soluble in chloroform (14.6 wt.%) has an oligomeric nature (Fig. 8). Some oligomers, however, are still entrapped in the chloroform-insoluble fraction.

3.5. Sulfur in polyaniline

Sulfur is present in all the PANI bases collected during synthesis (Fig. 9). The content of sulfur in the samples increases with the reaction time. It is much higher than in the standard PANI prepared in the presence of strong acids [31], 0.3 wt.%, and it has often been neglected in the literature [33]. Please note a certain similarity between Fig. 9 and the temperature profile in Fig. 3; this means that the sulfur content increases during the exothermic oxidation phases, as expected.

Support for the occurrence of sulfonation is found in the FTIR spectra. Sulfonate groups attached to the aromatic rings have been identified by the absorption peaks [39] at 1040 and 695 cm^{-1} (Fig. 10). These bands correspond to the S=O and S–O stretching vibration modes. The presence of these bands in the spectra of alkali-treated samples confirms that sulfonate groups are covalently bonded to the reaction intermediates during reaction, and not only on the completed oligomer or polymer. It seems that aniline molecules present at low acidity can also be sulfonated to *o*-aminobenzenesulfonic acid, which

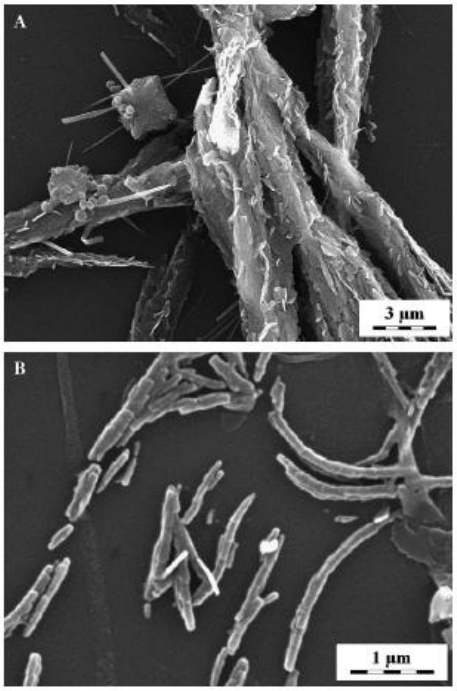

Fig. 5. SEM images of the oligomeric products obtained on silicon windows after the reaction time $t = 5$ min. Two magnifications (A,B).

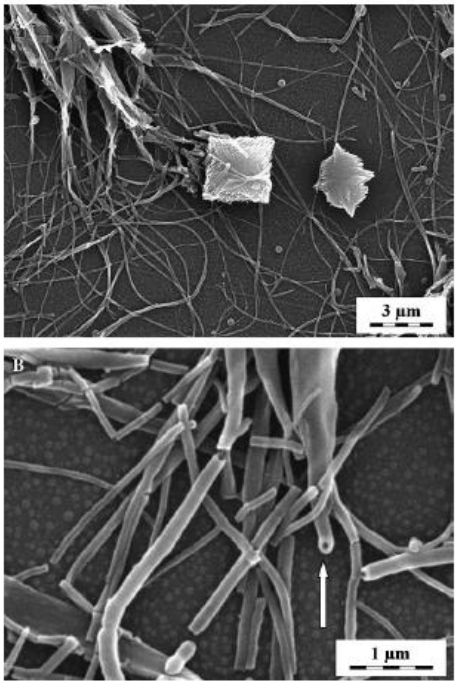

Fig. 6. SEM images of the polyaniline nanotubes produced on silicon windows after the reaction time $t = 34$ min. The internal cavity of a nanotube is marked by an arrow at the bottom micrograph. Two magnifications (A,B).

is subsequently copolymerized with aniline [40]. The sulfonate groups interact with protonated imine nitrogens in neighbouring chains and thus stabilize the supramolecular structure produced by PANI by ionic bonding [40,41].

3.6. Conductivity

Conductivity is a key parameter for this type of polymers; for typical PANI it attains the values of units S cm^{-1} [2,31]. The oligomeric products isolated in the early stages of oxidation in 0.4 M acetic acid are non-conducting, having the conductivity 2.4×10^{-10} S cm^{-1}, the conductivity of product after the completion of reaction is 0.078 S cm^{-1}. The reduced conductivity is a consequence of the two-component nature of the product composed of non-conducting oligomers and conducting PANI.

4. Discussion

4.1. Historical background

In 1856, Perkin oxidized the crude aniline, containing some toluidines, with potassium dichromate [42]. In addition to a black precipitate [42,43] (most likely, a mixture of aniline black and PANI in present terminology [44–46]), he was able to extract a purple dye, mauveine (Fig. 11A), the first

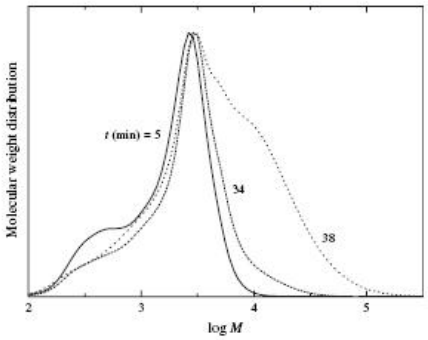

Fig. 7. Weight distributions of molecular weights M (normalized to a peak value) of the intermediates in the oxidation of aniline obtained after reaction times $t = 5$ (full line), 34 (dashed line), and 38 min (dotted line).

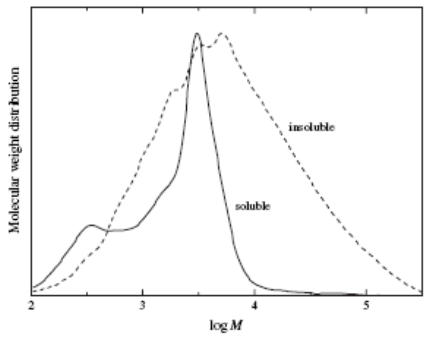

Fig. 8. Weight distributions of molecular weights M (normalized to a peak value) of the chloroform-soluble (full line) and chloroform-insoluble (dashed line) fractions of the final oxidation product.

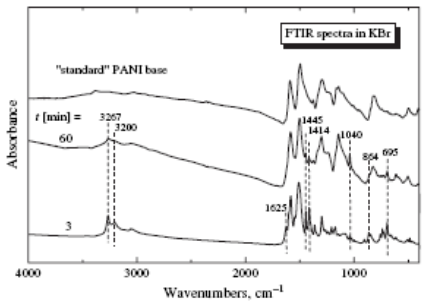

Fig. 10. FTIR spectra of samples collected at the beginning of aniline oxidation in acetic acid, $t = 3$ min, and of the final product, at $t = 60$ min. The spectrum of the PANI base, corresponding to its standard preparation in the acidic medium [31], is shown for comparison.

industrially produced dyestuff. The later oxidation of pure aniline reported in 1896 led to pseudomauveine [43] (Fig. 11B). This means that soluble protonated phenazinium structures are produced during the oxidation of aniline, and non-protonated phenazine units have been suggested as a major component in the insoluble polymeric product, aniline black [47,48] and in PANI [49]. The generation of phenazine units in PANI has also been predicted by semi-empirical quantum chemical calculations [28], and often been reported to be a result of ageing processes in PANI [50–54].

4.2. The principles of aniline oxidation

The oxidation of aniline in solutions of strong acids is the currently accepted method for preparing a conducting polymer, *i.e.*, PANI [1,2,31]. Under these reaction conditions, aniline is present as an anilinium cation, and its oxidation leads to PANI in which the aniline constitutional units are linked with a strong preference for the *para*-positions [1,54] (Fig. 1). This is generally accepted in all the proposed reaction mechanisms [1,29,55–57] and also experimentally confirmed by the oxidation of PANI to *p*-quinone [50]. Such PANI has good conductivity and, although the reaction conditions have been widely varied in the search for conductivity improvement [58,59], the high acidity of the medium has been maintained as a rule.

Oxidation started in mildly acidic [60] or even in alkaline medium [27,61] proceeds more easily [62] compared with strongly acidic media. Quantum chemical calculations have shown that aniline, which is present at pH > 4.6 mainly as a neutral molecule, is more readily oxidized than the anilinium cation [28]. These calculations also show the importance of *ortho*-coupling besides the prevalent *para*-coupling of the aniline molecules (Fig. 12A).

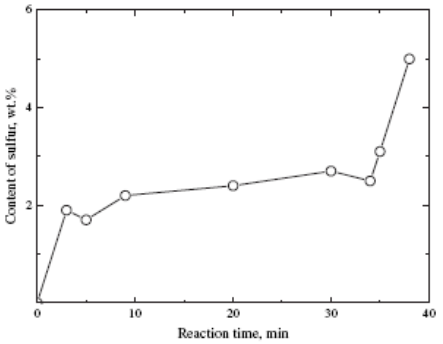

Fig. 9. The content of sulfur in the product of aniline oxidation in 0.4 M acetic acid collected after specified reaction time and deprotonated with 1 M ammonium hydroxide.

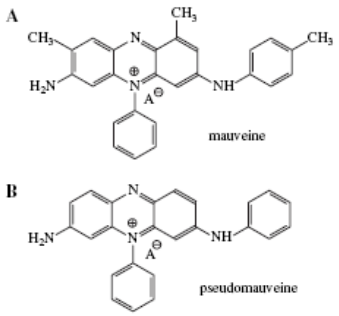

Fig. 11. (A) Mauveine, the first industrially produced synthetic dyestuff, and (B) pseudomauveine [42].

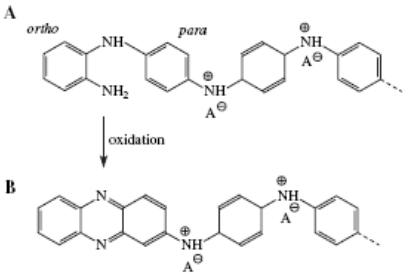

Fig. 12. (A) During the oxidation in mildly acidic media, aniline molecules couple in both the *ortho*- and *para*-positions. (B) Further oxidation of *ortho*-coupled units yields a phenazine unit, *e.g.*, at the beginning of the PANI chain [28].

The presence of *ortho*-coupled aniline molecules [63,64] in the early oxidation products resembles the situation in the oxidation of *o*-phenylenediamine [65]. Its electrochemical polymerization results in PANI-like chains with pendant amino groups but, under acidic conditions, ladder-like units of the phenazine type (Fig. 12B) were produced preferentially [66]. As the oxidation of aniline proceeds, the pH gradually decreases (Fig. 3), and this is the reason why the conversion of *ortho*-coupled aniline molecules to phenazine units is initiated (Fig. 12B). The oxidation of *o*-aminodiphenylamine, an intermediate of aniline oxidation, also yields oligomers comprising phenazine units as components [67]. When aniline has been oxidized in the media of various acidity, the initial oxidation products had optical absorption with a maximum at 370 nm [30,33], shifting to the 500 nm region, which could be assigned to the increasing conjugation in the oligomers [68] or to the formation of phenazine structures [69].

The newly produced phenazine units, or their segments, may act as initiation centres for the growth of conventional PANI, subject to the condition that pH < 2 and the intermediate pernigraniline units become protonated. Once growth starts, the aniline constitutional units are linked in the *para*-positions, due to the formation of the conducting conjugated system represented by protonated pernigraniline [25]. The propagation proceeds with a preference over initiation of PANI chains, as is illustrated by the high molecular weight of the products (Fig. 7). The resulting chains are thus expected to have a phenazine head segment and a tail of *para*-linked aniline constitutional units (Fig. 12B).

4.3. Phenazine structures in FTIR spectra

The spectrum of the final oxidation product is close to the spectrum of the PANI base prepared by a conventional method in solutions of strong acids [31] (Fig. 10). Some additional peaks are marked by dashed lines in the spectrum of the final product prepared in 0.4 M acetic acid. They are well distinguished in the spectrum of aniline oligomers (Fig. 10) and can be assigned to phenazine units (Fig. 12B). The band at 1625 cm^{-1} corresponds to the absorption of the C=C ring-stretching vibration in newly-formed substituted phenazine-like segments [70] together with the band observed at 1414 cm^{-1}, attributable to a totally symmetric stretching of the phenazine heterocyclic ring [71,72]. Phenazine-like units can also be recognized through the bands at 1208 cm^{-1} and by their contribution to the bands at 1144 and 1108 cm^{-1}. The presence of significant amount of 1,2,4-trisubstituted rings, indicative of the formation of branched and/or substituted phenazine-like segments, is revealed by the bands [41] at 864 and 858 cm^{-1}. The peaks attributable to phenazine units are more pronounced in the oligomers produced at the beginning of polymerization [35] (Fig. 10). We suppose that these peaks are overlapped by the spectrum of the newly formed *para*-coupled chains, which are generated in large excess.

4.4. Hydrogen bonding

The two relatively strong bands in the FTIR spectra, with maxima at 3267 and 3200 cm^{-1} (Fig. 10), have often been attributed to different types of intra- and inter-molecular hydrogen-bonded N–H stretching vibrations of secondary amines, N–H···N [73]. Hydrogen bonding in N–H···O, where oxygen atom belongs to a sulfonate group (discussed in Section 3.5), is also possible [35,74–77]. The presence of hydrogen bonding is indicative of the self-organization of PANI chains into supramolecular assemblies, like thin films [78–81] and nanotubes [24]. They are not found in the spectra of PANI having the common granular morphology, and seem to be associated here with the presence of nanotubes.

5. The concept of nanotube formation

5.1. Aniline oxidation

The following scenario is offered: aniline oxidation, which starts in mildly acidic conditions, at pH > 4, results in the coupling of aniline molecules in *ortho*- and *para*-positions to produce oligomers having, on average, 50–60 constitutional units. They are non-conducting. As the acidity increases, the newly *ortho*-coupled units become oxidized to phenazine units. The growth of oligomer chains proceeds to yield polymer chains at still higher acidity, pH < 2, when the intermediate pernigraniline unit can be protonated. This is reflected in the fast exothermic polymerization of aniline, producing long PANI chains.

Under highly acidic conditions, pH ~ 0–1, which are typical for PANI preparation, the proportion of phenazine participation is reduced in favour of the formation of *para*-coupled chains, which are generated in large excess. Moreover, the phenazine units become protonated [82], $pK_a = 1.2$.

5.2. Nucleation of nanotubes

The aniline oligomers produced in the early stages of oxidation are insoluble in the reaction medium; the solubility of

aniline dimers, semidines, is low [60]. Oligomers precipitate, often with frequent needle-like crystallite offsprings (Fig. 5A, upper left corner). These crystallites serve as templates for the future nucleation of PANI nanotubes.

When the acidity of the reaction mixture becomes sufficiently high, the phenazine units may initiate the propagation of polymer chains. Due to their flat structure, such hydrophobic units adsorb on the available surfaces. On solid surfaces, they nucleate the growth of PANI thin films [83,84] or the coatings of microparticles [85]. When adsorbed on added water-soluble polymer, they start the growth of colloidal dispersion particles [86,87]. The walls of the oligomer needle-like crystals similarly act as sites for the adsorption of the phenazine entities.

Various crystals present in the reaction mixture become coated with a thin conducting polymer film [21], similarly as macroscopic surfaces [88,89], or serve as centres for PANI growth [60]. The coating with PANI depends on the nature of the surface. The adsorption of phenazine units at the surface of needle-like oligomer offsprings is selective, due to the obvious anisotropy of the crystallites. We assume that the phenazine units are adsorbed on the walls of oligomer crystallites, leaving the front surfaces uncoated. In this way, the nucleus of the nanotubes is produced as a sleeve on an oligomer needle. The size of the crystallite inside determines the inner diameter of the future nanotube. Nanotubular structures with a rectangular hole, obviously produced by this mechanism, have been reported in the literature [90], and support this mechanism. The thickness of the nanotube wall corresponds to the thickness of the deposited PANI film, *e.g.*, on glass [84] ~100 nm, and is proportional to the molecular weight of the PANI chains [91], *i.e.* to their extended chain length. The front surfaces of this nanotubular nucleus have exposed phenazine units adjacent to the crystallite front.

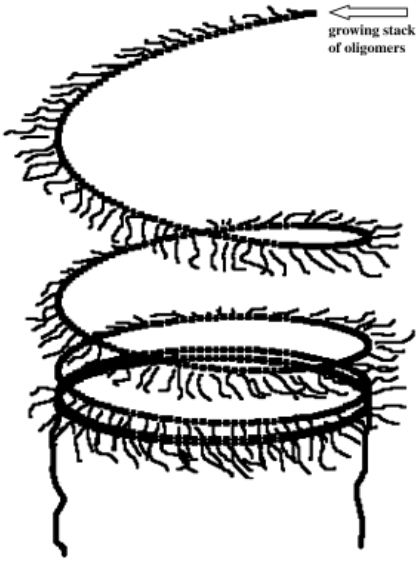

Fig. 13. The phenazine units at the start of PANI chains (squares) stack on each other, and PANI chains extend from them. The individual spiral threads are shown as being separated just for the clarity of illustration, we believe, however, that each thread closely copies the previous one and there is no separation between them. Hydrogen bonding and ionic interactions between the chains in the neighbouring threads stabilize the nanotubular structure. The oligomer crystallites nucleate the growth but the nanotube grows on its own without any external template.

5.3. The growth of a nanotube

In addition to their hydrophobic character promoting phase separation, phenazine derivatives (Fig. 12B) have a flat molecular structure that is able to produce columnar aggregates supported by $\pi-\pi$ electron interactions [92,93]. The newly produced phenazine units thus add to the exposed units at the nanotubular nucleus (Fig. 13). The PANI chains are growing from them in the preferred direction given by molecular geometry (Fig. 12B). Assembly of the terminal phenazine units thus binds the PANI chain-beginnings together. The self-ordering produced is further stabilized during the chain growth of PANI counterparts by hydrogen bonding and ionic interactions. That is why the nanotube continues to grow without any guide and with an internal cavity determined by nucleus size. This concept can be supported by the observation of nanotubular growth in polycarbonate membranes, which continue to grow beyond the membrane limits, still preserving the nanotubular morphology [94].

The growth of one-dimensional structures can also be initiated without any template. In this case, we assume that phenazine terminal units associate with each other more loosely. Stacks of one-dimensional fibrils of phenosafranines (including phenazine structures) of 1 nm diameter, which corresponds approximately to the size of a phenazine heterocycle [95], have been reported in the literature [69]. PANI chains extending from them produce a brush. A nanorod or nanowire without an internal cavity is produced instead of a nanotube. Such nanorods are observed to accompany the nanotubes (Fig. 2), and their mutual proportions are likely to be pH-dependent. At $pH < 2$, the phenazine heterocycles become protonated [82], the resulting phenazinium units are hydrophilic, and their ability to guide the self-ordering of polymer chains is lost. The common granular morphology of PANI is then produced [31].

The concept of soft templates, currently used in the literature [6,11,12,16], assumes the existence of micelles produced by aniline salts and the growth of PANI chains in such micellar structures. In this sense, the present model is similar in that it assumes the presence of a suitable template for the production of a nucleation site. The template nature, however, is proposed to be different, being produced by aniline oligomers rather than by a monomer. The salts of aniline with bulky organic acids [16], which may have limited solubility and crystallize

from the reaction medium, may produce a suitable template for the start of nanotubular growth [21].

5.4. The role of PANI conductivity in the polymerization of aniline

Another point is pertinent for the discussion of nanotubular growth. The oxidation of aniline to PANI is a redox process, in which the electrons are abstracted from aniline molecules and transferred to an oxidant. Peroxydisulfate accepts the electrons and converts to sulfate (Fig. 1). When PANI is produced, being a conducting polymer, it mediates the transfer of electrons between the aniline molecule and an oxidant [96]. This means that the aniline constitutional unit which is added to the growing end of a PANI nanotube can be oxidized, not only by the peroxydisulfate molecule in the vicinity, but also by *any* oxidant molecule that is close to the whole growing nanotube; the electrons are transferred through the conducting body of the already-produced PANI nanotube, without the necessity for oxidant and aniline molecules to meet directly. The probability that the PANI nanotube will grow thus increases with its length or, more generally, the mass of the produced PANI. It is thus much higher than the probability of aniline oxidation outside such a structure, which would lead to the nucleation of a new nanotube. This mechanism explains the auto-acceleration effect in aniline polymerization [56,57,97], and the topological connectivity of the PANI structure that is produced.

6. Conclusions

Polyaniline obtained by the chemical oxidation of aniline is produced in various morphologies. The reaction mechanism changes according to the acidity, which increases during the oxidation. The oxidation of neutral aniline molecules at moderate acidity, pH > 4, results in the formation of oligomers. They are composed of aniline constitutional units linked in both *ortho*- and *para*-positions. At higher acidity, neutral aniline molecules become protonated to anilinium cations, which are more difficult to oxidize but yield similar products. The oxidation of *ortho*-coupled units at higher acidity produces phenazine structures. These are adsorbed at the available surfaces and self-organize. It is proposed that they initiate the growth of PANI chains at pH < 2; a protonated pernigraniline intermediate is then produced. Chain growth proceeds with a strong preference for the coupling of aniline constitutional units in the *para*-positions.

It is proposed that needle-like oligomer crystallites serve as template sites for the growth of nanotubes after they become coated with PANI. Nanotubular growth proceeds beyond the template nucleus, without any external guide. The terminal phenazine units self-assemble and guide the growth of PANI chains, thus producing a nanotube wall. Once the tubular growth has started, each thread of the produced spiral copies the previous one. Hydrogen bonding and ionic interactions between the neighbouring PANI chains stabilize the supramolecular nanotubular structure.

Acknowledgments

The authors thank the Grant Agency of the Academy of Sciences of the Czech Republic (A4050313 and A400500504) and the Ministry of Education, Youth, and Sports of the Czech Republic (ME 847), and the Federal Agency for Science and Innovations (2005 RI-12.0/004/028) for the financial support. Thanks are due to J. Hromádková from the Institute of Macromolecular Chemistry and to M. Cieslar from Charles University in Prague for the microscopic characterization of samples and to G. Ćirić-Marjanović from the University of Belgrade for helpful comments.

References

[1] Genies EM, Boyle A, Lapkowski M. Synth Met 1990;36:139.
[2] Trivedi DC. In: Nalwa HS, editor. Handbook of organic conductive molecules and polymers, vol. 2. Chichester: Wiley; 1997. p. 505–72.
[3] Quadrat O, Stejskal J. J Ind Eng Chem 2006;12:352.
[4] Huang J, Wan M. J Polym Sci Part A Polym Chem 1999;37:1277.
[5] Long Y, Zhang L, Ma Y, Chen Z, Wang N, Zhang Z, et al. Macromol Rapid Commun 2003;24:938.
[6] Zhang Z, Wei Z, Zhang L, Wan M. Acta Mater 2005;53:1373.
[7] Konyushenko EN, Stejskal J, Šeděnková I, Trchová M, Sapurina I, Cieslar M, et al. Polym Int 2006;55:31.
[8] Zhang X, Manohar SK. J Am Chem Soc 2005;127:14156.
[9] Zhang X, Goux WJ, Manohar SK. J Am Chem Soc 2004;126:4502.
[10] Zhang XY, Kolla HS, Wang XH, Raja K, Manohar SK. Adv Funct Mater 2006;16:1145.
[11] Chiou N-R, Epstein AJ. Adv Mater 2005;17:1679.
[12] Huang K, Wan M, Long Y, Chen Y, Wei Y. Synth Met 2005;155:495.
[13] Huang J. Pure Appl Chem 2006;78:15.
[14] Kan J, Zhang S, Jing G. J Appl Polym Sci 2006;99:1848.
[15] Li D, Kaner RB. J Am Chem Soc 2006;128:968.
[16] Zhang L, Zhang L, Wan M, Wei Y. Synth Met 2006;156:454.
[17] Stejskal J, Špírková M, Riede A, Helmstedt M, Mokreva P, Prokeš J. Polymer 1999;40:2487.
[18] Chattopadhyay D, Chakraborty M, Mandal BM. Polym Int 2001;50:538.
[19] McCarthy PA, Huang J, Yang S-C, Wang H-L. Langmuir 2002;18:259.
[20] Jing X, Wang Y, Wu D, She L, Guo Y. J Polym Sci Part A Polym Chem 2004;44:1014.
[21] Diez I, Tauer K, Schulz B. Colloid Polym Sci 2004;283:125.
[22] Diez I, Tauer K, Schulz B. Colloid Polym Sci 2006;284:1431.
[23] Zhang Z, Wei Z, Wan M. Macromolecules 2002;35:5937.
[24] Zhang L, Long Y, Chen Z, Wan M. Adv Funct Mater 2004;14:693.
[25] Fu Y, Elsenbaumer RL. Chem Mater 1994;6:671.
[26] Sbaite P, Huerta-Vilca D, Barbero C, Miras MC, Motheo AJ. Eur Polym J 2004;40:1445.
[27] Gospodinova N, Mokreva P, Terlemezyan L. Polymer 1993;34:2438.
[28] Ćirić-Marjanović G, Trchová M, Stejskal J. Collect Czech Chem Commun 2006;71:1407.
[29] Ding Y, Padias AB, Hall Jr HK. J Polym Sci Part A Polym Chem 1999;37:2569.
[30] Neoh KG, Kang ET. Polymer 1993;34:3921.
[31] Stejskal J, Gilbert RG. Pure Appl Chem 2002;74:857.
[32] Palaniappan S, Saravanan C, John A. J Macromol Sci Pure Appl Chem A 2005;42:891.
[33] Venancio EC, Wang P-C, MacDiarmid AG. Synth Met 2006;156:357.
[34] Stejskal J, Kratochvíl P, Jenkins AD. Collect Czech Chem Commun 1995;36:4135.
[35] Trchová M, Šeděnková I, Konyushenko EN, Stejskal J, Holler P, Ćirić-Marjanović G. J Phys Chem B 2006;110:9461.
[36] Kolla HS, Surwade SP, Zhang X, MacDiarmid AG, Manohar SK. J Am Chem Soc 2005;127:16770.

[37] Pillalamarri SK, Blum FD, Tokuhiro AT, Story JG, Bertino MF. Chem Mater 2005;17:227.
[38] Cheng D, Ng S-C, Chan HSO. Thin Solid Films 2001;477:15.
[39] Şahin Y, Pekmez K, Yıldız A. Synth Met 2002;131:7.
[40] Yang C-H, Chih YK, Cheng H-E, Chen C-H. Polymer 2005;46:10688.
[41] Socrates G. Infrared and Raman characteristic group frequencies. New York: Wiley; 2001. p. 78–167.
[42] Meth-Cohn O, Smith M. J Chem Soc Perkin Trans 1994;1:5.
[43] Meth-Cohn O, Travis AS. Chem Br 1995;31:547.
[44] Cao Y, Andreatta A, Heeger AJ, Smith P. Polymer 1989;30:2305.
[45] Mazeikiene R, Malinauskas A. Synth Met 2000;108:9.
[46] Ayad MM, Shenashin MA. Eur Polym J 2004;40:197.
[47] Green AG, Johnson W. Ber 1913;46:3769.
[48] Hedayatullah M. Bull Soc Chim Fr 1972;7:2957.
[49] Geniès EM, Lapkowski M, Penneau JF. J Electroanal Chem 1988;249:97.
[50] Mathew R, Mattes BR, Espe MP. Synth Met 2002;131:141.
[51] Chen C-H. J Appl Polym Sci 2003;89:2142.
[52] Cruz-Silva R, Romero-García J, Angulo-Sánchez JL, Flores-Loyola E, Farias MH, Castillón FF, et al. Polymer 2004;45:4711.
[53] Trchová M, Matějka P, Brodinová J, Kalendová A, Prokeš J, Stejskal J. Polym Degrad Stab 2006;91:114.
[54] Chen L, Yu Y, Mao H, Lu X, Zhang W, Wei Y. Synth Met 2005;149:129.
[55] Wei Y, Tang X, Sun Y. J Polym Sci Part A Polym Chem 1989;27:2385.
[56] Wei Y, Sun Y, Tang X. J Phys Chem 1989;93:4878.
[57] Geng Y, Li J, Sun Z, Jing X, Wang F. Synth Met 1998;96:1.
[58] Stejskal J, Hlavatá D, Holler P, Trchová M, Prokeš J, Sapurina I. Polym Int 2004;53:294.
[59] Blinova NV, Stejskal J, Trchová M, Prokeš J. Polymer 2006;47:42.
[60] Cases F, Huerta F, Garcés P, Morallón E, Vázquez JL. J Electroanal Chem 2001;501:186.
[61] Wang X, Liu N, Yan X, Zhang W, Wei Y. Chem Lett 2005;34:42.
[62] Liu X-X, Zhang L, Li Y-B, Bian L-J, Su Z, Zhang L-J. J Mater Sci 2005;40:4511.
[63] Zimmermann A, Künzelmann U, Dunsch L. Synth Met 1998;93:17.
[64] Cruz-Silva R, Ruiz-Flores C, Arizmendi L, Romero-García J, Arias-Marin E, Moggio I, et al. Polymer 2006;47:1563.
[65] Ichinohe D, Muranaka T, Kise H. J Appl Polym Sci 1998;70:717.
[66] Tu X, Xie Q, Xiang C, Zhang Y, Yao S. J Phys Chem B 2005;109:4053.
[67] Cotarelo MA, Huerta F, Mallavia R, Morallón E, Vázques JL. Synth Met 2006;156:51.
[68] Laska J, Widlarz J. Polymer 2005;46:1485.
[69] Komura T, Ishihara M, Yamaguchi T, Takahashi K. J Electroanal Chem 2000;493:84.
[70] Li X-G, Duan W, Huang M-R, Yang Y-L. J Polym Sci Part A Polym Chem 2001;39:3989.
[71] Viva FA, Andrade EM, Molina FV, Florit MI. J Electroanal Chem 1999;471:180.
[72] Dines TJ, MacGregor LD, Rochester CH. Phys Chem Chem Phys 2001;13:2676.
[73] Holly S, Sohár P. In: Láng L, Prichard WH, editors. Absorption spectra in the infrared region (theoretical and technical introduction). Budapest: Akadémiai Kiadó; 1975. p. 69.
[74] Vien DL, Colthup NB, Fateley WG, Grasselli JG. The handbook of infrared and Raman characteristic frequencies of organic molecules. New York: Academic Press; 1991.
[75] Kieffel Y, Travers JP, Ermolieff A, Rouchon D. J Appl Polym Sci 2002;86:395.
[76] Lin X, Zhang H. Electrochim Acta 1996;41:2019.
[77] Coates J. Encyclopedia of analytical chemistry. In: Meyers RA, editor. Interpretation of infrared spectra: a practical approach. Chichester: Wiley; 2000. p. 10815–37.
[78] Trchová M, Sapurina I, Prokeš J, Stejskal J. Synth Met 2003;135–136:305.
[79] Wu G-C, Yeh Y-R, Chen J-Y, Chiou Y-H. Polymer 2001;42:2877.
[80] Sapurina I, Osadchev AYu, Volchek BZ, Trchová M, Riede A, Stejskal J. Synth Met 2002;129:29.
[81] Šeděnková I, Trchová M, Blinova NV, Stejskal J. Thin Solid Films 2006. doi:10.1016/j.tsf.2006.05.038.
[82] Inzelt G, Puskas Z. Electrochim Acta 2004;49:1969.
[83] Malinauskas A. Polymer 2001;42:3957.
[84] Stejskal J, Sapurina I. Pure Appl Chem 2005;77:815.
[85] Okubo M, Fujii S, Minami H. Colloid Polym Sci 2001;279:139.
[86] Stejskal J. J Polym Mater 2001;18:225.
[87] Stejskal J, Sapurina I. J Colloid Interface Sci 2004;274:489.
[88] Wang P-C, Huang Z, MacDiarmid AG. Synth Met 1999;101:852.
[89] Onoda M, Tada K, Shinkuma A. Thin Solid Films 2006;499:61.
[90] Li G, Pang S, Xie G, Wang Z, Peng H, Zhang Z. Polymer 2006;47:1456.
[91] Stejskal J, Riede A, Hlavatá D, Prokeš J, Helmstedt M, Holler P. Synth Met 1998;96:55.
[92] Crispin X, Cornil A, Friedlein R, Okudaira KK, Lemaur V, Crispin A, et al. J Am Chem Soc 2004;126:11889.
[93] Kokunov YV, Gorbunova YE, Khmelevskaya LV. Russ J Inorg Chem 2005;50:1184.
[94] Tagowska M, Palys B, Jackowska K. Synth Met 2004;142:223.
[95] Sáez EI, Corn RM. Electrochim Acta 1993;38:1619.
[96] Kocherginsky NM, Lei W, Wang Z. J Phys Chem A 2005;109:4010.
[97] Tzou K, Gregory RV. Synth Met 1992;47:267.

Appendix D

Elena N. Konyushenko, Jaroslav Stejskal, Miroslava Trchová, Jiří Hradil, Jana Kovářová, Jan Prokeš, Miroslav Cieslar, Jeong-Yuan Hwang, Kuei-Hsien Chen, and Irina Sapurina,

Multi-wall carbon nanotubes coated with polyaniline,

Polymer **47:** 5715–5723 (2006)

Available online at www.sciencedirect.com
SCIENCE DIRECT
ELSEVIER
Polymer 47 (2006) 5715–5723
polymer
www.elsevier.com/locate/polymer

Multi-wall carbon nanotubes coated with polyaniline

Elena N. Konyushenko [a], Jaroslav Stejskal [a,*], Miroslava Trchová [a], Jiří Hradil [a], Jana Kovářová [a], Jan Prokeš [b], Miroslav Cieslar [b], Jeong-Yuan Hwang [c,d], Kuei-Hsien Chen [c,d], Irina Sapurina [e]

[a] Institute of Macromolecular Chemistry, Academy of Sciences of the Czech Republic, 162 06 Prague 6, Czech Republic
[b] Charles University Prague, Faculty of Mathematics and Physics, 121 16 Prague 2, Czech Republic
[c] Institute of Atomic and Molecular Sciences, Academia Sinica, Taipei, Taiwan
[d] Center for Condensed Matter Sciences, National University, Taipei, Taiwan
[e] Institute of Macromolecular Compounds, Russian Academy of Sciences, St. Petersburg 199004, Russia

Received 23 March 2006; received in revised form 23 May 2006; accepted 26 May 2006
Available online 30 June 2006

Abstract

Multi-wall carbon nanotubes (CNT) were coated with protonated polyaniline (PANI) *in situ* during the polymerization of aniline. The content of CNT in the samples was 0–80 wt%. Uniform coating of CNT with PANI was observed with both scanning and transmission electron microscopy. An improvement in the thermal stability of the PANI in the composites was found by thermogravimetric analysis. FTIR and Raman spectra illustrate the presence of PANI in the composites; no interaction between PANI and CNT could be proved. The conductivity of PANI-coated CNT has been compared with the conductivity of the corresponding mixtures of PANI and CNT. At high CNT contents, it is not important if the PANI coating is protonated or not; the conductivity is similar in both cases, and it is determined by the CNT. Polyaniline reduces the contact resistance between the individual nanotubes. A maximum conductivity of 25.4 S cm^{-1} has been found with PANI-coated CNT containing 70 wt% CNT. The wettability measurements show that CNT coated with protonated PANI are hydrophilic, the water contact angle being ~40°, even at 60 wt% CNT in the composite. The specific surface area, determined by nitrogen adsorption, ranges from 20 $m^2 g^{-1}$ for protonated PANI to 56 $m^2 g^{-1}$ for neat CNT. The pore sizes and volumes have been determined by mercury porosimetry. The density measurements indicate that the compressed PANI-coated CNT are more compact compared with compressed mixtures of PANI and CNT. The relaxation and the growth of dimensions of the samples after the release of compression have been noted.

Keywords: Conducting polymer; Carbon nanotubes; Conductivity

1. Introduction

Interest in nanotechnology has greatly stimulated research on carbonaceous materials, such as fullerenes and carbon nanotubes (CNT). Development of nanostructures afforded by conducting polymers, *viz.* polyaniline (PANI) and polypyrrole, proceeds independently and includes the preparation of nanotubes [1–3] and nanofibres [4–7], as well as the coating of various substrates with a thin polymer film [8,9]. The combination of both types of materials on a nano-size level is thus an obvious challenge. This approach is illustrated by the coating of CNT with conducting polymers. The deposition process follows the same principle as the coating of polymer fibres having diameters in micrometre range [10], which is a well-established technique for the preparation of conducting textiles [11].

Both single-wall CNT [12–14] and multi-wall CNT [15–22] have been coated with PANI or polypyrrole *in situ* during the polymerization of the respective monomers. Conducting polymers have been deposited electrochemically in some cases [12,13,17–19,23] but the chemical polymerization of aniline salts using ammonium peroxydisulfate as an oxidant remains

* Corresponding author. Tel.: +420 296 809351; fax: +420 296 809410.
E-mail address: stejskal@imc.cas.cz (J. Stejskal).

0032-3861/$ - see front matter © 2006 Elsevier Ltd. All rights reserved.
doi:10.1016/j.polymer.2006.05.059

the most popular way for the preparation of PANI coatings [14,20,22,24–27].

Carbon nanotubes coated with conducting polymers have been proposed for widely differing applications, including an amperometric biosensor for DNA [18] or choline [19], a sensor for nitrogen oxide [28], an acidity sensor [29], a contact in plastic electronics [30], and in electrorheology [16,31]. PANI nanofibrils have been suggested as candidates for field-emitting applications [32]; the PANI-coated CNT might prove to be an even more promising material. Improvement of the mechanical properties of composites has been mentioned as a frequent goal [21,33–35].

Both carbonaceous materials and conducting polymers [36–38] have been used separately as supports for catalytic systems in the design of fuel cells. Electronic and proton conductivities are keywords in this field [39]. Electrodes combining carbon black or graphite and conducting polymers have been proposed only recently [40–42]. The use of CNT would introduce another dimension, the nanostructure. Such composites have already been used in other energy-conversion applications, such as hydrogen production by electrolysis [43,44] and energy storage in supercapacitors [25].

Having in mind the potential applications of conducting polymers combined with CNT, we have concentrated, in the present paper, on the coating of multi-wall CNT with PANI, using both the conducting protonated form and a non-conducting base [45]. The resulting composite materials have then been characterized with respect to their morphology, thermal stability, conductivity, porosity, wettability, and other characteristics.

2. Experimental

2.1. The coating of CNT with PANI

Multi-wall CNT (L.MWNCTs-2040, Conyuan Biochemical Technology Co., Taipei, Taiwan; specific surface area 40–300 $m^2 g^{-1}$, diameter 20–40 nm, length 5–15 μm) have been coated with PANI *in situ* during the oxidative polymerization of aniline [46] (Fig. 1). Aniline hydrochloride (2.59 g, 20 mmol) was dissolved in ethanol to provide 50 mL of solution, and ammonium peroxydisulfate (5.71 g, 25 mmol) was similarly dissolved in water to yield 50 mL of solution.

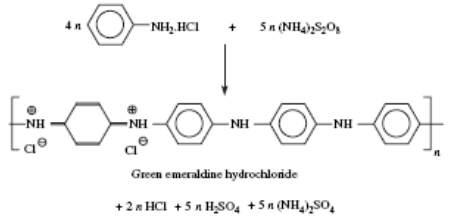

Fig. 1. The oxidation of aniline hydrochloride with ammonium peroxydisulfate yields polyaniline hydrochloride.

The monomer and then the oxidant solutions were added to various portions of CNT to start the polymerization of aniline. The reaction mixture used for the coating of CNT thus contained 0.2 M aniline hydrochloride and 0.25 M ammonium peroxydisulfate in ethanol (50 vol%)–water. The reaction mixture (100 mL) produces 2 g of PANI salt [46]. Composites containing more than 80 wt% CNT could not be prepared in this way because the volume of the reaction mixture was too low to accommodate all the CNT.

The PANI-coated CNT have been collected as solids on a filter, rinsed with 0.2 M hydrochloric acid, then with acetone, and dried at ambient atmosphere. In a portion of the samples, conducting PANI was converted to a non-conducting PANI base by immersion of the composites in excess of 1 M ammonium hydroxide.

Mixtures of protonated PANI or PANI base with CNT for comparative characterization have been prepared by mechanical blending of the components for 10 min with a pestle and mortar. Protonated PANI, for use in blending, has been prepared as above, but in water without ethanol [46].

2.2. Characterization

Electron scanning micrographs have been taken with a JEOL 6400 microscope (Japan), transmission investigations with JEOL JEM 2000FX microscope. Thermogravimetric analysis (TGA) was performed, in air flow (50 $cm^3 min^{-1}$) at a heating rate of 10 °C min^{-1}, with a Perkin Elmer TGA 7 Thermogravimetric Analyzer.

Specific surface area was determined with a Quantasorb apparatus (Quantachrome, USA) using nitrogen as sorbate. Mercury porosimetry was used to characterize the pore size of substrates with a ThermoFinigan PASCAL 440 apparatus in the pore-size range 4 nm–15 μm. The mean pore radius was calculated from the specific surface area and pore volume, assuming the model of cylindrical pores as $r = 2000\,V/S$, where r (nm) is the mean pore radius, V ($cm^3 g^{-1}$) is the pore volume obtained from mercury porosimetry, and S ($m^2 g^{-1}$) is the specific surface area according to the thermal desorption of nitrogen. The porosity was calculated from the pore volumes and true density d of the composite as $p = V/(V + d^{-1})$.

Infrared spectra in the range 400–4000 cm^{-1} were recorded, at 64 scans per spectrum at 2 cm^{-1} resolution, using a fully computerized Thermo Nicolet NEXUS 870 FTIR Spectrometer with DTGS TEC detector. Samples were dispersed in potassium bromide and compressed into pellets. Raman spectra, with the excitation in the visible range of a HeNe 633 nm laser, were collected on a Renishaw inVia Reflex Raman microscope using a 50× objective and 10 s accumulation time. The power was always kept low to avoid destruction of the samples.

The conductivity was measured by a four-point van der Pauw method on pellets compressed at 700 MPa with a manual hydraulic press using a current source SMU Keithley 237 and a Multimeter Keithley 2010 voltmeter with a 2000 SCAN 10-channel scanner card. For non-conducting PANI bases, a two-point method using a Keithley 6517 electrometer was

applied. Before such measurements, circular gold electrodes were deposited on both sides of the pellets.

The density of a composite was evaluated using a Sartorius R160P balance by weighing the pellets in air and immersed in decane. The wettability was assessed with a contact-angle measuring system OCA20, Dataphysic (Germany).

3. Results and discussion

3.1. The course of polymerization

The dispersion of carbonaceous materials in the aqueous medium used for the polymerization of aniline is difficult due to their hydrophobicity. That is why surfactants have often been added to the reaction mixture [15,26,47,48]. In the present case, we have used ethanol (50 vol%) as a component of the reaction medium to avoid this problem. The oxidation of aniline is an exothermic reaction and its course can easily be followed by monitoring the reaction temperature (Fig. 2). A solution of aniline hydrochloride in ethanol containing CNT has been mixed with an aqueous solution of the oxidant. The temperature rose from 20 °C to about 26 °C due to the ethanol–water heat of mixing. After an induction period, the next increase in the temperature is associated with the exothermic polymerization of aniline. The peak temperatures have reached 41–46 °C. This indicates that the conversion of aniline to PANI has practically been complete, as later confirmed by determining the yield of reaction [46], >90%.

The presence of CNT in the reaction mixture significantly accelerates the rate of aniline oxidation. Even 1 wt% of CNT (relative to aniline) reduces the reaction time from 64 min to 17 min by shortening the induction period (Fig. 2). The reaction time decreases on a semi-logarithmic scale about linearly as the content of CNT in the reaction mixture has grown (Fig. 3). A similar accelerating effect has also been reported with single-wall CNT [49].

There are two possible explanations for the observed acceleration of oxidation. The first is based on the assumption of

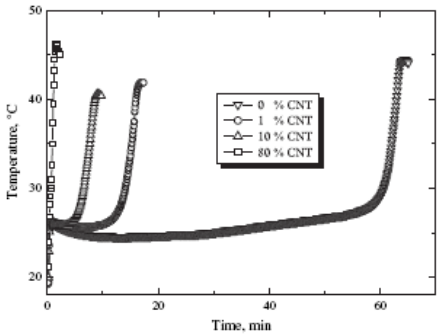

Fig. 2. The course of aniline polymerization in the presence of CNT. The compositions are given as wt% of CNT in the composites.

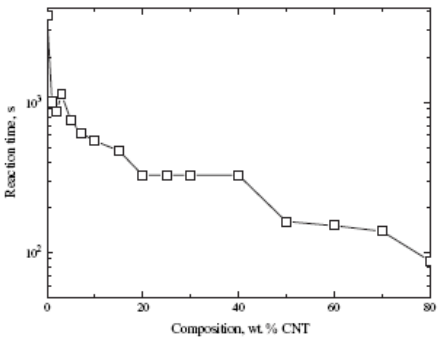

Fig. 3. The rate of composite formation in dependence on the composite composition.

heterogeneous catalysis. The oligomeric aniline intermediates adsorbed at the substrate, having a large surface area, like textile fibres [10] or silica gel [50], start the growth of PANI chains more readily. The CNT have also a high surface area and that is why they could act in a similar manner. Philip et al. [27] proposed the principle of heterogeneous catalysis to be operative in the case of CNT; the oxidation of aniline gets faster at the surface of CNT, resulting in the core–shell morphology of the products (Figs. 4 and 5).

The second explanation is based on the fact that CNT are conducting, *i.e.* they are able to transfer electrons. The oxidation of aniline is a typical redox reaction, in which the electrons are abstracted from aniline molecules and accepted by an oxidant, peroxydisulfate, which converts to sulfate (Fig. 1). In a classical reaction concept, the molecules of aniline and oxidant are expected to meet, and consequently react. It has recently been proposed that conducting materials can mediate the transfer of electrons [51]; CNT can obviously undertake such a role and transfer the electrons between the reductant and oxidant. This means that the aniline molecule at the surface of CNT can exchange electrons, and thus convert to PANI, with any oxidant molecule that is also in contact with CNT, and not only with the oxidant in the close vicinity of the aniline molecule involved. This fact dramatically increases the probability for an aniline molecule to be oxidized to a PANI constitutional unit. The PANI chains growing at the CNT surface are also conducting and thus participate in the electron transfer from the aniline unit that is being added to the PANI chain-end and CNT. That is why the non-conducting textile fibres, after being coated with conducting PANI, also accelerate the polymerization of aniline [10].

3.2. Morphology of PANI-coated CNT

Scanning electron microscopy (SEM) illustrates a uniform coating of CNT with PANI (Fig. 4). The coated CNT become thicker as the amount of deposited PANI increases. The uniform deposition of PANI on the CNT is similarly demonstrated

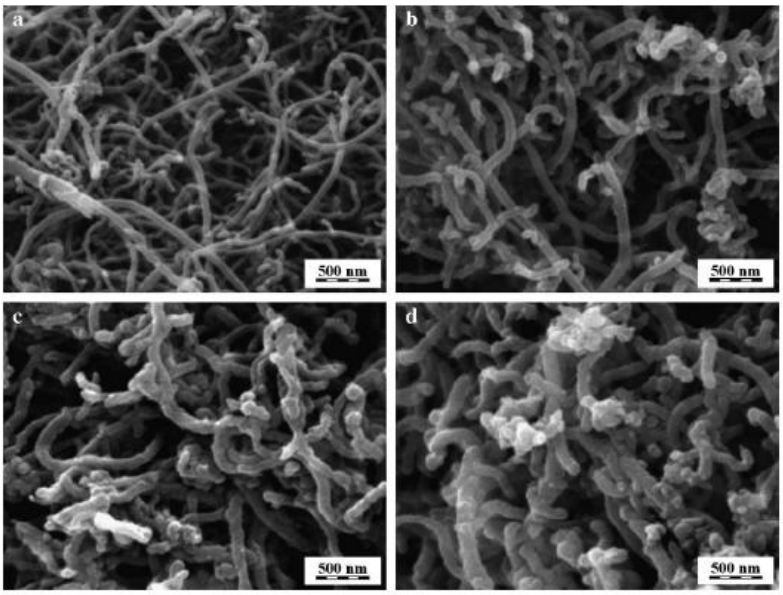

Fig. 4. Original MWCNT (a) and those coated with 50 wt% (b), 70 wt% (c) and 80 wt% PANI (d).

by transmission electron microscopy (TEM), which shows the bilayered structure of coated CNT (Fig. 5). As the internal cavity is well discernible, we conclude that the coating with PANI takes place only at the outer surface of the CNT. The polymerization of aniline inside the CNT is hindered by the restricted access of reactants to the interior of the CNT. The "droplets" of PANI on CNT have been observed by Yu et al. [26] at low (1 wt%) PANI loadings while coaxial core–shell agglomerates were produced at higher content (20 wt%) of PANI. Generally, the complete and uniform coating of CNT with a conducting polymer has been reported in the literature [17,23,25,27], in agreement with the present results.

Various modes of functionalization of CNT, *e.g.*, with carboxyl groups [20] or *p*-phenylenediamine [27,52], have been done to improve the interaction of PANI with CNT in the preparation of tubular nanocomposites. The surface of the CNT has also been modified, *e.g.*, by oxidation in nitric acid [13,19,23] or with permanganate [27], to enhance the deposition of conducting polymer. In the present paper, we demonstrate that the deposition of PANI by surface polymerization [50] proceeds well, even on the neat CNT, without any pre-treatment, if the appropriate reaction conditions have been used. This is in accordance with the well-known fact that uniform PANI films are produced by *in situ* polymerization on hydrophobic surfaces [53], and CNT satisfy this condition. The conducting polymer, however, is not covalently bonded to the carbon nanotubes. The aniline oligomers are adsorbed [9] at the surface of CNT and start the growth of polyaniline coating there. Uniform coatings with conducting polymers have thus been obtained by this technique on textiles [11,13,54] and carbon fibres [55] as well as on polymer nanofibres [56]. A good deposition of PANI on CNT is thus not surprising.

3.3. Thermal stability

Thermogravimetric analysis shows the deprotonation of PANI salts in the composites in the temperature region below 200 °C (Fig. 6) and the beginning decomposition of PANI at higher temperatures [57]. Polyaniline protonated with hydrochloric acid has a low thermal stability with respect to deprotonation; the performance could be improved by selecting another acid, like methanesulfonic acid [58]. The thermal stability of PANI in the composite is somewhat better compared with neat PANI (Fig. 6). Neat CNT are stable up to 650 °C and become completely decomposed above 750 °C, in accordance with data reported in the literature [22,26]. The residue of 0.6 wt% confirms that the metal catalyst used in the preparation of CNT has been removed from CNT.

3.4. Raman spectra

Raman spectroscopy is a useful tool for the characterization of carbonaceous materials. The typical G-band (derived from

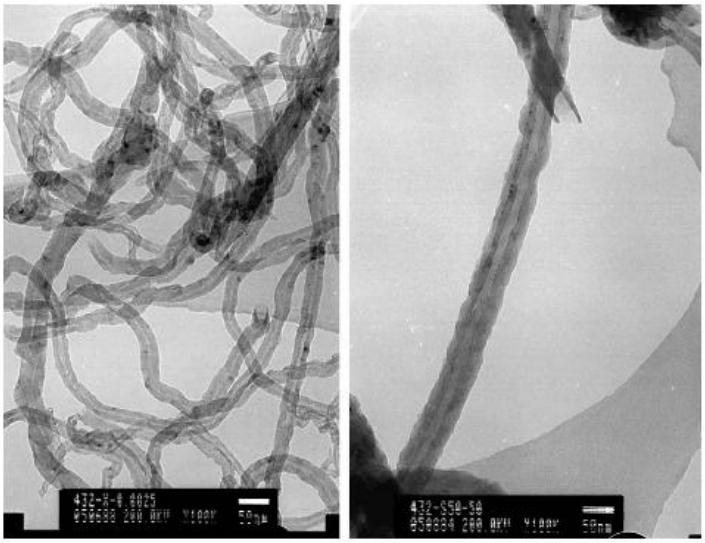

Fig. 5. Original CNT (left) and CNT after coating (right) with polyaniline (50 wt%) at the same magnification.

the graphite-like mode) is situated at 1574 cm^{-1} in the spectrum of neat CNT (Fig. 7). In contrast to the graphite G-band, which exhibits a single Lorentzian peak, the band for CNT has a shoulder extending to higher wavenumbers. Disorder-induced D-band is situated at 1326 cm^{-1} and its second-order harmonic D′-band is found at 2643 cm^{-1}. After the coating of CNT with PANI, the spectrum of this polymer dominates in all samples. This observation confirms that good coating of CNT with PANI has been achieved. The peaks in the spectra are typical of protonated PANI and are located at 1593, 1504, 1330, and 1171 cm^{-1}. Their positions remain practically unchanged for all contents of CNT. We have observed the relative decrease and a shift of the second-order of the disorder-induced band D′ which indicates a less perfect structure for the nanotubes embedded in the polymer [59]. In some cases, Raman spectroscopy showed indications of

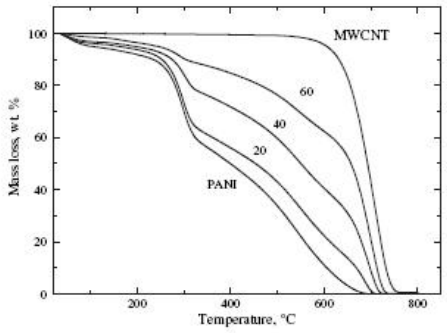

Fig. 6. Thermogravimetric analysis of PANI-coated CNT. The content of CNT (wt%) is given at the individual curves.

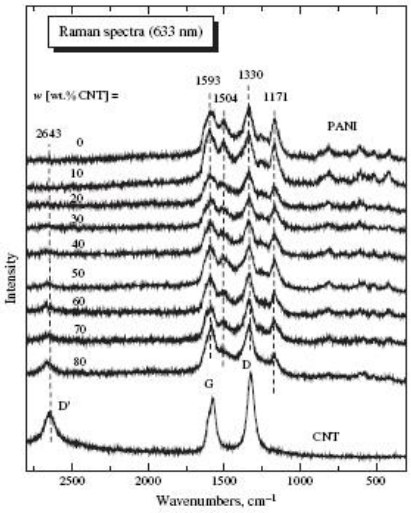

Fig. 7. Raman spectra of carbon nanotubes coated with PANI.

possible interaction between single-wall CNT and conducting polymers [60]. In contrast to polymer-functionalized CNT, where strong effects of the polymer on the Raman signal of CNT have been observed [61,62], no interaction between CNT and PANI could be proved by Raman spectra in the present study.

3.5. FTIR spectra

Raman-active D- and G-bands are inactive in IR spectra because they are forbidden due to the symmetry of the carbon network. That is why the FTIR spectra of neat CNT are featureless (Fig. 8). After coating with PANI, the spectra also reflect the presence of the polymer overlayer. The spectrum of PANI prepared in ethanol–water mixtures is very close to the spectrum of PANI sulfate [8] prepared in an aqueous medium. The main bands are situated at 1560 cm^{-1} (with a shoulder at 1607 cm^{-1}), 1482, 1408, 1301, 1242, 1137, 803, and 575 cm^{-1}. The fact that polymer is protonated in part by sulfate anions is demonstrated by the presence of the peak at 575 cm^{-1}, which is attributed to a stretching vibration in the sulfate anion [63].

Some authors have reported that an interaction between multi-wall CNT and conducting polymers manifested itself by the shifts in FTIR spectra [25,26,48], while no interaction between CNT and PANI was found by Karim et al. [13]. Baibarac et al. [59] showed that composites of PANI and single-wall CNT were different when they had been prepared by adding dispersed single-wall CNT to the polymer solutions or when they have been prepared by chemical polymerization

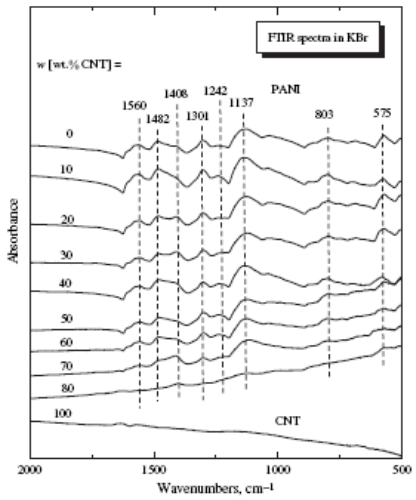

Fig. 8. FTIR spectra of carbon nanotubes coated with PANI.

of aniline in the presence of single-wall CNT. In the present case, the spectrum of PANI exhibits changes in the intensity in the region at about 1400 cm^{-1} probably corresponding to the hydrogen-bonded C–N^{+} stretching vibration [64] and at about 1242 cm^{-1}, which is interpreted as a C–$N^{+\bullet}$ stretching vibration in the polaron structure of PANI [65]. The prominent 1137 cm^{-1} band assigned to a vibration mode of the –$NH^{\bullet+}$– structure [66] exhibits a slight variation in its shape. Baibarac et al. [59] described the intensity increase of this band to charge transfer between the PANI and CNT. The electronic interaction between a semiconductor, like a conducting polymer, and carbon, like graphite or CNT, has also been suggested in the literature [67]. The question whether the molecular interaction between PANI and CNT takes place cannot be answered on the basis of present FTIR spectra.

3.6. Conductivity of PANI–CNT mixtures

Four series of samples have been prepared for the conductivity measurements: mixtures of PANI with CNT and PANI-coated CNT, PANI being either in the conducting protonated state or as a non-conducting PANI base.

The mixtures of protonated PANI with CNT show simple behaviour, the conductivity gradually increasing from 0.9 S cm^{-1} for PANI hydrochloride to a maximum at 7.7 S cm^{-1} for a mixture with 70 wt% CNT (Fig. 9a). The neat CNT could not be compressed to a pellet, as is necessary for conductivity measurement.

The mixtures of PANI base with CNT exhibit typical percolation behaviour (Fig. 9a). The conductivity of PANI base suddenly increases as the percolation threshold, located at 4 wt% of CNT, is passed. At this concentration of the conducting component, the first conducting pathways are produced in the composite. The percolation limit is lower than that expected for spherical particles (~16 vol%) and reflects the nanotubular character of CNT in the mixture. On the other hand, the percolation limit was estimated to be between 15 and 20 wt% CNT in a similar composite of CNT with polypyrrole [68]. The different degrees of dispersion of the CNT in the polymer matrix may be responsible for the observed difference.

3.7. Conductivity of PANI-coated CNT

The dependence of conductivity on CNT content for CNT coated with the conducting form of PANI is similar to that of corresponding mixtures (Fig. 9b). At low fractions of CNT, the conductivity is determined by the PANI as the main component. It increases moderately from 0.42 S cm^{-1} for neat PANI with increasing CNT content. The decrease in the contact resistance of CNT afforded by a PANI coating [69] results in the maximum composite conductivity of 25.4 S cm^{-1} at 70 wt% CNT. This is a much higher conductivity than that of the order of 10^{-1} S cm^{-1} reported for similar composites by some authors [20,48], and comparable with other reported results [24,47,70] that are of the order of 10^{0}–10^{1} S cm^{-1}. At higher CNT content, the conductivity

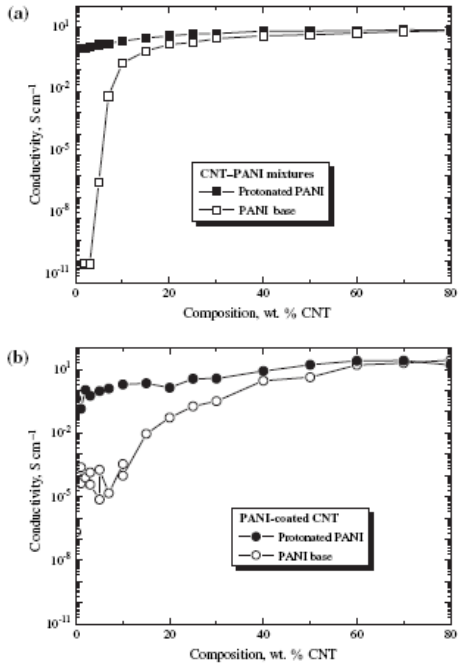

Fig. 9. The conductivity of carbon nanotubes mixed (a) or coated (b) with protonated PANI (filled symbols) and PANI base (open symbols).

was reduced; the amount of PANI is not sufficient to provide good contact between the CNT and the resistance between the CNT increases. Reduction of the thickness of the PANI coating could possibly be the way to increase the composite conductivity by introducing the tunneling mechanism of conduction.

The increase in the conductivity of CNT coated with PANI base with increasing content of CNT is slower (Fig. 9b), compared with the corresponding mixtures (Fig. 9a). At low concentrations of CNT, the direct electrical contact between CNT is prevented by the surface coating with a non-conducting PANI base and the percolation threshold is thus practically not distinguishable. Yet, the coating with PANI base seems to reduce the contact resistance between CNT. The resulting conductivity of CNT coated with PANI base thus reaches 19.6 S cm^{-1} at 70 wt% CNT. The conductivity is thus comparable with that of the CNT coated with protonated PANI. We are obviously dealing with interfacial phenomena between the CNT separated with a thin coating of PANI. A non-conducting PANI base is not a true insulator, but it can probably mediate the charge-carrier transfer over short distances between the neighboring CNT, similarly to the protonated conducting form.

3.8. Contact-angle measurements

The contact angle of water on "standard" PANI hydrochloride is [71] 49°. When PANI has been prepared in ethanol (50 vol%)–water mixture, the contact angle was 43°. The enhanced wettability is possibly due to the sulfonation of aromatic rings under these reaction conditions. The contact angles of CNT coated with protonated PANI are about ~40° (Fig. 10) up to 60 wt% CNT in the composite. The composite is thus hydrophilic and behaves as a neat PANI. This is not surprising considering the core–shell morphology of the composite (Fig. 5). At higher contents of CNT, the contact angles could not be measured. The water droplet penetrated into the composite, possibly as a result of higher porosity. This means that the contact angle of neat CNT could not be determined but we expect that, by analogy with graphite, they are more hydrophobic; the contact angle of water on graphite is 79°. The mixtures of PANI with CNT behave differently. Even a small fraction of CNT in PANI increases the contact angle towards the level expected for neat CNT (Fig. 10). Despite the hydrophobic behaviour, above 10 wt% CNT, water penetrated the samples, and contact angles again could not be determined.

3.9. Surface area and porosity

Basic properties of the porous structure of CNT coated with PANI were determined by standard methods, such as mercury porosimetry and thermal desorption of nitrogen (Table 1). The specific surface area of PANI, 20.2 m^2 g^{-1}, is lower than that of PANI prepared by, *e.g.*, mechanochemical synthesis [72], 69.7 m^2 g^{-1}. The surface areas of PANI-coated CNT are in the range from 12 to 55 m^2 g^{-1}. They are proportional to the micropore content, *i.e.* the pore area where the adsorption interactions occur. The highest values represent a good sorption ability of such materials.

Mercury porosimetry allows us to determine the pore volume and pore-size distribution. The pore volumes are in range from 0.4 to 2.5 cm^3 g^{-1} (Table 1). The mean pore radii

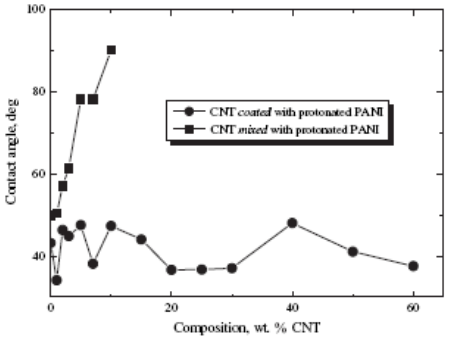

Fig. 10. Water contact angles on PANI-coated CNT and on the mixtures of protonated PANI with CNT.

Table 1
Porosity parameters of PANI-coated CNT

CNT (wt%)	Pore volume ($cm^3 g^{-1}$)	Specific surface area ($m^2 g^{-1}$)	Porosity (%)	Mean pore radius (nm)	Most frequent radius (nm)
0	0.42	20.2	30	432	35
10	0.87	48.8	47	36	61
20	0.58	19.3	37	61	82
30	0.63	12.9	39	97	71
40	1.04	50.0	51	42	56
50	0.99	34.9	50	57	60
60	1.65	51.9	62	64	47
70	1.41	31.0	59	91	40
80	0.92	20.6	48	89	53
100	2.54	56.5	72	90	20

calculated from the specific surface area and pore volume are in an interval from 35 to 96 nm. Such pores are in the area of mesopores. Pore-size distribution curves have two maxima, as illustrated on the PANI-coated CNT (20 wt%) (Fig. 11). The first, at about 750 nm, reflects the interstices between the nanotubes, and the second, at 65 nm, represents the actual pores. The porosity was calculated from pore volume values and the true density of the composite. Values from 30 to 72% are common for a wide range of adsorbents.

3.10. Density

The density of "standard" PANI hydrochloride is [46] 1.33 g cm^{-3} and the density of PANI base 1.24 g cm^{-3}. The density of materials containing the protonated form of PANI was always higher than with the composites of PANI base, as expected (Fig. 12). This applies both to mixtures of PANI with CNT and to PANI-coated CNT. The dependence of density on the content of CNT, however, is different for these two sample sets. The density of PANI-coated CNT increases with increasing CNT content, and the density of neat CNT can be estimated by extrapolation as 1.9 g cm^{-3}. The density of mixtures, on the contrary, has a decreasing trend. In the latter case,

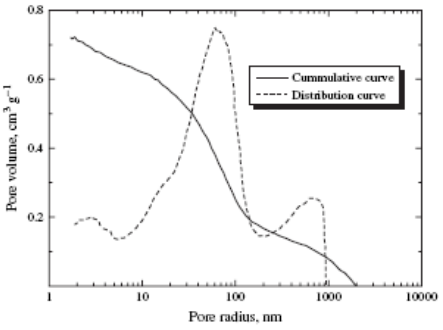

Fig. 11. Example of the pore-size distribution obtained by mercury porosimetry for the PANI-coated CNT (20 wt%).

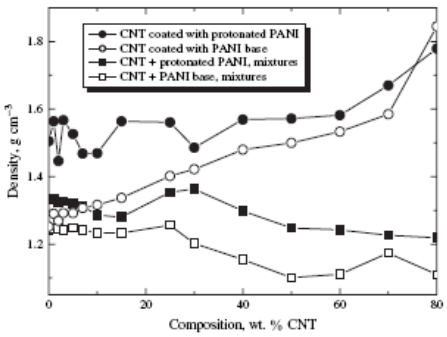

Fig. 12. Densities of CNT coated (circles) or mixed (squares) with PANI in the conducting protonated state (filled symbols) or as a non-conducting PANI base (open symbols).

the low apparent density has to reflect the porous structure of composites. We have indeed observed that the dimensions of the pellets used for the density measurements increase during a number of hours after the compression of the material at 700 MPa. The relaxation, manifested as an increase in pellet diameter, has often exceeded 10%. Such a process is expected to be associated with the formation of macropores within the sample.

4. Conclusions

The presence of CNT in the reaction mixture used for the oxidation of aniline dramatically increases the rate of PANI formation. Electron microscopy shows that CNT become coated with PANI during the *in situ* polymerization of aniline. The coating is uniform and its thickness increases with increasing content of PANI in the composite. The thermal stability of PANI in the composites with CNT is better than the stability of neat PANI. All composites completely disintegrate after heating to 700–750 °C. FTIR and Raman spectra confirm the presence of PANI in the samples; interaction between the two components, PANI and CNT, could not be proved.

The mixtures of CNT with PANI base show typical percolation behaviour, while the dependence of the conductivity of PANI base-coated CNT on the content of CNT is smooth. At high content of CNT, it is not important whether the coating is conducting (with protonated PANI) or non-conducting (with PANI base). The conductivity is controlled by the CNT. The highest conductivity, 25.4 S cm^{-1}, has been recorded for CNT (70 wt%) coated with protonated PANI.

CNT coated with protonated PANI are hydrophilic, like neat PANI, up to 60 wt% CNT in the sample, the contact angle for water being ~40°. The samples with higher content of CNT could not be characterized because the water droplet penetrated into the sample. Mixtures of PANI and CNT behave quite differently and are more hydrophobic than PANI-coated CNT.

The specific surface areas of PANI-coated CNT were between 20 $m^2 g^{-1}$ for protonated PANI and 56 $m^2 g^{-1}$ for neat CNT, the pore volume increased from 0.42 $cm^3 g^{-1}$ for PANI to 2.54 $cm^3 g^{-1}$ for CNT. While the density of PANI-coated CNT increases with increasing content of CNT in the samples, this parameter decreases in mixtures of PANI with CNT. The compressed PANI-coated CNT are thus more compact compared with the mixtures containing a similar fraction of CNT, which are porous. All these parameters indicate that PANI-coated CNT might constitute useful materials for various applications, *e.g.*, in fuel cells.

Acknowledgments

The authors thank the Academia Sinica, Taipei, Taiwan, for the support of Czech–Taiwanese cooperation, the Grant Agency of the Academy of Sciences of the Czech Republic (A4050313 and A400500504), the Ministry of Education, Youth, and Sports of the Czech Republic (MSM 0021620834 and ME 847), and the Federal Agency for the Science and Innovations (N2005-RI-12.0/004/028) for financial support.

References

[1] Zhang LJ, Wan MX. Nanotechnology 2002;13:750.
[2] Zhang Z, Wei Z, Zhang L, Wan M. Acta Mater 2005;53:1373.
[3] Konyushenko EN, Stejskal J, Šeděnková I, Trchová M, Sapurina I, Cieslar M, et al. Polym Int 2006;55:31.
[4] Huang J, Kaner RB. Angew Chem Int Ed 2004;43:5817.
[5] Nickels P, Dittmer WU, Beyer S, Kotthaous JP, Simmel FC. Nanotechnology 2004;15:1524.
[6] Ma Y, Zhang J, He H. J Am Chem Soc 2004;126:7097.
[7] Kim B-K, Kim YH, Won K, Chang H, Choi Y, Kong K-J, et al. Nanotechnology 2005;16:1177.
[8] Geng Y, Li J, Sun Z, Jing X, Wang F. Synth Met 1998;96:1.
[9] Stejskal J, Sapurina I. Pure Appl Chem 2005;77:815.
[10] Tzou K, Gregory RV. Synth Met 1992;47:267.
[11] Martin CR. Handbook of conducting polymers. In: Skotheim TA, Elsenbaumer RL, Reynolds JR, editors. 2nd ed. New York: M Dekker; 1998. p. 409–21.
[12] Vivekchand SRC, Sudheendra L, Sandeep M, Govindaraj A, Rao CNR. J Nanosci Nanotechnol 2002;2:631.
[13] Karim RM, Lee CJ, Park Y-T, Lee MS. Synth Met 2005;151:131.
[14] Ham HT, Choi YS, Jeong N, Chung IJ. Polymer 2005;46:6308.
[15] Wu M, Snook GA, Gupta V, Shaffer M, Fray DJ, Chen GZ. J Mater Chem 2005;15:2297.
[16] Choi HJ, Park SJ, Kim ST, Jhon MS. Diam Relat Mater 2005;14:766.
[17] Guo D-J, Li H-L. J Solid State Electrochem 2005;9:445.
[18] Cheng G, Zhao J, Tu Y, He P, Fang Y. Anal Chim Acta 2005;533:11.
[19] Qu F, Yang M, Jiang J, Shen G, Yu R. Anal Biochem 2005;344:108.
[20] Zhang X, Zhang J, Liu Z. Appl Phys A 2005;80:1813.
[21] Wu T-M, Lin Y-W, Liao C-S. Carbon 2005;43:734.
[22] Sainz R, Benito AM, Martínez MT, Galindo JF, Sotres J, Baró AM, et al. Adv Mater 2005;17:278.
[23] Han G, Yuan J, Shi G, Wei F. Thin Solid Films 2005;474:64.
[24] Cochet M, Maser WK, Benito AM, Callejas AM, Martínez MT, Benoit J-M, et al. Chem Commun 2001;1450.
[25] Deng MG, Yang BC, Hu YD. J Mater Sci 2005;40:5021.
[26] Yu Y, Che B, Si Z, Li L, Chen W, Xue G. Synth Met 2005;150:271.
[27] Philip B, Xie J, Abraham JK, Varadan VK. Polym Bull 2005;53:127.
[28] An KH, Jeong SY, Hwang HR, Lee YH. Adv Mater 2004;16:1005.
[29] Kaempgen M, Roth S. J Electroanal Chem 2006;586:72.
[30] Lefenfeld M, Blanchet G, Rogers JA. Adv Mater 2003;15:1188.
[31] Park SJ, Park SY, Cho MS, Choi HJ, Joo J. Mol Cryst Liq Cryst 2004;425:21.
[32] Wang C, Wang Z, Li M, Li H. Chem Phys Lett 2001;341:431.
[33] Wang M, Pramoda KP, Goh SH. Polymer 2005;46:11510.
[34] Chae HG, Sreekumar TV, Uchida T, Kumar S. Polymer 2005;46:10925.
[35] Zeng H, Gao C, Wang Y, Watts PCP, Kong H, Cui X, et al. Polymer 2006;47:113.
[36] Drelinkiewicz A, Waksmundzka-Góra A, Makowski W, Stejskal J. Catal Commun 2005;6:347.
[37] Samant PV, Rangel CM, Romwero MH, Fernandes JB, Figueiredo JL. J Power Sources 2005;151:79.
[38] Holzhauser P, Bouzek K, Bastl Z. Synth Met 2005;155:501.
[39] Treptow F, Jungbauer A, Hellgardt K. J Membr Sci 2006;270:115.
[40] Rajesh B, Thampi KR, Bonard JM, Mathieu HJ, Xanthopoulos N, Viswanathan B. Electrochem Solid State Lett 2004;7:A404.
[41] Wu Y, Li L, Jing-Hong L, Xu BQ. Carbon 2005;43:2579.
[42] Park JC, Kim JS, Jung DH. Macromol Res 2002;10:181.
[43] Navarro-Flores E, Omanovic S. J Mol Catal A Chem 2005;242:182.
[44] Damian A, Omanovic S. J Power Sources, in press.
[45] Stejskal J, Kratochvíl P, Jenkins AD. Polymer 1996;37:367.
[46] Stejskal J, Gilbert RG. Pure Appl Chem 2002;74:857.
[47] Zhang X, Zhang J, Wang R, Liu Z. Carbon 2004;42:1455.
[48] Yu Y, Ouyang C, Si Z, Chen W, Wang Z, Xue G. J Polym Sci Part A Polym Chem 2005;43:6105.
[49] Zhou Y, He B, Li H. J Electrochem Soc 2004;151:A1052.
[50] Stejskal J, Trchová M, Fedorova S, Sapurina I. Langmuir 2003;19:3018.
[51] Kochergirsky NM, Lei W, Wang Z. J Phys Chem A 2005;109:4010.
[52] Philip B, Xie J, Abraham JK, Varadan VK. Smart Mater Struct 2004; 13:N105.
[53] Huang Z, Wang P-C, MacDiarmid AG, Whitesides G. Langmuir 1997;13:6480.
[54] Varesano A, Dall'Acqua L, Tonin C. Polym Degrad Stab 2005;89:125.
[55] Paligová M, Vilčáková J, Sáha P, Křesálek V, Stejskal J, Quadrat O. Physica A 2004;335:421.
[56] Dong H, Prasad S, Nayme V, Wayne Jr EJ. Chem Mater 2004;16:371.
[57] Trchová M, Matějka P, Brodinová J, Kalendová A, Prokeš J, Stejskal J. Polym Degrad Stab 2006;91:114.
[58] Prokeš J, Stejskal J. Polym Degrad Stab 2004;86:187.
[59] Baibarac M, Baltog I, Lefrant S, Meveller JY, Chauver G. Chem Mater 2003;15:4149.
[60] Ferrer-Anglada N, Kaempgen M, Skákalová V, Detlaf-Weglikowska U, Roth S. Diam Relat Mater 2004;13:256.
[61] Gao C, Jin YZ, Kong H, Whitby RLD, Acquah SFA, Chen GY, et al. J Phys Chem B 2005;109:11925.
[62] Zeng H, Gao C, Yan D. Adv Funct Mater 2006;16:812.
[63] Socrates G. Infrared and Raman characteristic group frequencies. New York: Wiley; 2001. p. 78–167.
[64] Holly S, Sohár P. Absorption spectra in the infrared region – theoretical and technical introduction. Budapest: Akadémiai Kiadó; 1975.
[65] Quillard S, Louarn G, Buisson JP, Boyer M, Lapkowski M, Pron A, et al. Synth Met 1997;84:805.
[66] Chiang JC, MacDiarmid AG. Synth Met 1986;13:193.
[67] Tchmutin IA, Ponomarenko AT, Krinichnaya EP, Kozub GI, Efimov ON. Carbon 2003;41:1391.
[68] Long Y, Chen Z, Zhang X, Zhang J, Liu Z. J Phys D Appl Phys 2004; 37:1965.
[69] Long Y, Zhang L, Ma Y, Chen Z, Wang N, Zhang Z, et al. Macromol Rapid Commun 2003;24:938.
[70] Feng W, Bai XD, Lian YQ, Liang J, Wang XG, Yoshino K. Carbon 2003; 41:1551.
[71] Shishkanova TV, Sapurina I, Stejskal J, Král V, Volf R. Anal Chim Acta 2005;553:160.
[72] Huang JX, Moore JA, Acquaye JH, Kaner RB. Macromolecules 2005; 38:317.

Appendix E

Elena N. Konyushenko, Natalia E. Kazantseva, Jaroslav Stejskal, Miroslava Trchová, Jana Kovářová, Irina Sapurina, Marina.M. Tomishko, Olga V. Demicheva, and Jan Prokeš,

Ferromagnetic behaviour of polyaniline-coated multi-wall carbon nanotubes containing nickel nanoparticles,

Journal of Magnetism and Magnetic Materials **320:** 231–240 (2008)

Available online at www.sciencedirect.com
ScienceDirect
ELSEVIER
Journal of Magnetism and Magnetic Materials 320 (2008) 231–240
Journal of magnetism and magnetic materials
www.elsevier.com/locate/jmmm

Ferromagnetic behaviour of polyaniline-coated multi-wall carbon nanotubes containing nickel nanoparticles

E.N. Konyushenko[a], N.E. Kazantseva[b,c], J. Stejskal[a,*], M. Trchová[a], J. Kovářová[a], I. Sapurina[d], M.M. Tomishko[e], O.V. Demicheva[e], J. Prokeš[f]

[a]*Institute of Macromolecular Chemistry, Academy of Sciences of the Czech Republic, Heyrovsky Sq. 2, 162 06 Prague 6, Czech Republic*
[b]*Polymer Center, Faculty of Technology, Tomas Bata University in Zlin, 762 72 Zlin, Czech Republic*
[c]*Institute of Radio Engineering and Electronics, Russian Academy of Sciences, Fryazino, Moscow region 141190, Russia*
[d]*Institute of Macromolecular Compounds, Russian Academy of Sciences, St. Petersburg 199004, Russia*
[e]*Karpov Institute of Physical Chemistry, State Scientific Center, Moscow 103064, Russia*
[f]*Charles University Prague, Faculty of Mathematics and Physics, 18200 Prague 8, Czech Republic*

Received 5 March 2007; received in revised form 21 May 2007
Available online 12 June 2007

Abstract

Multi-wall carbon nanotubes (CNT) containing the residual nickel catalyst nanoparticles have been coated with a conducting polymer, polyaniline (PANI), directly during the oxidation of aniline in ethanol (50 vol%)–water mixture. The microscopy reveals that, at 20 wt% of PANI, the polymer is deposited on CNT, at 50 wt% of PANI, free PANI is found to accompany the nanotubes. The latter observation has been confirmed by the Raman spectroscopic mapping. The conductivity of composites of protonated PANI and CNT is practically independent of composition, 0–80 wt% CNT, and is 1–2 S cm^{-1}. The conductivity of similar composites with a non-conducting PANI base increased from 10^{-7} S cm^{-1} to 10^{0} S cm^{-1} as the CNT content increased, without any percolation transition. The content of nickel catalyst, responsible for the ferromagnetic behaviour of CNT, has been determined by thermogravimetric analysis as 28.5 wt% in the original CNT. Nickel, which is incorporated in the CNT, does not dissolve in the acid medium used for the preparation of PANI. Its presence manifests itself in the field dependence of magnetization of neat CNT and by the frequency dispersion of complex permeability of PANI–CNT composites with CNT concentration above 40 wt%. The high value of the coercivity of nickel-incorporated CNT as well as the character of magnetic spectra of CNT-rich composites with PANI can be explained by the cooperative effects in the magnetic system of strongly coupled ferromagnetic nanoparticles encapsulated in thin carbon shells.

Keywords: Multi-wall carbon nanotube; Conducting polymer; Polyaniline coating; Nickel nanoparticle; Conductivity; Permittivity; Permeability

1. Introduction

Carbon in various forms, like graphite or carbon black, is an inert material in many aggressive media, it has good thermal stability, and good electrical conductivity. Carbon is a material of a choice as a catalyst support or as electrodes in batteries, supercapacitors, and fuel cells. Graphite or carbon black have often been used as a component in antistatic and conducting composites, materials for electromagnetic interference shielding, or in conducting adhesives.

Carbon nanotubes (CNT) represent the youngest allotropic form of carbon having a high degree of constitutional organization. They exist as two fundamental forms, single-wall and multi-wall CNT. The high degree of organization and high aspect ratio are responsible for their unique electric, magnetic, and mechanical properties. Multi-wall CNT are produced on industrial scale by the chemical-vapour deposition, and have recently become relatively inexpensive. They have the bulk conductivity of 10^{0}–10^{1} S cm^{-1}, low apparent density, high surface area, porosity, and gas permeability. They have been successfully tested as electrodes in eletrocatalytic applications and in power sources, as components of electronics and field

*Corresponding author. Tel.: +420 296 809 351; fax: +420 296 809 410.
E-mail address: stejskal@imc.cas.cz (J. Stejskal).

0304-8853/$ - see front matter © 2007 Elsevier B.V. All rights reserved.
doi:10.1016/j.jmmm.2007.05.036

emitters [1,2], etc. CNT have been used in polymer composites with improved electrical, thermal, flammability, and mechanical properties [3–6].

Since the discovery of CNT, attention has been given to its surface modification in order to get separated and uniformly dispersed CNT and to produce useful composite materials. Several methods of CNT surface modification have already been developed: the intercalation with potassium, bromine, and iodine [7], the proton irradiation [8], the treatment by hydrogen plasma [3], and coating of CNT with conducting polymers, like polypyrrole [9] or polyaniline (PANI) [10–12]. The chemical doping increases the density of free charge-carriers and thereby enhances the electrical and thermal conductivity of CNT [7]. Proton irradiation results in C–H bond formation in CNT [8] and gives rise to the formation of large numbers of atomic vacancies and carbon interstitials which influence magnetic properties of CNT. The surface modification of CNT with conducting polymers [9–12] also brings forward a new direction in applications.

The methods of the coating of CNT, e.g., with PANI, have been recently elaborated [12]. The polymer overlayer of tens of nanometres thickness can be produced on the individual CNT. In such composite materials, PANI acts as an adhesive of the individual CNT. The conductivity of PANI–CNT composites is virtually independent of the degree of protonation of PANI, i.e. on its conductivity, when the CNT content is above 50 wt% [12]. On the other hand, when the content of CNT is less than 20 wt%, the conductivity of composite is controlled by PANI. Then the conductivity of CNT can be reduced after the conversion of protonated coating to a non-conducting PANI base. Each CNT is then coated with a thin film of a polymer dielectric, preventing the mutual contact of nanotubes. Such type of materials is potentially useful in the electromagnetic interference shielding [13].

PANI coating converts the original hydrophobic surface of CNT to hydrophilic one [12] and provides a good compatibility with other hydrophilic compounds [14]. This improves the processes at the interface composite–water and enhances the efficiency of some catalytic processes [15]. PANI is a mixed proton and electron conductor [16,17]. This is important in processes that involve the simultaneous transport of protons and electrons, e.g. in hydrogen evolution reactions [18] or in fuel-cell electrodes [17,19]. Conducting polymers exhibit redox properties; in the combination with CNT they have also been used as electrodes in supercapacitors [20–22]. The PANI–CNT composites have been used in the design of detectors and sensors [23–25].

CNT prepared by chemical-vapour deposition method often include metal nanoparticles, which serve as catalytic centers for the nanotubular growth during CNT preparation. The ferromagnetic metals (Fe, Co, and Ni) and their alloys are used as catalysts and their nanoparticles are incorporated into CNT. The residual catalyst is removed as a rule, by dissolution in strong acids, leaving pure CNT. On the other hand, if left in CNT, the presence of ferromagnetic metals results in magnetically functionalized CNT. For instance, iron-filled aligned multi-wall CNT shows significant uniaxial magnetic anisotropy related to the cylindrical shape of the aligned iron particles. Such materials may find application in future magnetic storage devices [26]. Other examples of such materials are CNT or PANI nanotubes filled with nickel, which have the coercivity an order of magnitude higher than that of bulk nickel [27,28].

PANI is typically prepared by the oxidation of aniline in acidic aqueous medium [29]. Most surfaces in contact with the reaction mixture used for the oxidation of aniline become coated with a thin PANI film [30,31]. This applies also to surfaces afforded by CNT, as demonstrated in a number of cases [12,32–34]. In the present paper, we have selected CNT containing the residual nickel-catalyst nanoparticles as a substrate for the coating with a conducting polymer, PANI. The properties of the resulting new composites are reported.

2. Experimental

2.1. The coating of CNT with PANI

Multi-wall CNT were prepared by the decomposition of methane on nickel catalyst [35]. PANI coating was produced by the oxidation of aniline hydrochloride dissolved in ethanol with an aqueous solution of ammonium peroxydisulfate [12]. Equal volumes of monomer and oxidant solutions have been added to CNT to start the polymerization which thus proceeded in ethanol (50 vol%)–water. The 100 mL of the reaction mixture containing 0.2 M aniline hydrochloride and 0.25 M ammonium peroxydisulfate produces about 2 g of PANI salt [29]. An ever-lower volume of reaction mixture was added to prepare the PANI–CNT composites with a higher CNT fraction. The progress of exothermic polymerization of aniline was monitored by recording the temperature of reaction mixture.

The solids after polymerization have been collected on a filter, rinsed with 0.2 M hydrochloric acid, acetone, and dried in air at ambient atmosphere. In a part of samples, conducting PANI was converted to non-conducting PANI base by immersion of composites in 1 M ammonium hydroxide.

2.2. Characterization

Electron scanning micrographs have been taken with a JEOL 6400 microscope (Japan), transmission investigations with JEOL JEM 2000FX microscope. Thermogravimetric analysis (TGA) was performed in airflow (50 $cm^3 min^{-1}$) at a heating rate 10 °C min^{-1} with a Perkin Elmer TGA 7 Thermogravimetric Analyzer.

Infrared spectra in the range of 400–4000 cm^{-1} were recorded at 64 scans per spectrum at 2 cm^{-1} resolution

using a fully computerized Thermo Nicolet NEXUS 870 FTIR Spectrometer with DTGS TEC detector. Samples were dispersed in potassium bromide and compressed into pellets. Raman spectra with HeNe 633 nm laser excitation were collected on the Renishaw inVia Reflex Raman microscope using a 50× objective and 10 s accumulation times. The power was always kept low to avoid damage of samples.

The conductivity was measured with a four-point van der Pauw method on pellets, compressed at 700 MPa with a manual hydraulic press, using a current source SMU Keithley 237 and a Multimeter Keithley 2010 voltmeter with a 2000 SCAN 10-channel scanner card. For non-conducting PANI bases, a two-point method using a Keithley 6517 electrometer was applied. Before such measurements, circular gold electrodes were deposited on both sides of the pellets.

The density of composite was evaluated using a Sartorius R160P balance by weighing the pellets in air and immersed in decane. The wettability has been assessed with a contact–angle measuring system OCA20, Dataphysic.

The samples for permittivity characterization were prepared in block shape with the base of 15 × 15 mm and thickness of 1 mm, those for dielectric and magnetic characterization were made by compressing the powders at 200 MPa in toroidal or cylindrical press forms. The toroids of outer diameter 8 mm, inner diameter 3.1 mm and thickness 2 mm were used for the investigation of a complex permeability. All measurements have been done in the range 1 MHz–3 GHz with an Impedance/Material Analyzer Agilent E4991 A. Cylindrical samples of PANI–CNT composites with outer diameter 1 mm and 15 cm length were used for the determination of permittivity and permeability by resonant cavity method at frequency range 2–10 GHz using panoramic standing-wave ratio meter. The magnetic measurements on neat CNT powders were performed by Faraday method [37] in magnetic fields up to 8 kOe.

3. Results and discussion

CNT, used as a substrate for coating with PANI, contain nickel particles. The metal particles having the size of tens of nanometres are well visible in transmission electron microscopy (TEM) micrographs (Fig. 1). Some of them are located outside the CNT, a part of them is integrated into CNT. These CNT have been coated in situ during the oxidation of aniline hydrochloride with a conducting polymer overlayer.

3.1. The coating of CNT with PANI

In order to disperse hydrophobic CNT or related carbonaceous substrates in water, surfactants have often been added to the reaction mixture in the literature [38–40]. Alternatively, the introduction of a water-miscible organic solvent, like ethanol, has similar effect [12]. A good contact between the reaction medium and CNT has been achieved in ethanol (50 vol%)–water mixtures used in the present study.

The oxidation of aniline is an exothermic reaction and its course is easily monitored by recording the reaction temperature [29]. The induction period is followed by the polymerization of aniline which manifests itself by the

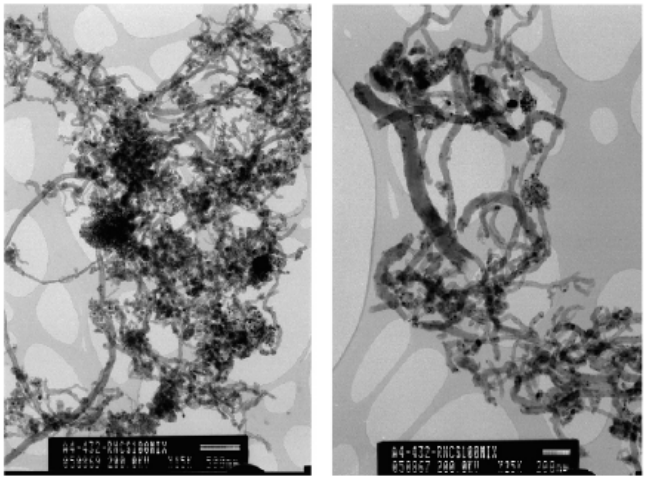

Fig. 1. TEM micrographs of CNTs containing nickel nanoparticles (two magnifications).

increase of temperature (Fig. 2). The dramatic shortening of the induction period after the introduction of CNT into reaction mixture is observed.

PANI grows on CNT (Fig. 3a) producing a core–shell morphology for the samples containing majority of CNT (Fig. 3b). The larger diameter of the PANI-coated CNT compared with neat CNT is well visible. The thickness of the coating estimated by TEM for similar CNT without nickel was 20–30 nm. In the composite having comparable amounts of components, 50 wt% PANI, conducting polymer constitutes separate regions (Fig. 3c). This will also be documented below by Raman spectroscopy. The addition of ethanol to reaction mixture has been reported to change the common granular morphology of PANI to fibrillar [41]. In the present study, however, the morphology of PANI prepared in ethanol (50 vol%)–water was strictly granular (Fig. 3d).

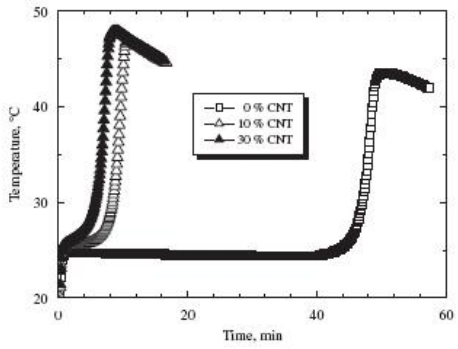

Fig. 2. The course of aniline polymerization in the presence of CNT. The compositions are given in wt% of CNT in the composite.

3.2. TGA

TGA demonstrates that the composites of PANI and CNT have been prepared (Fig. 4). The typical features of PANI degradation are observed [12]. The mass loss in temperature range below 200 °C reflects the deprotonation of PANI, the loss of its acid, and humidity. The decomposition of PANI starts above 300 °C. We can see an improvement of PANI stability with increasing content of CNT in the composite. CNT destruction begins above 550 °C. CNT with a removed catalyst leave after exposure to 800 °C a residue less than 1 wt% [12]. In the present case, the residue is 28.5 wt% and can be attributed to the nickel catalyst and/or its oxidation products.

The coating of CNT with PANI proceeds in acidic medium, pH being determined by dissolved aniline hydrochloride and

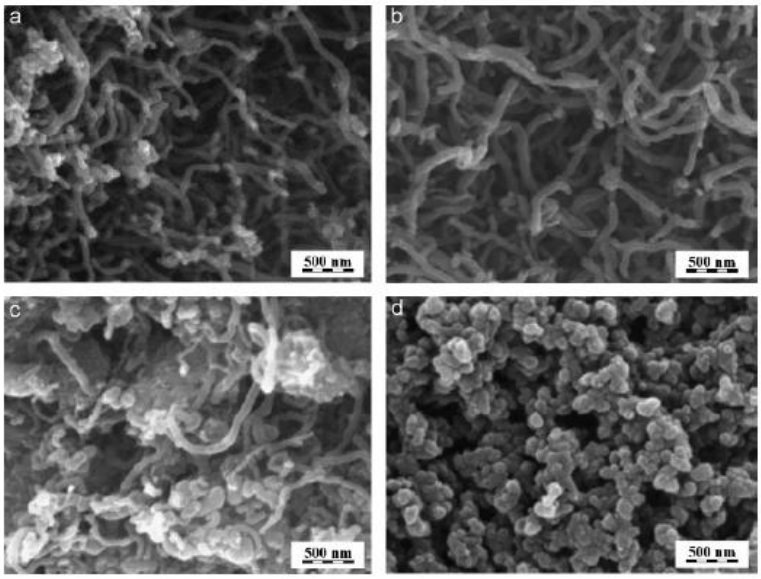

Fig. 3. SEM micrographs of (a) original CNT, (b) those coated with 20 wt% PANI, (c) 50 wt% PANI, and (d) neat PANI.

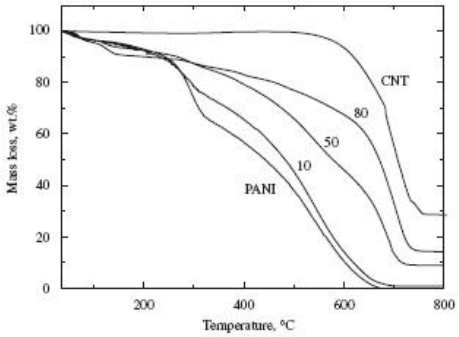

Fig. 4. Thermogravimetric analysis of PANI-coated CNT. The content of CNT (wt%) is given at the individual curves.

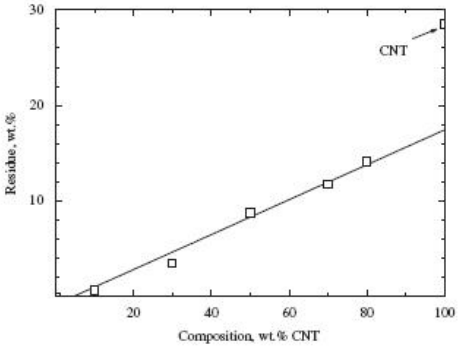

Fig. 5. The residue after TGA experiments, i.e. after heating of PANI–CNT composites to 800 °C in air.

later by sulfuric acid generated as a by-product [29]. It is a question, if and to what extent a residual nickel catalyst dissolves under these conditions. We find that the fraction of residues is directly proportional to the content of CNT in the composite, as expected (Fig. 5). When we extrapolate the data to neat CNT, we obtain the 18.3 wt% content of nickel and/or its compounds. The initial CNT, however, had a residue of 28.5 wt%. We conclude that approximately one third of nickel catalyst has dissolved in acid medium during the polymerization. It has been reported that the PANI coating of nickel reduces its oxidation and corrosion [42]. We thus speculate that the soluble portion of nickel is located outside the CNT, while the catalyst incorporated directly in CNT is not accessible to acid medium and is therefore preserved.

3.3. Raman and FTIR spectra

The PANI–CNT powders were analyzed also by Raman microscopy. The mapping was used to demonstrate that PANI constitutes separate regions in the composite having comparable amounts of components, 50 wt% PANI (Figs. 6–8) as suspected on the basis of SEM micrographs (Fig. 3c). The circular area was randomly selected at the sample surface and the Raman spectra were collected from different spots of the sample (Fig. 6). During the mapping, the picture was built, which shows the intensity of Raman signal at different peaks (Fig. 7). The grey scale of the spectra (Fig. 8) corresponds to the sample areas (Fig. 7), black colour being associated with neat CNT. One can clearly observe the border between two phases of the sample, PANI and CNT. This also means that some CNT have not been completely coated with PANI.

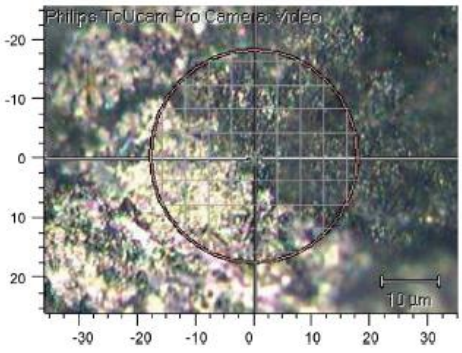

Fig. 6. Selected circular area of powdered PANI–CNT composite with 50 wt% PANI as observed by the optical microscope.

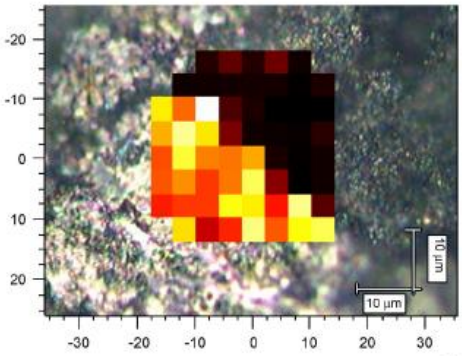

Fig. 7. Intensity of Raman signal at different sample areas ($3 \times 3\ \mu m^2$) obtained during mapping of selected circular area (Fig. 6).

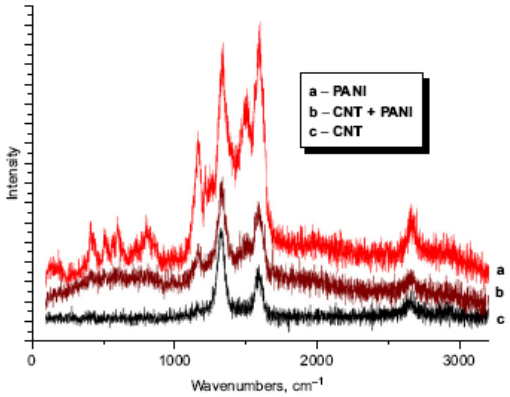

Fig. 8. Raman spectra of (a) PANI, (b) composite area, and (c) CNT. The grey scale in the plot corresponds to the areas shown in Fig. 7.

FTIR spectra of neat CNT are relatively featureless (Fig. 9). The broad band with maximum at about 1428 cm^{-1} and two sharp peaks at 879 and 712 cm^{-1} in the spectrum of CNT are most probably connected with the normal modes of the CO_3^{2-} anion, probably from $NiCO_3$, present in the sample. The broad bands at 789 and 582 cm^{-1} are difficult to assign. The spectrum of neat PANI prepared in ethanol–water mixtures is very close to the spectrum of PANI sulfate prepared in an aqueous medium. The main bands are situated at 1562 cm^{-1} (with a shoulder at 1607 cm^{-1}), 1480, 1408, 1301, 1243, 1127, 800, and 575 cm^{-1}. The fact that polymer is protonated mainly by sulfate anions is demonstrated by the presence of the peak at 575 cm^{-1}, which is attributed to the vibration in the sulfate anion [43]. When the content of CNT increases in the composite, the spectra change. The intensity of the PANI bands decreases. The most significant feature is disappearance of the peak observed at 575 cm^{-1} in the spectrum of PANI. When the content of CNT is 50 wt%, this peak shifts to 615 cm^{-1} and its intensity increases with the content of CNT. At the same time a small but sharp peak is observed at 980 cm^{-1}, and its intensity also increases with the content of CNT.

3.4. Conductivity

The conductivity of PANI-coated CNT, 1–2 S cm^{-1}, practically does not depend on the content of CNT in the composite (Fig. 10). The conductivity of neat PANI, 1.0 S cm^{-1}, is lower than in the case of "standard" PANI [29], 4.4 S cm^{-1}, because the preparation took place in ethanol–water mixture instead of water. An unpronounced increase in the conductivity to 1–2 S cm^{-1} is marginal and suggests that the CNT are slightly more conducting than PANI. The PANI glues the CNT and decreases the contact resistance between individual CNT [32]. A possible small

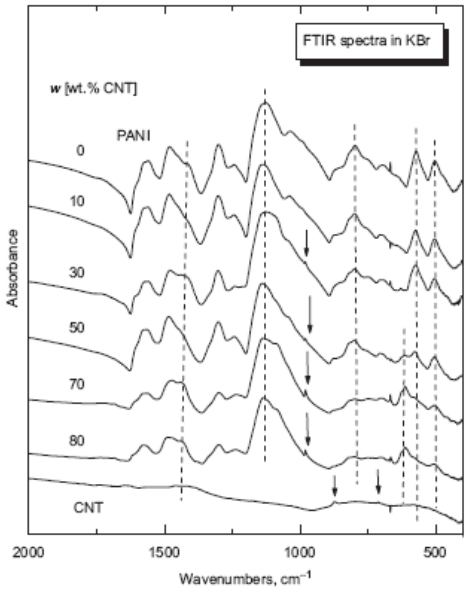

Fig. 9. FTIR spectra of PANI–CNT composites.

decrease in conductivity at high CNT contents may be interpreted as being caused by the increasing contact resistance, due to the insufficient availability of PANI in the interstitial space.

The conversion of protonated PANI coating to a non-conducting PANI base reduces the conductivity down to

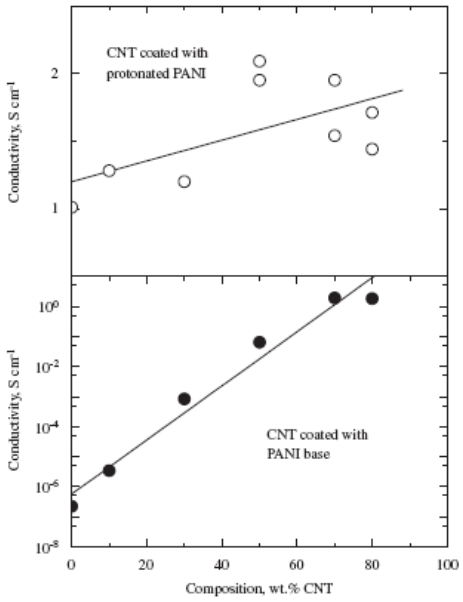

Fig. 10. The dependence of conductivity of CNT coated with protonated PANI (top) and with PANI base (bottom) for composites having various CNT content.

10^{-7} S cm^{-1} at low CNT contents (Fig. 10). The conductivity increases with increasing CNT content, without any percolation transition, otherwise observed for the mixture of PANI base with CNT [12]. This result confirms that the CNT are coated with PANI and thus cannot be in direct mutual contacts assumed in the percolation behaviour.

The mechanical integrity of compressed samples was poor, considerably lower compared with analogous CNT that have not contained the residual catalyst [12]. The attempts to test the thermal stability of composites [44] at 175 °C have failed because of the electrical contact with the samples has been lost even before reaching the working temperature.

3.5. Density and wettability

The specific mass of neat CNT is 0.5 g cm^{-3}, the density determined by helium pycnometry was 2.36 g cm^{-3} [35]. The densities of PANI-coated CNT have been measured by the Archimedes method on compressed pellets and they have an apparent character reflecting their porosity. The density of composites increases with increasing content of CNT (Fig. 11), and its value extrapolated for neat CNT is 1.72 g cm^{-3}. The composites thus contain voids and are likely to have a good permeability for vapours and gases.

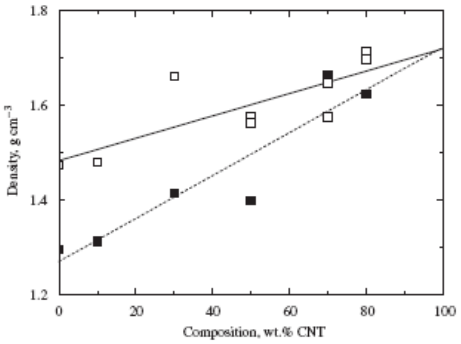

Fig. 11. Density of CNT coated with protonated PANI (open squares) or with PANI base (full squares).

This is important for the applications in the fuel-cell electrodes and sensors.

Water contact angle could be measured only at 0–30 wt% CNT in the samples and was 42°, close to the value of 49° reported for bulk PANI hydrochloride [36]. At higher content of CNT, water droplet placed on a pellet penetrated the sample, and contact angle could not be determined. This implies that PANI-coated CNT are hydrophilic [12] and, similarly like density results, suggest the porous structure of composites.

3.6. Complex permittivity

The permittivity spectra of PANI-coated CNT display the relaxation type of frequency dispersion up to 30 wt% of CNT (Fig. 12). At low frequencies in MHz range, both the real and imaginary parts of complex permeability of composites, ε' and ε'', increase rapidly with increasing CNT content. As the concentration of more conducting CNT phase increases up to formation of infinite conducting network, the averaged value of effective complex permittivity in low-frequency range approaches the infinity. The region, assumed to be connected with the width of critical transition from semi-conducting to conducting state, in the case of PANI–CNT composites is 10–30 wt% CNT. In frequency range from 5 to 10 GHz, the composites with a high concentration of CNT (above 30 vol% of CNT) exhibit the values of $\varepsilon' \sim 30$ and $\varepsilon'' \sim 17$.

In the contrast to the differences in conductivity of CNT coated with conducting or non-conducting form of PANI (Fig. 10), there was not any notable difference in the magnitude and character of frequency dependence of permittivity between the PANI–CNT with the protonated (Fig. 12a,c) and deprotonated composites (Fig. 12b,d). Consequently, the frequency dependence of permittivity is determined by the electronic structure and shape of CNT [45], rather than by the properties of PANI interlayer.

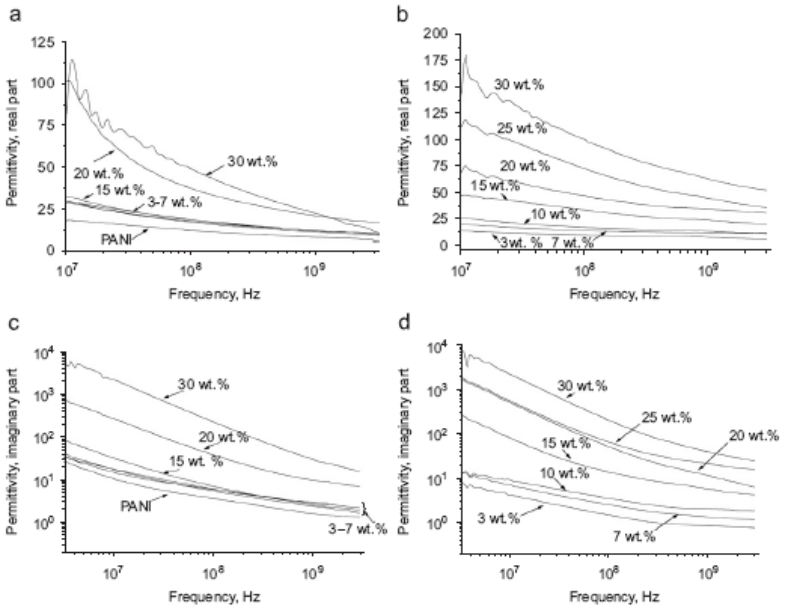

Fig. 12. The frequency dependence of real (a, b) and imaginary parts (c, d) of complex permittivity of CNT coated with conducting (left) and nonconducting (right) form of PANI. The content of CNT is given at the individual curves.

3.7. Complex permeability and magnetic hysteresis

Magnetic spectra, frequency dependences of complex permeability, $\mu^*(f)$, of PANI–CNT composites with different ratio of PANI and CNT are presented in Fig. 13. The composites with 10–40 wt% CNT do not exhibit any ferromagnetic properties; the real part of permeability, μ', is around the unity and the magnetic losses, μ'', are close to zero in the frequency range from 1 MHz to the 10 GHz. The ferromagnetic behaviour of composites appears when the CNT content increases to 50 wt%, which approximately corresponds to 10 wt% of nickel. The character of $\mu^*(f)$ indicates that single-domain nickel nanoparticles (single-domain-size criterion for nickel particles is 6–7 nm [46,47]) in CNT are exchange-coupled. This is revealed by magnetic dispersion and two resonance peaks on the $\mu''(f)$, the first located in low-frequency range, 1–10 MHz, and the second in high-frequency range, 1–3 GHz. By increasing CNT up to 80 wt%, nickel content increases, and thus enhances both permeability components in specified frequency regions.

The dynamic magnetic behaviour of PANI–CNT composites is in a good agreement with magnetostatic measurements of nickel-incorporating CNT powders. It is a ferromagnetic material with saturation magnetization $M_S = 0.5\,\mathrm{emu\,g^{-1}}$ (Fig. 14) and low remanent magnetization $M_r = 0.035\,\mathrm{emu\,g^{-1}}$. By comparison with few tens oersted coercivities of bulk nickel, the coercivity $H_C = 35\,\mathrm{Oe}$ was observed in CNT (Fig. 14). Such high coercivity of nickel-incorporating CNT can be explained by the high value of the effective anisotropy in one-dimensional exchange-coupled system formed by nickel nanoparticles encapsulated in thin carbon shells (Fig. 1) [48,49].

Consequently, the ferromagnetism of CNT containing nickel nanoparticles has two reasons: (1) the carbon shell protects nickel from oxidation, and (2) the large shape anisotropies and inner diameter of CNT give rise to single-domain one–dimensional system. Two types of particle interactions, viz. magnetic–dipole and exchange interactions, are operative [48]. The cooperative effects lead to the increase in the internal magnetic field that acts on each particle. Taking into account a few works that provide evidence that in some carbon structure, e.g. fullerene encapsulated nickel nanoparticles [50] or CNT produced by arc-discharge method [51], and under special treatment of graphitic structure [52], the unusual magnetic properties of CNT maybe due to the enhanced interaction between ferromagnetic nanoparticles under the influence of electronic structure of graphene layers.

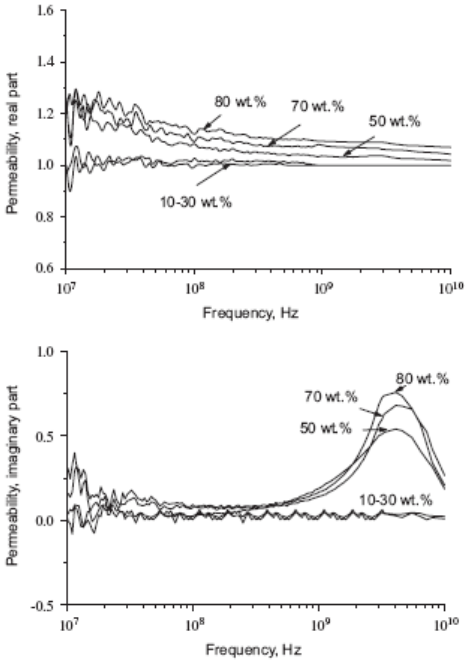

Fig. 13. The frequency dependence of real (top) and imaginary (bottom) parts of complex permeability of CNT coated with protonated conducting PANI. The content of CNT is given at the individual curves.

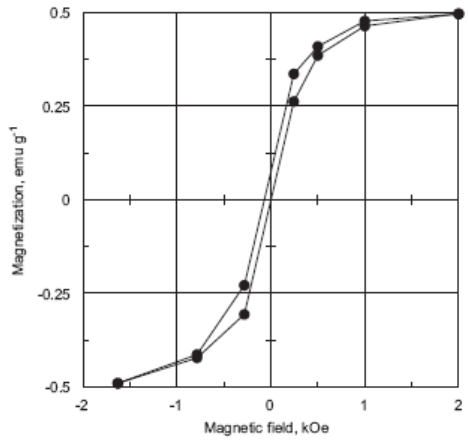

Fig. 14. Magnetic hysteresis loop of neat CNT containing nickel nanoparticles.

4. Conclusions

(1) CNT immersed in the reaction mixture used for the production of PANI become coated with this conducting polymer. Only below 50 wt% of CNT, PANI produces separate regions.
(2) Conductivity of protonated PANI–CNT composites was 1–2 S cm^{-1}, regardless of the composition, 0–80 wt% CNT. Protonated PANI coating is converted to a non-conducting one by immersion in ammonium hydroxide solution and conductivity of composites can be reduced down to 10^{-7} S cm^{-1} at low CNT contents. The compositional dependence of conductivity does not exhibit the percolation behaviour.
(3) The coating of CNT with protonated PANI changes the originally hydrophobic surface to hydrophilic, the water contact angle for protonated PANI coating being 42°.
(4) The ferromagnetism of neat CNT and CNT-rich composites is due to the presence of incorporated nickel-catalyst nanoparticles inside the holes and defects of nanotubes. In spite of the fact that nickel nanoparticles are single-domain particles. They display cooperative magnetic properties, due to the formation of one-dimensional nanosystem, which manifest itself in the presence of frequency dispersion of complex permeability in broad frequency range.

Acknowledgments

The authors thank the Grant Agency of the Czech Republic (202/06/0416), Grant Agency of the Academy of Sciences of the Czech Republic (A4050313 and A400500504), the Ministry of Education, Youth, and Sports of the Czech Republic (ME 847 and ME 833, MSM 0021620834), Department of Materials Sciences, Russian Academy of Sciences (01-07/391), and the Russian Foundation for Basic Research (06-08-01162) for financial support.

References

[1] P.G. Collins, M.S. Arnold, P. Avouris, Science 292 (2001) 706.
[2] A.G. Rinzler, J.F. Hafner, P. Nikolaev, L. Low, S.G. Kim, D. Tomanek, P. Nordlander, D.T. Colbet, R.E. Smalley, Science 269 (1995) 1550.
[3] Y.H. Lin, J.-S. Huang, H.-T. Chiu, Polym. Polym. Compos. 9 (2001) 351.
[4] V. Mottaghitalab, G.M. Spinks, G.G. Wallace, Synth. Met. 152 (2005) 77.
[5] T. Koshiwagi, E. Grulke, J. Hilding, K. Groth, R. Harris, K. Butler, J. Shields, S. Kharchenko, J. Douglas, Polymer 45 (2004) 4227.
[6] M. Sarno, G. Gorrasi, D. Sanniano, A. Sorrentino, P. Ciambelli, V. Vittoria, Macromol. Rapid Commun. 25 (2004) 1963.
[7] A.M. Rao, P.C. Eklund, S. Bandow, A. Thess, R.E. Smalley, Nature 388 (1997) 257.
[8] Y. Ma, P.O. Lehtinen, A.S. Foster, R.M. Neiminen, Phys. Rev. B. 72 (2005) 085451.

[9] K. Yu, Z. Zhu, Q. Li, Appl. Phys. A 77 (2003) 811.
[10] J. Fan, M. Wan, D. Zhu, B. Chang, Z. Pan, S. Xie, Synth. Met. 102 (1999) 1266.
[11] J. Deng, X. Ding, W. Zhang, Y. Peng, J. Wang, X. Long, P. Li, A.S.C. Chan, Eur. Polym. J. 38 (2002) 2497.
[12] E.N. Konyushenko, J. Stejskal, M. Trchová, J. Hradil, J. Kovářová, J. Prokeš, M. Cieslar, J.Y. Hwang, K.H. Chen, I. Sapurina, Polymer 47 (2006) 5715.
[13] M. Paligová, J. Vilčáková, P. Sáha, P. Křesálek, J. Stejskal, O. Quadrat, Physica A 335 (2004) 421.
[14] Y. Jie, S. Zeng-Min, X. Tao, New Carbon Mater. 18 (2003) 95.
[15] G. Inzelt, M. Pineri, J.W. Schultze, M.A. Voroyntsev, Electrochim. Acta 45 (2000) 2403.
[16] D. Coutinho, Z.W. Yang, J.P. Ferraris, K.J. Balkus, Micropor. Mesopor. Mater. 81 (2005) 321.
[17] M.E. Kompan, I.Yu. Sapurina, J. Stejskal, Tech. Phys. Lett. 32 (2006) 213.
[18] A. Damian, S. Omanovic, J. Power Sources 158 (2006) 464.
[19] Z. Qi, M.C. Lefebvre, P.G. Pickup, J. Electroanal. Chem. 459 (1998) 9.
[20] M.D. Deng, B.C. Yang, Y.D. Hu, J. Mater. Sci. 40 (2005) 5021.
[21] E. Frackowiak, V. Khomenko, K. Jurewicz, K. Lota, F. Beguin, J. Power Sources 153 (2006) 413.
[22] V. Gupta, N. Miura, Mater. Lett. 60 (2006) 1466.
[23] M. Guo, J. Chen, J. Li, B. Tao, S. Yao, Anal. Chim. Acta 532 (2005) 71.
[24] E. Granot, B. Basnar, Z. Cheglakov, E. Katz, I. Willner, Electroanalysis 18 (2006) 26.
[25] M. Kaempgen, S. Roth, J. Electroanal. Chem. 586 (2006) 72.
[26] T. Mĕhl, D. Elefant, A. Graff, R. Kozhuharova, A. Leonhardt, I. Mönch, M. Ritshel, P. Simon, S. Groudeva-Zotova, C.M. Schneider, J. Appl. Phys. 93 (2003) 7894.
[27] J. Bao, Q. Zhou, J. Hong, Z. Xu, Appl. Phys. Lett. 81 (2002) 4592.
[28] H. Cao, C. Tie, Z. Xu, J. Hong, H. Sang, Appl. Phys. Lett. 78 (2001) 1592.
[29] J. Stejskal, R.G. Gilbert, Pure Appl. Chem. 74 (2002) 857.
[30] J. Stejskal, M. Trchová, S. Fedorova, I. Sapurina, J. Zemek, Langmuir 19 (2003) 3013.
[31] J. Stejskal, I. Sapurina, Pure Appl. Chem. 77 (2005) 815.
[32] M. Cochet, W.K. Maser, A.M. Benito, M.A. Callejas, M.T. Martinez, J.-M. Benoit, J. Schreiber, O. Chauvet, Chem. Commun. (2001) 1450.
[33] X. Zhang, J. Zhang, Z. Liu, Appl. Phys. A 80 (2005) 1813.
[34] R. Sainz, A.M. Benito, M.T. Martínez, J.F. Galindo, J. Sotres, A.M. Baró, B. Corraze, O. Chauvet, W.K. Maser, Adv. Mater. 17 (2005) 278.
[35] M.M. Tomishko, G.N. Permyakov, M.Yu. Zezin, V.S. Beskov, A.V. Mikhailova, A.M. Alekseev, A.V. Putilov, Theor. Found. Chem. Eng. 33 (1999) 370.
[36] T.V. Shishkanova, I. Sapurina, J. Stejskal, V. Král, R. Volf, Anal. Chim. Acta 553 (2005) 160.
[37] R.T. Lewis, Rev. Sci. Instrum. 42 (1971) 31.
[38] Y. Yu, B. Che, Z. Si, L. Li, W. Chen, G. Xue, Synth. Met. 150 (2005) 271.
[39] X. Zhang, J. Zhang, R. Wang, Z. Liu, Carbon 42 (2004) 1455.
[40] M. Omastová, S. Podhradská, J. Prokeš, I. Janigová, J. Stejskal, Polym. Degrad. Stab. 82 (2003) 251.
[41] J. Kan, S. Zhang, G. Jing, J. Appl. Polym. Sci. 99 (2006) 1848.
[42] H. Cao, C. Tie, Z. Xu, J. Hong, H. Sang, Appl. Phys. Lett. 78 (2001) 1592.
[43] R.M. Silverstein, G.C. Bassler, T.C. Morrill, Spectrometric Identification of Organic Compounds, fifth ed., Wiley, New York, 1991.
[44] J. Prokeš, J. Stejskal, Polym. Degrad. Stab. 86 (2004) 187.
[45] C.A. Grimes, C. Mungle, D. Kouzoudis, S. Fang, P.C. Eklund, Chem. Phys. Lett. 319 (2000) 460.
[46] S.V. Vonsovskii, Magnetism, Nauka, Moscow, 1971 (Chapter 23, pp. 800–805).
[47] A.A. Bukhaev, D.V. Ovchinnikov, N.I. Nurgazizov, E.F. Kukovitskii, M. Klaiber, R. Weisendanger, J. Phys. Solid State 40 (1998) 1163.
[48] R.S. Iskhakov, S.V. Komagortsev, A.D. Balaev, A.V. Okotrub, A.G. Kudashov, V.L. Kuznetsov, Yu.V. Butenko, JETP Lett. 78 (2003) 236.
[49] S.V. Komagortsev, R.S. Iskhakov, E.A. Denisova, A.D. Balaev, V.G. Myagkov, N.V. Bulina, A.G. Kudashov, A.V. Okotrub, Tech. Phys. Lett. 31 (2005) 454.
[50] G.H. Lee, S.H. Hun, J.W. Jeong, H.-C. Ri, J. Magn. Magn. Mater. 246 (2002) 404.
[51] A.S. Kotosonov, D.V. Shilo, A.P. Moravsky, Phys. Solid State 44 (2002) 666.
[52] P. Esquinazi, D. Spemann, R. Hohne, A. Setzer, K.-H. Han, T. Butz, Phys. Rev. Lett. 91 (2003) 227201.

Appendix F

Jaroslav Stejskal, Irina Sapurina, Miroslava Trchová,
and Elena N. Konyushenko,
Oxidation of Aniline: Polyaniline Granules, Nanotubes, and Oligoaniline Microspheres,
Macromolecules, in press.

obio1/yma-yma/yma-yma/yma99907/yma3908d07z | xppws | 23:ver.6 | 4/6/08 | 23:44 | Msc: ma-2007-02601q | TEID: cdm00 | BATID: ma5b38

Oxidation of Aniline: Polyaniline Granules, Nanotubes, and Oligoaniline Microspheres

Jaroslav Stejskal,*,† Irina Sapurina,‡ Miroslava Trchová,† and Elena N. Konyushenko†

Institute of Macromolecular Chemistry, Academy of Sciences of the Czech Republic, 162 06 Prague 6, Czech Republic, and Institute of Macromolecular Compounds, Russian Academy of Sciences, St. Petersburg 199004, Russia

Received November 22, 2007; Revised Manuscript Received February 19, 2008

ABSTRACT: Aniline was oxidized with ammonium peroxydisulfate in solutions of strong acid (0.1 M sulfuric acid), weak acid (0.4 M acetic acid), or alkali (0.2 M ammonium hydroxide). The properties of the oxidation products and their morphology are controlled by the initial acidity of the medium and the acidity profile during the oxidation; the acidity increases because sulfuric acid is a byproduct. Conducting polyaniline nanogranules, nanotubes, or nonconducting oligoaniline microspheres were obtained, respectively. FTIR spectra suggest that the oligomers produced by the oxidation of neutral aniline molecules at the beginning of oxidation are similar, regardless of the acidity of the medium. Neutral aniline molecules, prevailing under alkaline conditions, are easily oxidized to aniline oligomers composed of *ortho*- and *para*-coupled aniline constitutional units. *Ortho*-coupled units are further converted by oxidative intramolecular cyclization to phenazines. It is proposed that, in acidic media, *N*-phenylphenazine units constitute the initiation centers for the subsequent polymerization of aniline, which takes place at pH < 2 when the intermediate pernigraniline chains become protonated. Anilinium cations, which dominate in strongly acidic media, are difficult to oxidize to oligomers, but they easily participate in the formation of polymer chains once their growth has started. The self-organization of phenazine units is responsible for the generation of polyaniline nanotubes. Partial sulfonation of aromatic amines occurs at higher pH, especially in alkaline media. The sulfonated oligomers stabilize aniline emulsions and enable the formation of oligoaniline microspheres, when the miscibility of aniline with aqueous medium is limited. The final oxidation products obtained in alkaline conditions contain only low-molecular-weight oligomers; the polymeric component is the dominating product only in strongly acidic media. Both components are present in various proportions when the oxidation takes place at intermediate pH ranges.

Introduction

Nanostructures produced by conducting polymers are likely to exhibit new electrical and optical properties due to the various organizations of polymer chains.[1,2] Polyaniline (PANI) is one of the most important conducting polymers. The oxidation of aniline typically proceeds in strongly acidic aqueous medium and is currently used for the synthesis of conducting PANI.[3] The granular morphology of PANI is observed as a rule.

Reports on the preparation of PANI nanotubes[4–7] and nanowires[8–13] now appear in the literature frequently. The pioneering papers have been published by the Wan group.[14–16] The presence of organic acid in the reaction mixture has been a typical feature of these syntheses.[7,11,14] It has been proposed that aniline salts with these acids form a special kind of template for the subsequent polymerization of aniline.[16,17] Later, however, the nanotubes were prepared in solutions of inorganic acids[18] or even in the absence of any added acid.[19] Another type of morphology, microspheres, was the product of aniline oxidation started in an alkaline medium.[20,21] The role of the acidity, rather than the nature of the acid employed, has recently been suggested to exert control over the chemistry of aniline oxidation[5,21,22] and, subsequently, the growth of PANI nanostructures.

During the oxidation of aniline with peroxydisulfate, the pH decreases because sulfuric acid is a byproduct (Figure 1). Any coupling of aniline molecules is connected with the abstraction of two hydrogen atoms that are released as protons. The whole oxidation is thus an intricate interplay of oxidation and protonation processes, depending on the starting pH and the acidity−time profile during the reaction. The present study demonstrates the role of acidity in the formation of the molecular structure of the oxidation products, and tries to provide some chemical clues to the generation of supramolecular assemblies.

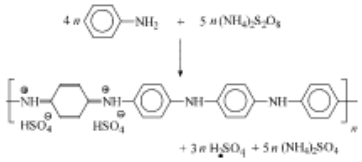

Figure 1. Stoichiometry of aniline oxidation with ammonium peroxydisulfate to polyaniline hydrogen sulfate in an acidic medium. Sulfuric acid and ammonium sulfate (or ammonium hydrogen sulfate) are byproducts.

Experimental Section

Oxidation of Aniline. Aniline (20 mmol, 1.86 g) was dissolved in various aqueous media: 0.1 M sulfuric acid, 0.4 M acetic acid, or 0.2 M ammonium hydroxide to 50 mL of solution. Ammonium peroxydisulfate (APS; 25 mmol, 5.71 g) was similarly dissolved to provide 50 mL of a solution, and the solutions of aniline and oxidant were mixed at 20 °C to start the oxidation. The reaction mixture thus always contained 0.2 M aniline and 0.25 M APS (Figure 1). The course of the exothermic polymerization was monitored with a digital thermometer, and the acidity changes were recorded with a pH meter. The solids were collected on a filter after 2 h, rinsed with water, and dried in air then over silica gel in a desiccator.

* To whom correspondence should be addressed. Fax: +420-296-809-410; e-mail: stejskal@imc.cas.cz.
† Academy of Sciences of the Czech Republic.
‡ Russian Academy of Sciences.

10.1021/ma702601q CCC: $40.75

ohio1/yma-yma/yma-yma/yma99907/yma3908d07z | xppws | 23:ver.6 | 4/6/08 | 23:44 | Msc: ma-2007-02601q | TEID: cdm00 | BATID: ma5b38

Table 1. Properties of Polyanilines Prepared in Aqueous Media of Various Acidities[a]

	0.1 M sulfuric acid	0.4 M acetic acid	0.2 M ammonium hydroxide
starting pH	2.4	4.5	10.4
terminal pH	1.0	1.1	3.0
morphology	granules	nanotubes	microspheres
conductivity of protonated form, S cm^{-1}	3.7	0.036	$<10^{-10}$
conductivity of corresponding base, S cm^{-1}	1.1×10^{-9}	7.9×10^{-9}	$<10^{-10}$
density, protonated/base, g cm^{-3}	1.402/1.227	1.338/1.256	
sulfur in PANI bases, wt %	0.9	1.8	2.0
molecular weight, M_w	39,400	32,200	4,080
polydispersity index, M_w/M_n	13.1	19.0	1.3

[a] 0.2 M Aniline was oxidized with 0.25 M ammonium peroxydisulfate at 20 °C. The corresponding bases were obtained by deprotonation with 1 M ammonium hydroxide. Conductivity was determined by a four-point method for conducting samples ($>10^{-5}$ S cm^{-1}) and with a two-point technique for nonconducting samples. Density was determined by weighing the samples in air and immersed in decane. Molecular weights and polydispersity were assessed by gel-permeation chromatography using *N*-methylpyrrolidone as the solvent.

A portion of the products was converted to PANI bases by overnight immersion in 1 M ammonium hydroxide, followed by separation and drying. Test samples have also been isolated after 4 min of reaction.

Characterization. Infrared spectra in the range of 400–4000 cm^{-1} were recorded at 64 scans per spectrum at 2 cm^{-1} resolution using a Thermo Nicolet NEXUS 870 FTIR spectrometer with a DTGS TEC detector. Samples were dispersed in potassium bromide and compressed into pellets. The spectra were corrected for the presence of moisture and carbon dioxide in the optical path. Optical spectra of the oxidation products dissolved in *N*-methylpyrrolidone were recorded with a Lambda 20 spectrometer (Perkin-Elmer, UK).

Results

Oxidation of Aniline in Media of Various Acidities. The oxidation of aniline in the solutions of strong acids, e.g., 0.1 M sulfuric acid, has become standard procedure for the preparation of a conducting polymer,[3] with the conductivity of the product of the order of at least units S cm^{-1} being the criterion of successful preparation. The oxidation products are polymers having a broad molecular-weight distribution (Table 1) and are obtained as fused nanogranules (Figure 2a). The characteristic absorption maxima in the UV–visible spectra recorded for solutions of PANI base in *N*-methylpyrrolidone are located at 324 and 618 nm, and correspond to the blue color of PANI base (Figure 3).

When the oxidation is started under mildly acidic conditions, e.g., in 0.4 M acetic acid, the conductivity of the product is reduced but its polymeric character is still retained (Table 1). The high polydispersity index is due to the bimodality of the distribution; the product is composed of polymeric and oligomeric components.[22] The formation of nanotubes is the most interesting feature of the reaction (Figure 2b). When the conductivity is not the main goal and the preference is given to the nanoscale morphology of the products, the oxidation of aniline under mildly acid conditions is the priority strategy. In the optical spectra, the first maximum is shifted to 336 nm and the second is shifted to 602 nm, in accord with the reduced conductivity and the presence of an oligomeric fraction (Figure 3).

Oxidation started in an alkaline medium, 0.2 M ammonium hydroxide, yields nonconducting aniline oligomers (Table 1) but the microspheres they create (Figure 2c) make them of interest. The single absorption maximum at 336 nm in the visible spectra corresponds to the brown color of the solution and reflects the absence of conjugation (Figure 3).

The Course of Oxidation. The oxidation process itself can be analyzed by following the time-dependence of the acidity (Figure 4) which increases in the course of reaction because sulfuric acid is a byproduct (Figure 1), and/or temperature (Figure 5), because the oxidation is exothermic. The oxidation in 0.1 M sulfuric acid starts at pH 2.4 and the decrease in pH is well visible (Figure 4). An athermal induction period is followed by exothermic polymerization,[3,23] during which the temperature of the reaction mixture increases (Figure 5). Similar oxidation under mildly acidic conditions, in 0.4 M acetic acid, starts immediately, as illustrated by the sudden drop in pH (Figure 4) and the evolution of heat (Figure 5). After the pH falls below ~3.5, the oxidation virtually stops and the mixture cools, just to be followed by the second exothermic phase, starting below ca. pH 2.5. The oxidation of aniline started in alkaline conditions, 0.2 M ammonium hydroxide, is fast, without any induction period (Figures 4 and 5). The ammonium hydroxide constituting the medium is neutralized in the course of oxidation by the sulfuric acid produced (Figure 1), and the final pH thus falls in the mildly acidic region.

Molecular Structure. FTIR spectra of *the final oxidation products* substantially differ from each other (Figure 6). The base forms of the oxidation products are better suited for the comparison of molecular structure rather than the protonated counterparts, because the spectral features of counter-ions are then absent. In addition to the main absorption bands of PANI base, located at 1585 and 1497 cm^{-1}, a shoulder at about 1630 cm^{-1} and bands at 1445 and 1414 cm^{-1} are present in the spectra of the products obtained in 0.4 M acetic acid and under alkaline conditions. We suppose that they correspond to the presence of *ortho*-coupled aniline units and phenazine-like units.[5,19] These peaks are not visible in the spectra of samples prepared in 0.1 M sulfuric acid. The peak at 1374 cm^{-1}, typical of standard PANI base and assigned to C−N stretching in the neighborhood of a quinonoid ring,[24] becomes reduced in the product prepared in less acidic conditions, e.g., in acetic acid. The peak located at 1040 cm^{-1} suggests the presence of sulfonate groups attached to the aromatic rings;[25] this is supported by the presence of sulfur in the samples (Table 1).

FTIR spectra of oxidation products collected in *the early stages of oxidation* in the solutions of a strong and a weak acid are, on the other hand, virtually identical (Figure 7). This is one of the most important observations of the present study. They are also identical with the spectra of the first oligomeric products of the oxidation of aniline in water, reported earlier,[19] and are very close to those observed for the oxidation products in an alkaline medium (Figure 7). The presence of the peaks at 1625, 1445, and 1414 cm^{-1} is a common feature of the all the early oxidation products. The last peak may be assigned to a totally symmetric stretching of the phenazine ring.[26,27] Phenazine-like units can also be detected by the bands at 1208 and 1136 cm^{-1} (Figure 7) and their contribution to the band at 1145 cm^{-1} is possible. The bands observed at 1445 and 1414 cm^{-1} in the spectrum of *o*-semidine (2-aminodiphenylamine), where they are much stronger than in the spectrum of *p*-semidine (4-aminodiphenylamine), support the presence of *ortho*-linked aniline constitutional units in the oligomers. The band at 1625 cm^{-1}, with a shoulder at ~1630 cm^{-1}, corresponds to the C═C stretching vibration in a phenazine-like segment,[28] including a contribution from C═N stretching vibrations.[29] The spectrum of phenazine itself displays the band at 1627 cm^{-1}. The ring-sulfonation of oligomers is especially favored when the oxidation proceeds in an alkaline medium, as is demonstrated by the absorption peak located at 1040 cm^{-1}.

ohio1/yma-yma/yma-yma/yma99907/yma3908d07z | xppws | 23:ver.6 | 4/6/08 | 23:44 | Msc: ma-2007-02601q | TEID: cdm00 | BATID: ma5b38

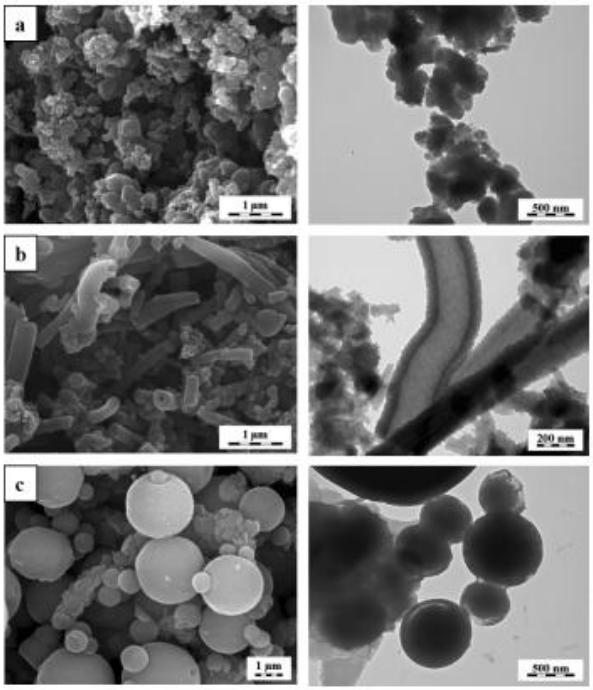

Figure 2. Scanning (left) and transmission (right) electron microscopy: (a) granular morphology typical for polyaniline prepared in strongly acidic solutions (0.1 M sulfuric acid); (b) oxidation of aniline under mildly acidic conditions (0.4 M acetic acid) produces nanotubes; (c) oligomeric microspheres obtained when the oxidation is initiated in alkaline medium (0.2 M ammonium hydroxide).

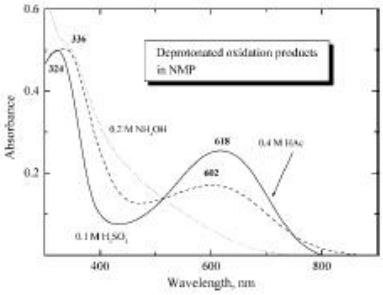

Figure 3. UV–visible spectra of the oxidation products converted to the base form and dissolved in *N*-methylpyrrolidone. Polyaniline was prepared in 0.1 M sulfuric acid (full line), and 0.4 M acetic acid (dashed line), and oligoaniline in 0.2 M ammonium hydroxide (dotted line). The first two products are blue, the last one is brown.

Discussion

Aniline is a weak base, $pK_a = 4.6$ at 25 °C.[30,31] In alkaline media, it exists mostly as neutral aniline molecules while, under strongly acidic conditions, the anilinium cations dominate (Figure 8). The neutral aniline molecules and anilinium cations have different electron density distributions and, consequently, different oxidation reactivity and reaction fate.[30]

Oxidation in an Alkaline Medium. Neutral aniline molecules are easily oxidized to produce a dimer (semidine), and to add further aniline molecules to produce higher oligomers (Figure 9). Both the *ortho* and *para* coupling of aniline molecules is possible.[32,33] That is why the oxidation products prepared in 0.2 M ammonium hydroxide do not produce a conjugated system and they are nonconducting. The degree of oligomerization is low, typically up to tens of aniline constitutional units (Table 1).

The *ortho*-coupled aniline units can further undergo oxidative cyclization to yield phenazine structures[34,35] (Figure 9). This type of reaction is well-known from the oxidation of *o*-phenylenediamine.[36,37] or branching and cross-linking reactions in PANI.[38–40] Phenazine units can be produced at any point in an oligomer chain.

Oxidation in a Solution of a Weak Acid. When the oxidation of aniline starts in mildly acidic conditions, at pH 4.5 in 0.4 M acidic acid (Figure 4), the reaction mixture is rich in both neutral aniline molecules and anilinium cations (Figure 8). Neutral aniline molecules are easily oxidized to oligomers as described above (Figure 9), and the released protons reduce the pH (Figure 4). The equilibrium between the aniline

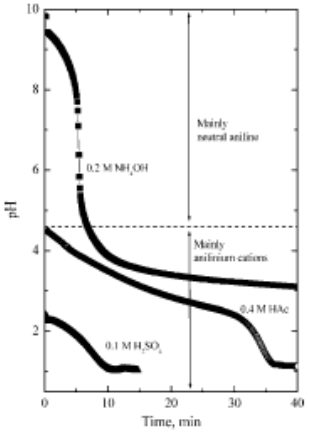

Figure 4. Acidity profiles during the oxidation of 0.2 M aniline with 0.25 M ammonium peroxydisulfate started in media of high acidity (0.1 M sulfuric acid), low acidity (0.4 M acetic acid), and in alkaline solutions (0.2 M ammonium hydroxide).

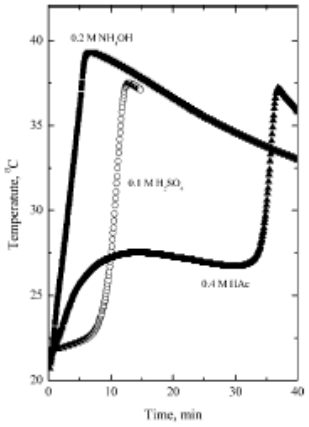

Figure 5. Temperature profile during the oxidation of 0.2 M aniline with 0.25 M ammonium peroxydisulfate started in media of high acidity (0.1 M sulfuric acid), low acidity (0.4 M acetic acid), and in alkaline solution (0.2 M ammonium hydroxide).

molecules and anilinium cations shifts in favor of the latter species (Figure 8). Anilinium cations are much more difficult to oxidize directly, because the electron pair on nitrogen, which is delocalized in neutral aniline molecules, becomes localized in the anilinium cation.[30] That is why the reaction virtually stops,[5,41] and the temperature starts to decrease (Figure 5). Yet, there is always equilibrium between the protonated and neutral species (Figure 8), both species always coexist, and the oxidation of neutral aniline molecules still proceeds with preference even if their content is very low. This is manifested by a continuing decrease in pH under such conditions (Figure 4). The situation corresponds to the induction period observed in the classical

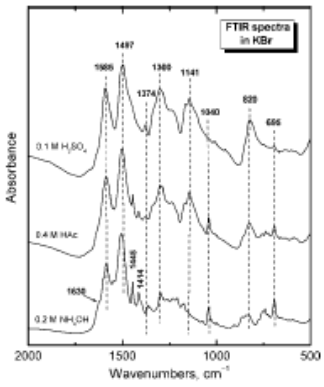

Figure 6. FTIR spectra of bases obtained by the deprotonation of samples prepared by the oxidation of aniline in 0.1 M sulfuric acid, 0.4 M acetic acid, or in 0.2 M ammonium hydroxide.

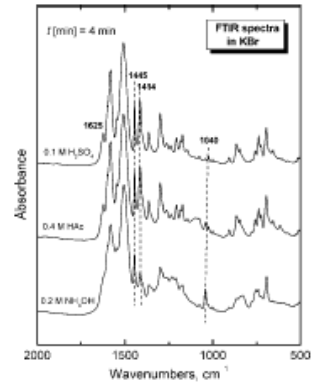

Figure 7. FTIR spectra of products isolated in the early stages of aniline oxidation (after 4 min) in 0.1 M sulfuric acid, 0.4 M acetic acid, or in 0.2 M ammonium hydroxide.

polymerization of aniline in acidic media. The situation changes when pH < 2 (Figure 4). Such conditions correspond to those of oxidation in strong acids, and indeed sulfuric acid is produced in the course of oxidation (Figure 1). The exothermic polymerization then follows (Figure 5).

Oxidation in a Solution of a Strong Acid. The induction period is a typical feature when anilinium cations are the dominating monomer species (Figure 5): the aniline molecules that can be oxidized are deficient, anilinium cations that are available are difficult to oxidize, and the reaction proceeds only very slowly. This reaction stage is followed by an exothermic polymerization (Figure 5). It is well-known that under such conditions the growth of PANI chains in the protonated pernigraniline form becomes feasible[42] (Figure 10). Anilinium cations cannot be oxidized directly but they are easily added to propagating PANI chains, once their growth has started. After the oxidant becomes depleted, pernigraniline is reduced by the residual aniline to the final product, a green emeraldine form

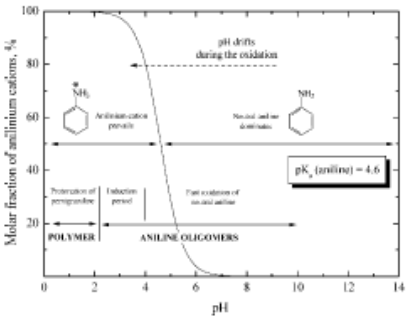

Figure 8. pH Drifts to lower values during the oxidation of aniline (Figure 4). The equilibrium between neutral aniline molecules and anilinium cations shifts in favor of the latter species.

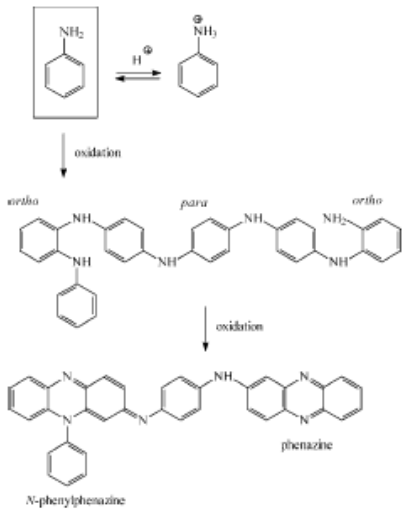

Figure 9. Proportions between neutral aniline molecules and anilinium cations depend on pH. Neutral aniline molecules are oxidized to oligomers having mixed *ortho*- and *para*-coupled aniline constitutional units. *Ortho*-coupled units may undergo intramolecular cyclization to produce phenazine structures.

of PANI.[23] Macromolecules are composed with a high preference by *para*-linked aniline constitutional units[43] (Figure 10).

While the propagation of PANI chains seems to be well established, the chain initiation mechanism is still open to discussion. We propose that species of the *N*-phenylphenazine type (Figure 9) act as initiation centers. During the induction period observed in acidic media, the highly deficient aniline is still the only species which is oxidized; the predominating anilinium cations are not prone to direct oxidation. The *ortho*-coupled aniline units produced by oxidation of neutral aniline are converted by intramolecular cyclization to *N*-phenylphenazine (Figure 9). Such structures have been identified in "aniline black" and synthetic dyes obtained by the oxidation of aniline,

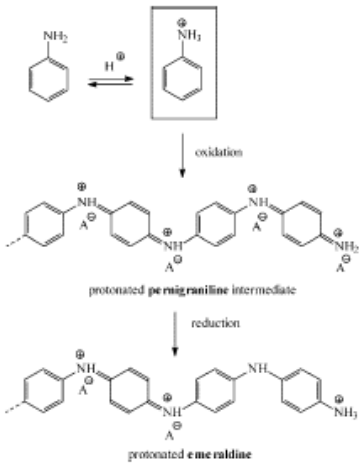

Figure 10. Polyaniline chains grow in blue protonated pernigraniline form by adding anilinium cations in *para* positions. At the end of oxidation they are reduced by excess aniline to the green emeraldine form.

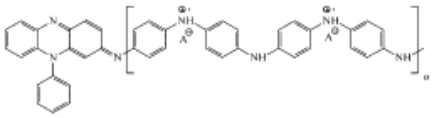

Figure 11. Structure of polyaniline chains, based on the proposition that a *N*-phenylphenazine head initiates the growth of an attached linear *para*-coupled polyaniline tail.

such as mauveine and pseudomauveine.[35,44] The formation of a phenazine heterocycle is promoted by an acidic medium.[45] Further oligomer growth, however, is suppressed due to their high oxidation potential of *N*-phenylphenazine and the low concentration of available neutral aniline. At pH < 2, mainly aniline dimers, trimers, and tetramers can be produced simultaneously by direct oxidation of neutral aniline molecules.[35] When the pH becomes sufficiently low, chain propagation from these initiation centers becomes feasible (Figure 10). The low number of initiation centers and the high propagation rate result in the formation of high-molecular-weight chains. Such polymer chains are then likely to contain a *N*-phenylphenazine head and a linear *para*-coupled PANI tail (Figure 11).

This concept is supported by FTIR spectra reported above. The formation of phenazine units was also suggested to explain the "middle peak" observed in cyclic voltammograms during the early stages of electrochemical oxidation of aniline.[46] Nonconducting aniline oligomers were produced, which passivated the electrode surface,[47] and only later a conducting PANI film grew on this layer. The UV–visible spectra recorded during the onset of aniline oxidation included absorption peaks,[32,48] which could be associated with the phenazine cycles.[49,50]

Polyaniline Nanotubes. The structure proposed in Figure 11 seems to explain some features of the supramolecular morphology produced by PANI. When the oxidation was carried out in the solution of a weak acid, e.g., 0.4 M acetic acid,[5,22] PANI nanotubes were obtained (Figure 2b). The ability of phenazines

to self-organize into microfibrils or nanobelts has been demonstrated in the literature.[51] The stacking of phenazine-based molecules was proposed to be due to the interplay of $\pi-\pi$ interactions, hydrogen bonding, and to be assisted by phase separation caused by hydrophobic effects.[51] The oligomers produced at the first stage of aniline oxidation similarly produce extended nanocrystallites by stacking mechanism.[5,19] These act as templates for the adsorption of *N*-phenylphenazines arising in solution during the induction period. The starting template place for nanotubular growth is thus produced by the short *N*-phenylphenazines stacked around the oligomeric nanocrystallite.[5] We can speculate that the further addition of phenazine units on the front of the tubular *N*-phenylphenazine stack guides its growth beyond the nanocrystallite template.[5] One-dimensional crystal growth is a distant but pertinent analogy. The subsequent growth of PANI chains from stacked *N*-phenylphenazines initiation centers (Figure 11) then gives rise to the walls of nanotubes. We believe that the nanowires grow by a closely related mechanism.

Oligoaniline Microspheres. The formation of microspheres, which is observed in the oxidation of aniline[20,21,52,53] or aniline derivatives[54] under weakly acidic or alkaline conditions, has another background. The neutral aniline is not always completely miscible with the aqueous medium and constitutes a separate phase. The oxidation then proceeds at the interface between the aniline droplets and the aqueous phase containing the oxidant. The nonconducting aniline oligomers (Table 1) form microspheres (Figure 2c) having a diameter of a few micrometers. They can be hollow or may possibly be partly filled with aniline (Figure 2c, right); the presence of aniline encapsulated in an overoxidized oligomeric shell facing the oxidant-rich medium may be responsible for some of the differences observed in the FTIR spectra (Figure 7).

The generation of microspheres can be understood by using the concept of surfactant-free emulsion polymerization. Such polymerization has been used for the preparation of polystyrene nanospheres and microspheres by introducing ionic moieties into the polymer structure during the radical polymerization, e.g., as end-groups from the peroxydisulfate,[55–57] other initiator fragments,[58] or by copolymerization with an ionic comonomer.[58,59] The process may be regarded as an *in situ* formation of a surfactant in emulsion polymerization. The polymerization then proceeds in the monomer droplets stabilized by the produced oligomers,[60] and the resultant polymer microspheres are stabilized by the surface charge of the ionic groups.

A similar scenario is offered in the case of aniline. The limited miscibility of 0.2 M aniline with 0.2 M ammonium hydroxide solution is clearly visible to the naked eye during the experiment. The substituted anilines are even less miscible with water, and that is the reason for the frequent observation of microspheres.[61,62] Aniline oligomers produced at the beginning of oxidation in alkaline media are partly sulfonated, as is confirmed by the presence of the absorption peak at[19] 1040 cm^{-1} in the FTIR spectra (Figure 7), and by the content of sulfur in the base (Table 1). Such oligomers may stabilize monomer droplets at micrometer-size dimensions, just as surfactants do, with the sulfonic groups being oriented at the droplet surface toward the aqueous phase with the aniline constitutional units in the direction of its interior.

Some microspheres seem to have a "stopper", a small sphere, on the surface (Figure 2c). Similar microspheres, composed of aniline oligomers, have been reported to have an opening, a hole.[20,21,53,62] These effects may be connected with the heat evolution during the polymerization leading to protrusion of aniline outside the spheres or with the evaporation of aniline encapsulated in the spheres during the drying of the samples at elevated temperature *in vacuo*.[63] No proof of any hypothesis has been provided so far.

Conclusions

The oxidation of neutral aniline molecules produces nonconducting oligomers composed of mixed *para*- and *ortho*-coupled aniline constitutional units, and various phenazine units, as a result of the cyclization of *ortho*-coupled units. At pH > 4, this is the only reaction that takes place.

At 4 > pH > 2, anilinium cations are the predominant aniline species in the system but they are difficult to oxidize. The oxidation reaction virtually does not proceed and this phase is known as an induction period. The highly deficient neutral aniline molecules are still the only species that are oxidized to yield short aniline oligomers, rich in phenazine units. That is why the early stages of oxidation always involve neutral aniline molecules and yield the similar type of oligomers regardless of the acidity of the medium. The acidity slowly decreases as a result of continuing oxidation. No polymer is produced at this stage. It is proposed that phenazine units act as the initiation centers for the future polymerization of aniline.

The polymerization proceeds only at pH < 2, when the intermediate pernigraniline form becomes protonated and makes this process feasible. *N*-phenylphenazine is proposed to be responsible for the initiation of chain growth. Anilinium cations easily participate in the propagation step to give high-molecular-weight PANI chains, until aniline or oxidant or both become depleted. The pH ranges given here have only informative guidance and the transition between them is smooth.

The pH decreases in the course of oxidation because sulfuric acid is a byproduct. Depending on the initial and final acidity of the reaction mixture, the mechanism of oxidation may change. The oxidation products always have an oligomeric component (produced by the oxidation of neutral aniline) and may have a polymeric fraction (generated by the polymerization involving anilinium cations) in varying proportions. Short oligomers comprising units of the phenazine type are proposed to self-assemble and promote the self-organized growth of polymer chains to supramolecular assemblies, such as nanotubes and nanowires. The limited miscibility of neutral aniline with the reaction medium is responsible for the formation of microspheres, which are stabilized by sulfonated oligoanilines.

Acknowledgment. We thank the Czech Grant Agency (202/06/0419 and 203/08/0686) and the Ministry of Education, Youth, and Sports of the Czech Republic (ME 847) for financial support.

References and Notes

(1) Aleshin, A. N. *Adv. Mater.* 2006, *18*, 17.
(2) Zhang, D.; Wang, Y. *Mater. Sci. Eng., B* 2006, *134*, 9.
(3) Stejskal, J.; Gilbert, R. *G. Pure Appl. Chem.* 2002, *74*, 857.
(4) Zhang, Z.; Wei, Y.; Zhang, L.; Wan, M. *Acta Mater.* 2005, *53*, 1373.
(5) Stejskal, J.; Sapurina, I.; Trchová, M.; Konyushenko, E. N.; Holler, P. *Polymer* 2006, *47*, 8253.
(6) Zhang, L. J.; Peng, H.; Hsu, C. F.; Kilmartin, P. A.; Travas-Sejdic, J. *Nanotechnology* 2007, *18*, 115607.
(7) Zhang, L. J.; Peng, H.; Zujovic, Z. D.; Kilmartin, P. A.; Travas-Sejdic, J. *Macromol. Chem. Phys.* 2007, *208*, 1210.
(8) Zhang, X.; Goux, W. J.; Manohar, S. K. *J. Am. Chem. Soc.* 2004, *126*, 4502.
(9) Li, D.; Kaner, R. B. *J. Am. Chem. Soc.* 2006, *128*, 968.
(10) (a) Huang, J. X.; Kaner, R. B. *J. Am. Chem. Soc.* 2004, *126*, 851. (b) Huang, J. X. *Pure Appl. Chem.* 2006, *78*, 15. (c) Huang, J.; Kaner, R. B. *Chem. Commun.* 2006, 367.
(11) Zhang, L.; Zhang, L.; Wan, M.; Wei, Y. *Synth. Met.* 2006, *156*, 454.
(12) Chiou, N.-R.; Lee, J.; Epstein, A. J. *Chem. Mater.* 2007, *19*, 3587.
(13) Chiou, N. R.; Lui, C. M.; Guan, J. J.; Lee, L. J.; Epstein, A. J. *Nature Nanotechnol.* 2007, *2*, 354.
(14) Huang, J.; Wan, M. *J. Appl. Polym. Sci.* 1999, *37*, 1277.
(15) Qiu, H.; Wan, M.; Matthews, B.; Dai, L. *Macromolecules* 2001, *34*, 675.

(16) Qiu, H.; Wan, M. *J. Polym. Sci., Part A Polym. Chem.* **2001**, *39*, 3485.
(17) Wei, Z.; Zhang, Z.; Wan, M. *Langmuir* **2002**, *18*, 917.
(18) Zhang, Z.; Wei, Z.; Wan, M. *Macromolecules* **2002**, *35*, 5937.
(19) Trchová, M.; Šeděnková, I.; Konyushenko, E. N.; Stejskal, J.; Holler, P.; Ćirić-Marjanović, G. *J. Phys. Chem. B* **2006**, *110*, 9461.
(20) Wang, X.; Liu, N.; Yan, X.; Zhang, W.; Wei, Y. *Chem. Lett.* **2005**, *34*, 42.
(21) Venancio, E. C.; Wang, P.-C.; MacDiarmid, A. G. *Synth. Met.* **2006**, *156*, 357.
(22) Konyushenko, E. N.; Stejskal, J.; Šeděnková, I.; Trchová, M.; Sapurina, I.; Cieslar, M.; Prokeš, J. *Polym. Int.* **2006**, *55*, 31.
(23) Pud, A. A.; Noskov, Yu. V.; Kassiba, A.; Fatyeyeva, K. Yu.; Ogurtsov, N. A.; Makowska-Janusik, M.; Bednarski, W.; Tabellout, M.; Shapoval, G. S. *J. Phys. Chem. B* **2007**, *111*, 2174.
(24) Kang, K. G.; Neoh, K. L.; Tan, T. C. *Prog. Polym. Sci.* **1998**, *23*, 277.
(25) Sahin, Y.; Pekmez, K.; Yildiz, A. *Synth. Met.* **2002**, *131*, 7.
(26) Viva, F. A.; Andrade, E. M.; Molina, F. M.; Florit, M. I. *J. Electroanal. Chem.* **1999**, *471*, 180.
(27) Dines, T. J.; MacGregor, L. D.; Rochester, C. H. *Phys. Chem. Chem. Phys.* **2001**, *13*, 2676.
(28) Li, X.-G.; Duan, W.; Huang, M.-R.; Yang, Y.-L. *J. Polym. Sci., Part A: Polym. Chem.* **2001**, *39*, 3989.
(29) Malinauskas, A.; Bron, M.; Holze, R. *Synth. Met.* **1998**, *92*, 127.
(30) Cram, D. J.; Hammond, G. S. *Organic Chemistry*; McGraw Hill: New York, 1964; pp 210–211..
(31) *CRC Handbook of Chemistry and Physics*, 76th Ed.; Lide, D. R., Frederikse, H. P. R., Eds.; CRC Press: New York, 1995; pp 8–49..
(32) Zimmermann, A.; Kunzelmann, U.; Dunsch, L. *Synth. Met.* **1998**, *93*, 17.
(33) Mazeikiene, R.; Niaura, G.; Malinauskas, A. *J. Electroanal. Chem.* **2005**, *580*, 87.
(34) Ćirić-Marjanović, *G.*; Trchová, M.; Stejskal, J. *Collect. Czech. Chem. Commun.* **2006**, *71*, 1407.
(35) (a) Ćirić-Marjanović, G.; Trchová, M.; Stejskal, J. *Int. J. Quantum Chem.* **2008**, *108*, 318. (b) Ćirić-Marjanović, G.; Konyushenko, E. N.; Trchová, M.; Stejskal, J. *Synth. Met.* , 000. in press, , doi:10.1016/j.synthmet.2008.01.005.
(36) (a) Chiba, K.; Ohsaka, T.; Ohnuki, Y.; Oyama, N. *J. Electroanal. Chem.* **1987**, *219*, 117. (b) Losito, I.; De Giglio, E.; Cioffi, N.; Malitesta, C. *J. Mater. Chem.* **2001**, *11*, 1812.
(37) Li, X. G.; Duan, W.; Huang, M.-R.; Rodriguez, L. N. J. *React. Funct. Polym.* **2005**, *62*, 261.
(38) Trchová, M.; Matějka, P.; Brodinová, J.; Kalendová, A.; Prokeš, J.; Stejskal, J. *Polym. Degrad. Stab.* **2006**, *91*, 114.
(39) Zhou, C.; Han, J.; Song, G; Guo, R. *Macromolecules* **2007**, *40*, 7075.
(40) Matnishyan, A. A.; Akhnazaryan, T. L. *Polym. Sci. Ser. B* **2007**, *49*, 139.
(41) Fu, Y.; Elsenbaumer, R. L. *Chem. Mater.* **1994**, *6*, 671.
(42) Madathil, R.; Ponrathnam, S.; Byrne, H. J. *Polymer* **2004**, *45*, 5465.
(43) Bacon, J.; Adams, R. N. *J. Am. Chem. Soc.* **1968**, *90*, 6596.
(44) (a) Meth-Cohn, O.; Smith, M. *J. Chem. Soc., Perkin Trans.* **1994**, *1*, 5. (b) de Melo, J. S.; Takato, S.; Sousa, M.; Melo, M. J.; Parola, A. J. *Chem. Commun.* **2007**, 2624.
(45) Tu, X.; Xie, Q.; Xiang, C.; Zhang, Y.; Yao, S. *J. Phys. Chem. B* **2005**, *109*, 4053.
(46) Geniès, E. M.; Lapkowski, M.; Penneau, J. P. *J. Electroanal. Chem.* **1988**, *249*, 97.
(47) Hong, S.-Y.; Park, S.-M. *J. Phys. Chem. B* **2007**, *111*, 9779.
(48) Neoh, K. G.; Kang, E. T.; Tan, K. L. *Polymer* **1993**, *34*, 3921.
(49) Wu, L.-L.; Luo, J.; Lin, Z.-H. *J. Electroanal. Chem.* **1997**, *440*, 173.
(50) He, D.; Wu, L.-L; Xu, B.-Q. *Eur. Polym. J.* **2007**, *43*, 3703.
(51) (a) Desvergne, J.-P.; Del Guerzo, A.; Bouas-Laurent, H.; Belin, C.; Reichwagen, J.; Hopf, H. *Pure Appl. Chem.* **2006**, *78*, 707. (b) Sun, X.; Hagner, M. *Langmuir* **2007**, *23*, 10441. (c) He, D.; Wu, Y.; Xu, B.-Q. *Eur. Polym. J.* **2007**, *43*, 3703.
(52) Zhang, L.; Wan, M.; Wei, Y. *Macromol. Rapid Commun.* **2006**, *27*, 888.
(53) Zhu, Y.; Hu, D.; Wan, M.; Wan, M.; Jiang, L.; Wei, Y. *Adv. Mater.* **2007**, *19*, 2092.
(54) Han, J.; Song, G.; Guo, R. *Adv. Mater.* **2006**, *18*, 3140.
(55) Žůrková, E.; Bouchal, K.; Zdeňková, D.; Pelzbauer, Z.; Švec, F.; Kálal, J.; Batz, H. G. *J. Polym. Sci., Polym. Chem. Ed.* **1983**, *21*, 2949.
(56) Tuin, G.; Peters, A. C. I.; vanDiemen, A. J. G.; Stein, H. N. *J. Colloid Interface Sci.* **1993**, *158*, 508.
(57) Ngai, T.; Wu, C. *Langmuir* **2005**, *21*, 8520.
(58) Liu, W.-J.; He, W.-D.; Wang, Y.-M.; Wang, D.; Zhang, Z.-C. *Polym. Int.* **2006**, *55*, 520.
(59) Peula, J. M.; Fernández-Barbero, A.; Hidalgo-Álvarez, R.; de las Nieves, F. J. *Langmuir* **1997**, *13*, 3938.
(60) Kühn, I.; Tauer, K. *Macromolecules* **1995**, *28*, 8122.
(61) Sanada, K.; Patil, R.; Ooyama, Y.; Yano, J.; Harima, Y. *Polym. J.* **2006**, *38*, 732.
(62) Han, J.; Song, G.; Guo, R. *Chem. Mater.* **2007**, *19*, 973.
(63) Im, S. H.; Jeong, U.; Xia, Y. *Nat. Mater.* **2005**, *4*, 671.

MA702601Q

Appendix G

Elena N. Konyushenko, Jaroslav Stejskal, Miroslava Trchová, Natalia V. Blinova, and Petr Holler,

Polymerization of aniline in ice,

Synthetic Metals, submitted, after revision (2008)

Polymerization of aniline in ice

Elena N. Konyushenko, Jaroslav Stejskal, Miroslava Trchová, Natalia V. Blinova, Petr Holler

Institute of Macromolecular Chemistry, Academy of Sciences of the Czech Republic, 162 06 Prague 6, Czech Republic

Abstract

It was observed that the oxidative polymerization of aniline proceeded well not only in the liquid mixtures (20 °C or –5 °C) but also in ice at –24 °C. The oxidative polymerization took place in the solutions of strong acid (0.1 M sulfuric acid) or weak acid (0.4 M acetic acid). It is proposed that the initially generated polyaniline participates in the further redox process, leading to new polyaniline formation. The molecules of the monomer (aniline) and oxidant (peroxydisulfate) thus react by transferring electrons through the conducting polyaniline, without the need to be in direct contact. The polymerization in the liquid phase or in the solid frozen state changes the morphology of the polyaniline. Polyaniline nanogranules or nanotubes are produced in the liquid state, while thin nanowires of 20 nm diameter connecting the submicrometre polyaniline particles have been observed when the polymerization took place in ice.

Keywords: Aniline, polyaniline, conducting polymer, redox reaction, nanotube, nanowire, electron transfer, ice, solid-state polymerization.

1. Introduction

Polyaniline (PANI), the most common conducting polymer [1,2], is typically prepared by the oxidation of aniline in an acidic aqueous medium [3]. It has been observed that the polymerization carried out at reduced temperature yielded PANI with a higher molecular weight [4] and higher degree of crystallinity [5], although the improvement of conductivity was marginal [5]. The higher molecular weight is of benefit when the mechanical properties of PANI are important, *e.g.*, when the solutions of PANI base in *N*-methylpyrrolidone are used to cast PANI membranes [6] or are spun to produce PANI fibres [7] or nanofibres [8].

The freezing point of the reaction mixture containing 0.2 M aniline hydrochloride and 0.25 M ammonium peroxydisulfate is –12 °C. In order to prevent freezing at lower temperatures in similar experiments, copious amounts of lithium chloride have been added into reaction mixture [4,9–14], which stayed liquid even at –40 °C. It has been observed, however, that the polymerization of aniline proceeds well, and to a high yield, even at –50 °C when the reaction mixture was frozen [5,15]. Although the polymerizations of monomers in crystals or solid monomer solutions are well known, and have been reviewed [16], this behavior in the present system of aniline oxidation is still rather unexpected.

Besides the polymerization in ice, solid-state reactions involving PANI have been described in the literature. The protonation reactions between PANI base and solid organic acids have been established [7,17–22]. The same approach, the mixing of the components in the solid state, has been successfully used for the preparation of PANI complexes with fullerene [23]. The mechanochemical polymerization of aniline, an oxidation of aniline in the solid state, has only recently been reported [24–26]. In this case, the aniline monomer and an oxidant produce a polymer as a result of the joint

mechanical grinding of the components. One would expect that, when the oxidation of aniline takes place in the solid state, like in the frozen medium, the process would be slow, if feasible at all, due to the restricted diffusion of reactants in the solids and the reduced probability of their contact. Yet, for reasons discussed below, the polymerization takes place easily even under such conditions.

Kocherginsky *et al.* [6,27] have demonstrated that the molecule of an oxidant and a reductant separated by a PANI membrane may undergo a redox reaction. This was achieved without any direct contact between the reacting molecules, by simply transporting an electron from the oxidant to the reductant through conducting PANI; the redox reaction between iron(III) chloride and ascorbic acid has been used as an example. This concept has been extended to the preparation of PANI by the oxidation of aniline with ammonium peroxydisulfate, solutions of the two components being separated by a PANI membrane [28]. It is elaborated in the present study to provide an understanding of the oxidative polymerization of aniline, which is a typical redox reaction, in a frozen aqueous reaction medium, *i.e.*, in ice.

2. Experimental

2.1. Oxidation of aniline

For the polymerizations in liquid state, aniline (0.2 M) was oxidized with ammonium peroxydisulfate (0.25 M) in 0.1 M sulfuric acid or in 0.4 M acetic acid (Figure 1). Solutions of a monomer and an oxidant were mixed at 20 °C or after pre-cooling at 0 °C or –5 °C to start the oxidation.

For the polymerizations in ice, the solutions of reactants were mixed at –5 °C in polyethylene containers and immediately cooled to –190 °C in liquid nitrogen. The solid frozen samples were then placed into a freezer at –24 °C. After 20 days, the green solid

content was melted and the PANI was isolated on a filter, rinsed with the corresponding acid, and acetone, and dried in air.

When estimating the rate of oxidation, the containers were removed after a specified time, their frozen content was transferred to excess of 1 M ammonium hydroxide, and left to melt there. The combination of the alkaline medium and the accompanying dilution stopped the conversion of aniline to PANI in 0.4 M acetic acid. The precipitated oxidation product was quickly collected on the filter, and thus separated from the residual oxidant and aniline, and dried. For polymerizations in 0.1 M sulfuric acid this approach was not successful, because the ice, which was white after removal from the freezer, turned green before it completely melted.

2.2. Characterization

Scanning electron micrographs were taken with a JEOL 6400 microscope (Japan). Molecular-weight distributions were assessed by gel-permeation chromatography using a 8 × 600 mm PLMixedB column (Polymer Laboratories, UK) operating with *N*-methylpyrrolidone and calibrated with polystyrene standards, with spectrophotometric detection. The samples were dissolved in *N*-methylpyrrolidone containing 0.025 g cm^{-3} triethanolamine for deprotonation of PANI, and 0.005 g cm^{-3} lithium bromide to prevent aggregation. Infrared spectra were recorded with a fully computerized Thermo Nicolet NEXUS 870 FTIR Spectrometer with a DTGS TEC detector. The spectra of the samples dispersed in potassium bromide were recorded in the transmission mode and corrected for the presence of carbon dioxide and water vapour in the optical path. The conductivity was measured with a four-point van der Pauw method, on pellets compressed at 700 MPa with a manual hydraulic press, using

as the SMU Keithley 237 and a Multimeter Keithley 2010 voltmeter with a 2000 SCAN 10-channel scanner card.

3. Results

3.1. The course of aniline polymerization: liquid aqueous medium and ice

The fact that the oxidation of aniline in an acidic aqueous medium yields PANI and the conversion of aniline to PANI is practically complete has been well established [2,3]. It is, however, implicitly assumed that the reaction medium is liquid. Nevertheless, it has been demonstrated that, even if the medium becomes frozen, the polymerization of aniline takes place [5]. The polymerization of 0.2 M aniline with 0.25 M ammonium peroxydisulfate (Figure 1) at 20 °C takes 15 min to complete in 0.1 M sulfuric acid or 40 min in 0.4 M acetic acid [29]. At –24 °C in ice, the process takes place in the solid state, the reaction is slower, yet still feasible. The originally white ice becomes gradually dark green. In 0.4 M acetic acid, the full conversion of aniline to PANI was achieved after 4 h (Figure 2). The similar oxidation of aniline in 0.1 M sulfuric acid was faster. When trying to estimate the rate of oxidation in this case, we have not been able to stop efficiently this process during the melting of ice.

3.2. Morphology

Polyaniline is known to exhibit a variety of supramolecular morphologies, such as thin films on various substrates [30,31], colloidal particles [32–36], nanotubes [29,37–40], nanowires [41–43], sometimes referred to as nanofibres [44,45], and hollow PANI microspheres [37,45,46]. It is likely that PANI morphology, based on the self-assembly of PANI chains, will also be affected by the liquid or solid state of the medium in which the polymerization takes place. It has already been shown that the

polymerization of aniline in the presence of hydroxypropylcellulose yields colloidal particles [15,34]. In the similar polymerization carried out in ice, a sponge-like macroporous composite has been obtained instead [15].

Granular morphology of PANI is typically obtained when the polymerization takes place at 20 °C in solutions of strong acids [28], such as 0.1 M sulfuric acid. At –5 °C, some indications of extended nanostructures are observed (Figure 3). If the similar reaction takes place in the solutions of weak acid [29], 0.4 M acetic acid, PANI nanotubes are the dominating product (Figure 4). A rough nanogranular "dotted" surface of the nanotubes, occasionally reported in the literature [15,47,48], should be noted. The morphology after polymerization in ice is different, irrespective of acid, and is constituted by particles of submicrometre size, mutually connected by nanofibres of *ca* 20 nm thickness (Figures 3, 4).

3.3. Molecular weights

The solutions of aniline always contain equilibrium concentrations of aniline as neutral molecules and anilinium cation in various proportions [49]. Aniline molecules dominate at low acidity or in alkaline solutions and the anilinium cations are present with preference in strongly acidic conditions. The oxidation of aniline molecules yields non-conducting oligomers, the oxidation of anilinium cations results in the formation of a conducting polymer [49]. The situation is even more complex because the acidity increases in the course of polymerization, where sulfuric acid is a by-product (Figure 1) and the proportions of both monomers change correspondingly. Any oxidation of aniline thus yields a mixture of a non-conducting oligomers and conducting polymer, their shares being widely varying depending on the reaction conditions.

The oxidation in 0.1 M sulfuric acid starts and proceeds at strongly acidic conditions, pH<2, and yields a polymer (Figure 5a). The traces of oligomers manifest themselves as an unpronounced shoulder in molecular-weight distributions (MWD) at low-molecular-weight part. This applies both to the polymerization in a liquid state at 20 °C and in ice at –24 °C. The MWD are monomodal, and shifted to higher molecular weights when the oxidation took place at low temperature. The weight-average molecular weight of PANI produced in ice was M_w = 30 400, the weight-to-number average molecular weight ratio M_w/M_n = 6.6. It has to be noted that the reproducibility of the GPC results is not very good; the molecular-weight averages depended on the calculation procedures and have to be regarded as relative estimates only.

The oligomers are the main component when the polymerization takes place in a solution of a weak acid, 0.4 M acetic acid (Figure 5b). The presence of polymer fraction is demonstrated by a broad peak at the high-molecular-weight region. Under such conditions the oxidation starts at pH 4.5 and the terminal acidity [50] is pH 1 and this acidity profile is responsible for the generation of oligomers at the beginning of oxidation and the growth of polymer chains at later stage. This two-component character is preserved also when the oxidation takes place in ice; only the proportion of polymeric fraction is considerably enhanced. The polymerization in ice yielded PANI having M_w = 23 200, and M_w/M_n = 5.6.

It should be mentioned that the presence of oligomers may be regarded as undesirable when the high conductivity and good processing properties are a goal [14]. On the other hand, such oligomers constitute an important template for the growth of PANI nanotubes and related morphologies [50,51].

3.4. Molecular structure

The molecular structure of PANI prepared at room temperature in solutions of strong acids is different compared with the samples prepared at mildly acidic conditions [50,51]. The spectrum of the PANI base prepared in the presence of 0.1 M sulfuric acid is similar to that reported in the literature [18,51–53] (Figure 6, spectrum **a**). Additional peaks situated at 1444, 1414, 1040, and 694 cm^{-1} are observed in the spectrum of the product prepared in 0.4 M acetic acid (Figure 6, marked by arrows in the spectrum **c**). They were assigned to aniline oligomers containing the phenazine units [50,51]. The bands at 1444 and 1414 cm^{-1} are probably related to mixed C–C stretching, and C–H and C–N bending vibrations observed in the spectra of the aniline oligomers [14,53]. The peak at 1040 cm^{-1} is possibly due o the S=O stretching vibration and suggests the presence of sulfonic groups on the aromatic rings [54]. The band at 695 cm^{-1} is characteristic of mono-substituted aromatic rings, terminal groups in aniline oligomers, which corresponds to GPC results [14] (Figure 5).

The corresponding spectra of PANI prepared in a frozen mixtures at –24 °C in 0.1 M sulfuric acid (Figure 6, spectrum **b**) and in 0.4 M acetic acid (spectrum **d**) are very close to the shape of the spectra of samples prepared at 20 °C, including the differences between these spectra described above. The main peaks corresponding to quinone and benzene ring-stretching deformations at 1589 and 1497 cm^{-1} are slightly red-shifted in case of samples prepared in a frozen mixture, which indicates the protonation of the samples. The presence of a small peak at 880 cm^{-1} signifies the presence of ammonium hydrogen sulfate (spectrum **e**) which protonates the sample. The spectra of samples prepared at reduced temperature (spectra **b** and **d)** contain also broad bands of ammonium sulfate (spectrum **f**) located at about 1413, 1088 and 612 cm^{-1}. This is explained as follows: the samples prepared in ice were transferred to the solution of ammonium hydroxide to stop the polymerization, and left to melt there. The solids

were quickly separated on a filter to separate any residual aniline and oxidant. The time was short enough to avoid any polymerization after melting but not sufficient to remove the ammonium hydrogen sulfate or ammonium sulfate, which are the reaction by-products (Figure 1). The traces of residual ammonium hydrogen sulfate, which is an equimolar compound of sulfuric acid and ammonium sulfate (Figure 1) from the formal point of view, are likely to partly protonate the PANI base.

3.5. Conductivity

The conductivity is the most important property of conducting polymers. The decrease of temperature from 20 °C to –24 °C leads to the increase in conductivity from 2.5 S cm^{-1} to 9.8 S cm^{-1} in 0.1 M sulfuric acid, and from 0.1 S cm^{-1} to 1.3 S cm^{-1} in 0.4 M acetic acid (Figure 7). This is in the accordance with the earlier observations that the conductivity of PANI is only slightly dependent on the temperature of polymerization [5]; the changes of one order of magnitude are regarded as "small", because the decrease in conductivity connected with deprotonation of PANI amounts to ten orders of magnitude. A little effect of molecular weight on the conductivity can be explained by the comparable probabilities of inter- and intra-molecular charge transports.

4. Discussion

4.1. Oxidation of aniline on polyaniline

Kocherginsky *et al.* [6,27] have investigated redox processes occurring at PANI membranes. They have shown that a molecule of a reductant, ascorbic acid, and an oxidant, iron(III) chloride, can react, *i.e.* supply and accept electrons without being in a direct contact, when separated by a conducting PANI membrane. Such a membrane enables the transfer of electrons from the reductant to an oxidant to occur. This concept

was extended to the polymerization of aniline [28]. Solutions of aniline hydrochloride (a reductant) and ammonium peroxydisulfate (an oxidant), separated by a PANI membrane, react in similar fashion to yield PANI by exchanging the electrons through the conducting polymer. Polyaniline was produced entirely on aniline side of the membrane.

The PANI that is produced *during* the polymerization of aniline may perform a similar role. Let us imagine a reaction mixture containing the molecules of a reductant (aniline salt) and an oxidant (ammonium peroxydisulfate), in the presence of already-produced and still growing PANI body (Figure 8). An active PANI chain-end will add aniline monomer as a new constitutional unit. The abstraction of two electrons is needed for the formation of a chemical bond between the aniline and the existing PANI chain. These are accepted by the oxidant molecule, peroxydisulfate, which is reduced to sulfate. The crucial point is that *any* oxidant molecule in contact with PANI particles, and not only the oxidant molecules in the close vicinity of growing chains, can accept electrons. The electrons travel through the conducting PANI phase from the locus of polymerization to the oxidant. Consequently, neither the aniline monomer nor the oxidant molecules need to diffuse to meet each other in order to react.

It should be noted that simultaneous transport of protons should be considered in order to maintain the electroneutrality of the system [27,28] and the role of PANI as a mixed proton and electron conductor may become of importance [55].

4.2. Polymerization in the frozen reaction mixture

The concept outlined above explains why the polymerization also takes place in a solid system in general and in a frozen aqueous medium, ice, in particular. Once the first traces of PANI have been formed, the molecules of aniline and peroxydisulfate

produce further PANI by transferring the electrons through the mass of existing PANI (Figure 3). We repeat that there is no need for the molecules to diffuse close to each other to react. As PANI grows by this mechanism, it gradually expands and penetrates the whole volume of the solidified reaction mixture; the electrons can then be transferred through the PANI structure, even over long distances. The resulting PANI structure thus has a connective character, and electrical contact between its parts is maintained, among others, also by PANI nanowires connecting the larger polymer particles (Figures 3, 4). The fact that the aniline molecule, which is added to the growing PANI structure, can react with *any* oxidant molecule which is close to PANI, and not only with the neighboring one (contact reaction in Figure 8) dramatically increases the probability of reaction. That is why the polymerization is relatively fast even in the solid system. This principle also explains the well-known autoacceleration effect in the oxidation of aniline [15,56,57]; the larger becomes the mass of PANI in the early stages of polymerization, more oxidant molecules are in its vicinity, and the probability of aniline molecules to react with any of them strongly increases. The reaction slows down only after oxidant or aniline molecules or both become depleted.

In a chemical translation, we can schematically describe the above process as follows (Figure 9): the oxidant (peroxydisulfate) removes electrons from the emeraldine form of PANI – at some point on a PANI macromolecule or a PANI particle – and converts it to the pernigraniline form. On the other hand, the addition of an aniline molecule to growing PANI chain at another location results in the formation of a new constitutional unit of PANI. The transfer of electrons from the added aniline molecules to pernigraniline regenerates the original emeraldine form at both reaction loci.

We would like to make here the following point: the polymerization of aniline takes place in contact with preformed nanostructures of PANI and it is not important,

from the chemical point of view, whether the surrounding reaction medium is liquid or solid. The differences in the molecular structure of the resulting PANI are negligible but the supramolecular morphology depends on the state of the reaction medium.

4.3. Concluding remarks

There are many questions that can be asked, yet the answers are not available. For instance, during the cooling of reaction mixture to freezing point, some of the components may become insoluble. This would result in the loci having the increased concentration, *e.g.* of aniline. The fact that sulfuric acid is produced especially at the places where ammonium peroxydisulfate accepts electrons from aniline may similarly produce a local increase in acidity. Such concentration inhomogeneities fixed in ice may affect the course of polymerization and the produced morphology.

5. Conclusions

(1) The oxidative polymerization of aniline with ammonium peroxydisulfate proceeds well, even when the aqueous reaction mixture is frozen and the oxidation of aniline takes place in the solid state, *i.e.* in ice. This is explained by the transfer of electrons from aniline to oxidant assisted by the conducting PANI phase. The aniline molecule can be converted to a polyaniline constitutional unit by providing two electrons. These are transferred through conducting PANI body to any oxidant molecules at its vicinity. The aniline thus can react with an oxidant without any direct contact of these two molecules.

(2) Granular PANI is produced in the liquid reaction mixtures in 0.1 M sulfuric acid, PANI nanotubes are produced in 0.4 M acetic acid. In the frozen mixtures at –24 °C, the products are composed of submicrometre PANI particles connected by PANI

nanowires of *ca* 20 nm diameter. The nanowires are expected to provide the electrical contact and participate in the electron transfer between larger polyaniline particles.

(3) A decrease in the reaction temperature from 20 °C in the liquid state and the polymerization in ice at –24 °C results in a small increase in the conductivity measured at room temperature. The conversion of aniline to polyaniline is practically complete in both cases. Polyaniline of higher molecular weight is produced at lower temperatures. FTIR spectroscopy suggests that the molecular structures of the PANI prepared in the liquid or in the solid state identical.

Acknowledgment. Authors thank the Grant Agency of the Academy of Sciences of the Czech Republic (A4050313 and A400500504) for financial support. Thanks are also due to Dr J. Prokeš from the Charles University of Prague for the conductivity measurements.

References

[1] E.T. Kang, K.G. Neoh, K.L. Tan, Prog. Polym. Sci. 23 (1998) 227.

[2] N. Gospodinova, L. Terlemezyan, Prog. Polym. Sci. 23 (1998) 1443.

[3] J. Stejskal, R.G. Gilbert, Pure Appl. Chem. 74 (2002) 857.

[4] P.N. Adams, P.J. Laughlin, A.P. Monkman, Synth. Met. 76 (1996) 157.

[5] J. Stejskal, A. Riede, D. Hlavatá, J. Prokeš, M. Helmstedt, P. Holler Synth. Met. 96 (1998) 55.

[6] N.M. Kocherginsky, W. Lei, Z. Wang, J. Phys. Chem. A 109 (2005**)** 4010.

[7] S. J. Pomfret, P.N. Adams, N.P. Comfort, A.P. Monkman, Polymer 41 (2000) 2265.

[8] J. Kameoka, R. Orth, Y.N. Yang, D. Czaplewski, R. Mathers, G.W. Coates, H.G. Craighead, Nanotechnology 14 (2003) 1124.

[9] L. H.C. Mattoso, A.G. MacDiarmid, A. J. Epstein, Synth. Met. 68 (1994) 1.

[10] P.N. Adams, P.J. Laughin, A.P. Monkman, A.M. Kenwright, Polymer 37 (1996) 3411.

[11] P.N. Adams, A.P. Monkman, Synth. Met. 87 (1997) 165.

[12] P.M. Beadle, Y.F. Nicolau, E. Banka, P. Rannou, D. Djurado, Synth. Met. 95 (1998) 29.

[13] D. Chao, J. Chen, X. Lu, L. Chen, W. Zhang, Y. Wei, Synth. Met. 150 (2005) 47.

[14] J. Laska, J. Widlarz, Polymer 46 (2005) 1485.

[15] J. Stejskal, M. Špírková, A. Riede, M. Helmstedt, P. Mokreva, J. Prokeš, Polymer 40 (1999) 2487.

[16] G.C. Eastmond Prog. Polym. Sci. 2 (1970) 1.

[17] J. Stejskal, I. Sapurina, M. Trchová, J. Prokeš, I. Křivka, E. Tobolková, Macromolecules 31 (1998) 2218.

[18] M. Trchová, J. Stejskal, J. Prokeš, Synth. Met. 101 (1999**)** 840 .

[19] H.-S. Xu, Z.-Y. Cheng, Q. M. Zhang, P.-C. Wang, A.G. MacDiarmid, Synth. Met. 108 (2000) 133.

[20] K. Potje-Kamloth, B.J. Polk, M. Josowicz, J. Janata, Chem. Mater. 14 (2002) 2782.

[21] D. Poussin, H. Morgan, P. J. S. Foot, Polym. Int. 52 (2003) 433.

[22] W. Lu, E. Smela, P. Adams, G. Zuccarello, B.R. Mattes, Chem. Mater. 16 (2004) 1615.

[23] I. Sapurina, M. Mokeev, V. Lavrentev, V. Zgonnik, M. Trchová, D. Hlavatá, J. Stejskal, Eur. Polym. J. 36 (2000) 2321.

[24] J. Gong, X.-J. Cui, Z.-W. Xie, S.-G. Wang, L.-Y. Qu Synth. Met. 129 (2002) 187.

[25] S. Yoshimoto, F. Ohashi, Y. Ohnishi, T. Nonami, Synth. Met. 145 (2004) 265.

[26] J. X. Huang, J.A. Moore, J.H. Acquaye, R.B. Kaner, Macromolecules 38 (2005) 317.

[27] N.M. Kocherginsky, Z. Wang, Synth. Met. 156 (2006) 558.

[28] N.V. Blinova, J. Stejskal, M. Trchová, G. Ćirić.Marjanović, I. Sapurina, J. Phys. Chem. B 111 (2007) 2440.

[29] E.N. Konyushenko, J. Stejskal, I. Šeděnková, M. Trchová, I. Sapurina, M. Cieslar, J. Prokeš, Polym. Int. 53 (2006) 31.

[30] I. Sapurina, A. Riede, J. Stejskal, Synth. Met. 123 (2001) 303.

[31] M.M. Ayad, M.A. Shenashin, Eur. Polym. J. 40 (2004) 197.

[32] J. Stejskal, P. Kratochvíl, S.P. Armes, S.F. Lascelles, A. Riede, M. Helmstedt, J. Prokeš, I. Křivka, Macromolecules 29 (1996) 6814.

[33] S. Maeda, D.B. Cairns, S.P. Armes, Eur. Polym. J. 33 (1997) 245.

[34] J. Stejskal, J. Polym. Mater. 18 (2001) 225.

[35] M. S. Cho, S.Y. Park, J.Y. Hwang, H.J. Choi, Mater. Sci. Eng. C 24 (2004) 15.

[36] J. Stejskal, I. Sapurina, Pure Appl. Chem. 77 (2005) 815.

[37] L. Zhang, M. Wan, Adv. Funct. Mater. 13 (2003) 815.

[38] L. Zhang, Y. Long, Z. Chen, M. Wan, Adv. Funct. Mater. 14 (2004) 693.

[39] M. Trchová, I. Šeděnková, E.N. Konyushenko, J. Stejskal, P. Holler, G. Ćirić-Marjanović, J. Phys. Chem. B 110 (2006) 9461.

[40] L. Zhang, H. Peng, C.F. Hsu, P.A. Kilmartin, J. Travas-Sejdic, Nanotechnology 18 (2007) 115607.

[41] J. Huang, R.B. Kaner, Angew. Chem. Int. Ed. 43 (2004) 5817.

[42] W. Zhong, J. Deng, Y. Yang, W. Yang, Macromol. Rapid Commun. 26 (2005) 395.

[43] D. Li, R.B. Kaner, Chem. Commun. (2005) 3286.

[44] D. M. Sarno, S.K. Manohar, A.G. MacDiarmid, Synth. Met. 148 (2005) 237.

[45] K. Huang, X.-H. Meng, M. Wan, J. Appl. Polym. Sci. 100 (2006) 3050.

[46] E.C. Venancio, P.-C. Wang, A.G. MacDiarmid, Synth. Met. 156 (2006) 357.

[47] H. Ding, M. Wan, Y. Wei, Adv. Mater. 19 (2007) 465.

[48] Y. Gao, S. Yao, J. Gong, L. Qu, Macromol. Rapid Commun. 28 (2007) 286.

[49] G. Ćirić-Marjanović, M. Trchová, J. Stejskal, Collect. Czech. Chem. Commun. 71 (2006) 1407.

[50] J. Stejskal, I. Sapurina, M. Trchová, E.N. Konyushenko, P. Holler, Polymer 47 (2006) 8253.

[51] M. Trchová, P. Matějka, J. Brodinová, A. Kalendová, J. Prokeš, J. Stejskal, Polym. Degrad. Stab. 91 (2006) 114.

[52] S. Quillard, G. Louarn, S. Lefrant, A.G. MacDiarmid, Phys. Rev. 50 (1994**)** 12496 .

[53] M.I. Boyer, S. Quillard, E. Rebourt, G. Louarn, J.P. Buisson, A.P. Monkman, S. Lefrant, J. Phys. Chem. B 102 (1998**)** 382.

[54] R. M. Silverstein, G. C. Bassler, and T. C. Morrill, Spectrometric Identification of Organic Compounds, 5th Ed., Wiley, New York, 1991.

[55] I. Yu. Sapurina, M. E. Kompan, A. G. Zabrodskii, J. Stejskal, M. Trchová, Russ. J. Electrochem. 43 (2007) 528.

[56] K. Tzou, R.V. Gregory, Synth. Met. 47 (1992) 267.

[57] Y.H. Geng, J. Li, Z.C. Sun, X.B. Jing, F.S. Wang, Synth. Met. 96 (1998) 1.

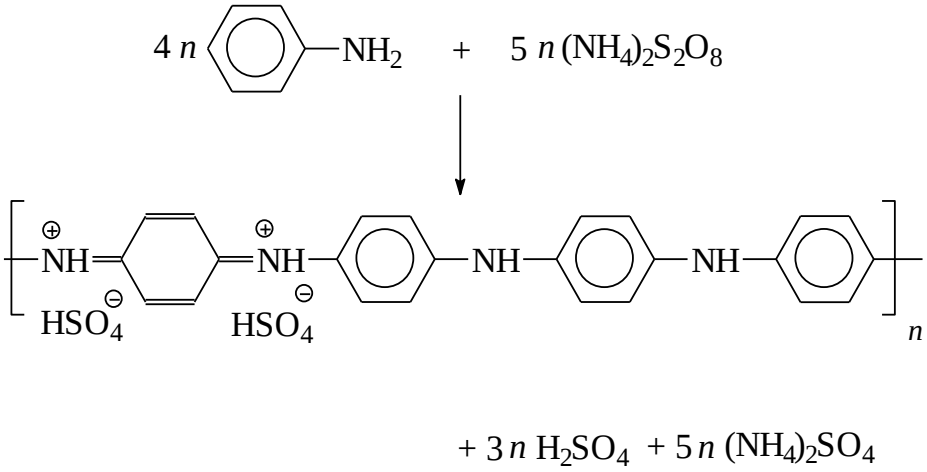

Fig. 1. **A**niline is oxidized with ammonium peroxydisulfate to PANI (hydrogen) sulfate. Sulfuric acid and ammonium sulfate are by-products.

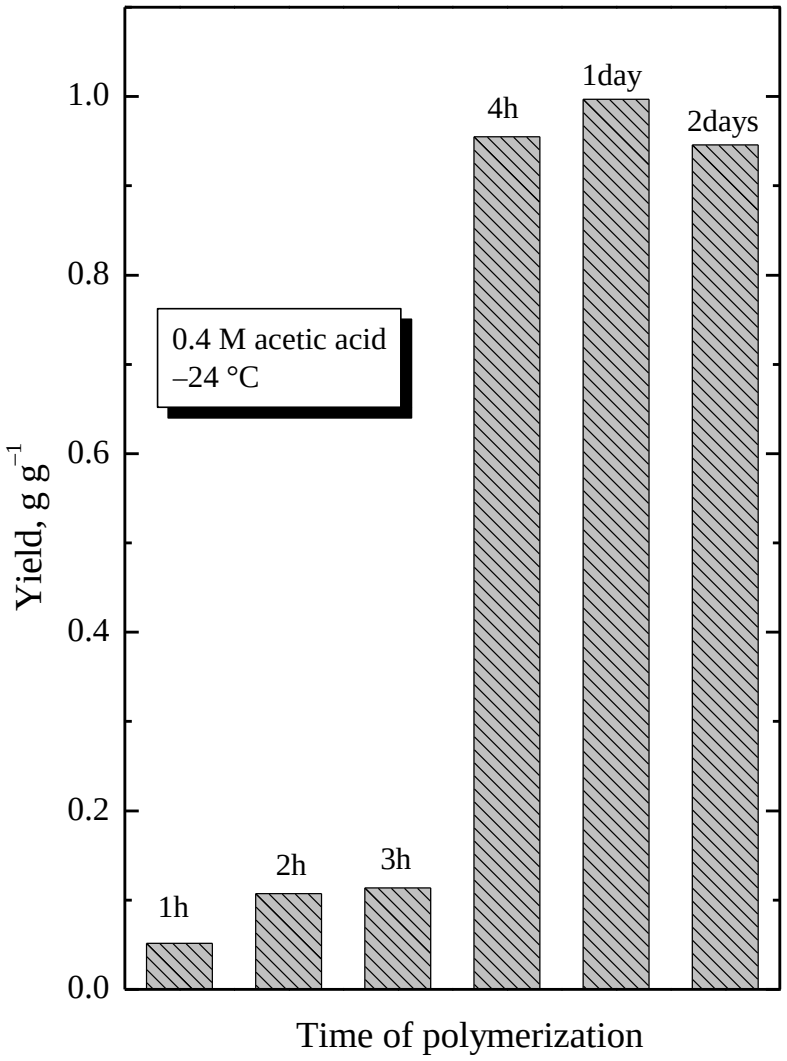

Fig. 2. The time-dependence of the yield of PANI (a polymer obtained from 0.2 M aniline monomer) in the oxidation of 0.2 M aniline with 0.25 M ammonium peroxydisulfate in 0.4 M acetic acid in ice at –24 °C.

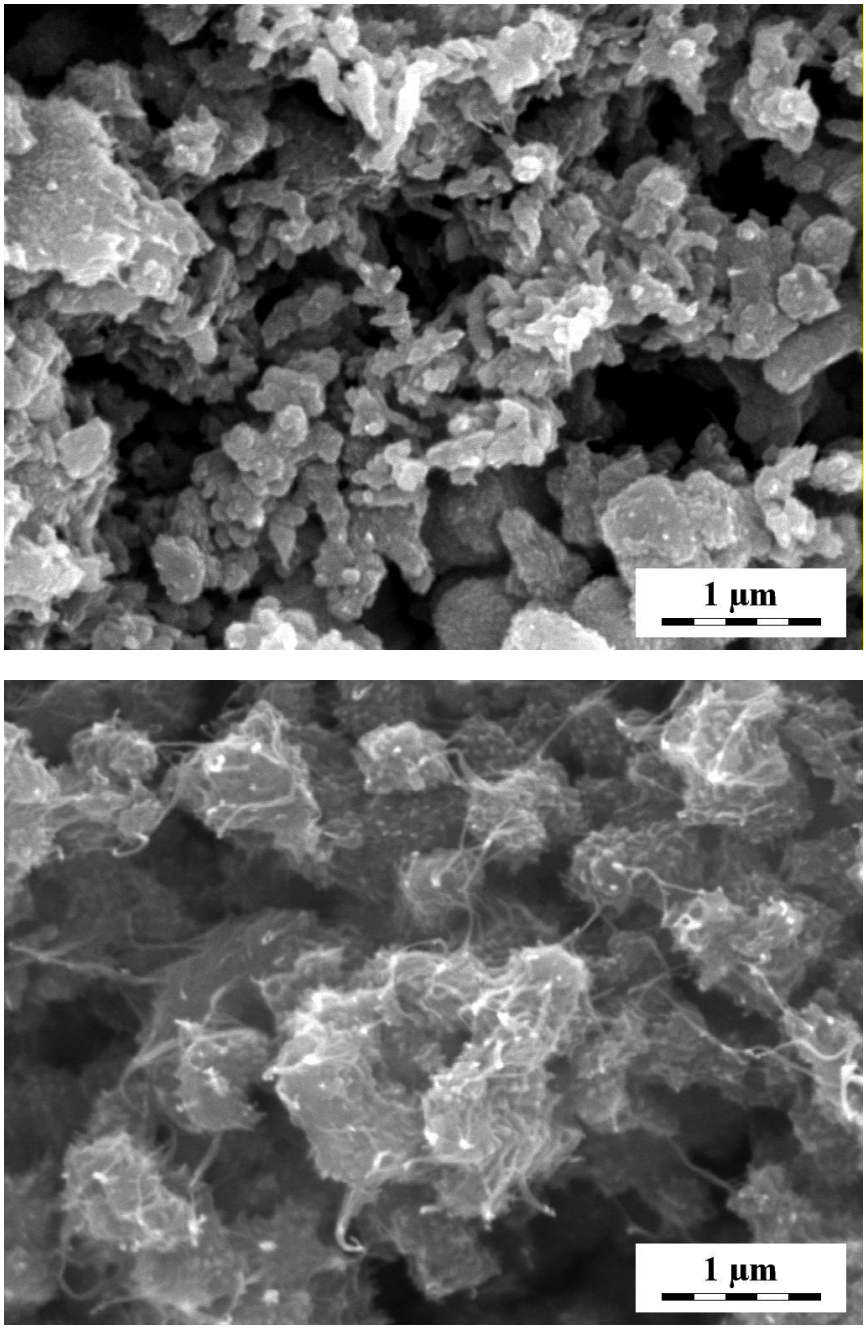

Fig. 3. The morphology of PANI prepared in 0.1 M sulfuric in the liquid state at –5 °C (top), and in the frozen reaction mixture at –25 °C (bottom).

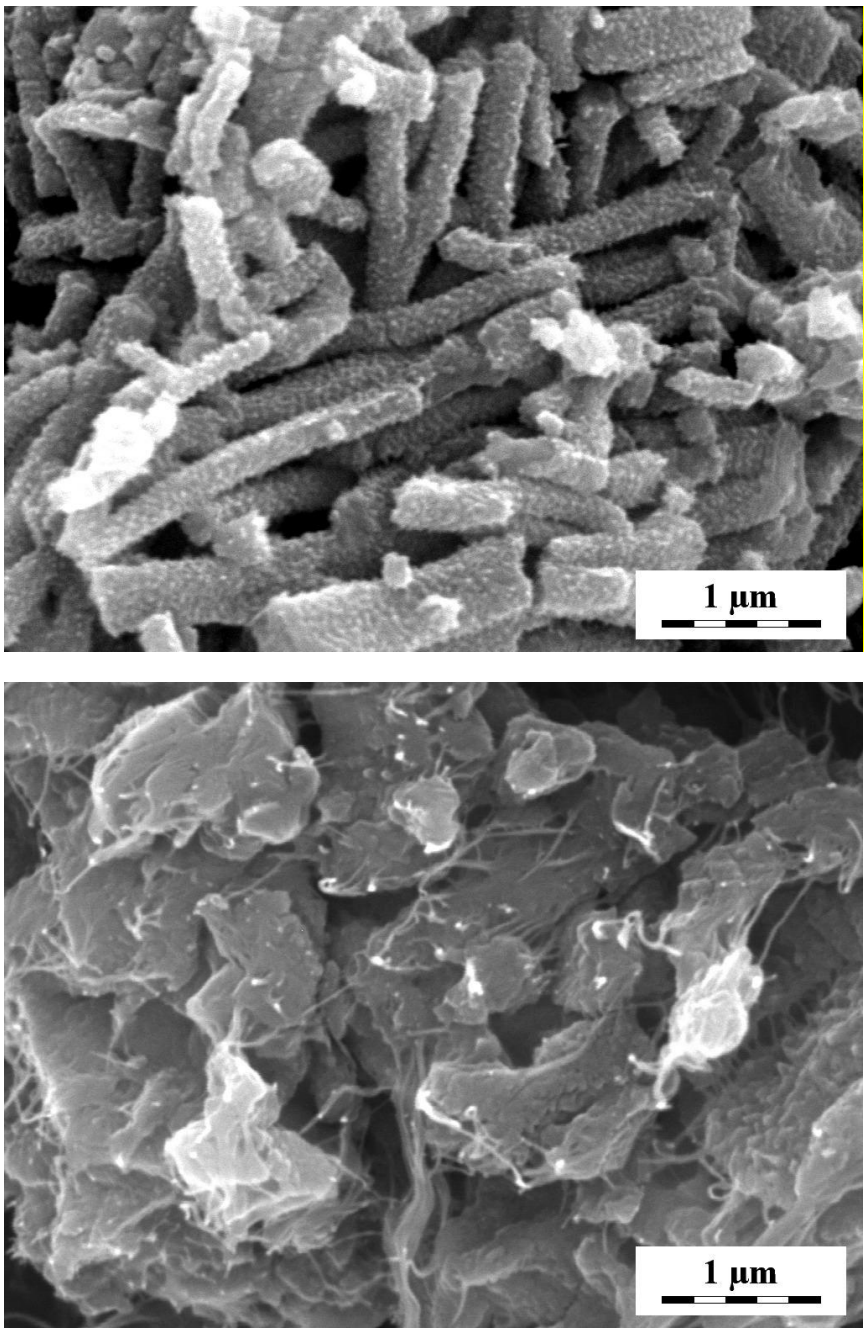

Fig. 4. The morphology of PANI prepared in 0.4 M acetic acid in the liquid state at –5 °C (top), and in the frozen reaction mixture at –25 °C (bottom).

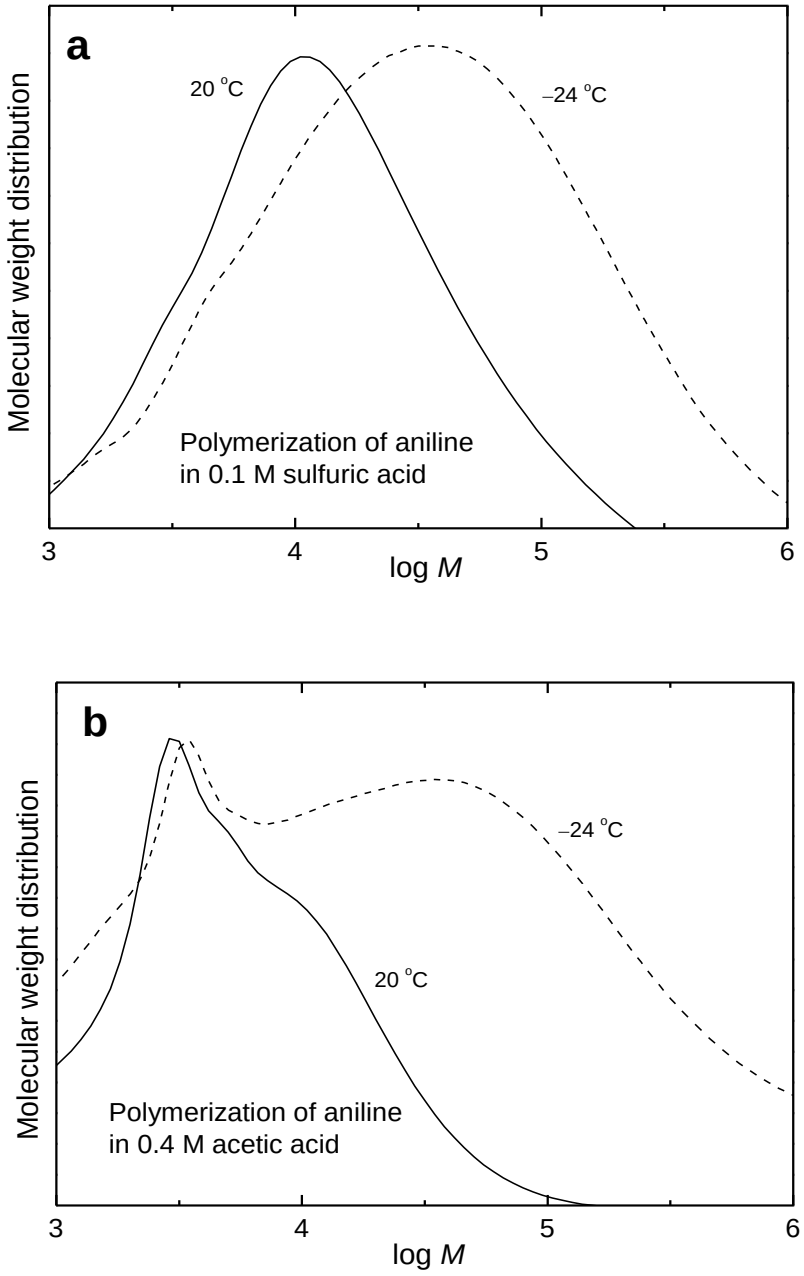

Fig. 5. Weight distributions of the molecular weight of PANI prepared in a liquid reaction mixture at 20 °C and in the frozen mixture at –24 °C (a) in 0.1 M sulfuric acid and (b) in 0.4 M acetic acid (bottom).

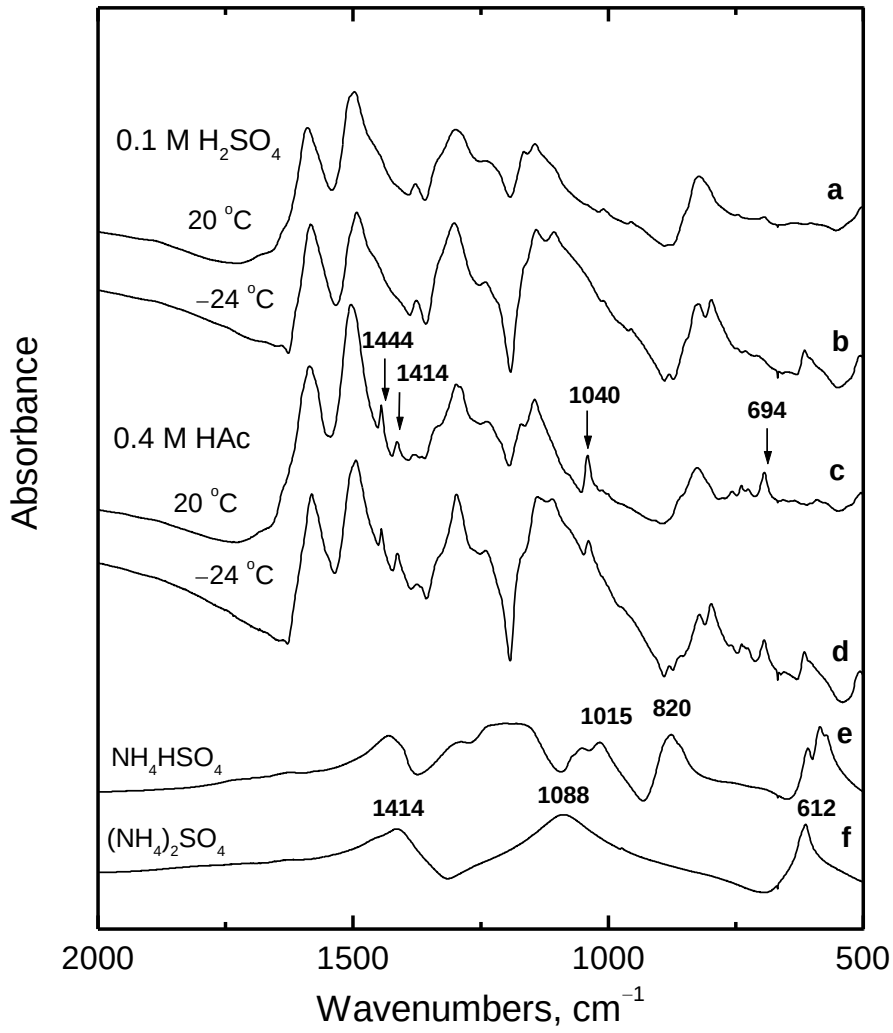

Fig. 6. The FTIR spectra of PANI bases obtained after deprotonation of the samples prepared in a liquid reaction mixture at 20 °C in 0.1 M sulfuric acid (**a**) and in 0.4 M acetic acid (**c**), the spectra of the deprotonated samples polymerized in frozen mixtures, in ice, at –24 °C in 0.1 M sulfuric acid (**b**) and in 0.4 M acetic acid (**d**), and the spectra of ammonium hydrogensulfate (**e**) and ammonium sulfate (**f**).

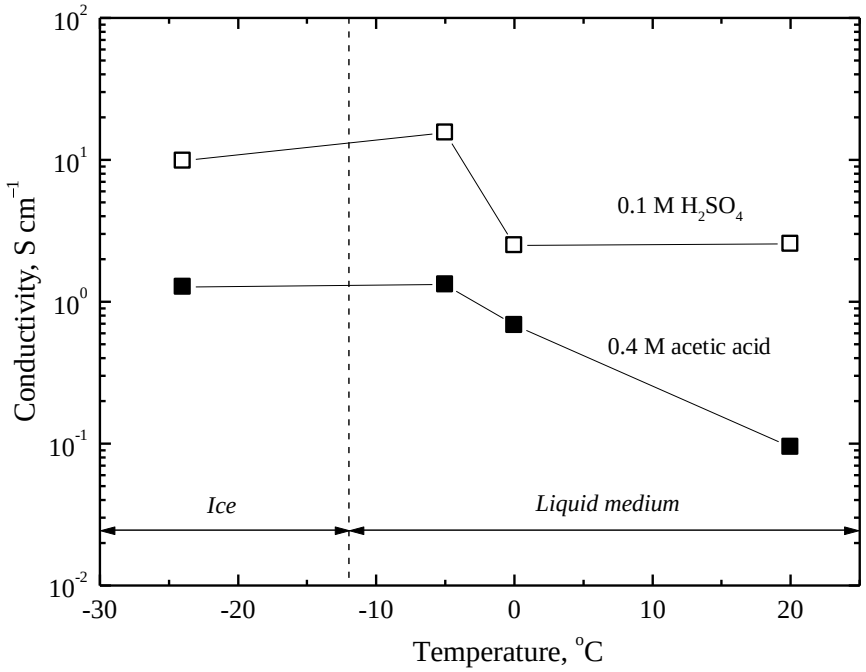

Fig. 7. The conductivity of PANI prepared at various temperatures in 0.1 M sulfuric acid (open squares) or 0.4 M acetic acid (full squares).

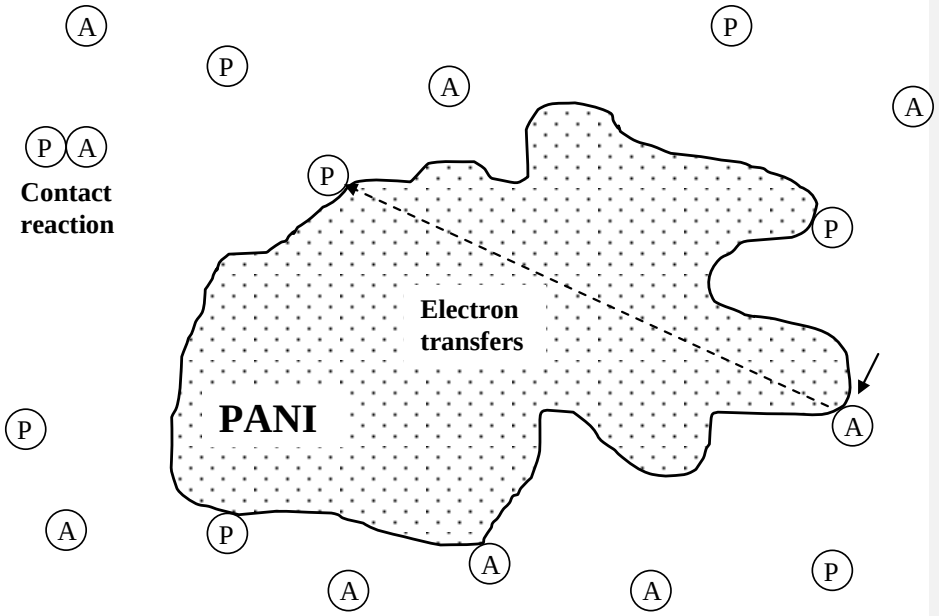

Fig. 8. A PANI chain growing in contact with PANI particles (marked by full arrow) adds an aniline monomer molecule (A) as a new constitutional unit. The electrons abstracted during the formation of the chemical bond incorporating the aniline molecule are transferred to the oxidant, peroxydisulfate molecule (P), which is reduced to sulfate. *Any* oxidant molecule in contact with PANI particles can accept electrons, which are transported through the conducting PANI phase (broken arrow) from the locus of polymerization. Aniline can also react with peroxydisulfate in the classical way, by exchanging electrons after physical contact between the molecules.

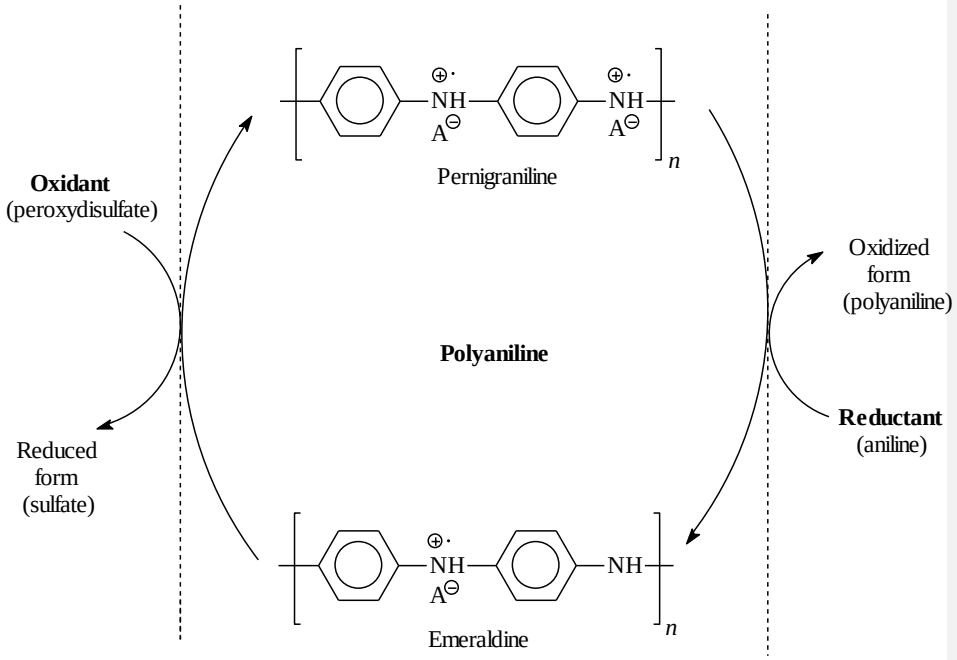

Fig. 9. The oxidant, peroxydisulfate, removes electrons from the emeraldine form of PANI, and converts it to pernigraniline. The addition of an aniline molecule to a growing PANI chain at another point results in the formation of a new constitutional unit. A transfer of electrons from the newly added aniline unit to the pernigraniline regenerates the original emeraldine form of PANI.